FACULTY OF SCIENCES

Where small molecules and polymer materials meet: triazolinedione chemistry at the interface

Kevin De Bruycker

Promotors:
Prof. Dr. Filip Du Prez
Prof. Dr. Johan Winne

Academic Year 2017–2018

Submitted to the Faculty of Sciences of Ghent University, in Fulfilment of the Requirements for the Degree of Doctor of Science: Chemistry

GHENT UNIVERSITY

FACULTY OF SCIENCES

WHERE SMALL MOLECULES AND POLYMER MATERIALS MEET: TRIAZOLINEDIONE CHEMISTRY AT THE INTERFACE

Kevin De Bruycker
Student number: 00800730

Supervisors: Prof. Dr. Filip Du Prez, Prof. Dr. Johan Winne

A dissertation submitted to the Faculty of Sciences of Ghent University, in fulfilment of the requirements for the degree of Doctor of Science: Chemistry

Academic year: 2017–2018

GHENT UNIVERSITY

Exam commission

Prof. Dr. Peter Dubruel (chair, Ghent University)

Prof. Dr. Karen De Clerck (Ghent University)

Prof. Dr. Annemieke Madder (Ghent University)

Dr. Laetitia Mespouille (University of Mons)

Prof. Dr. Bart Jan Ravoo (University of Münster)

Prof. Dr. Johan Winne (co-promotor, Ghent University)

Prof. Dr. Filip Du Prez (promotor, Ghent University)

Research funded by the Research Foundation – Flanders

Onderzoek gefinancieerd door het Fonds Wetenschappelijk Onderzoek – Vlaanderen

"Failure is the fog through which we glimpse triumph."

Guy Pearce

Dankwoord

Tijdens mijn doctoraat heb ik talloze keren gezegd dat een werkende toepassing van TAD-chemie typisch heel leuk en fascinerend is. Die toepassing werkend krijgen, dat is het echte probleem. Hoewel er gelukkig af en toe een eureka moment was (anders zou het toch wel een héél triestig doctoraat zijn), was dit onderzoek net zoals de meeste projecten: er waren vooral veel tegenslagen met de bijhorende frustraties. Ik ben dan ook veel mensen dankbaar voor de steun en hulp de afgelopen jaren.

In de eerste plaats wil ik prof. Filip Du Prez bedanken om mij een positie aan te bieden in zijn onderzoeksgroep. De afgelopen vier jaar heb ik me nooit ongewenst gevoeld in zijn bureau en stond hij altijd klaar om raad, hulp of een motiverende babbel te bieden. Bij Filip kon ik altijd mijn mening kwijt, ook al was deze meestal rechttoe rechtaan, zonder enige verbloeming. Zijn inzet en onvoorstelbare positieve ingesteldheid dragen heel sterk bij tot de aangename sfeer binnen de groep.

Naast mijn promotor ben ik ook mijn copromotor prof. Johan Winne zeer dankbaar. Johan zijn deur stond altijd open voor de kleine en minder kleine 'synthetische problemen': een mislukte reactie, een rare NMR, een nood aan nieuwe ideeën om een bepaalde component te synthetiseren of simpelweg een bevestiging van mijn eigen ideeën onder de vorm van een 'Johan approved' stempel. Altijd werd ik met een glimlach in zijn bureau ontvangen en nooit ben ik met lege handen weer vertrokken.

Uiteraard wil ik alle leden van de PCR-groep bedanken die voor een leuke werkatmosfeer in de labo's zorgden. Hoewel ik het heel aangenaam vond om met jullie samen te werken, heb ik ook veel plezier beleefd aan de tijd die we samen spendeerden op de vele activiteiten zoals happy hours, teambuildings, 'komen drinken' avonden, house warming parties en kerstfeestjes, die meestal vrij memorabel waren.

Waar een poging om *alle* huidige en vroegere leden van de groep bij naam te bedanken sowieso gedoemd is om te mislukken, verdienen sommigen toch wat extra aandacht. De bijdrage van Bernhard aan alle doctoraten wordt regelmatig onderschat, maar niets is zo onterecht. Bedankt voor de technische ondersteuning, het uitvoeren van analyses en om de hele groep draaiend te houden. Maarten en Chiel zou ik willen bedanken om voor mij te kiezen als begeleider voor hun masterthesis en voor hun bijdrage aan enkele hoofdstukken van deze thesis. Bastiaan en Hannes, mijn dank is groot voor vele grappige momenten in labo 4, waar ik de grootste tijd van mijn doctoraat samen met jullie gevestigd was. Oğuz, thanks for the many fun moments we shared during your time in the PCR-group, but more importantly for being a good friend afterwards. Finally, I would like to thank Oliver and Jiaojun for the work on my PhD topic during their research stay in the PCR-group. I can only hope you learned as much from me as I learned from you.

Ook buiten de eigen onderzoeksgroep waren meerdere personen bij dit doctoraatswerk betrokken die ik allen heel dankbaar ben. Prof. José Martins en Tim Courtin stonden garant voor een excellente NMR dienstverlening, terwijl de vele LC-MS en HRMS metingen uitgevoerd werden door Jan Goeman. Met vragen rond administratie, bestellingen, onkosten, verzenden van pakjes enz. werd ik altijd snel en vriendelijk geholpen door Carine, Christel, Paul, Queenie of Veerle.

Tot slot wil ik mijn vrienden en familie bedanken voor de fantastische momenten die we de afgelopen jaren samen hadden en hun interesse in wat ik ganse dagen uitspook. In het bijzonder wil ik mijn ouders uit de grond van mijn hart bedanken. Ondertussen heb ik al negen jaar gespendeerd aan het studeren en werken aan de unief, en al die tijd hebben ze me onvoorwaardelijk gesteund. Zonder hen zou dit alles niet mogelijk geweest zijn.

Table of Contents

Abbreviations

μCC	Microcontact chemistry
μCP	Microcontact printing
ABS	Acrylonitrile butadiene styrene terpolymer
ACN	Amphiphilic co-network
AE	Alder-ene
AFM	Atomic force microscopy
AI	Aziridinium imide
AIBN	α,α′-Azoisobutyronitrile
ARGET-ATRP	ATRP with activators regenerated by electron transfer
ATR-FTIR	Attenuated total reflectance infrared spectroscopy
ATRP	Atom-transfer radical polymerisation
ATPR-TAD	TAD-tagged ATRP initiator
bisTAD	Bivalent triazolinedione
BuTAD	4-Butyl-1,2,4-triazoline-3,5-dione
Cbz	Carboxybenzyl
CTA	Chain transfer agent
CuAAC	Cu (I)-catalysed azide-alkyne cycloaddition
$Đ$	Dispersity
DA	Diels-Alder
DABCO	1,4-Diazabicyclo[2.2.2]octane
DABCO-Br	Tetrameric 1,4-diazabicyclo[2.2.2]octanebromide complex
DBTL	Dibutyltin dilaurate
DCM	Dichloromethane
DDMAT	*S*-1-Dodecyl-*S*′-(α,α′-dimethyl-a″-acetic acid)trithiocarbonate

DEAD	Diethyl azodicarboxylate
DiBAl−H	Diisobutylaluminium hydride
DIPEA	Diisopropylethylamine
DMA	*N*,*N*-dimethylacrylamide
DMPA	2,2-Dimethoxy-2-phenylacetophenone
DMSO	Dimethyl sulfoxide
DMSO-d_6	Deuterated dimethyl sulfoxide
DMTA	Dynamic mechanical thermal analysis
DPPA	Diphenyl phosphoryl azide
DR1	Disperse Red 1
DSC	Differential scanning calorimetry
E	Young's modulus
EAS	Electrophilic aromatic substitution
ECS	(Ethoxycarbonyl)semicarbazide
EDG	Electron donating group
EDX	Energy-dispersive X-ray spectroscopy
EPM	Electrostatic potential map
EWG	Electron withdrawing group
FTIR	Fourier transform infrared spectroscopy
G′	Storage modulus
G″	Loss modulus
HDEO	*trans*,*trans*-2,4-Hexadiene-1-ol
HDI	Hexamethylene diisocyanate
HDI_3	Isocyanurate-based trimer of HDI
HLB	Hydrophilic-lipophilic balance
HMQC	Heteronuclear multiple-quantum correlation
Ini	Initiating radical
IPDI	Isophorone diisocyanate
$IPDI_3$	Isocyanurate-based trimer of IPDI
IR	Infrared

(isocyanate$_3$)–alcohol	Shorthand notation for trivalent alkenes or dienes based on an isocyanate trimer and an unsaturated alcohol
IZ	Iminium-urazolide zwitterion
LbL	Layer-by-layer
LC-MS	Liquid chromatography - mass spectrometry
Lg	Leaving group
MDI	4,4′-methylene diphenyl diisocyanate
MDI-TAD	4,4′-(4,4′-methylenediphenyl)-bis-(1,2,4-triazoline-3,5-dion)
M_w	Weight average molecular weight
NBD	7-Nitrobenz-2-oxa-1,3-diazole
NBD-Cl	4-Chloro-7-nitro-1,2,3-benzoxadiazole
NBDA	NBD-acrylate
NHS	*N*-hydroxysuccinimide
NMR	Nuclear magnetic resonance
NO_2PhTAD	4-(4′-nitrophenyl)-TAD
PD	Polarised diradical
Pd/C	Palladium on carbon
PDMA	Poly(*N*,*N*-dimethylacrylamide)
PDMS	Poly(dimethylsiloxane)
PDMS-TLa	Thiolactone-functional PDMS
PEG	Poly(ethylene glycol)
PFPTAD	4-Perfluorophenyl-TAD
PhTAD	4-Phenyl-1,2,4-triazoline-3,5-dione
PhTAD-COOH	4-(4′-Carboxyphenyl)-1,2,4-triazoline-3,5-dione
PMA	Poly(methyl acrylate)
PNP	*p*-nitrophenyl
polyHEA	Poly(2-hydroxyethyl acrylate)
ppm	Parts per million
PVA	Poly(vinyl alcohol)
rAE	retro-Alder-ene
RAFT	Reversible addition fragmentation transfer

rDA	retro-Diels-Alder
R_F	Fluorinated 'ponytail'
R_FTAD	4-(1*H*,1*H*,2*H*,2*H*-perfluorodecyl)-1,2,4-triazoline-3,5-dione
ROMP	Ring-opening metathesis polymerisation
rt	Room temperature
SAM	Self-assembled monolayer
SAXS	Small-angle X-ray scattering
SBC	Poly(styrene-*co*-butadiene)
SBS	Poly(styrene-butadiene-styrene) triblock copolymer
SI-ATRP	Surface-initiated ATRP
SIS	Poly(styrene-isoprene-styrene) triblock copolymer
SEC	Size exclusion chromatography
SEM-EDX	EDX with electron beam excitation
SF	Soluble fraction
SWCA	Static water contact angle
TAD	1,2,4-Triazoline-3,5-dione
TAIC	Trichloroacetyl isocyanate
TDI	Toluene diisocyanate
TDI_3	Isocyanurate-based trimer of TDI
TEM	Transmission electron microscopy
T_g	Glas transition temperature
TGA	Thermogravimetric analysis
THF	Tetrahydrofuran
TLa	Thiolactone
TLaAm	Acrylic TLa-containing monomer
TLa-NCO	α-Isocyanato-γ-thiolactone
TLaSt	Styrenic TLa-containing monomer
ToF-SIMS	Time-of-flight secondary ion mass spectrometry
UV	Ultraviolet
wt%	Weight %
XPS	X-ray photoelectron spectroscopy

Chapter I

General aim and outline

I.1 Introduction

More than a decade ago, the concept of 'click chemistry' was introduced by Sharpless and co-workers, together with a list of criteria.[1] Essentially, these reactions must be robust, fast, high-yielding and should allow efficient linking of various molecules with easily separable side-products. Nevertheless, products can be separated from side-products and reagents by several techniques in organic synthesis, while these techniques are often not applicable for polymeric substrates. Moreover, polymers are typically synthesised on a (very) large scale, which complicates the purification even more. Therefore, the click concept proved to be especially useful in the context of polymer modifications, and resulted in the synthesis of polymer architectures that are not readily obtained via traditional reactions.[2–4]

Next to the well-known Cu (I)-catalysed azide-alkyne cycloaddition (CuAAC), historically the first click reaction,[5] many other ligation methods were re-explored over the years and re-branded as 'click', such as the nucleophilic ring-opening of epoxides or additions to unsaturated carbon-carbon bonds. However, because not many reactions – if any – meet all of Sharpless' original criteria, this term was often used quite loosely and rather became a synonym for any fast and efficient process. Therefore, a slightly altered set of criteria was introduced by a number of research groups, including ours, which defines true click chemistry for applications in polymer science.[6,7] For example, the requirement of an equimolar amount of reagents was introduced, which allows polymer-polymer ligations without the need to isolate the product from a blend of polymers.[8]

Despite the continued misuse of the term and the ongoing search for the perfect click reaction, the concept of click chemistry is very useful and might as well be considered as a way of thinking and designing an experiment, rather than a strict set of rules and definitions. In this context, many applications in the area of material science profit from these fast and highly efficient click-like reactions. For example, most of the commercial polymers are mixed with additives prior to the shaping of the material to improve their bulk properties, after which coatings can be applied to alter the interaction of the material with its surroundings.[9,10] Because typically neither the additives nor the coatings are chemically bound to the polymer, leaching or delamination, respectively, are common issues that result in a decrease in material performance of the material over time.[11,12] These problems can be solved by covalently linking specific moieties to the polymer, while a significant increase in processing time is avoided by using one of the click-inspired chemistries.

Triazolinedione (TAD) chemistry represents another example of a known and well studied ligation method[13–16] that recently regained a lot of interest because of the click-like reactivity towards a variety of unsaturated substrates. For example, the research groups of Barbas and Madder reported on the efficient bioconjugation of TAD reagents with tyrosine and (unnatural) furylalanine residues in peptides and proteins via an electophilic aromatic substitution.[17–19] Later, our research group demonstrated the high reactivity of triazolinediones for conjugated dienes and isolated alkenes, in a Diels-Alder or an Alder-ene reaction, respectively, by producing block copolymers and cross-linked plant-oil-based materials.[20,21] In fact, these compounds are generally considered as the strongest dieno-

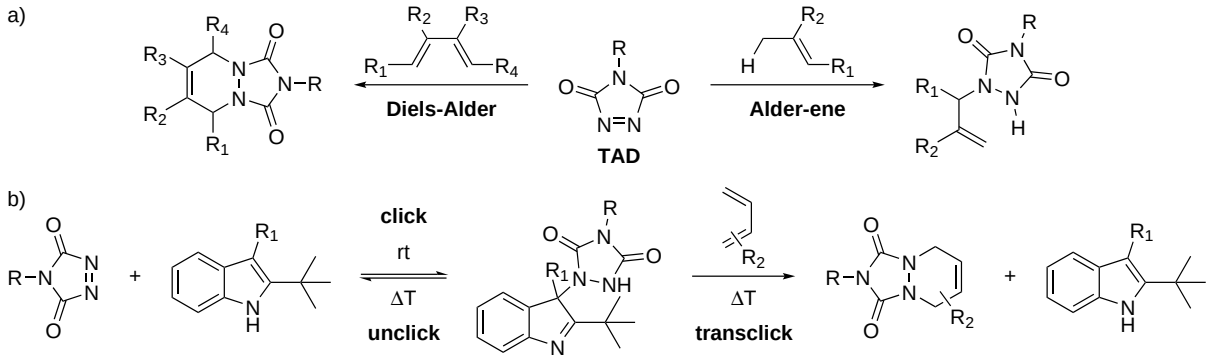

Scheme I.1: **(a)** Reactivity of a triazolinedione (TAD) towards dienes (left) or isolated alkenes (right) in a Diels-Alder or Alder-ene reaction, respectively. **(b)** A reversible Alder-ene reaction between a TAD and an indole, followed by an irreversible Diels-Alder reaction. This click-unclick-click cascade is an example of a transclick reaction.

and enophiles in organic chemistry (Scheme I.1a).[22,23] TAD reactions are typically complete within a time scale of seconds to minutes, proceed at room temperature without the need of a catalyst, are high-yielding and thus meet many criteria of a click reaction. Moreover, when TADs are reacted with an indole rather than a simple alkene, reversibility of the Alder-ene adduct is observed at elevated temperatures (Scheme I.1b). Our group further explored this dynamic TAD-indole 'click-unclick' reaction and eventually developed the 'transclick' concept in analogy with a transesterification, describing an unclick-click cascade transferring a TAD moiety from its indole-adduct to another reaction partner.[20] This concept was subsequently applied for the generation of reversible polymer conjugates and dynamic cross-linked materials.

The general aim of this doctoral work has been the exploration of TAD-based chemistry as a tool for highly efficient reactions at interfaces. These interfacial reactions include both modifications of solid substrates with solubilised TAD compounds, *i.e.* reaction at the solid-liquid interface, as well as the synthesis and functionalisation of polymeric beads and microcapsules, *i.e.* reactions in a liquid-liquid biphasic system. In the former case, local concentration effects should be expected to significantly influence the reaction kinetics, whereas identifying complementary reaction partners that are soluble in two orthogonal liquids will pose the greatest challenge in the latter case. While some low molecular weight TAD-compounds are known to be volatile at a reduced pressure, reactions at the gas-liquid or the gas-solid interface (*e.g.* chemical vapour deposition) are out of the scope of this dissertation.

I.2 Outline

Despite their somewhat 'exotic' reputation, triazolinediones are unique reagents in organic synthesis, which have also found various applications in different research disciplines. Therefore, **Chapter II** offers a detailed discussion of the available TAD reagents, together with their synthesis strategies.[24] Furthermore, it also gives an overview of the reactivity and the most important applications in the field of polymer science. The first part of this manuscript thus serves as a theoretical background of the chemical platform that is used throughout this doctoral work.

Because no general synthetic strategy is available to obtain functional triazolinediones, **Chapter III** discusses the development of scalable syntheses for triazolinediones that bring functionality to a material. Apart from these tailored compounds, cross-linked materials containing TAD-complementary groups are synthesised and characterised as well. These materials are applied in a final stage to illustrate the applicability of the functional TADs for surface modifications.

Chapter IV explores the possibility to alter the wetting properties of various readily available bulk polymers using fluorinated triazolinediones that were synthesised in Chapter III.[25] Both a surface modification, in which the solid material is submerged in a solution of the TAD compound, and a homogeneous treatment in solution are investigated. The impact of the modification on the surface properties is quantified by contact angle goniometry, while the results are rationalised by a combination of bulk- and surface analysis techniques.

In contrast to the modification of an unsaturated polymer, **Chapter V** demonstrates the deposition of a TAD-based coating with a controlled thickness on an inorganic substrate.[26] First, a TAD-reactive silane is grafted on a silicon wafer, which is then alternatingly reacted with a bivalent TAD and a trivalent diene. In this way, a coating can be deposited very rapidly in a layer by layer fashion.

Rather than covering the full surface of a substrate with a TAD-based coating, **Chapter VI** describes the use of microcontact chemistry to pattern a functional TAD on a surface.[27] In the first phase, an irreversibly reacting TAD-compatible substrate is synthesised, which is used to optimise the printing process of a triazolinedione 'ink'. Next, a reversibly reacting indole is grafted on a silicon wafer to develop and optimise TAD transclick reactions in an interfacial system, *i.e.* from a surface-bound indole to a competitive partner in solution. Both this chapter and the previous one are the result of a collaboration with the group of Prof. Bart Jan Ravoo (University of Münster, Germany).

Just like other 'click' chemistries, the triazolinedione platform is not perfect and revealed some of its drawbacks during the course of this doctoral work. **Chapter VII** provides an overview on these limitations in the context of liquid-liquid biphasic systems. Next, thiolactone chemistry is introduced as a complementary strategy that shares some of the strengths, yet is not hampered by these TAD-related issues. Finally, the applicability of

this thiolactone ligation method for the synthesis of polymeric particles via an interfacial polymerisation is demonstrated.

Because thiolactones also allow for a fast one-pot double modification, **Chapter VIII** explores this chemistry as an alternative cross-linking strategy for the generation of amphiphilic silicone-based co-networks. Rather than a macrophase separation (*cf.* interfacial polymerisations), a characteristic nanophase separation of hydrophilic and hydrophobic domains is targeted, which should allow the networks to swell in both water and organic solvents. After the synthesis of multiple thiolactone-functional silicones, these hydrophobic polymers are reacted with acrylate-terminated poly(ethylene glycol) as hydrophilic component. Different network structures are synthesised, functionalised, and their amphiphilic character is assessed.

Besides the research projects discussed in chapters III–VII, multiple other TAD-related topics have been investigated in the framework of this PhD research as well. However, these topics have mainly been focused on very specific applications and have typically relied to a great extent on the expertise of our collaboration partners. Therefore, they are not included in this dissertation. For example, in collaboration with the research group of Prof. Karen De Clerck (Ghent University), we show that the delamination resistance of composite materials containing poly(styrene-*block*-butadiene-*block*-styrene) nanofibres can be tuned by modifying the fibres with triazolinediones.[28,29] In collaboration with the group of Joël Lyskawa (University of Lille, France), on the other hand, we demonstrate the electrochemical generation of TAD moieties on glassy carbon surfaces, which are subsequently used to further functionalise the surface.[30]

Chapter IX gives a general conclusion of the described work and addresses some future perspectives.

Finally, **Chapter X** provides a summary of this manuscript in Dutch.

I.3 Bibliography

1. H. C. Kolb, M. G. Finn, K. B. Sharpless, *Angew. Chem. Int. Ed.* **2001**, *40*, 2004–2021.
2. C. J. Hawker, V. V. Fokin, M. G. Finn, K. B. Sharpless, *Aust. J. Chem.* **2007**, *60*, 381–383.
3. A. Inglis, S. Sinnwell, M. Stenzel, C. Barner-Kowollik, *Angew. Chem. Int. Ed.* **2009**, *48*, 2411–2414.
4. P. L. Golas, K. Matyjaszewski, *Chem. Soc. Rev.* **2010**, *39*, 1338–1354.
5. M. Meldal, C. W. Tornøe, *Chem. Rev.* **2008**, *108*, 2952–3015.
6. C. Barner-Kowollik, F. E. Du Prez, P. Espeel, C. J. Hawker, T. Junkers, H. Schlaad, W. Van Camp, *Angew. Chem. Int. Ed.* **2011**, *50*, 60–62.
7. P. Espeel, F. E. Du Prez, *Macromolecules* **2015**, *48*, 2–14.
8. W. Xi, T. F. Scott, C. J. Kloxin, C. N. Bowman, *Adv. Funct. Mater.* **2014**, *24*, 2572–2590.
9. G. Pritchard, *Plastics Additives: A Rapra Market Report*, iSmithers Rapra Publishing, United Kingdom, **2005**, p. 208.
10. I. Holme, *Surf. Coat. Int. Part B* **2006**, *89*, 343–363.
11. D. Price, K. Pyrah, T. R. Hull, G. J. Milnes, J. R. Ebdon, B. J. Hunt, P. Joseph, C. S. Konkel, *Polym. Degrad. Stab.* **2001**, *74*, 441–447.
12. D. J. Kind, T. R. Hull, *Polym. Degrad. Stab.* **2012**, *97*, 201–213.
13. B. T. Gillis, J. D. Hagarty, *J. Org. Chem.* **1967**, *32*, 330–333.
14. R. C. Cookson, S. S. H. Gilani, I. D. R. Stevens, *J. Chem. Soc. C* **1967**, *1967*, 1905–1909.
15. G. B. Butler, *Ind. Eng. Chem. Prod. Res. Dev.* **1980**, *19*, 512–528.
16. S. Rádl in *1,2,4-Triazoline-3,5-Diones*, *Vol. 67* (Ed.: R. K. Alan), Academic Press, **1996**, book section 2, pp. 119–205.
17. H. Ban, J. Gavrilyuk, C. F. Barbas, *J. Am. Chem. Soc.* **2010**, *132*, 1523–1525.
18. H. Ban, M. Nagano, J. Gavrilyuk, W. Hakamata, T. Inokuma, C. F. Barbas, *Bioconjugate Chem.* **2013**, *24*, 520–532.
19. K. Hoogewijs, D. Buyst, J. M. Winne, J. C. Martins, A. Madder, *Chem. Commun.* **2013**, *49*, 2927–2929.
20. S. Billiet, K. De Bruycker, F. Driessen, H. Goossens, V. Van Speybroeck, J. M. Winne, F. E. Du Prez, *Nat. Chem.* **2014**, *6*, 815–821.

21. O. Türünç, S. Billiet, K. De Bruycker, S. Ouardad, J. Winne, F. E. Du Prez, *Eur. Polym. J.* **2015**, *65*, 286–297.

22. W. H. Pirkle, J. C. Stickler, *Chem. Commun. (London)* **1967**, *1967*, 760–761.

23. G. B. Butler, *Polym. Sci. U.S.S.R.* **1981**, *23*, 2587–2622.

24. K. De Bruycker, S. Billiet, H. A. Houck, S. Chattopadhyay, J. M. Winne, F. E. Du Prez, *Chem. Rev.* **2016**, *116*, 3919–3974.

25. K. De Bruycker, M. Delahaye, P. Cools, J. Winne, F. E. Du Prez, *Macromol. Rapid Commun.* **2017**, *38*, 1700122.

26. B. Vonhören, O. Roling, K. De Bruycker, R. Calvo, F. E. Du Prez, B. J. Ravoo, *ACS Macro Lett.* **2015**, *4*, 331–334.

27. O. Roling, K. De Bruycker, B. Vonhören, L. Stricker, M. Körsgen, H. F. Arlinghaus, B. J. Ravoo, F. E. Du Prez, *Angew. Chem. Int. Ed.* **2015**, *54*, 13126–13129.

28. S. van der Heijden, K. De Bruycker, R. Simal, F. Du Prez, K. De Clerck, *Macromolecules* **2015**, *48*, 6474–6481.

29. S. van der Heijden, L. Daelemans, K. De Bruycker, R. Simal, I. De Baere, W. Van Paepegem, H. Rahier, K. De Clerck, *Compos. Struct.* **2017**, *159*, 12–20.

30. W. Laure, K. De Bruycker, P. Espeel, D. Fournier, P. Woisel, F. E. Du Prez, J. Lyskawa, *Langmuir* **2017**, submitted.

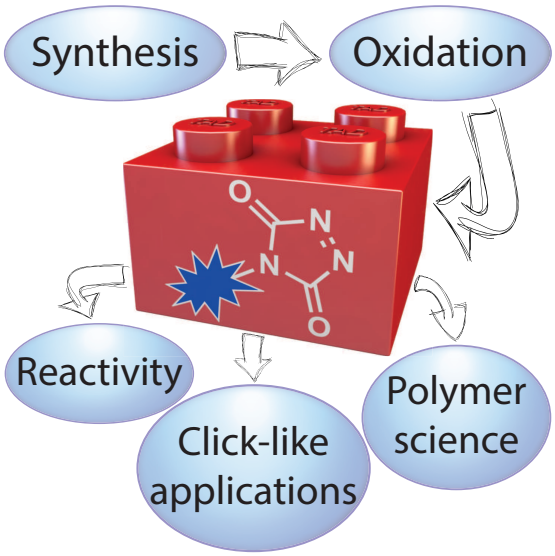

Abstract

Triazolinediones are unique reagents in organic synthesis, which have also found wide applications in different research disciplines, in spite of their somewhat 'exotic' reputation. Nevertheless, because the general use of triazolinediones has always been hampered by the limited commercial and synthetic availability of such reagents, this chapter offers a detailed discussion of the available TAD reagents, together with their synthesis strategies. Moreover, it also gives an overview of the reactivity and the most important applications in the field of polymer science. This chapter thus aims to serve as a practical guide for researchers that are interested in exploiting and further developing the exceptional click-like reactivity of triazolinediones in various applications.

Published as

K. De Bruycker, S. Billiet, H. A. Houck, S. Chattopadhyay, J. M. Winne, F. E. Du Prez, *Chemical Reviews* **2016**, *116*, 3919–3974.

Chapter II

Introduction to triazolinedione chemistry

II.1 Introduction

The remarkable bond-forming reactivity of azodicarbonyl derivatives towards normally 'unreactive' unsaturated hydrocarbon substrates was first recognised in the pioneering 1920s work by Otto Diels *et al.*[1] This seminal finding would lead to the development of the famous and transformative Diels-Alder reaction, as reagents such as diethyl azodicarboxylate (DEAD) were found to spontaneously form a quantitative 1:1 adduct with cyclopentadiene at room temperature without the need for additives or catalysts (Scheme II.1a).[1,3] The even more reactive *cis*- or cyclic azodicarbonyl analogues, however, were excluded from

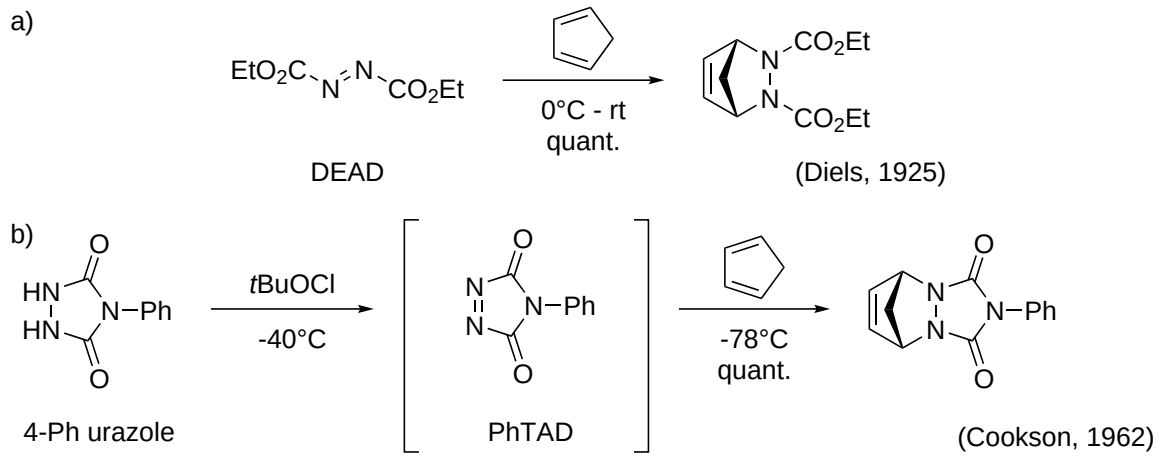

Scheme II.1: **(a)** Initial observation of azodicarbonyl reactivity with hydrocarbon substrates,[1] and **(b)** first useful transformation of a (*in situ* prepared) TAD reagent.[2]

these initial studies, although a 4-substituted 1,2,4-triazoline-3,5-dione ('triazolinedione' or TAD) was reported as early as 1894 by Thiele and Stange.[4] In fact, as a result of the problematic synthesis and purification of TAD compounds, their use as a dienophile in a Diels-Alder reaction was not established before the 1960s, when Cookson *et al.* obtained pure crystalline 4-phenyl-TAD (Cookson's reagent) for the first time (Scheme II.1b).[2,5] Cookson's procedure is now properly considered as a major breakthrough in the field of TAD chemistry, as it was followed by a wide range of investigations into the unique reactivity and many synthetic applications of TAD-bearing compounds, which have continued to grow to this day.

With a Diels-Alder-type reactivity which is, respectively, 30 000 and 1000 times faster than that of DEAD[6–8] and tetracyanoethylene,[9,10] triazolinediones are generally considered as the most reactive bench-stable dienophiles[6,11] and enophiles.[12] Moreover, as their reactivity depends to a certain extent on the nature of the 4-substituent, electron-poor 4-aryl substituents can even further increase the electrophilicity up to the point that TAD reagents, for example 4-(4-nitrophenyl)-TAD, become too reactive to be isolated.[13–15] Nevertheless, once isolated, most triazolinediones are generally easy to handle and are stable for prolonged periods when stored in a cold environment (*i.e.* −18 °C) in the absence of light and moisture.[2,16,17]

Although the synthesis and chemistry of simple TAD reagents is well understood,[18,19] in more recent applications, such as in click chemistry and/or modern polymer chemistry (*vide infra*), functional or 'tailored' TAD reagents are often required to harness the full potential of the exceptional TAD reactivity. Although the use of such functional TAD compounds enables unprecedented applications, research into this area is hampered by the limited synthetic accessibility of these compounds, even by today's high standards.

A survey of known practical synthesis methods for TAD compounds reveals that these almost invariably involve the oxidation of the corresponding 1*H*,2*H*-1,2,4-triazolidine-3,5-dione ('urazole'), as in Cookson's original procedure (Scheme II.1b).[2] For the assembly of these heterocyclic precursor urazoles, a large variety of methods is now available, using a number of simple starting materials. Likewise, many different oxidation methods for urazoles have been explored, with varying degrees of efficiency and chemoselectivity. Despite all of these methodological developments, the 'tailored' synthesis of triazolinediones

is still no trivial matter and often involves critical strategic choices, as there are no 'general' methods. The limited commercial availability of TAD reagents and the synthetic challenges encountered in preparing (functional) TAD compounds thus continue to serve as a major bottleneck for TAD-chemistry-based research and applications. For this reason, rather than providing a complete and detailed discussion of every synthetic route and oxidation method, the first section in this chapter (section II.2) aims to provide an informative overview of the most relevant ones in view of this doctoral work.

In the following section (section II.3), an overview of the reactivity of triazolinediones will be provided. While TADs are highly activated species and can participate in a large variety of reactions, only a brief discussion of the most important reaction partners and possible side reactions will be provided herein. Finally, the TAD reactivity is illustrated by a selection of applications (section II.4), which are actively investigated in our research group and are thus of specific relevance for this doctoral work. For a more comprehensive discussion of possible applications, or a complete overview of TAD syntheses, the reader is referred to our review on TAD chemistry.[20]

II.2 Synthesis of functionalised triazolinediones

The first report on the synthesis of a 1,2,4-triazolidine-3,5-dione (urazole) dates back to 1887, when Pinner noted a peculiar reaction between phenylhydrazine and urea, the outcome of which depends on the ratio of the reactants (Scheme II.2).[21] If only one equivalent of urea is used, 1-phenylsemicarbazide (**1**) is obtained, while an excess of urea leads to a cyclic compound (**2**). Since Pinner envisioned that other analogues of 1-phenyl-1,2,4-triazolidine-3,5-dione can be synthesised as well, he introduced the name 'urazole' for this class of five-membered heterocyclic compounds.

Because a 4-substituted 1,2,4-triazoline-3,5-dione is mostly obtained through oxidation of

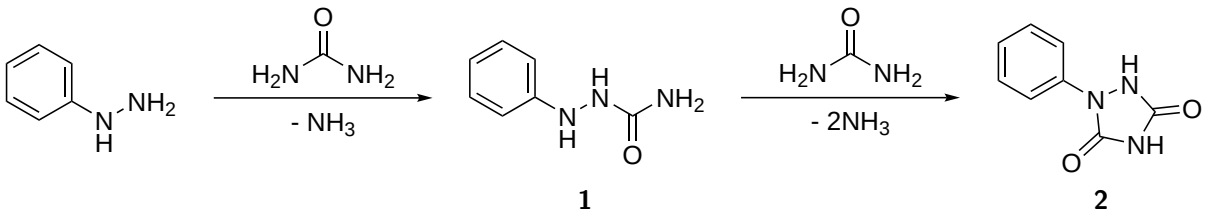

1 **2**

Scheme II.2: Reaction of urea with phenylhydrazine, as reported by Pinner.[21]

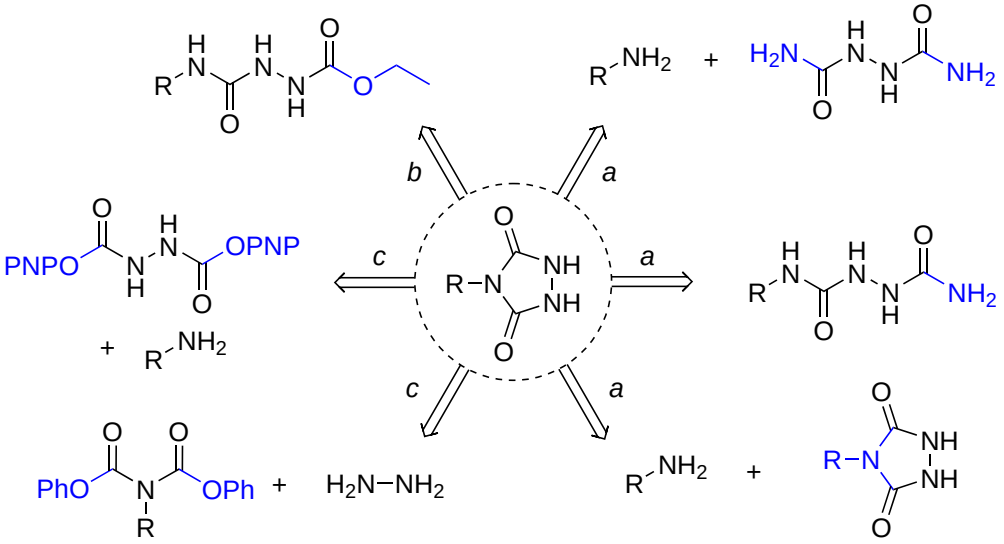

Figure II.1: Brief overview of the possible synthetic strategies to obtain 4-substituted 1,2,4-triazolidine-3,5-diones (urazoles). PNP = *p*-nitrophenyl.

the corresponding urazole (*vide supra*), this section will first discuss the possible synthetic pathways to produce such compounds. Figure II.1 provides a brief overview of the possible synthetic strategies, which can be categorised based on the nature of the required starting materials, building blocks and intermediates.

The oldest synthetic routes for 4-substituted urazoles,[4,22] used before the second half of the twentieth century, were all based on hydrazodicarboxamide intermediates or derivatives thereof (*a*, Figure II.1).[20] However, the optimisation of reaction conditions can be very tedious and the overall substrate scope remains fairly limited as a result of the required harsh reaction conditions. Therefore, this one-step procedure was not suitable in the framework of this thesis and will not be further discussed in this chapter. Nevertheless, it seems to be especially feasible in an industrial environment, where a single batch typically yields hundreds of grams of product without the need of intermediate purifications.

The more efficient modern methods are distinguished by the use of 1-alkoxycarbonyl semicarbazides as alternative (and more activated) urazole precursors (*b*, Figure II.1). These key intermediates for urazole synthesis are commonly referred to as 'semicarbazides' in this context, which will also be done in this chapter. As semicarbazides themselves can be assembled in a number of efficient ways, these alternative routes will be discussed within the first section (II.2.1), devoted to the synthesis and cyclisation of semicarbazide intermediates.

Apart from the widely adopted semicarbazides and hydrazodicarboxamides, some alternative urazole precursors have also been explored (*c*, Figure II.1).[20,23–25] These less common synthetic schemes were mainly developed for a very specific purpose, such as the possibility to synthesise urazoles bearing certain functionalities that are not tolerated by the more conventional methods. Because of their highly specialised character, they were not considered for this doctoral work and will thus not be discussed in this chapter.

While there is a vast choice of routes and starting materials to prepare 'functional' urazoles, certain chemical functionalities are incompatible with all of them. In this case, an alternative can be found in procedures that transform available simple 4-substituted urazoles into more elaborate ones. Therefore, section II.2.2 will provide the reader with examples and possibilities in the chemoselective modification of 4-substituted urazoles.

Unless noted otherwise, all the urazoles that are described in the following sections, have also been successfully oxidised to the corresponding TAD compounds (*cf*. Scheme II.1b). However, the exact oxidant can greatly vary depending on the exact urazole, since there are no generally applicable oxidation approaches. Therefore, this section will conclude with a summary of the most relevant oxidants for this doctoral work (section II.2.3).

II.2.1 Urazoles via semicarbazides

In 1961, more than seven decades after Thiele's original synthesis based on hydrazodicarboxamide intermediates,[4] Zinner and Deucker were the first to propose a synthetic scheme for urazoles that actually improved upon the methods based on Thiele's original approach.[26] Rather than using biurea starting materials, they synthesised 4-phenyl and 4-butyl urazole (R = Ph and Bu resp.) through cyclisation of the corresponding 4-substituted 1-(ethoxycarbonyl)semicarbazide (**3**, Scheme II.3), which only requires mild reaction conditions. Significantly, these 'semicarbazides' can be generated by simply mixing an isocyanate with ethyl carbazate (in itself a readily available condensation product of cheap hydrazine and diethyl carbonate) and is thus a very convenient approach.

While the isocyanate-based two-step approach is characterised by significantly higher overall yields and much milder reaction conditions compared to the original urazole synthesis (*vide infra*), it took ten years for this strategy to gain the attention of the wider scientific community. Cookson and co-workers were the first to publish an efficient

synthetic procedure for 4-phenyl-1,2,4-triazoline-3,5-dione starting from hydrazine, diethyl carbonate and phenyl isocyanate in 1971 (Scheme II.3).[27] This procedure includes the generation of ethyl carbazate (**4**), the subsequent reaction with phenyl isocyanate and cyclisation to obtain 4-phenyl urazole – according to Zinner and Deucker – and the final oxidation to the triazolinedione. As this sequence was widely adopted thereafter, it became generally known as the Cookson method,[23] and triazolinediones became regularly referred to as Cookson reagents.[2,28,29]

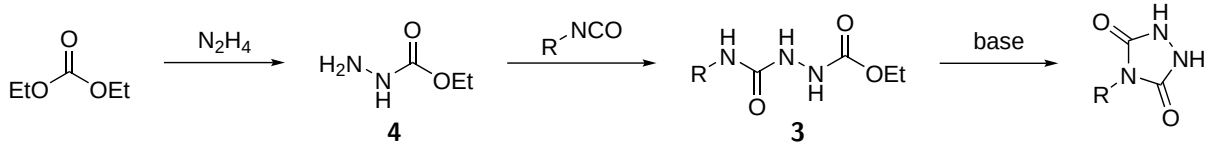

Scheme II.3: Cookson/Zinner-Deucker synthesis of urazoles.

The Cookson method for urazole synthesis (or Zinner-Deucker synthesis) has found many applications, where the main differences are found in synthetic strategies to obtain the semicarbazides (*vide infra*). Thus, these will be discussed in more detail in this section before a final discussion of the semicarbazide cyclisation step itself. Scheme II.4 provides a summary of the alternative semicarbazide syntheses, based on three different strategic bond disconnections. For the purposes of this review, the different semicarbazide syntheses will be discussed according to the class of readily available starting materials that can be used to introduce the R-group on the 4-position: isocyanates, carboxylic acids, or amines. The modification or derivatisation of R-groups on the semicarbazide stage will also be briefly discussed.

It should be noted that in the discussed syntheses, ethyl carbazate can generally be substituted by methyl carbazate, as demonstrated by Bausch *et al.* as well as by Little *et al.*[30,31] The resulting 1-methoxycarbonyl semicarbazides can be processed in the same way as the regular 1-ethoxycarbonyl semicarbazides, so a further distinction between both will not be made.

II.2.1.1 Semicarbazides from isocyanates

As a result of the high reactivity of isocyanates, these readily react at room temperature with ethyl carbazate (**4**) to give the corresponding semicarbazide adducts (Scheme II.3) in excellent yields (up to 100 %), typically after stirring overnight. If the reaction mixture is

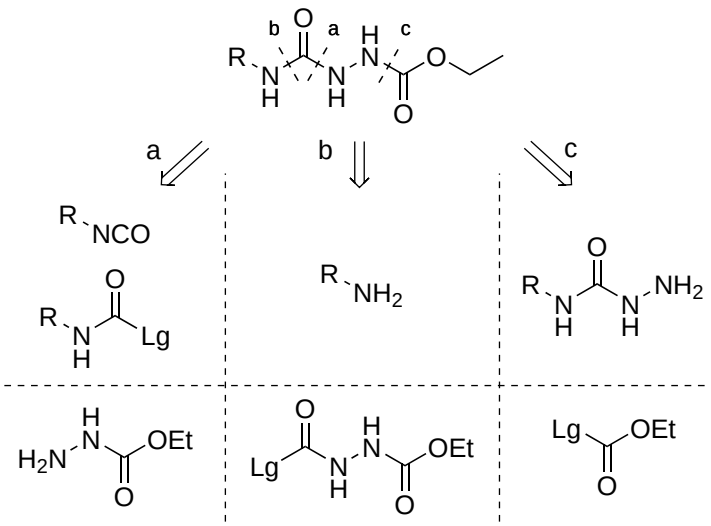

Scheme II.4: Summary of the possible synthetic strategies for the production of 4-substituted 1-(ethoxycarbonyl)semicarbazides with the corresponding starting materials. Lg = leaving group.

heated, complete conversions can be achieved in a matter of hours. The role of the solvent is not critical, but as the semicarbazide products tend to precipitate from hydrophobic solvents such as toluene, the use of such solvents vastly simplifies the workup to the point that after collecting and drying the solids, there is generally no more need for a further purification step.

Although the original Cookson method was mainly used for the synthesis of 4-phenyl semicarbazides (and urazoles) from phenyl isocyanate,[26,27,32,33] the substrate scope was quickly expanded to include a wide range of isocyanates as well. An analysis of the available literature reveals that the structural variations in the obtained semicarbazides are only limited by the availability and reactivity of the isocyanates themselves.[20,34] This means semicarbazides bearing a chemical functionality for further modifications are not easily accessible by this strategy because of the general incompatibility with isocyanates. However, Yamada and Shimizu did report a synthesis of 3-chloropropyl semicarbazide (**5**, Figure II.2),[35,36] in which the alkylchloride can be used as a functional handle to introduce various nucleophilic groups, while Read and Richardson reported on the synthesis of a semicarbazide bearing a carboxybenzyl-protected amine (**6**), which – after deprotection – can be derivatised by various electrophilic groups.[14] On the matter of (industrial) scalability, Chandrasekhar *et al.* prepared nearly 4 kg of 4-phenyl urazole in one batch with an overall yield exceeding 90 %.[37]

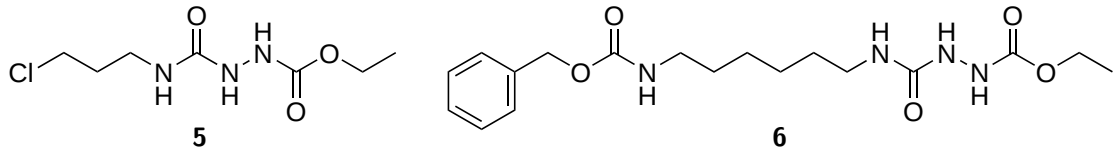

Figure II.2: Examples of semicarbazides bearing a latent functionality. The urazole derived from **6** was modified (section II.2.2.2) prior to oxidation.

The Cookson method can also be used for the preparation of bis-semicarbazides when the corresponding diisocyanate is used. The possibility to convert bulk chemicals used in polyurethane synthesis, such as 4,4′-methylene diphenyl diisocyanate (MDI),[38] into the corresponding bivalent triazolinedione (bisTAD) reagents obviously attracted the interest of polymer chemists. Early reports by Wald and Wamhoff as well as Butler and co-workers triggered the development of a wide range of difunctional semicarbazides (and TAD reagents), as depicted in Figure II.3 (compounds **7** to **14**).[39–43] These bivalent compounds also attracted attention in the patent literature, with reports on the transformation of some of the industrially relevant diisocyanates.[44] Recently, our group synthesised a novel divalent semicarbazide (and bisTAD reagent) based on isophorone diisocyanate (**15**, Figure II.3).[45]

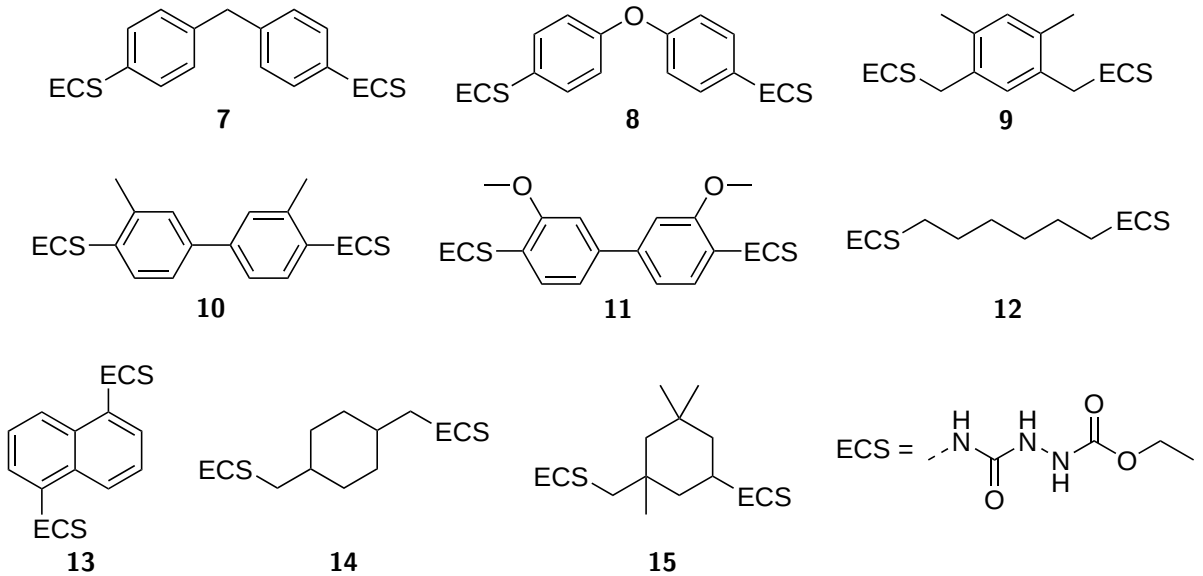

Figure II.3: Reported divalent semicarbazides by combining ethyl carbazate with the corresponding diisocyanate. ECS = (ethoxycarbonyl)semicarbazide.

Finally, a couple of examples are known in literature to prepare the target 1-(ethoxycarbonyl)semicarbazides from the corresponding isocyanates in a sequence where the order of bond forming steps is altered,[26,46] *i.e.* via 4-substituted semicarbazides (Scheme II.5). A first example was already provided by Zinner and Deucker, who reacted 4-phenyl

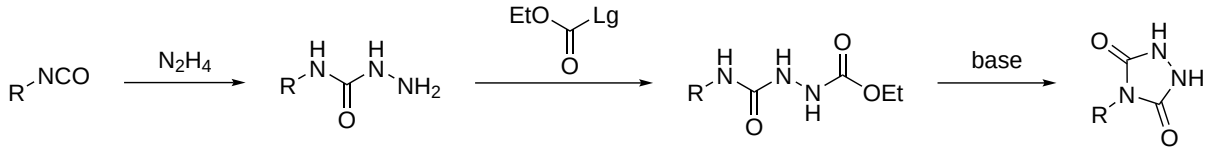

Scheme II.5: Alternative synthesis of 4-substituted urazoles from isocyanates, in which the order of bond forming steps is altered compared to the common Cookson method.

semicarbazide with ethyl chloroformate (Scheme II.5, R = Ph and Lg = Cl) to obtain 1-(ethoxycarbonyl)-4-phenyl semicarbazide.[26] Later, Pesson and Dupin substituted ethyl chloroformate by diethyl carbonate (Lg = OEt) to perform the same reaction.[47] Since the decreased reactivity of diethyl carbonate required harsher (alkaline) reaction conditions, the product is also immediately cyclised to the urazole under these conditions (*vide infra*). However, overall, this strategy is usually less practical with regard to isolation of compounds, generally lower yielding, and, in case ethyl chloroformate is used, is also more costly than the Cookson method.[26,37]

II.2.1.2 Semicarbazides from carboxylic acids

Despite the ease and versatility of the Cookson method, typically accompanied by a high yield of the overall synthesis, the method is limited by the structural variety in commercially available isocyanates (section II.2.1.1). Therefore, a lot of research has been performed to obtain semicarbazides from alternative starting materials. As in fact isocyanate-free synthetic schemes have been developed (*vide infra*), most 'alternative' procedures are actually based on the Cookson method, where an isocyanate is prepared *in situ*, avoiding the isolation or purification of hazardous intermediates. Thus, the Cookson method has been extended to the preparation of semicarbazides from simple carboxylic acids.

A carboxylic acid can easily be converted into an acyl azide, which upon heating will readily rearrange into an isocyanate with the expulsion of nitrogen gas. The well-known Curtius rearrangement is a classical 19th century organic reaction,[55–57] but its first application for the synthesis of urazoles was only reported in 1990.[58] The acyl azide intermediates can be prepared in one step from carboxylic acids using an azidating agent such as diphenyl phosphoryl azide (DPPA, **16**, Scheme II.6), or via an intermediate acid chloride that can be reacted with sodium azide (Scheme II.6, bottom). While acyl azide intermediates can be isolated, the crude product or reaction mixture can be directly used for the Curtius

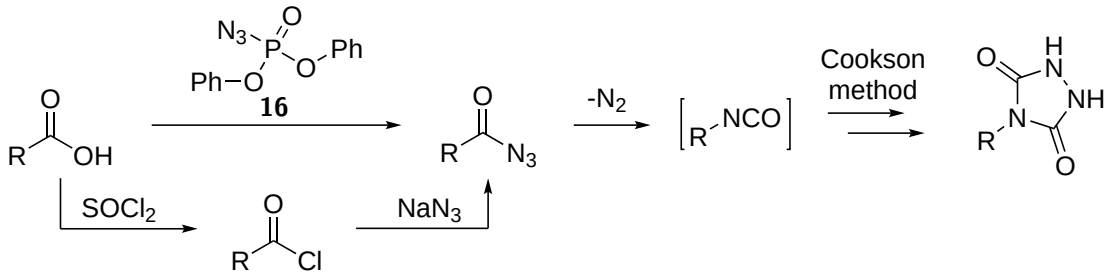

Scheme II.6: Extension to the Cookson method by *in situ* generation of an isocyanate via the Curtius rearrangement of an acyl azide. The latter compound can be obtained in one step using DPPA (**16**) or in two steps via an activated carbonyl derivative such as an acid chloride[28,48–52] or a mixed anhydride (not shown).[53,54]

rearrangement to the corresponding isocyanate. Again, toluene is a favored solvent for this thermal reaction, which demonstrates the compatibility with the Cookson method. Thus, upon completion of the Curtius rearrangement, ethyl carbazate can simply be added to the reaction mixture, upon which the desired semicarbazide will precipitate.

Shimada *et al.* first applied the one-step procedure – using DPPA – to obtain the corresponding acyl azides of a range of interesting fluorescent (**17** and **18**) or chromophoric carboxylic acids (**19**, Figure II.4).[29,58] Likewise, Yamada and co-workers reported the synthesis of a highly fluorogenic semicarbazide, starting from quinoxalinone 2-propionic acid (**20**).[35,59,60] Later, Little *et al.* claimed that this synthetic scheme is also applicable to a wide range of carboxylic acids.[31] The main advantage of using (relatively expensive) DPPA to generate the acyl azide, as compared to the acyl chloride/sodium azide route, is that sequential one-pot reactions are possible that afford the semicarbazide from the corresponding carboxylic acid without the need of any intermediate workup or solvent switch. For instance, Read and Richardson applied such a one-pot procedure to synthesise a pyrene derived with a longer spacer (**21**).[14]

Mallakpour and co-workers developed an efficient three step procedure, using activated carboxylic acids (**22**–**26**, Figure II.4) by first transforming them in an acid chloride or a mixed anhydride with thionyl chloride[28,48–52] or ethyl chloroformate[53,54] respectively. The resulting acyl derivative can then be reacted with sodium azide to obtain the acyl azide in high to excellent yields by a simple precipitation from the reaction mixture (76–96 %). Since the Curtius rearrangement itself is a clean reaction, with only nitrogen gas as a side product, heating a pure acyl azide basically yields the pure isocyanate, which explains why the semicarbazides in this three-step process can be acquired in much higher yields

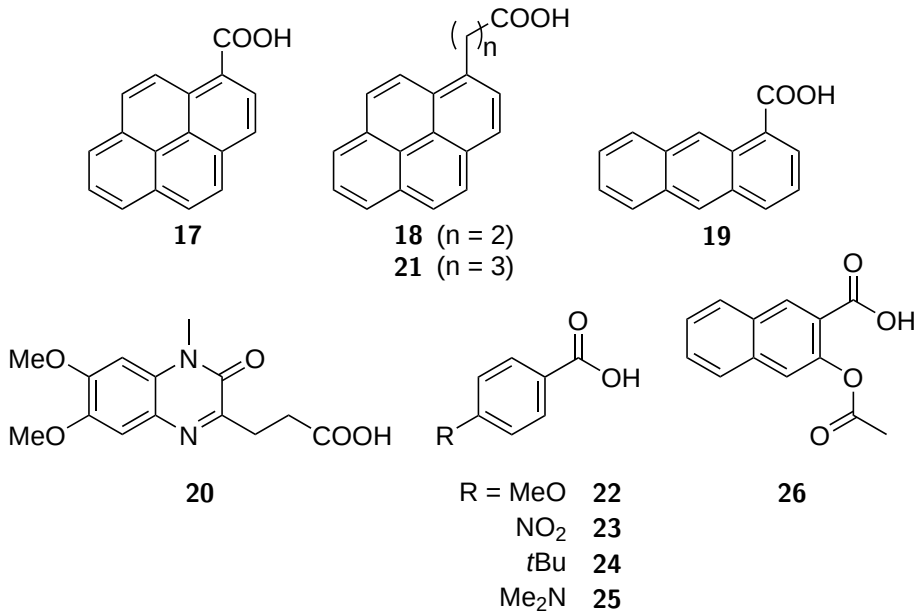

Figure II.4: Carboxylic acids used for the synthesis of semicarbazides by generating an isocyanate *in situ* via the Curtius rearrangement. The acetyl ester is hydrolysed during cyclisation of the semicarbazide derived from **26** (see section II.2.2.1).[51]

than the corresponding one-pot procedure, up to the level of those obtained from pure isocyanates (96–98 %). However, the substrate scope for this acyl azide isolation-based sequence seems limited to benzoic acid derivatives (**22**–**25**), as no examples of aliphatic carboxylic acids have been reported so far. Thus, the strength of this protocol critically relies on the ease of purification of the acyl azide intermediates.

In conclusion, the one-pot procedure to convert carboxylic acids into the corresponding semicarbazides using DPPA not only stands out in operational practicality, but it also has the widest possible substrate scope.

II.2.1.3 Semicarbazides from amines

In analogy with the synthesis of semicarbazides from carboxylic acids using a Curtius rearrangement (section II.2.1.2), isocyanates can be readily obtained *in situ* by combining an amine, or its hydrochloride salt, with phosgene. After removal of gaseous hydrochloric acid, addition of ethyl carbazate to the resulting reaction mixture thus leads to the formation of semicarbazides as demonstrated by Paquette and co-workers for the synthesis of chiral semicarbazides from optically pure amines (**27**–**29**, Figure II.5).[16,17] Later, the use of safer alternatives to the gaseous phosgene were demonstrated as well, *i.e.* trichloromethyl chloroformate (diphosgene)[14] and bis(trichloromethyl) carbonate (triphosgene).[61,62]

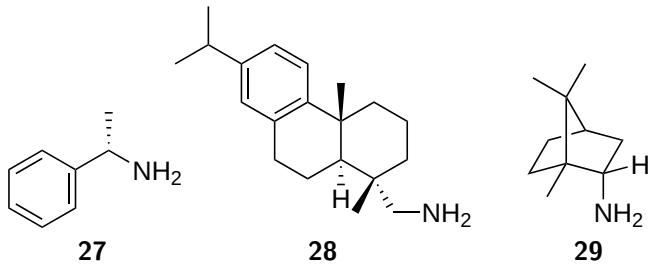

Figure II.5: Treatment of enantiomerically pure amines, *i.e.* (*S*)-(−)-α-methylbenzylamine (**27**), (+)-dehydroabietylamine (**28**) and (+)-endo-bornylamine (**29**), with phosgene and ethyl carbazate (**4**) gave the corresponding semicarbazides in quantitative yield.

The reaction of an amine with (di- or tri-)phosgene results only in the formation of the desired isocyanate and hydrochloric acid. In the absence of acid-sensitive moieties, this gas is easily removed and the isocyanate is obtained in essentially pure form, resulting in high yields of the target semicarbazide.[17] However, as a result of safety issues with regard to the use of isocyanates and especially phosgene, alternative isocyanate-free methods have been developed for the production of semicarbazides from amines, which altogether avoid the use and even intermediate formation of hazardous and less readily available isocyanates (as compared to amines and anilines).[63] Two distinct methods to perform this truly isocyanate-free semicarbazide synthesis can be found in literature (Scheme II.7).

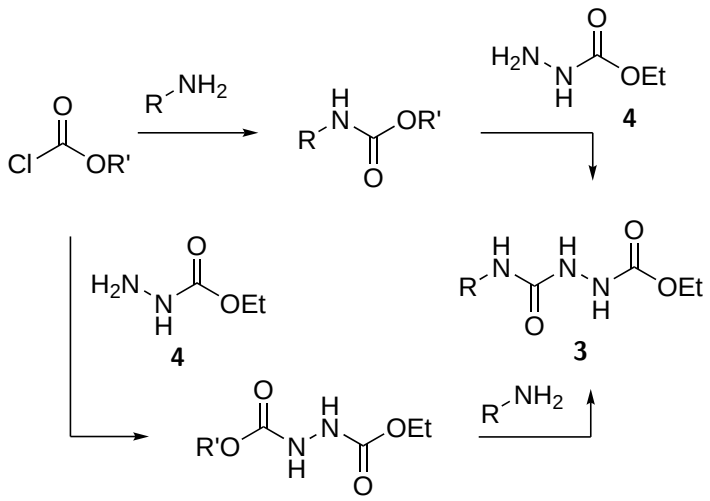

Scheme II.7: Different synthetic strategies to produce a semicarbazide (**3**) in an isocyanate-free manner from amines. R' = *p*−NO_2Ph,[63–65] Ph[23] or Et.[66]

The most straightforward strategy for the isocyanate-free production of semicarbazides closely follows the Cookson method (synthetic strategy *a* in Scheme II.4), wherein activated carbamates are used as synthetic equivalents to isocyanates (Scheme II.7, top). In a first step, the amine is reacted with a chloroformate, resulting in the generation of a

carbamate, which is subsequently reacted with ethyl carbazate to obtain the corresponding semicarbazide. Mallakpour and co-workers, who were the first to develop this synthetic route, reported multiple procedures with different reactive carbamate intermediates. The reactivity of these carbamates towards ethyl carbazate is determined by the chloroformate reagent used in the first step.

The reaction of substituted anilines with *p*-nitrophenyl chloroformate gives a quite reactive carbamate (R' = *p*-nitrophenyl, Scheme II.7).[63] In fact, the intermediate carbamate can be considered as a 'blocked' isocyanate, since *p*-nitrophenol is readily released upon refluxing in toluene, yielding the corresponding isocyanate. Apart from the synthesis of already known semicarbazides, this blocked isocyanate approach appears to be advantageous compared to the Curtius rearrangement for certain substrates, as, for example, 4-(2-nitrophenyl)semicarbazide could not be synthesised from 2-nitrobenzoic acid, while it was obtained from 2-nitroaniline in high yield.[63,66] Nevertheless, the yield of the different semicarbazides varies from 36 % up to 85 % and is therefore highly dependent on the substituents of the aniline. While Mallakpour's original procedure includes isolation of the carbamate, Barbas and co-workers more recently developed a one-pot procedure using an excess of chloroformate and ethyl carbazate, directly giving semicarbazides, with varying success.[67–69] Nevertheless, good to quantitative yields (63–100 %) were achieved for very interesting "clickable" semicarbazide products with a pending azide (**30**–**32**) or alkyne moiety (**33**, Figure II.6).[64,67,69–71] Lower yields resulted when 4-ethynylaniline or 4-aminoacetophenone were used as starting compounds.[64,68,69]

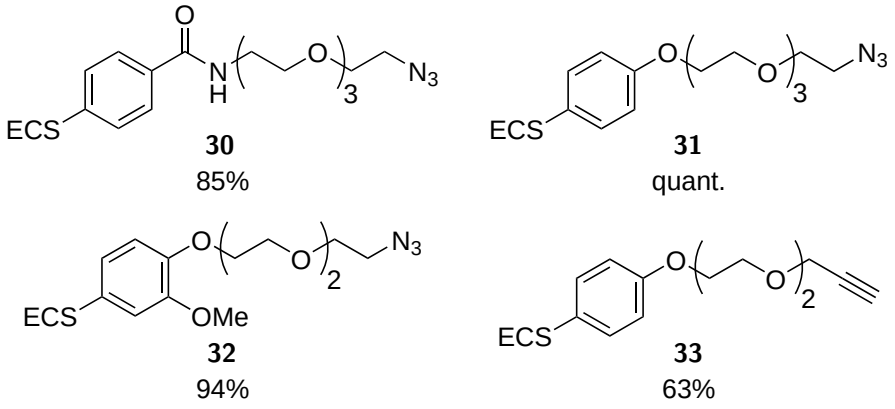

Figure II.6: Semicarbazides with a pending azide or alkyne moiety obtained in good yields via the corresponding *p*-nitrophenyl carbamate.[64,67,70,71] The urazole derived from **31** was modified (sections II.2.2.2 and II.2.2.5) prior to oxidation. ECS = (ethoxycarbonyl)semicarbazide.

The use of ethyl chloroformate, and subsequent transformation of the less reactive ethyl carbamates (R' = Et, Scheme II.7) derived from substituted anilines, was also studied by Mallakpour and Rafiee.[66] Based on this less reactive carbamate intermediate, a successful one-pot procedure was developed starting from anilines that can also give the urazole compound directly by a spontaneous *in situ* cyclisation reaction (section II.2.1.5), without intermediate purification and using mild reaction conditions. The yields of the isolated urazoles are very similar compared to the analogous *p*-nitrophenyl chloroformate protocol (*vide supra*), but the overall process is clearly more efficient, cheaper and less hazardous. Possible substrates include nitroaniline isomers, *p*-chloroaniline and *p*-toluidine.

An alternative strategy to obtain semicarbazides in an isocyanate-free manner from the corresponding amines encompasses the synthesis of a reactive intermediate out of ethyl carbazate to which the amine is added (Scheme II.7, bottom). A first example of such a reactive intermediate is reported by Breton and Turlington who used phenyl chloroformate to obtain ethyl phenyl hydrazine-1,2-dicarboxylate (R' = Ph).[23] This reactive hydrazine dicarboxylate can be used to transform aliphatic amines under very mild conditions with a high yield (76–93 %). Nevertheless, no reaction was observed when aniline was used, even at elevated temperatures, which is explained by its decreased nucleophilicity compared to the alkyl amines. In a similar synthesis, Adamo and co-workers used *p*-nitrophenyl chloroformate (R' = $p-NO_2Ph$) to obtain a more reactive ethyl carbazate derivative, which was subsequently reacted *in situ* with a range of structurally diverse aliphatic amines (Figure II.7) to obtain the corresponding semicarbazide in acceptable yields (54–71 %).[64,65] Both protocols use an excess of amine and therefore require a purification step in which the produced semicarbazide is separated from the unreacted amine.

Little *et al.* introduced the use of carbonyldiimidazole to transform a carbazate in the corresponding activated carbonyl compound (Scheme II.7, bottom).[31] The resulting intermediate is sufficiently reactive to transform both aliphatic amines and anilines. This synthetic scheme can also be applied for the synthesis of semicarbazides with azide and alkyne residues as well.[68,69] Similarly, phosgene can also be used to generate the reactive 2-(ethoxycarbonyl)hydrazinecarbonyl chloride from ethyl carbazate (OR' = Cl, Scheme II.7, bottom). While this reactive intermediate is very sensitive to water, it can be purified and isolated as a white, crystalline solid.[72,73] It readily reacts with both aliphatic amines and

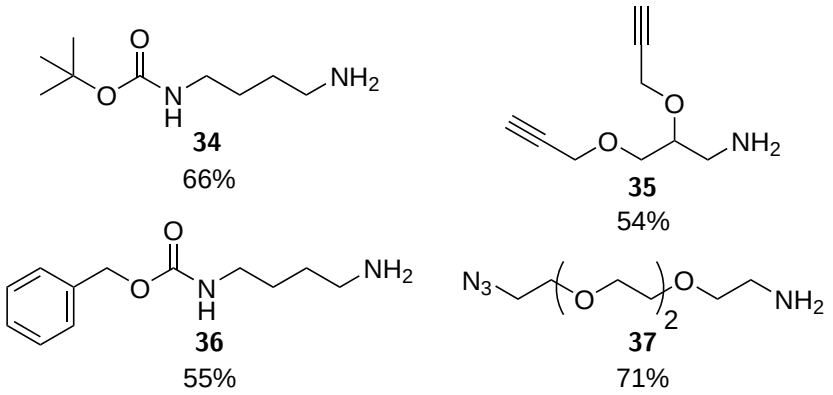

Figure II.7: Overview of the aliphatic amines that are successfully reacted with a reactive hydrazine dicarboxylate to produce the corresponding semicarbazide:[64,65] *N*-Boc-1,4-butanediamine (**34**), bis(prop-2-ynyloxy)propan-1-amine (**35**), *N*-Cbz-1,4-butandiamine (**36**) and 11-azido-3,6,9-trioxaundecan-1-amine (**37**). The urazole derived from **36** was modified (section II.2.2.2) prior to oxidation.

fluorinated anilines,[74–76] however, since phosgene is required to produce this intermediate, this procedure is much more hazardous than other 'isocyanate-free' protocols, while phosgene-mediated isocyanate-based routes tend to be higher yielding (*vide supra*).

II.2.1.4 Modification of semicarbazides

The synthesis of semicarbazides (*vide supra*) does not tolerate too many chemical functionalities, so that functional urazoles and TAD reagents are more challenging synthetic targets. One way around this problem is the chemoselective modification of semicarbazide or urazole intermediates. While plenty of methods are available to modify urazoles (section II.2.2), only a few modifications on the semicarbazide intermediates have been reported. For instance Yamada and Shimizu reacted 3-chloropropyl semicarbazide (**5**) with sodium azide to produce the corresponding azide-bearing semicarbazide **38** (Scheme II.8a) with a yield of 95 %.[35] Mallakpour and Nasr-Isfahani reported the efficient reduction of 4-(4-nitrophenyl) semicarbazide (**39**, Scheme II.8b) to the corresponding amine (**40**) using tin (II) chloride as a reductant, thus providing a reliable synthetic handle for further transformations using electrophilic reagents (*e.g.* amide bond formation).[49]

II.2.1.5 Cyclisation

Most semicarbazides discussed above can be readily cyclised to the corresponding urazole. Thus, only a limited amount of protocols can be found throughout all reported syntheses. A clear rationale to why a certain method should be preferred over another one is rarely

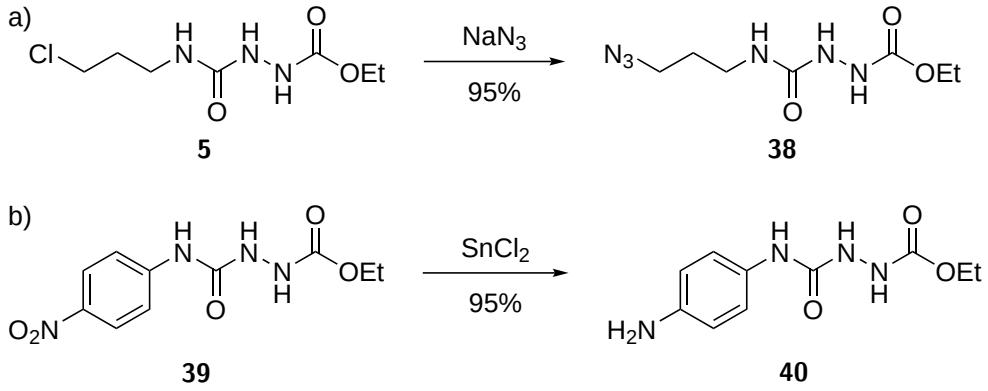

Scheme II.8: Examples of semicarbazide modification by either **(a)** an S_N2 substitution[35] or **(b)** a reduction.[49]

provided. In general, however, the cyclisation of a semicarbazide is achieved using mildly basic conditions in a protic solvent.[17,26,32,75,77]

The original Cookson method reports a simple treatment of the semicarbazide with an aqueous potassium hydroxide solution at reflux temperature to effect cyclisation of the semicarbazide to the urazole. When the cyclisation is completed, as a result of the acidity of the formed urazole,[8,30] the urazole is obtained as a water-soluble potassium salt (solvated urazolyl anion), which, upon acidification of the solution to pH $\approx$ 1–2, precipitates from the aqueous medium as a neutral compound.

While Cookson's method for urazole synthesis is very practical, and the cyclisation is typically finished in 2–3 hours, with a nearly quantitative yield, the reaction conditions can lead to obvious side reactions. Hydrolysis of the hydrazine carboxylate itself, followed by decarboxylation (Scheme II.9a), is usually not a problem, except when the R-group is extremely electron withdrawing and/or severely sterically encumbering.[13,31] Hydroxide-mediated hydrolysis is more likely to occur in the R-groups, as was noticed by Gilbertson and Ryan, in the partial displacement of the 4′-fluorine atom when these reaction conditions were used to cyclise 1-ethoxycarbonyl-4-(pentafluorophenyl) semicarbazide (**41**, Scheme II.9b).[75] Nevertheless, despite these possible (but predictable) side reactions, this cyclisation is often the method of choice for urazoles that easily crystallise from the acidic aqueous solution, in particular those with an aromatic 4-substituent.[78]

A somewhat milder alternative to an aqueous potassium hydroxide solution involves sodium ethoxide in refluxing ethanol. This widely adopted method also allows the isolation of urazoles in high yields, but longer reaction times of up to 24 hours have to be taken

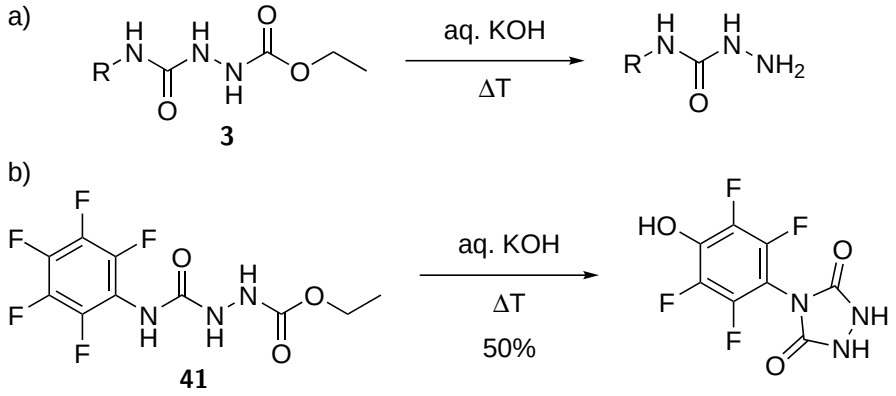

Scheme II.9: Two examples of possible side reactions during the cyclisation of semicarbazides in a refluxing aqueous potassium hydroxide solution. **(a)** hydrolysis of an ethoxycarbonyl semicarbazide (**3**), followed by decarboxylation results in the corresponding semicarbazide[31] while **(b)** the base might participate in nucleophilic substitution reactions.[75]

into account. Often, these reaction conditions represent the best choice if the substituent on the urazole, such as an aliphatic residue, prevents it from precipitating from an acidified aqueous solution.[31,78] This is mainly because this procedure is compatible with a non-aqueous work-up to isolate certain urazoles as an oil.

Potassium carbonate can also be used as a base, rather than the much stronger ones applied in the previous systems. As a result of these milder conditions, higher yields can be obtained with some problematic substrates although longer reaction times are necessary.[74,75] This protocol can be used in both water as well as in alcoholic solvents.[31,59,75] The elegant one-pot urazole synthesis by Mallakpour *et al.* (*vide supra*) uses triethylamine to mediate the cyclisation of semicarbazides in acetone as solvent.[66]

Finally, semicarbazides can also be cyclised under neutral but high temperature (pyrolysis) conditions. Similarly to Thiele-type procedures based on hydrazodicarboxamide intermediates,[4] heating the neat semicarbazide to 200–250 °C produces the corresponding urazole in good yields (65–75 %).[17,79,80] In general, such pyrolysis conditions are only applied on the rare occasion that a semicarbazide is resistant to either of the conventional base-mediated cyclisations[17] or if a concurrent urazole modification is desired (section II.2.2).[80]

To the best of our knowledge, the mechanism of the cyclisation of semicarbazides has not been extensively studied or considered in much detail. For this, we would like to propose herein two possible mechanisms, which are both consistent with experimental observations and account for the rate enhancing effects of added base (Scheme II.10).[62,81]

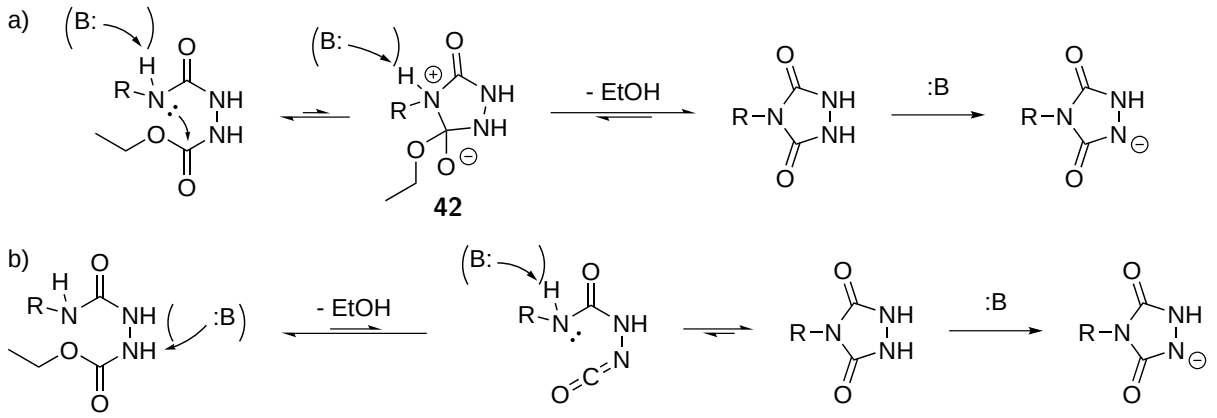

Scheme II.10: Two plausible mechanisms for the cyclisation of semicarbazides, consistent with the experimental observations. The elimination of ethanol can occur either **(a)** after or **(b)** prior to the intramolecular addition of the 4-semicarbazide nitrogen to the 1-semicarbazide carbonyl.

The first mechanism, shown in Scheme II.10a, is based on the proposal by Ghorbani-Choghamarani *et al.*,[62] and consists of the intramolecular addition of the 4-semicarbazide nitrogen to the 1-semicarbazide carbonyl with the formation of a charged intermediate (**42**). Consequent elimination of ethanol yields the corresponding urazole. Since both the addition and the elimination are reversible processes, the equilibrium can be shifted to the urazole by physical removal of the produced ethanol, *cf.* pyrolysis conditions. The presence of a base can increase the efficiency of the reaction at different stages. First, it can assist the addition step by proton abstraction, either before or after formation of the charged intermediate. Next, the elimination step can also be assisted by an alkaline environment since this will result in an increased population of the charged alkoxide intermediate **42** compared to the corresponding protonated species. Finally, as a result of the relatively low pK_a value (~ 5) of the urazole protons,[8,30] the product will be deprotonated by the base, which results in an irreversible step in the mechanism.

An alternative mechanism is shown in Scheme II.10b and is very similar to the first proposal. However, in this case, ethanol is eliminated first with the formation of a neutral isocyanate-type intermediate, after which the urazole is formed as a result of an intramolecular addition. The existence of a similar transient isocyanate has been demonstrated earlier by pyrolysis of a hydrazinecarbonyl chloride in toluene with the elimination of hydrochloric acid.[72]

The cyclisation step in the fragmentation-addition mechanism shown in Scheme II.10b is favored over the acylation-type cyclisation step on stereoelectronic grounds when the

tendency for side reactions as a function of the utilised base is taken into account. At this time, we find no evidence to favor one pathway over the other, but a systematic investigation of different N-alkylated semicarbazides might lead to further insight into this matter.

II.2.2 Urazole modification

Despite the fact that the aforementioned synthetic procedures can already accommodate a large structural variety in the synthesised urazoles, these syntheses are often not compatible with a lot of sensitive chemical functionalities. When desired, these functionalities should thus be introduced in a post-cyclisation step in which either a latent functionality is transformed or a protecting group is removed (*cf.* semicarbazide modifications in section II.2.1.4). From a strategic point of view, having a 'reactive' urazole for the introduction of more elaborate 4-substituents, avoids the cumbersome optimisations that are often required to obtain an efficient urazole synthesis.

In principle, unsubstituted urazole **43** can be transformed into various 4-substituted urazoles through a chemoselective reaction that can discriminate between the nucleophilic 4- and 1- (or 2-) nitrogen sites (Scheme II.11a). In literature, however, to the best of our knowledge, only one such reaction has been reported, using methylolamines at neutral or slightly alkaline pH (Scheme II.11b).[82,83] While this strategy has apparently been successfully applied for the synthesis of multivalent urazoles in patent literature, no further examples could be found. Moreover, systematic studies by Arndt *et al.* on the regioselectivity of reactions of urazoles,[22] seem to contradict the reported regioselectivity in this aminal-forming reaction. Taking into account that the hydrazide NH-moieties are not only more nucleophilic but also much more acidic ($pK_a \approx 5$) than the imide NH ($pK_a \approx 7.5$),[30] we propose that the aminal formation with urazole **43** actually gives a mixture of 1- and 4-substituted regioisomers. Thus, urazole **43** cannot be used as a

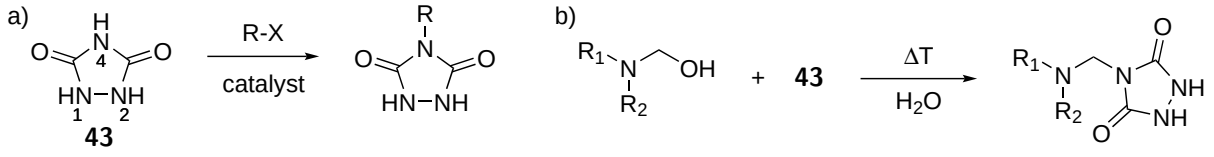

Scheme II.11: Modification of unsubstituted urazole (**43**). **(a)** General scheme for the chemoselective reaction of the nucleophilic 4-nitrogen site and **(b)** an example of such a modification in which methylolamine acts as the electrophile.[82,83]

starting material to efficiently prepare 4-substituted urazoles (and the corresponding TAD reagents).

In the remainder of this section, an overview of the chemical transformations of 4-substituted urazoles is provided, together with various urazole building blocks that can be orthogonally functionalised. Examples have been selected to offer the reader some broad synthetic considerations and insights in reaction conditions that are compatible with urazole moieties, and allow a chemoselective modification of the urazole substrates.

II.2.2.1 Modification during semicarbazide cyclisation

Under the standard semicarbazide cyclisation conditions, it can be possible to concomitantly transform other functional groups in certain urazole substrates, which can release a useful synthetic handle. For example, ester hydrolysis readily occurs in aqueous base conditions, giving a urazole with a carboxylic acid functionality (**45**, R = H, Scheme II.12a) starting from ester-functionalised semicarbazides (**44**).[84,85] The same cyclisation in ethanol or methanol as solvent, gives a transesterification of the alcohol part (R = Me).[85,86] More interestingly, urazoles with hydroxyl functions can be obtained in the same way from ester hydrolysis where the semicarbazide is part of the alcohol moiety.[51] Burgert and Stadler developed a purely thermal cyclisation protocol in which volatile ethoxytrimethylsilane is released from semicarbazide **46** (Scheme II.12b) to give 4-hydroxyphenyl urazole (**47**).[80]

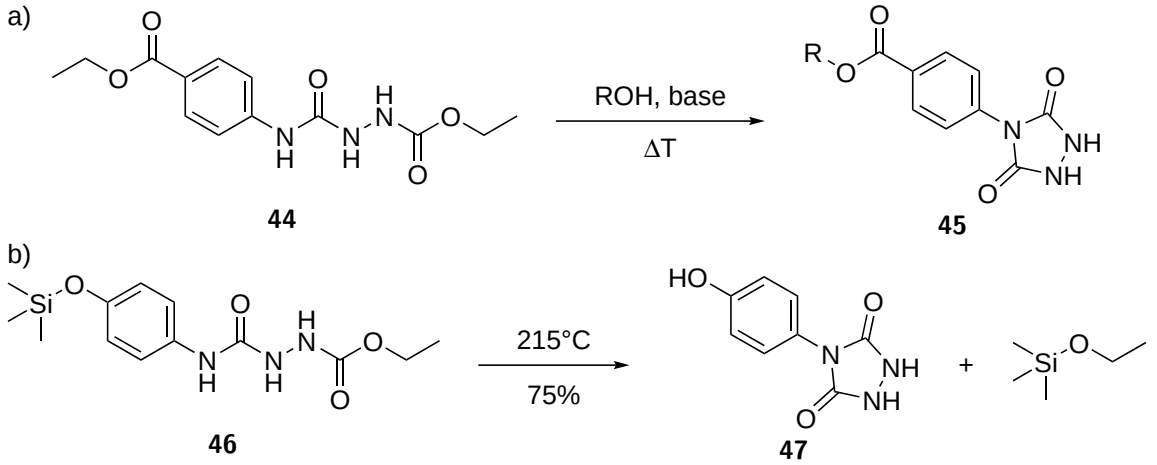

Scheme II.12: Chemical modification of a functional group during the cyclisation of the semicarbazide. **(a)** Depending on the solvent, either transesterification or hydrolysis can occur, yielding urazole **45** with R = Et (94 %),[85] Me (91 %)[86] or H (78–95 %).[84,85] **(b)** Trimethylsilylethers were demonstrated to cleave during a purely thermal cyclisation protocol.[80]

II.2.2.2 Urazole substrates in hydrogenation or hydride addition reactions

Urazole moieties seem to be highly resistant to reductive conditions such as catalytic hydrogenations, opening up a number of strategies to introduce new functionalities. For example, the interesting 4-(4-aminophenyl) urazole (**49**) is readily obtained by hydrogenation of the nitro-group in **48** using Adams' catalyst (PtO_2)[35] or palladium on carbon (Pd/C, Scheme II.13a).[86,87] Alkene hydrogenations in urazole substrates using PtO_2 have also been reported.[88] Aliphatic amines can be generated from the corresponding azides via simple hydrogenation using either palladium[35] or palladium (II) hydroxide[67,70] catalysts (Scheme II.13b), the latter of which is reported to give the best yields. A carboxybenzyl (Cbz) group is also readily removed by a catalytic (Pd/C) hydrogenation in urazoles with a Cbz-protected amine (*cf.* urazole derived from **36**, Figure II.7).[14,64] These deprotections are helped by adding formic acid to the reaction mixture, thereby generating the formate salts rather than the free amines.[14]

Urazoles are also stable towards hydride reductions, as demonstrated by the transformation

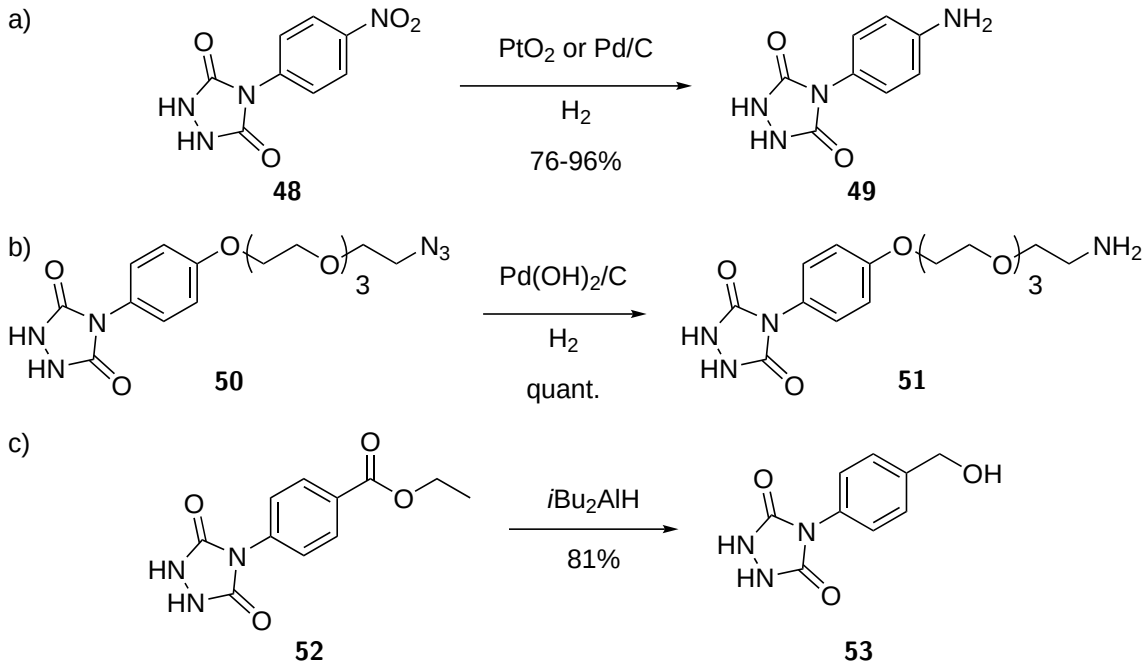

Scheme II.13: Examples of reductive urazole modifications. Amines can be obtained by a catalytic hydrogenation of **(a)** a nitro-group or **(b)** an azide. **(c)** Selective hydride reduction of the ester in urazole **52** is possible as well. Due to reactivity reasons (section II.3), only the hydrochloride salt of 4-(4-aminophenyl) urazole (**49**) can be oxidised to the corresponding triazolinedione.[89,90] To the best of our knowledge, products **51** and **53** were never oxidised, but are further modified using electrophilic reagents (section II.2.2.3).

of the ester group in urazole **52** (Scheme II.13c) to the corresponding benzylic alcohol (**53**), using an excess of diisobutylaluminium hydride (DiBAl−H), as reported by Yamada and co-workers.[35,59]

II.2.2.3 Derivatisation of amino-, hydroxy- and (activated) carboxy-urazoles

Reactive chemical functionalities such as amines, hydroxyls and (activated) carboxylic acids are incompatible with standard urazoles syntheses, but can be introduced on urazole substrates in a number of straightforward ways (sections II.2.2.1 and II.2.2.2). Thus, these reactive moieties can be used as synthetic handles for further derivatisation of urazoles.

The use of 4-(4-aminophenyl) urazole (**49**) as a versatile intermediate to prepare a range of functional TAD reagents has been extensively explored (Scheme II.14). Reaction with trimellitic anhydride gives the corresponding imide (**54**, Scheme II.14, left).[91] In a fully analogous reaction, the aniline is transformed in imides with a 1,8-naphthalimidophenyl (**55**),[92,93] phthalimidophenyl (**56**)[94,95] or tetrabromophthalimidophenyl (**57**)[96] substituent by using the appropriate anhydride. These reactions all occur in a mildly acidic environment at elevated temperatures and provide the products in good yields (76-98 %). Rather than using maleic anhydride, Bauer *et al.* used *N*-methoxycarbonyl maleimide to transform the aliphatic amine of urazole compounds **58** and **59** (Scheme II.15) into a maleimide (not shown).[64,70] Good yields of 70-85 % were obtained.

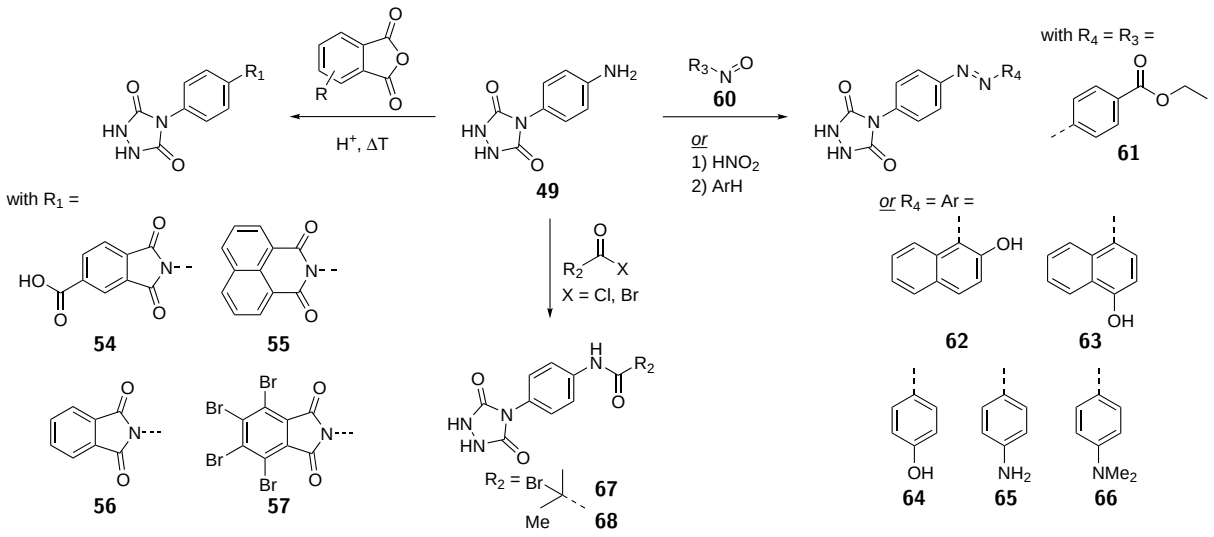

Scheme II.14: Reactions of 4-(4-aminophenyl) urazole (**49**). Except for urazoles **61** and **67**, none of the given compounds were oxidised to their corresponding triazolinediones.

Starting from 4-(4-aminophenyl) urazole, azo compounds can also be readily obtained. Reaction of aniline **49** with nitrosobenzene derivative **60**, for example, produces azo compound **61** (Scheme II.14, right).[86] An alternative route towards azo dyes comprises of the diazotisation of the same aniline using sodium nitrite in acidic medium.[49] Subsequent reaction of the diazonium salt with an electron-rich aromatic compound, either in acidic or basic media, yields the corresponding azo dye (**62**–**66**) in varying yields (66–97 %).

Recently, our group reported a simple procedure using pyridine as a mildly basic solvent to couple amino-urazole **49** with a functional acid bromide, giving a robust amide derivative (**67**, Scheme II.14, bottom).[87,97] In fact, the amide is an initiator for copper-mediated polymerisations with a urazole moiety and was used for this exact purpose. An acylation with acetyl chloride has also been achieved in neutral dimethyl acetamide (**68**).[98]

The use of hydroxyl functions in urazole substrates has been considerably less explored, and also seems more problematic. A good illustration can be found in the work of Shimizu *et al.* towards the synthesis of fluorescent TAD reagents, wherein urazole **53** (Scheme II.13) was reacted with an acid chloride.[35,59] However, this straightforward esterification proved to be rather difficult with problems pointing towards the typical basic reaction conditions used for such reactions. In fact, in the presence of a base, the acidic urazole ($pK_a \approx 5$) is readily deprotonated,[30] which will give an anion that can compete with the hydroxyl function as a nucleophile. Shimizu *et al.* solved this problem by running the reaction under acidic conditions in the absence of base at elevated temperatures. Read and Richardson reported similar issues when they tried to couple 4-(6-aminohexyl) urazole with dansyl chloride, where competitive urazole acylation led to low yields (25 %).[14] However, in the amide bond forming conditions using the much less basic pyridine with amino-urazole **49** (*vide supra*), the urazole acylation does not seem to be problematic.

Based on the above observations, it can be concluded that acylation reactions on urazoles should preferably not be performed in the presence of an excess of strong bases ($pK_a > 5$) as this will likely lead to competitive urazole acylations.

Activated carboxylic acid intermediates such as *N*-hydroxysuccinimide (NHS) esters have also been successfully coupled with amino-functional urazoles. These activated esters are reported to selectively react with the amines and do not give urazole acylation, even in the

presence of a catalytic or equimolar amount of base (triethylamine or diisopropylethylamine (DIPEA)). Barbas and co-workers prepared two rhodamine-bearing urazoles by reacting NHS-activated carboxy-X-rhodamine (**69**) with the amine **51** or **58** (Scheme II.15a). However, yields are not reported.[67,69] Similarly, Adamo *et al.* reported on the successful reaction of 4-(4-aminobutyl) urazole with an NHS ester of poly(ethylene glycol) in 82 % yield.[64] Modern amide coupling reagents have also been used to derivatise amino-functional urazoles. Bauer *et al.* demonstrated the use of HATU in the presence of DIPEA to attach 1-fluorocyclooct-2-ynecarboxylic acid (**70**) to a urazole with an amine functionality (**59**) in 51 % yield (Scheme II.15b).[70] In general, however, these coupling reagents are not always preferred because of the difficult removal of waste products from the urazole compound and the risk for urazole acylation in the presence of an excess of base.

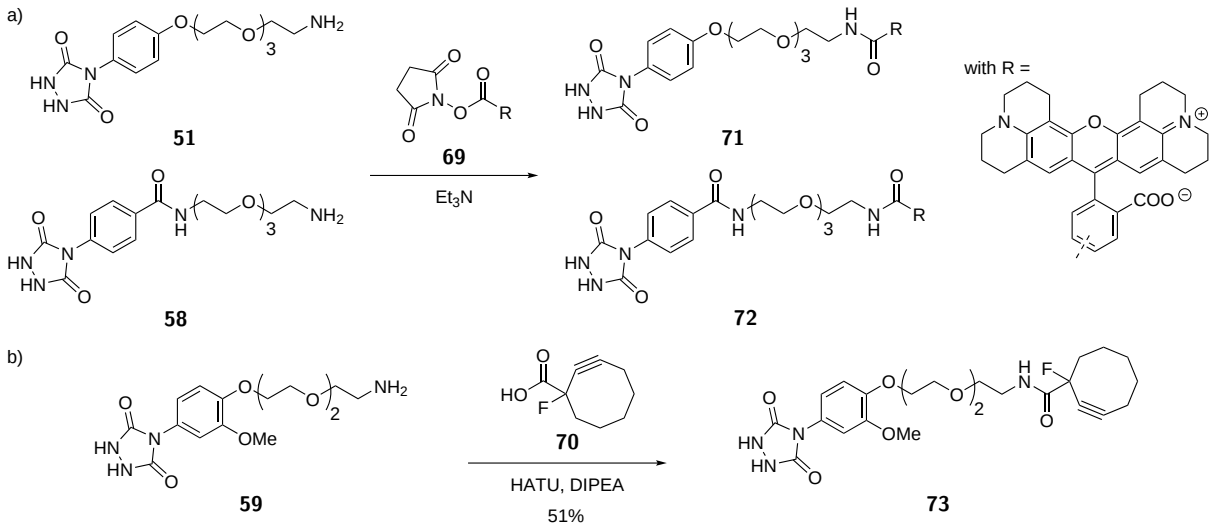

Scheme II.15: Examples of modifications on urazoles with an aliphatic amine using **(a)** an NHS-activated carboxy-X-rhodamine (**69**) or **(b)** a combination of 1-fluorocyclooct-2-ynecarboxylic acid (**70**) and HATU as coupling reagent.

The use of carboxylic acid derivatives as synthetic handles in urazoles has been very limited. This is likely because urazoles are expected to interfere with most reactions of carboxylic acids (as they are similar in acidity). Apart from the transesterification and hydrolysis examples shown in section II.2.2.1, Seidel *et al.* have demonstrated the aminolysis of methyl ester **45** (Scheme II.12, R = Me) with aqueous ammonia, resulting in 4-(4-urazolyl)benzamide.[86] While this reaction readily occurs at room temperature with an excellent yield (91 %) in a matter of hours, it is reported to fail when other 4-(4-urazolyl)benzoic acid derivatives (**45**) are used.[86] Ketones have also been used to functionalise urazoles with limited success. Adamo *et al.* reacted 4-(4-acetylphenyl)

urazole with O-benzylhydroxylamine and O-(prop-2-ynyl)hydroxylamine to obtain the corresponding Schiff base in very low yields (7–23 %).[64] Dey and Purkayashtha obtained yields up to 65 % for a similar derivatisation.[99] In conclusion, carboxyl- and carbonyl-type substrates seem less promising for the straightforward modification of urazoles.

II.2.2.4 Electrophilic aromatic substitution

In the case of PhTAD, the aromatic ring is electronically activated towards electrophilic aromatic substitutions. Indeed, Keana *et al.* reported the synthesis of water soluble TAD reagents by reacting 4-aryl urazoles (**74**, Scheme II.16) with chlorosulfuric acid at elevated temperatures.[100] The obtained sulfonyl chloride **75** could be isolated and subsequently hydrolysed in water to yield the corresponding sulfonic acid (**76**). The sulfonyl chloride **75** could also be immobilised on aminopropylsilylated silica gel via a sulfonamide link (**77**).

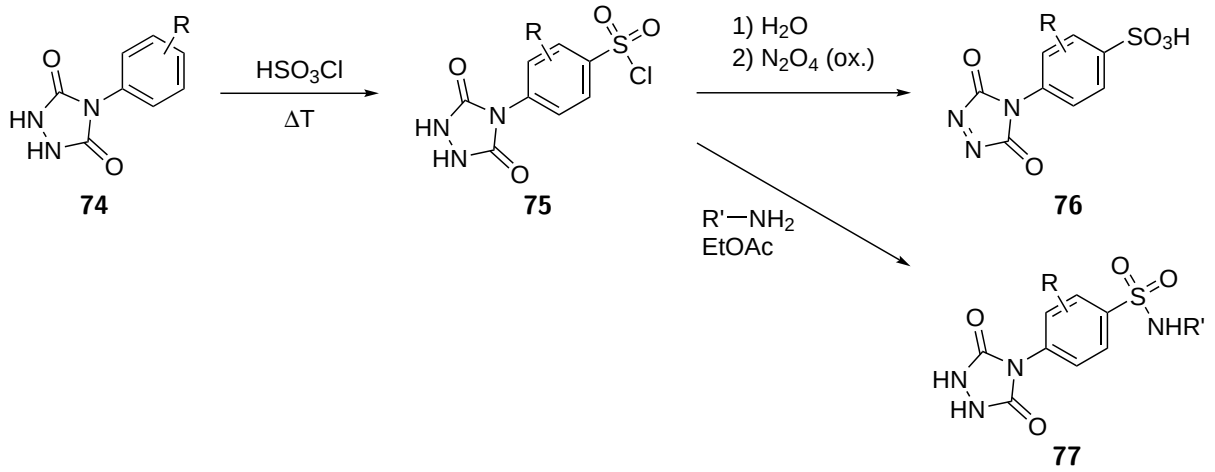

Scheme II.16: Sulfonation of 4-aryl urazoles allows the synthesis of water soluble TAD reagents and the immobilisation of triazolinediones on silica gel.[100]

II.2.2.5 'Click' modification of urazoles

By definition, click reactions are the most reliable methods to introduce covalent links between two moieties. For this, Barbas and co-workers developed azide containing urazoles, using different synthetic approaches (section II.2.1.3). These azido-urazoles were successfully reacted with an alkyne in a copper catalysed Huisgen 1,3-dipolar cycloaddition. Using this strategy, urazoles bearing a cyclic RGD peptide,[67,69] a poly(ethylene glycol) chain[68] or aplaviroc,[68] *i.e.* a HIV entry inhibitor, were obtained in moderate to high yields (52–95 %). Thus, the azido-urazole compounds are probably the most versatile synthetic intermediates

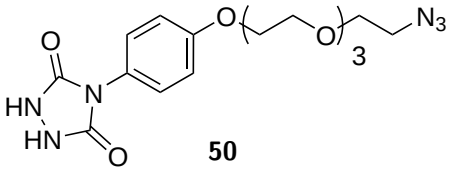

50

Figure II.8: Urazole derived from semicarbazide **31** (Figure II.6).

for functional TAD synthesis, although their synthesis is quite long and expensive (*e.g.* 11 % overall yield over 8 steps[69,101] from commercial materials for **50**, Figure II.8), thereby prohibiting large-scale applications.

II.2.3 Oxidation of 4-substituted urazoles to their corresponding 1,2,4-triazoline-3,5-diones

The first oxidation was serendipitously observed by Thiele when he sought to dissolve a silver salt of an unsubstituted 4*H*-urazole in concentrated nitric acid, a common solvent for heavy metals and their salt derivatives.[4] However, instead of just observing a fast dissolution process, a bright red colour also appeared, which was attributed to the formation of an azodicarbonamide oxidation product. Nevertheless, pure triazolinediones could not be obtained, and their modes of reactivity could not be studied, before Cookson's seminal work in the 1960s. Until today, all practical methods to synthesise TAD reagents proceed via a final oxidation step of a urazole precursor.

While the oxidation of urazoles is a straightforward reaction, it can sometimes be a bottleneck of triazolinedione synthesis. Although urazoles are in fact readily oxidised by most oxidants, these reactions are hard to perform because of two interrelated issues, *i.e.* the chemoselectivity of the oxidant and the reactivity of the resulting TAD compounds. Especially isolation of TAD reagents from reaction mixtures can be challenging. Ideal oxidation methods should thus be highly chemoselective, give one single triazolinedione reaction product, and generate no waste products or only waste products that are readily removed. Both the oxidant and its reduced forms should not react with the TAD compound. Unfortunately, there are no generally successful approaches, and developing a successful protocol is often a question of trial and error, balancing the kinetics of several processes. For some applications, an '*in situ*' oxidation method is preferred, which avoids the isolation problem, but usually exacerbates the chemoselectivity problem. Because of these reasons,

a myriad of oxidation procedures was presented over the years. Nonetheless, today, only a few oxidants are still commonly applied for the synthesis of triazolinediones. Therefore, only the most important methods are described in this section, while a more complete overview is provided in our review on TAD chemistry.[20]

Stickler and Pirkle[32] developed a straightforward protocol for the oxidation of urazoles by making use of gaseous dinitrogen tetroxide (N_2O_4), which is known to be in equilibrium with nitrogen dioxide ($NO_{2(g)}$, Scheme II.17).[102,103] The use of dinitrogen tetroxide, which is a liquid below 20 °C, can convert urazoles to their corresponding triazolinediones in an almost traceless manner, as the gaseous oxidant can be used in excess without compromising the straightforward isolation procedure. The residues obtained from simple evaporation of the reaction mixture thus contain little contaminants and pure, bench stable TAD reagents can be obtained by a twofold sublimation of the residue. The toxic gas N_2O_4 can be handled in liquid form, but a solution of this gas in an inert solvent can also be employed to achieve less hazardous handling procedures.[14,100,104] This reaction can also be performed in more polar solvents such as ethyl acetate, which broadens the scope of the classical nitric acid procedure considerably, which is typically limited to (hydrophobic) chloroform- or dichloromethane soluble TAD reagents.[85]

Although the N_2O_4/NO_2-method seems to be widely applicable to many urazole substrates, some electron rich aryl groups tend to give competitive electrophilic aromatic nitration reactions, as evidenced during the attempted oxidation of 4-(4-hydroxyphenyl) urazole (Scheme II.18).[80] Nevertheless, the N_2O_4-based oxidation is still one of the most effective and reliable methods to obtain TAD reagents of a high analytical quality since the volatiles are readily removed, while interference of the formed water can greatly be excluded by the simple addition of an appropriate desiccant, such as anhydrous $NaSO_4$.[32,104]

Besides gaseous dinitrogen tetroxide (N_2O_4), a second major chemical class of oxidants

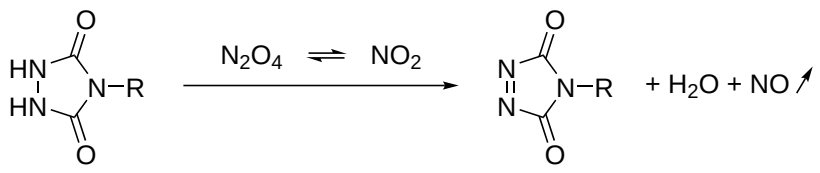

Scheme II.17: General oxidation scheme of nitrogen (IV) and nitrogen (V) oxides, affecting the conversion of urazoles towards their triazolinedione counterparts.

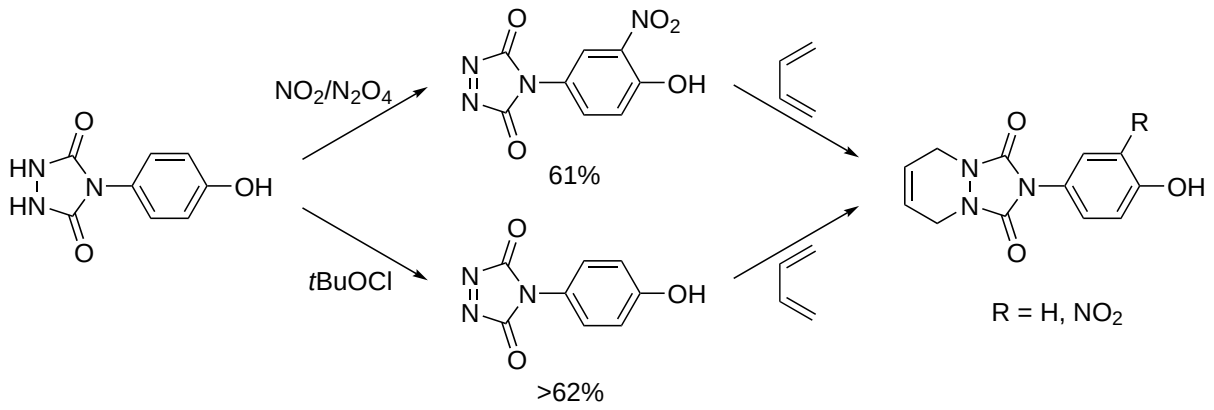

Scheme II.18: Oxidation of 4-(4-hydroxyphenyl) urazole, illustrating the advantageous use of *t*-BuOCl over electrophilic oxidants for electron rich aromatic substrates.[80]

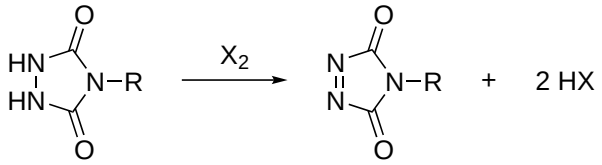

Scheme II.19: General representation of a halogen-mediated urazole oxidation.

used to convert urazoles into triazolinediones comprises halogens and their derivatives (Scheme II.19). However, elemental chlorine and bromine often give low yields for urazole oxidations, presumably due to their limited chemoselectivity and because of the acid sensitivity of the formed TAD compounds.[105] Cookson, on the other hand, achieved a more controlled oxidation process by using tert butyl hypochlorite for the oxidation of 4-phenyl urazole in dry acetone at low temperatures (−50 °C to −78 °C).[2] This method remains a well-established oxidation procedure that can be carried out on a large scale and in the presence of a broad range of known 4-substituents. Especially the ability to oxidise urazoles containing electron-rich substituents is of advantage compared to more electrophilic reagents (*e.g.* nitrogen (IV) oxides and halogens), as was illustrated by Burgert and Stadler for the oxidation of a sensitive – 4-(4-hydroxyphenyl) – urazole (Scheme II.18).[80]

In order to avoid the use and handling of hazardous active halogen species, a number of alternative reagents and procedures have been developed that rely on the slow generation of halogen-based oxidants.[20] Moreover, a heterogenous character of a halogen mediated oxidation procedure can be achieved by simply using a solid supported reagent. This usually gives shorter reaction times and a more efficient removal of salts by filtration. Zolfigol, Mallakpour and co-workers reported on the use of the tetrameric complex of

1,4-diazabicyclo[2.2.2]octane and bromine (DABCO-Br)[52] to generate active bromine species *in situ*[52] which was found to be a particularly useful heterogeneous reagent that does not require the addition of any additives to facilitate the workup. Besides the mild conversion of low molecular weight (divalent) urazole components, this bromine complex was also found to be suitable for the heterogeneous oxidation of polymers bearing urazole end groups, which has very recently been demonstrated in our group.[87] Therefore, this oxidant is still the method of choice to easily obtain the various triazolinediones for this PhD research.

II.3 Overview of the reactivity of triazolinediones

TAD reagents have an overall resemblance in chemical structure with the more widely known maleimides, which are a well-established class of important synthetic tools for a wide range of applications, including click chemistry.[106–108] Indeed, also their modes of reactivity show some important similarities. Nevertheless, TAD compounds react much faster than maleimides and can also participate in a larger variety of pericyclic reactions with a much wider range of substrates, and with simple olefins in particular.[9,109,110] TAD reagents also have a higher intrinsic thermodynamic driving force than maleimides. Thus, whereas many maleimide-based conjugation reactions are reversible processes, most TAD-based reactions are completely irreversible. An important difference is the relative lack of (controlled) reactivity that TAD reagents show towards typical nucleophiles such as amines and thiols.

In terms of reactivity, TAD compounds have often been compared with singlet oxygen.[111–113] Indeed, both singlet oxygen and TADs show a great preference for Diels-Alder, ene-type, and (2+2)-cycloaddition reactions for more or less the same range of substrates (electron rich or non-polarised olefins). This similarity in reactivity can also be related to a correspondence in the particular arrangement and energies of the frontier orbitals (HOMO and LUMO), with a filled and an empty π^*-type orbital of very similar energy (Figure II.9).[114]

In essence, TAD and singlet oxygen have a strong preference for orbital-controlled reactions and favor delocalised π-cloud type substrates over typical localised or ionic nucleophiles. A major difference in terms of practicality between singlet oxygen and TAD reagents, however, is their life time. Many TAD compounds can be isolated and stored for prolonged

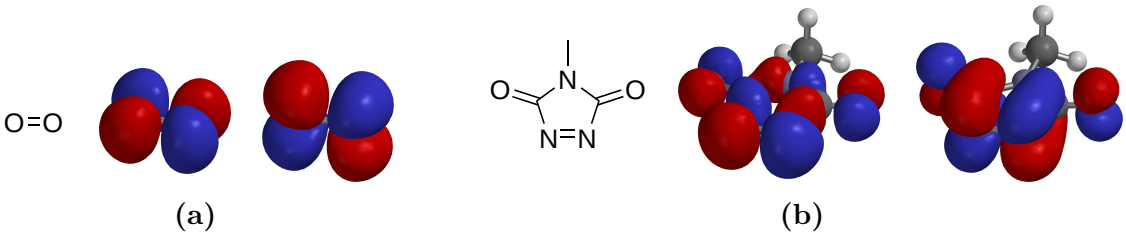

Figure II.9: The similar reactivity of **(a)** singlet oxygen and **(b)** 4-methyl-TAD can be related to their similar frontier orbitals. In both cases, the HOMO (left) and LUMO (right) are orthogonal π^*-type orbitals with a similar energy.

periods (*vide supra*), while singlet oxygen only has a half-life of a few microseconds in most organic solvents. Moreover, TAD reagents offer the possibility to introduce a wide range of functionality (R-groups), instead of just effecting oxygenations.

The preferred reaction partners and reactivity modes of TAD reagents are outlined in Scheme II.20, of which the Diels-Alder- and Alder-ene reactions are the most relevant for this doctoral work and will thus be briefly discussed in dedicated sections II.3.1 and II.3.2.[18] Apart from these very fast conjugation reactions in which carbon-nitrogen bonds are formed, TAD reagents can engage in a wide range of other reactions. These secondary

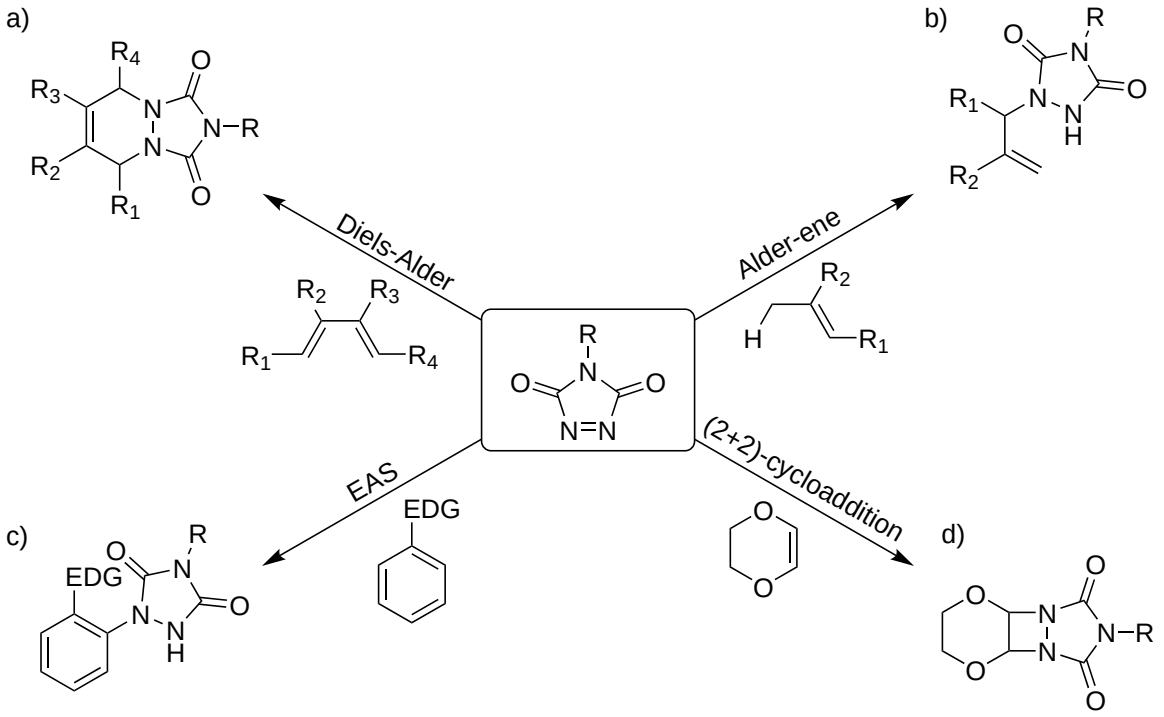

Scheme II.20: Four most relevant reactions involving TAD molecules: **(a)** Diels-Alder reaction, **(b)** Alder-ene reaction, **(c)** Electrophilic Aromatic Substitution (EAS) with an activated aromatic system (EDG = Electron Donating Group) and **(d)** (2 + 2)-cycloaddition.

reaction modes are often much less selective but also much slower than the ones shown in Scheme II.20. Nevertheless, these reactions can be observed as undesired side reactions, and will also be briefly discussed in this section (section II.3.3). A more detailed overview of the reactivity of TAD molecules is discussed in a variety of review articles.[7,12,18–20,115]

II.3.1 Diels-Alder reaction

The original discovery of the Diels-Alder (DA) reaction is actually closely linked to the chemistry of azodicarbonyl compounds (*vide supra*, Scheme II.1). Since its discovery, the DA reaction has been developed into one of the most efficient and widely applicable organic bond-forming reactions. The DA reaction allows the introduction of two new carbon-carbon σ-bonds and up to four new stereocenters,[116] with very pronounced and predictable levels of chemo-, stereo- and regioselectivity. Generally, the reaction requires elevated temperatures, but many DA reactions can also be effected at low temperature by using simple catalysts.[117] The DA reaction is a highly atom-economical process and, at least in theory, the bond forming process can be reversed, giving a retro-Diels-Alder (rDA) reaction that releases the original reaction partners.[118] This dynamic feature of the DA/rDA reaction has been used in a range of interesting applications in organic synthesis such as temporary protection of dienes,[119,120] scavenging of dienes from complex reaction mixtures,[121] and capturing and releasing transient reaction intermediates.[122] In polymer chemistry, the rDA reaction has been used to design covalently adaptable materials that show interesting properties such as healing[123] and remendability.[124]

The DA reaction has an enormous substrate scope, but TAD compounds were relatively late entries to the Diels-Alder toolbox. However, since Cookson's original report of an instantaneous reaction between PhTAD and cyclopentadiene at −78 °C,[2] TADs have become an intensively studied class of DA substrates, acquiring the reputation of being the fastest dienophile that can be isolated.[18,114] The exceptional reactivity of triazolinediones can be appreciated by the fact that their reaction with 'good' Diels-Alder dienes is almost instantaneous and quantitative even at quite low temperatures (−78 °C to −50 °C, *e.g.* Scheme II.1).

Reactions with less reactive dienes, such as anthracene or styrene, still proceed smoothly at room temperature (Scheme II.21a–b). The reaction between anthracene and TAD is very

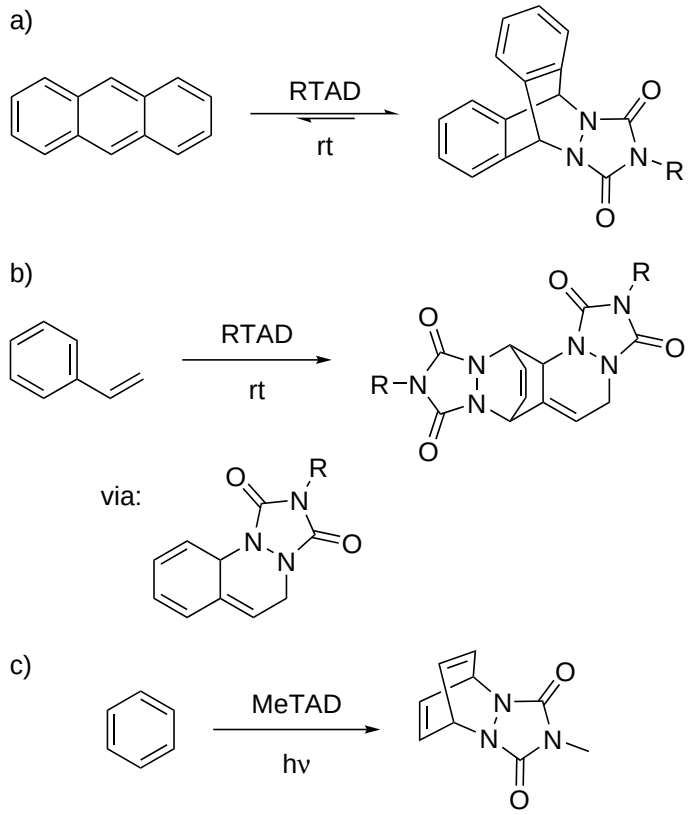

Scheme II.21: **(a)** 1:1 adduct of TAD and anthracene (reversible at room temperature), **(b)** 1:2 adduct of TAD and styrene (TAD and styrene react to form a diene that reacts *in situ* with another TAD moiety) and **(c)** photochemical adduct of benzene and TAD.

fast at room temperature, but it is also one of the few DA reactions that shows reversibility at room temperature,[109] related to the aromatic stability of the diene. In the case of styrene, which does normally not react with dienophiles even at elevated temperatures, a 1:2 adduct is quantitatively formed via a highly reactive diene intermediate that cannot be isolated (Scheme II.21b).[5] Reaction of styrene with just one equivalent of a TAD compound thus leads to a clean conversion of half of the styrene into the bis-adduct with TAD. Sheridan and co-workers found that while benzene, naphtalene and phenantrene do not readily react with TAD compounds, Diels-Alder adducts of these can be obtained by a photochemical DA reaction (Scheme II.21c)[125–129] or with the aid of an acid catalyst.[130]

II.3.2 Alder-ene reaction

The Alder-ene (AE) reaction (also referred to as ene reaction) can be defined as the reaction of an alkene bearing an allylic hydrogen (the ene) with a double bond (enophile) and was first described by Kurt Alder in 1943 (Scheme II.22).[131] During his Nobel lecture in 1950

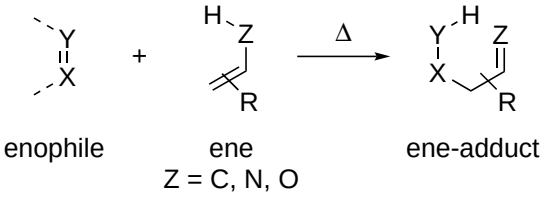

Scheme II.22: General reaction scheme of an Alder-ene reaction.

it was classified as an '*indirect substitution addition*' or '*ene synthesis*'.[132] It belongs to a general class of pericyclic reactions and comprises the migration of a σ-bonded hydrogen atom, the formation of a new C−C σ-bond at the expense of a C−C π-bond and the displacement of the initial π-bond.[133]

Despite the great potential in organic synthesis of the ene reaction,[137] the applications of the AE reaction have been rather limited as compared to the DA reaction. One reason for this is the unfavorable activation entropy and enthalpy, related to the highly ordered transition state with relatively poor orbital overlap, which results in much slower reaction rates.[138] Indeed, the AE reaction often requires extreme conditions (high pressure

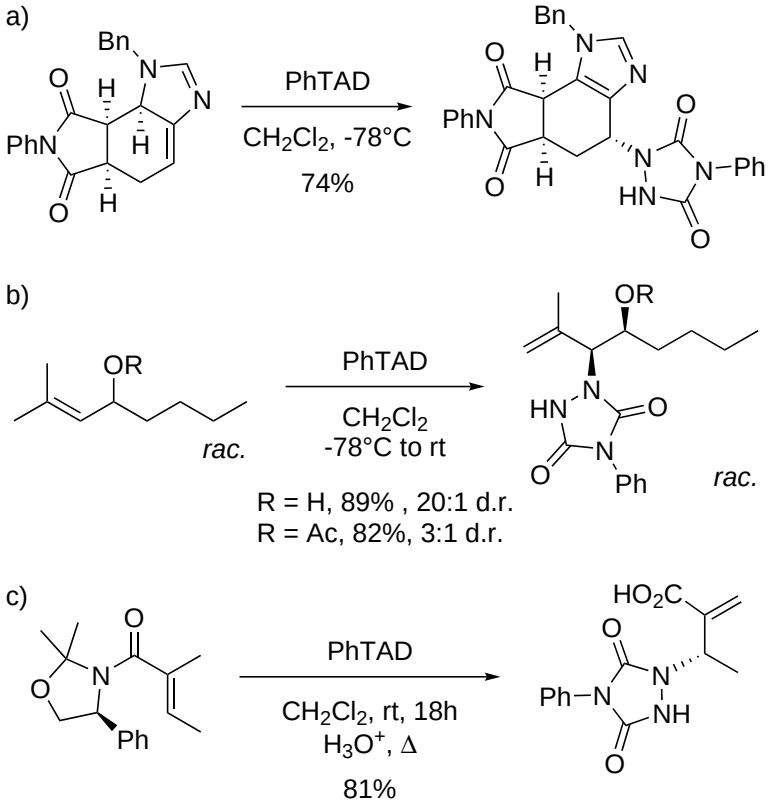

Scheme II.23: **(a)** DA cycloadducts of 4-vinylimidazoles are viable substrates for high yielding and highly diastereoselective ene reactions with TAD,[134] **(b)** regio- and diastereoselective ene reaction of 4-phenyl-TAD with chiral allylic alcohols[135] and **(c)** reaction between 2,2-dimethyloxazolidines and PhTAD.[136]

and temperature close to or above 200 °C), especially in the case of intermolecular ene reactions. The use of Lewis acid catalysts can lead to much enhanced reaction rates at lower temperature, but the issue of regioselectivity, in the common case where more than one allylic hydrogen is present in the ene substrate, has limited such methods mostly to intramolecular applications (ene cyclisations).[139] The introduction of highly reactive enophiles such as TAD compounds, however, has opened the door to quite reliable and even selective intermolecular ene reactions. Just a few years following Cookson's isolation of TAD compounds, its use as a potent enophile was found in room temperature reactions with simple alkene substrates, giving *N*-allylurazole adducts in quantitative yields.[6] A number of more recent illustrative TAD-based AE reactions are shown in Scheme II.23.

The mechanism of the TAD-based ene reactions has been a matter of some debate in the literature, where a six-electron concerted pericyclic process has been discarded in favor of a stepwise route involving the formation of a zwitterion aziridinium imide (AI, Scheme II.24).[140,141] The exact mechanism for subsequent hydrogen transfer is unclear but studies by Squillacote and co-workers suggest the involvement of an open form polarised diradical (PD) intermediate, and also that this mechanism might actually be solvent-dependent.[142,143]

Because of the (very) high activation barriers for typical ene reactions, it is not unexpected that the retro-Alder-ene (rAE) reaction has only rarely been observed in comparison to

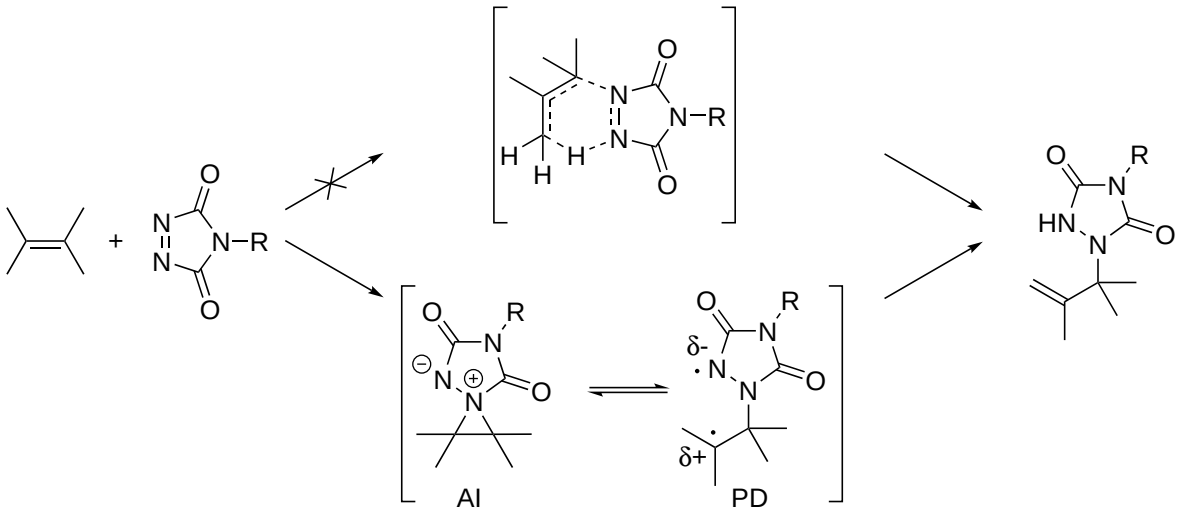

Scheme II.24: Alder-ene reaction between a mono-olefin and a TAD molecule. Two mechanisms are depicted: **(a)** a concerted pericyclic process via a six-membered ring transition state and **(b)** a stepwise route (via an aziridinium (AI) or a polarised diradical (PD) transition state).

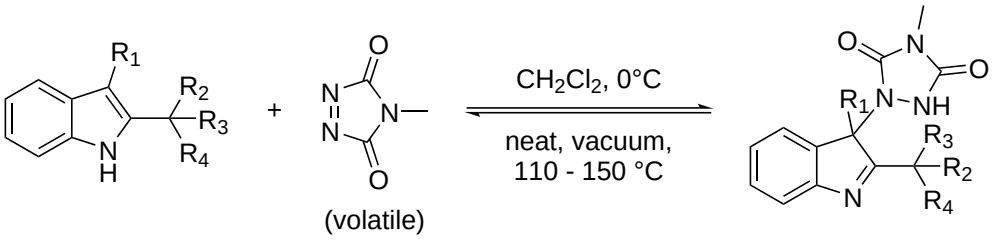

Scheme II.25: The 2,3-π-bond of certain indoles can be protected via the ene reaction with a TAD compound. Heating the adduct under vacuum allows the deprotection by removal of the volatile MeTAD.

the retro-DA reaction.[137,144] Most of the described thermoreversible AE reactions require pyrolysis-type conditions and are thus of limited value in synthetic applications.[137,145] Based on the much higher kinetic reactivity of TAD compounds as enophiles, one might expect to find ene reactions with these reagents that can be reversible in reasonable temperature intervals. However, so far only one example has been reported in literature. Baran and Corey described in 2003 the possibility to thermoreversibly protect an indole functionality.[111] Indoles readily and selectively form ene adducts, even at 0 °C. By simply heating the adduct, a rAE reaction will take place, which allows removal of a volatile TAD reagent, and gives the indole moiety (Scheme II.25).

II.3.3 Secondary reaction modes of TADs and important side reactions

As was proven in the previous sections, TAD compounds are highly reactive towards electron rich delocalised π-cloud type substrates, including simple alkenes, of which a qualitative empirical reactivity scale is provided in Figure II.10. In the case that there are no such suitable reaction partners available, TAD compounds can undergo a whole range of other reactions, albeit with slower kinetics. Thus, these reactions are often observed

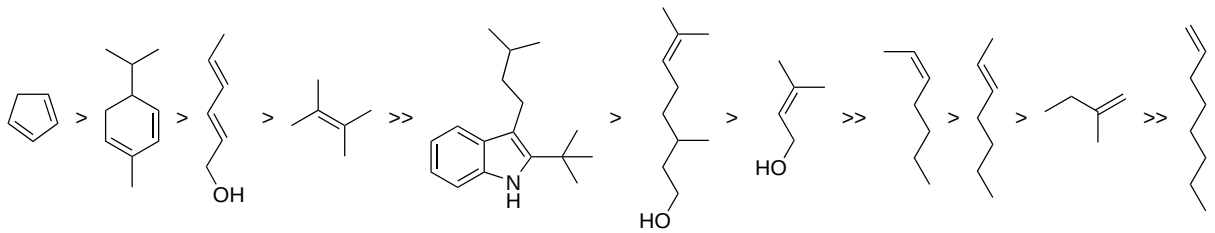

Figure II.10: Relative reaction rates as observed in a head-to-head analysis (in DMSO-d_6) of different representative reaction partners for triazolinediones. The symbol "$>$" indicates that a selectivity for the left substrate is observed ($>50\,\%$ adduct formation), while the symbol "$\gg$" indicates a complete selectivity.

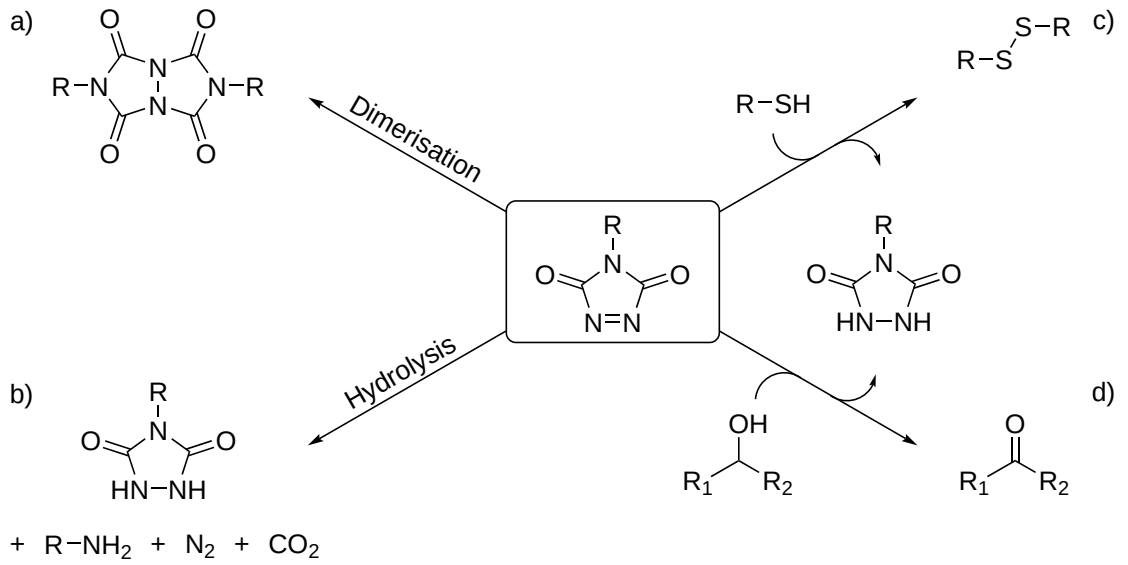

Scheme II.26: Important side reactions involving TAD. **(a)** dimerisation of TAD under UV irradiation or when heated above 160 °C, **(b)** hydrolysis of TAD, **(c)** oxidation of thiols and **(d)** oxidation of alcohols to aldehydes or ketones.

as undesired side reactions or as decomposition reactions. The main types of these 'slow' TAD reactions are summarised in Scheme II.26.

As already mentioned, some TAD molecules are not stable enough (or too reactive) to be isolated. However, in crystalline form, reagents such as PhTAD are relatively stable up to 160 °C and can be stored for several months in a dark, cold environment without significant decomposition.[5] However, when PhTAD is exposed to UV irradiation (for a longer period of time) or to temperatures above 160 °C, dimerisation through self-condensation occurs (Scheme II.26a).[146] Thus, this dimerisation process – actually the loss of nitrogen gas – puts an upper limit on reaction temperatures that can be employed when working with TAD reagents.

Although quite a few reactions of TAD compounds are actually conducted in water as solvent,[67,68] hydrolysis of TAD is a feasible process.[109] When stored in water for longer times, TAD compounds will slowly hydrolyse, giving the corresponding urazole and amine as final decomposition products (Scheme II.26b). This problem can usually be avoided by storing TAD compounds in a dry medium and container. The presence of acid or base can accelerate the hydrolysis, which needs to be taken into account when working in non-neutral media.

As can be expected from section II.2.3, TAD compounds are also redox active com-

pounds, acting as oxidants for substrates such as thiols,[147] leading to disulfide formation (Scheme II.26c). Also alcohols[148] can be oxidised (Scheme II.26d). In some cases, these mild oxidation reactions are actually synthetically useful, giving a clean oxidation under relatively neutral conditions.

In spite of all the different modes of reactivity that are available to TAD compounds, most TAD reactions of the type described in sections II.3.1 and II.3.2 are surprisingly chemo-, regio- and even stereoselective, even in the presence of competing reaction partners. This is because of the very pronounced kinetic selectivity TAD reagents have (*cf.* Figure II.10). Another feature that contributes to this orthogonal behaviour of a TAD reagent, is the fact that although it is a highly electrophilic species, it reacts only very slowly with classical (ionic) nucleophiles with 'localised' electron density.

A notable chemoselectivity issue in TAD reactions can arise in the presence of basic amines. The reaction of TADs with basic amines depends on a number of factors, and also a distinction has to be made between primary, secondary and tertiary amines. In combination with primary and secondary amines, TAD compounds can promote an acylation-type reaction of the amine, ultimately giving a urea derivative (Scheme II.27a).[71] The reaction proceeds via a nucleophilic attack of the amine that leads to the ring-opened species, which quickly expels N_2 and CO gas with the formation of a urea. In the case of tertiary amines, the reaction follows a different course after initial ring opening, and can react with another

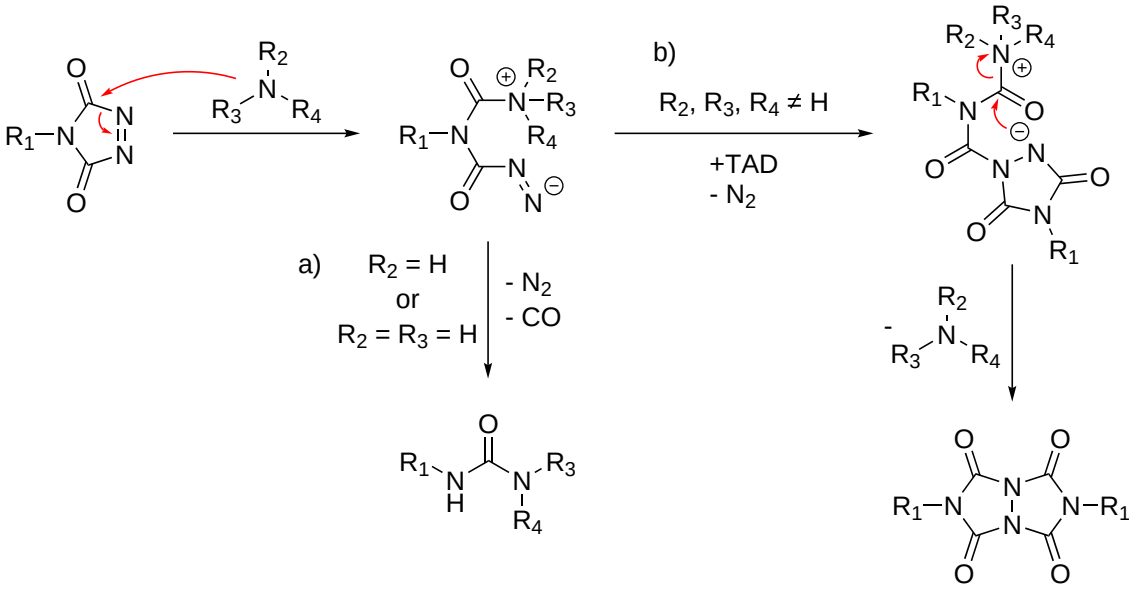

Scheme II.27: Reaction mechanism of the unwanted side reaction between TAD and **(a)** primary/secondary amines and **(b)** tertiary amines.[71,149,150]

TAD molecule. The original amine is then expelled to form the dimer as can be seen in Scheme II.27b, and thus acts as a TAD-dimerisation catalyst.[149,150] These side reactions can be suppressed by prior protonation of the amines (*e.g.* by adjusting the pH of the reaction medium), or by using substrates that are (much) more reactive than amines (such as Diels-Alder-type dienes). Anilines are usually less problematic, and mostly give EAS reaction with TAD, without significant urea formation or TAD dimerisation.

Given the very high reactivity, the release of nitrogen gas at elevated temperatures (*vide supra*) and the high nitrogen content of triazolinediones, these moieties could be considered to result in explosive compounds. Indeed, electron-deficient azo derivatives and low molecular weight azides are notorious because of their explosive nature.[151,152] However, to the best of our knowledge, TADs were never reported, also not in the course of this PhD research, to exhibit such an explosive or shock-sensitive behaviour.

II.4 The use of triazolinediones in polymer science

Following the introduction of TAD-compounds as versatile reagents in organic synthesis in the 1960s, the polymer community also developed an interest for the unique reactivity of TADs. Most of the early literature appeared in the 1970s and mainly dealt with the modification of polydienes. Nevertheless, this particular subject remains highly relevant, since research to further enhance the material properties still continues to date.[153,154] Therefore, this section will first discuss the application of triazolinediones as polydiene modifiers with the influence on the properties of the final material (section II.4.1). Next, two distinct examples are discussed in which the exceptional reactivity of TADs allowed the production of new, unprecedented polymeric materials (sections II.4.2 and II.4.3).

II.4.1 Triazolinedione modification of polydienes

The major application of triazolinediones in polymer science, so far, lies in the low-temperature modification of polydienes, both in academic[12] and industrial context.[155–159] The alkene-TAD ene reaction is very versatile and gives an atom efficient and site selective way to functionalise substrates that are otherwise quite hard to chemically modify in a reliable way (Scheme II.28).[7]

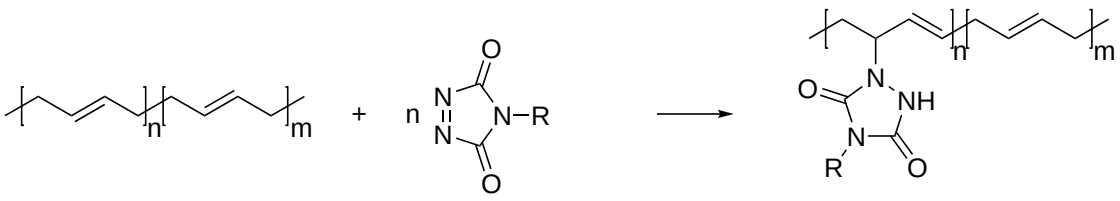

Scheme II.28: Reaction between polybutadiene and TAD.

TAD-based modification of polydienes was introduced in the early 1970s by Saville[38] using natural rubbers, and was later on more extensively studied by Butler *et al.*[9,34] A wide range of polydienes (polybutadiene, polyisoprene, random styrene-butadiene copolymer and a 1:1 alternating copolymer of furan and maleic anhydride) were modified with monofunctional TAD molecules. Although, theoretically, it is possible to add 4 mole of reactant per repeating unit (*i.e.* 4 'active' C-H bonds), the solubility of the obtained polymers plays a significant role, and the subsequent reactions are usually kinetically disfavored. Polymers with modification degrees ranging from 5 until 100 % can be obtained, in which the polymers with lowest conversion demonstrated elasticity, which was an indication for possible secondary – supramolecular – cross-linking reactions (higher conversion led to rigid amorphous polymers with high T_g).

Follow-up studies on TAD-functionalised polydienes[160,161] ruled out covalent cross-linking and supported the hypothesis that the highly polar pendant urazole groups have pronounced inter- and intramolecular hydrogen bonding interactions (Figure II.11a), which can be related to properties such as elasticity, changes in solubility character, thermal behaviour

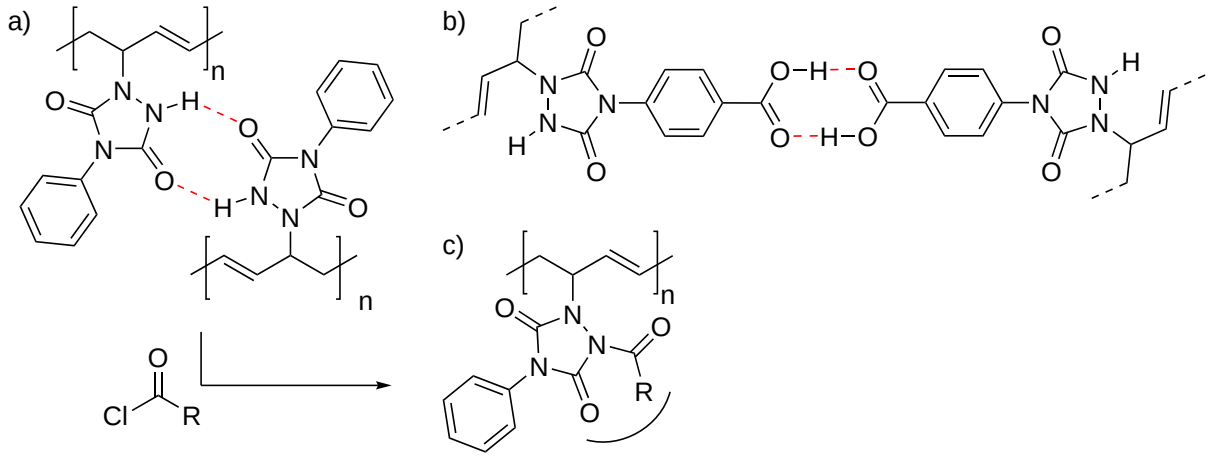

Figure II.11: **(a)** Secondary cross-linking of a polybutadiene functionalised with PhTAD and **(b)** extra secondary cross-linking of polybutadiene functionalised with a 4-carboxy-derivative of PhTAD. **(c)** The acidic urazole proton can be (partially) acylated, thereby blocking the self-associating behaviour.

and tensile strength. However, since this urazole-based association behaviour is physical in nature, the polymer remains soluble. Stadler *et al.* studied this hydrogen bond network formation in detail using star-shaped polybutadienes.[162,163]

Extending upon the concept of urazole-based hydrogen bonding networks (*cf.* Figure II.11a), Stadler *et al.* explored a range of TAD reagents that would enhance this supramolecular behaviour, including hydroxyl-, nitro- and carboxyl- functional TAD molecules.[164] It was shown that the addition of a hydroxyl group as an extra hydrogen bond donor resulted in the formation of extended 'junction zones' instead of point-like linkages. The use of a nitro-functionalised TAD moiety showed a similar hydrogen bonding behaviour as the original PhTAD complexes, and were used to convert the polybutadienes into ionomers.[165] The modification of polydienes with the 4-carboxy derivative of PhTAD (PhTAD-COOH) was first described in patent literature[84,166,167] and later Hilger *et al.* studied the hydrogen-bonding behaviour in these materials, which was found to be similar to that of a covalently cross-linked material up to 80 °C (Figure II.11b).[168] The mechanical properties were superior to those of PhTAD-based H-bonded networks, and actually comparable to thermoplastic elastomers of the covalent multiblock copolymers type, with high modulus and tensile strength.[85,169–174]

Because the attached urazole groups contain a quite acidic proton ($pK_a \approx 5$), further modifications of this strong hydrogen bond donor are relatively straightforward. Following a simple acylation reaction that 'caps' this acidic N−H group, polymers with a wider range of properties can be obtained by using different acid chloride modifiers, while the supramolecular self-associating behaviour is also blocked (Figure II.11c).[175] The degree of modification can be easily controlled by the amount of PhTAD, and the type of modification can be controlled by the choice of the acylating group. In this way, also optically active acid chlorides can be introduced on polydienes.[176]

Not only modification with monofunctional components was attempted but also bisTAD molecules were reacted with the aforementioned polydienes, resulting in highly cross-linked polymer networks.[34,177] De Lucca Freitas and Stadler studied the characteristics of the network formation in the reaction of polybutadiene and 4,4′-(4,4′-methylenediphenyl)-bis--(1,2,4-triazoline-3,5-dion) (MDI-TAD). This reaction was studied in solution as a model system, which allowed monitoring of the cross-linking kinetics, as a function of the gelation

process[178,179] and the primary molecular weight of the polymer matrix.[180] In later studies, a variety of cross-linkers (containing azo-dyes[181] or poly(ethylene glycol) chains[182,183]) and matrices[158,159] were used to obtain different network properties.

Next to the solution modification of polydienes, the surface modification of these polymers was investigated as well. Cutts *et al.* treated surfaces of elastomers with TAD components (both mono- and bifunctional).[184] In this way not only the adhesion could be improved, but also resistance to peeling with flexible paints improved while the surface tack of the elastomers reduced. This proved to be an advantageous method over the prior art (chlorination and halogen donor techniques), particularly because the applied triazolinediones are relatively mild and non-corrosive. In a recent study in collaboration with our group, van der Heijden *et al.* showed that the properties of styrene-butadiene-styrene (SBS) electrospun fibres could be tuned by their reaction with PhTAD and TAD cross-linkers.[185] These nanofibres could subsequently be applied for tuning the delamination resistance of composite materials.[186]

Very recently, Zhao *et al.* introduced triazolinediones as an efficient post-polymerisation tool for ring-opening metathesis polymerisation (ROMP) derived polymers. The TAD based Alder-ene reaction was used to efficiently post-functionalise well-defined ROMP polymers. Both monofunctional and bifunctional TAD molecules were employed to functionalise and cross-link poly(*N*-propyl-5-norbornene-exo-2,3-dicarboximide).[187]

II.4.2 Natural plant oils as a versatile feedstock monomer for new materials

The synthesis of polymer materials is a chemical process that typically requires precise control of reaction conditions, dedicated reaction vessels and raw materials (monomers) of high chemical purity. As the use of TAD-based click chemistry was expanding,[87] our group showed interest in natural plant oils as complementary partners for TAD reagents. Although most plant oils contain a large number of olefinic bonds, only very limited chemical transformations can be effected on these natural synthetic handles, often requiring catalysts and/or harsh reactions conditions.

An initial study demonstrated the reactivity and versatility of triazolinediones by cross-

linking crude, readily available plant oils with bifunctional TAD-molecules at room temperature.[45] Although a wide range of plant oils was successfully transformed in polymer networks, the gelation kinetics and resulting material properties varied as a function of the plant oil composition. In general, a higher fraction of polyunsaturated fatty acids resulted in both shorter gelation times and a higher glass transition temperature (T_g) of the obtained plant oil network. Furthermore, by simply varying the amount of cross-linker or the structure thereof, the T_g could be varied in a range of more than 70 °C independent from the applied plant oil.

In a subsequent collaboration of our group with the group of Tang, plant oil-based triblock copolymers were prepared from monomers derived from soybean oil.[188] The TAD-based 'fatty acid click coupling' strategy was employed to site-selectively create chemical junctions between the middle blocks of the triblock copolymers, improving tensile strength and resulting in excellent elastic recovery characteristics.

II.4.3 Clicking and transclicking TAD-bearing substrates

Our group was the first one to formally investigate the click-like behaviour of TAD chemistry with a range of simple olefin-type substrates.[87] The positive outcome of this study led to the introduction of a general click chemistry platform, based on hetero-Diels-Alder reactions of TAD reagents. These TAD-click reactions do not require additives or a catalyst and proceed readily at or even below room temperature. It was shown that the involved reactions were upscalable, quantitative (high yielding) under equimolar conditions, ultrafast (showing rate constants that go up to 160 000 $L\,mol^{-1}\,s^{-1}$[189]), and typically resulted in a single reaction product, even when a mixture of two reactive substrates is offered to one equivalent of a TAD reagent. A very wide range of ene-type reaction partners are available that give irreversible reactions with these click-like characteristics (Scheme II.29a).

Based on Baran's click-unclick TAD-based reaction for indoles (Scheme II.29b, see also Scheme II.25),[111] our group described that the combination of a high thermodynamic forward driving force, as is required by click chemistry ideals, is only very rarely observed in combination with a kinetically feasible backward reaction. Such a dynamic feature usually goes hand-in-hand with either low 'forward' yields or with hard-to-control free radical chemistry. Thus, this unique example of a dynamic TAD-indole reaction opened

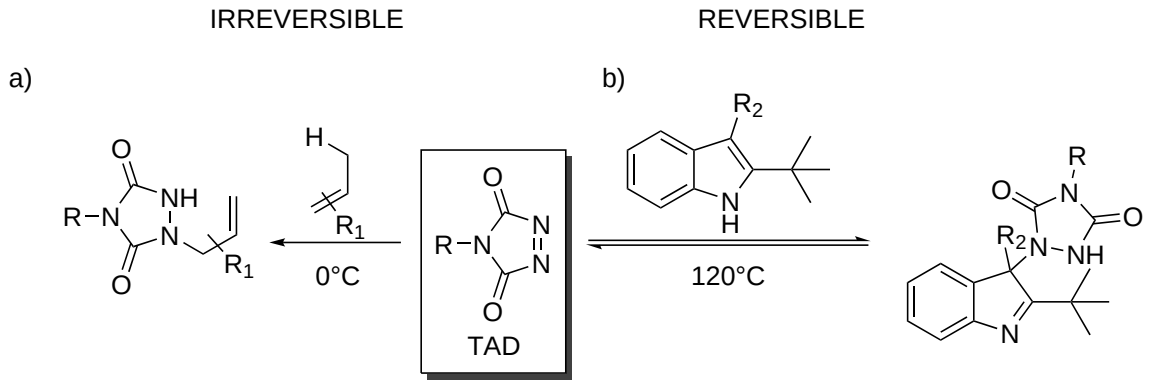

Scheme II.29: **(a)** Irreversible Alder-ene type reaction with a 1,2,4-triazoline-3,5-dione and **(b)** reversible Alder-ene reaction by replacement of the alkene derivative by a 1*H*-indole.

possibilities for unprecedented applications of TAD chemistry in a macromolecular context.

As an initial demonstration of dynamic TAD-click reactions, our group reported a linear indole-functionalised polyurethane, making use of an indole-diol, which was then cross-linked with a bifunctional TAD reagent.[87] The resulting PU-network, containing TAD-indole cross-links, could be molded, recycled and processed at elevated temperatures without loss of material properties. In one illustrative test, the stiff cross-linked material was broken into small fragments and then put into a mold under pressure for 30 minutes at 120 °C. A pristine sample was retrieved from the mold after cooling.

Although the indole-TAD 'unclick' reaction is an efficient and clean process, it is not practically feasible to fully 'reverse' this click reaction in the case of non-volatile reagents, because the indole and TAD reagents will reform the adduct quantitatively at room temperature. However, by adding an alternative reaction partner for TAD, which is known to result in an irreversible adduct formation, the TAD-indole adduct can be completely unclicked, while another substrate is now clicked onto the TAD reagent. For this unprecedented concept in click chemistry applications, the term '*transclick reaction*' was introduced (Scheme II.30) for *any covalent linking process that subsequently can be triggered to form a new bond with an alternative or orthogonal reaction partner, and at the same time release one of the original binding partners, in which both bond-forming steps meet the usual requirements for click reactions.*[87] Indeed, it was shown that both low molecular weight and macromolecular TADs and indoles react in an equimolar ratio to afford the TAD-indole Alder-ene adduct (*e.g.* a block copolymer). When this adduct is heated in the presence of one equivalent of a conjugated diene, the TAD molecule is

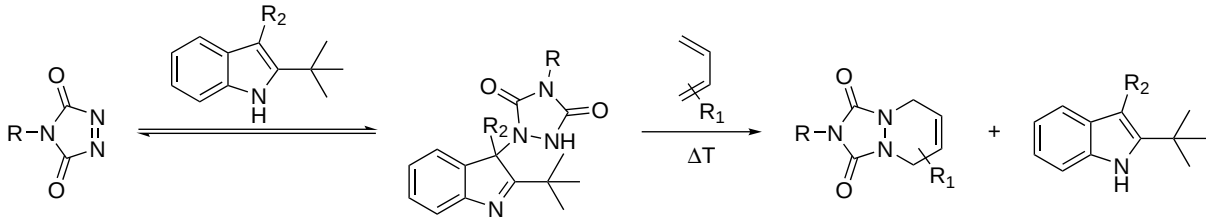

Scheme II.30: Example of a *transclick* reaction: reversible Alder-ene reaction between a 1,2,4-triazoline-3,5-dione and a 1*H*-indole, followed by an irreversible Diels-Alder reaction (all under click conditions).

completely and selectively transferred to this diene, resulting in a new Diels-Alder adduct and the release of the original indole compound without any side reactions.

II.5 Conclusions

Triazolinediones are very reactive species that can participate in a whole range of reactions with specific classes of olefin-type substrates. Despite their high reactivity, many TAD reagents can be isolated in pure form and are bench stable compounds, while more functionalised and/or sensitive TAD compounds can be easily generated *in situ* or used as a freshly prepared solution.

TAD-reactions are characterised by a very pronounced kinetic selectivity towards electron rich π-systems, predominantly resulting in very fast hetero-Diels-Alder and hetero-Alder-ene type reactions. Importantly, many TAD-based reactions match all of the typical click chemistry requirements. Moreover, the extraordinary kinetics of TAD-based reactions have also resulted in the development of unprecedented 'dynamic' click reactions, including our introduction of the concept of 'transclick' reactions as a means to program or direct successive and selective covalent exchange reactions.

The interest of using TAD reagents for various applications has clearly known a renaissance in the last decade, partially related to the search for orthogonal, yet highly reactive modular click chemistry tools. Therefore, it can be expected that the further development of TAD-based applications will be hampered by the limited availability of these reagents. While the oxidation of 4-functionalised urazoles is the only practical method to obtain useful TAD reagents (section II.2.3) and can prove to be quite cumbersome, the real issue in tailored TAD synthesis is the limited versatility in the assembly of urazole precursor

compounds. Indeed, other 'clickable groups' are often introduced via a simple one-step reaction of a functional commercial compound without major chemoselectivity issues, *e.g.* the condensation of propargylamine with an activated carboxylic acid. However, a similar strategy is not readily applied in the case of urazoles.

Functional urazoles are not commercially available and their synthesis requires harsh reaction conditions (section II.2.1). Moreover, the urazole moiety itself is acidic and competes with other nucleophiles, leading to many chemoselectivity problems in further modification reactions (section II.2.2). Therefore, only common urazole substrates, such as 4-phenyl or 4-butyl urazole, and numerous bis-urazoles have been synthesised on (very) large scale and with high yields from cheap starting materials. Urazoles bearing an additional functionality such as a functional handle, 'clickable' group, fluorescent group or bioactive molecule often require more tedious multi-step procedures or extensive reaction optimisation. However, ongoing research efforts, including in our group, are actively researching generic synthetic strategies for functional urazoles that are not hampered by these chemoselectivity issues.

For niche applications that do not require large amounts of TAD reagents, such as in biomedical research, the cost of their synthesis is not an issue. Consequently, many heterobifunctional TAD reagents have been developed, some of which have even been commercialised for small scale use. For large scale adoption and further developments in the field of TAD-based click chemistry, on the other hand, the chemical community is in need of short, scalable, and versatile synthesis methods for simple functionalised urazoles. In this aspect, this doctoral work is no exception, since tailored reagents are typically required when one wants to perform TAD reactions at the interface.

II.6 Bibliography

1. O. Diels, J. H. Blom, W. Koll, *Justus Liebigs Ann. Chem.* **1925**, *443*, 242–262.
2. R. C. Cookson, S. S. H. Gilani, I. D. R. Stevens, *Tetrahedron Lett.* **1962**, *3*, 615–618.
3. O. Diels, K. Alder, *Justus Liebigs Ann. Chem.* **1928**, *460*, 98–122.
4. J. Thiele, O. Stange, *Justus Liebigs Ann. Chem.* **1894**, *283*, 1–46.
5. R. C. Cookson, S. S. H. Gilani, I. D. R. Stevens, *J. Chem. Soc. C* **1967**, *1967*, 1905–1909.
6. W. H. Pirkle, J. C. Stickler, *Chem. Commun. (London)* **1967**, *1967*, 760–761.
7. G. B. Butler, *Ind. Eng. Chem. Prod. Res. Dev.* **1980**, *19*, 512–528.
8. S. Ohashi, K.-W. Leong, K. Matyjaszewski, G. B. Butler, *J. Org. Chem.* **1980**, *45*, 3467–3471.
9. A. G. Williams, G. B. Butler, *J. Org. Chem.* **1980**, *45*, 1232–1239.
10. M. A. Zolfigol, H. Nasr-Isfahani, S. Mallakpour, M. Safaiee, *Synlett* **2005**, *2005*, 761–764.
11. J. Sauer, *Angew. Chem. Int. Ed. Engl.* **1967**, *6*, 16–33.
12. G. B. Butler, *Polym. Sci. U.S.S.R.* **1981**, *23*, 2587–2622.
13. M. E. Burrage, R. C. Cookson, S. S. Gupte, I. D. R. Stevens, *J. Chem. Soc. Perkin Trans. 2* **1975**, *1975*, 1325–1334.
14. G. Read, N. R. Richardson, *J. Chem. Soc. Perkin Trans. 1* **1996**, *1996*, 167–174.
15. M. A. Zolfigol, M. Bagherzadeh, S. Mallakpour, G. Chehardoli, A. Ghorbani-Choghamarani, N. Koukabi, M. Dehghanian, M. Doroudgar, *J. Mol. Catal. A: Chem.* **2007**, *270*, 219–224.
16. J. M. Gardlik, L. A. Paquette, *Tetrahedron Lett.* **1979**, *20*, 3597–3600.
17. L. A. Paquette, R. F. Doehner, *J. Org. Chem.* **1980**, *45*, 5105–5113.
18. S. Rádl in *1,2,4-Triazoline-3,5-Diones*, *Vol. 67* (Ed.: R. K. Alan), Academic Press, **1996**, book section 2, pp. 119–205.
19. I. K. Korobitsyna, A. V. Khalikova, L. L. Rodina, N. P. Shusherina, *Chemistry of Heterocyclic Compounds* **1983**, *19*, 117–136.
20. K. De Bruycker, S. Billiet, H. A. Houck, S. Chattopadhyay, J. M. Winne, F. E. Du Prez, *Chem. Rev.* **2016**, *116*, 3919–3974.
21. A. Pinner, *Ber. Dtsch. Chem. Ges.* **1887**, *20*, 2358–2360.

22. F. Arndt, L. Loewe, A. Tarlan-Akön, *Istanbul Univ. Fen Fak. Mecm. Seri A* **1948**, *13A*, 127–146.

23. G. W. Breton, M. Turlington, *Tetrahedron Lett.* **2014**, *55*, 4661–4663.

24. W. Chai, Y. Chang, J. D. Buynak, *Tetrahedron Lett.* **2012**, *53*, 3514–3517.

25. W. Chai, E. Nguyen, J. Doran, K. Han, A. Weatherbie, D. Fernandez, S. Karimi, R. Mynam, C. Humphrey, S. Rana, J. D. Buynak, *Tetrahedron Lett.* **2013**, *54*, 2308–2310.

26. G. Zinner, W. Deucker, *Arch. Pharm.* **1961**, *294*, 370–372.

27. R. C. Cookson, S. S. Gupte, I. D. R. Stevens, C. T. Watts, *Org. Synth.* **1971**, *51*, 121–127.

28. S. Ogawa, S. Ooki, M. Morohashi, K. Yamagata, T. Higashi, *Rapid Commun. Mass Spectrom.* **2013**, *27*, 2453–2460.

29. K. Shimada, T. Oe, T. Mizuguchi, *Analyst* **1991**, *116*, 1393–1397.

30. M. J. Bausch, B. David, P. Dobrowolski, C. Guadalupe-Fasano, R. Gostowski, D. Selmarten, V. Prasad, A. Vaughn, L. H. Wang, *J. Org. Chem.* **1991**, *56*, 5643–5651.

31. T. Little, J. Meara, F. Q. Ruan, M. Nguyen, M. Qabar, *Synth. Commun.* **2002**, *32*, 1741–1749.

32. J. C. Stickler, W. H. Pirkle, *J. Org. Chem.* **1966**, *31*, 3444–3445.

33. B. T. Gillis, R. A. Izydore, *J. Org. Chem.* **1969**, *34*, 3181–3187.

34. G. B. Butler, A. G. Williams, *J. Polym. Sci. Polym. Chem. Ed.* **1979**, *17*, 1117–1128.

35. S. Yamada, M. Shimizu, *Preparation of 1,2,3-triazoline-3,5-dione and 1,2,3-triazolidine-3,5-dione derivatives as phosphorescent or chemiluminescent dienophile reagents for analysts of vitamin D and analogs*, **1992**, JP04005287.

36. C. H. Hassall, A. Krohn, C. J. Moody, W. A. Thomas, *J. Chem. Soc. Perkin Trans. 1* **1984**, *1984*, 155–164.

37. B. Chandrasekhar, G. B. Kumar, S. Mallela, S. B. Bhirud, *Org. Prep. Proced. Int.* **2004**, *36*, 469–472.

38. B. Saville, *J. Chem. Soc. D* **1971**, *1971*, 635–636.

39. K. Wald, H. Wamhoff, *Chem. Ber.* **1978**, *111*, 3519–3523.

40. K. B. Wagener, K. A. Matyasjewski, G. B. Butler, *J. Polym. Sci. Polym. Lett. Ed.* **1979**, *17*, 129–137.

41. K. A. Matyjaszewski, K. B. Wagener, G. B. Butler, *J. Polym. Sci. Polym. Lett. Ed.* **1979**, *17*, 65–77.

42. K. B. Wagener, S. R. Turner, G. B. Butler, *J. Polym. Sci. Part B: Polym. Lett.* **1972**, *10*, 805–816.

43. Y.-C. Lai, G. B. Butler, *J. Macromol. Sci. - Chem.* **1985**, *22*, 1443–1461.

44. R. L. Sowerby, *Urazoles compositions useful as additives for functional fluids*, **1987**, WO8707892.

45. O. Türünç, S. Billiet, K. De Bruycker, S. Ouardad, J. Winne, F. E. Du Prez, *Eur. Polym. J.* **2015**, *65*, 286–297.

46. T. Tsuji, *Pharm. Bull.* **1954**, *2*, 403–411.

47. M. Pesson, S. Dupin, *Bull. Soc. Chim. Fr.* **1962**, *29*, 250–254.

48. S. E. Mallakpour, A.-R. Hajipour, H. Raheno, *J. Appl. Polym. Sci.* **2002**, *85*, 1141–1146.

49. S. E. Mallakpour, H. Nasr-Isfahani, *Indian J. Chem. Sect. B: Org. Chem. Incl. Med. Chem.* **2002**, *41*, 169–174.

50. S. Mallakpour, S. Rezazadeh, *Iran. Polym. J.* **2004**, *13*, 29–38.

51. S. Mallakpour, Z. Rafiee, *Polymer* **2007**, *48*, 5530–5540.

52. M. A. Zolfigol, G. Chehardoli, E. Ghaemi, E. Madrakian, R. Zare, T. Azadbakht, K. Niknam, S. Mallakpour, *Monatsh. Chem.* **2008**, *139*, 261–265.

53. S. Mallakpour, Z. Rafiee, *Polym. Bull.* **2006**, *56*, 293–303.

54. S. Mallakpour, Z. Rafiee, *J. Appl. Polym. Sci.* **2007**, *103*, 947–954.

55. T. Curtius, *J. Prakt. Chem.* **1894**, *50*, 275–294.

56. T. Curtius, *Ber. Dtsch. Chem. Ges.* **1893**, *26*, 403–410.

57. T. Curtius, *Ber. Dtsch. Chem. Ges.* **1894**, *27*, 778–781.

58. K. Shimada, T. Oe, *Anal. Sci.* **1990**, *6*, 461–463.

59. M. Shimizu, T. Takahashi, S. Uratsuka, S. Yamada, *J. Chem. Soc. Chem. Commun.* **1990**, *1990*, 1416–1417.

60. M. Shimizu, S. Kamachi, Y. Nishii, S. Yamada, *Anal. Biochem.* **1991**, *194*, 77–81.

61. J. Flagothier, C. Warnier, S. Dammicco, C. Lemaire, A. Luxen, *RSC Adv.* **2013**, *3*, 24936–24940.

62. A. Ghorbani-Choghamarani, M. Nikoorazm, G. Azadi, *Chin. Chem. Lett.* **2014**, *25*, 451–454.

63. S. Mallakpour, Z. Rafiee, *Synth. Commun.* **2007**, *37*, 1927–1934.

64. R. Adamo, M. Allan, F. Berti, E. Danieli, Q.-Y. Hu, *Tyrosine ligation process*, **2013**, WO2013009564.

65. A. Nilo, M. Allan, B. Brogioni, D. Proietti, V. Cattaneo, S. Crotti, S. Sokup, H. Zhai, I. Margarit, F. Berti, Q.-Y. Hu, R. Adamo, *Bioconjugate Chem.* **2014**, *25*, 2105–2111.

66. S. Mallakpour, Z. Rafiee, *Synlett* **2007**, *2007*, 1255–1256.

67. H. Ban, J. Gavrilyuk, C. F. Barbas, *J. Am. Chem. Soc.* **2010**, *132*, 1523–1525.

68. H. Ban, M. Nagano, J. Gavrilyuk, W. Hakamata, T. Inokuma, C. F. Barbas, *Bioconjugate Chem.* **2013**, *24*, 520–532.

69. C. F. Barbas, H. Ban, J. Gavrilyuk, *Tyrosine bioconjugation through aqueous ene-like reactions*, **2011**, WO2011079315.

70. D. M. Bauer, I. Ahmed, A. Vigovskaya, L. Fruk, *Bioconjugate Chem.* **2013**, *24*, 1094–1101.

71. Q.-Y. Hu, M. Allan, R. Adamo, D. Quinn, H. Zhai, G. Wu, K. Clark, J. Zhou, S. Ortiz, B. Wang, E. Danieli, S. Crotti, M. Tontini, G. Brogioni, F. Berti, *Chem. Sci.* **2013**, *4*, 3827–3832.

72. C. D. Hurd, F. F. Cesark, *J. Am. Chem. Soc.* **1967**, *89*, 1417–1422.

73. D. S. Campbell, A. J. Tinker, P. G. Mente, *Reagents for graft copolymers*, **1983**, EP0065366.

74. T. J. Gilbertson, *4-Substituted phenyl-1,2,4-triazoline-3,5-diones and their dihydro analogs as analytical reagents*, **1982**, US4366320.

75. T. J. Gilbertson, T. Ryan, *Synthesis* **1982**, *1982*, 159–160.

76. T. Vidal, V. Pevere, *Process for preparing hydrazo-silane compounds using an alkoxylated hydrazocarboxylate precursor*, **2009**, WO2009003955.

77. G. Zinner, B. Böhlke, *Arch. Pharm.* **1966**, *299*, 43–55.

78. S. Alakurtti, T. Heiska, A. Kiriazis, N. Sacerdoti-Sierra, C. L. Jaffe, J. Yli-Kauhaluoma, *Bioorg. Med. Chem.* **2010**, *18*, 1573–1582.

79. K. Schmitt, G. Driesen, L. Ther, W. Pfaff, *Verfahren zur Herstellung von 3, 5-Dioxo-triazolidinen Process for the preparation of 3, 5-dioxo-triazolidinen*, **1965**, DE1200825.

80. J. Burgert, R. Stadler, *Chem. Ber.* **1987**, *120*, 691–694.

81. K.-H. Park, L. J. Cox, *Tetrahedron Lett.* **2002**, *43*, 3899–3901.

82. L. Rottmaier, R. Merten, *Triazolidine-3,5-dione condensed with amine-formaldehyde, and its preparation*, **1982**, EP0044417.

83. L. Rottmaier, R. Merten, *Triazolidine-3,5-dione/formaldehyde/amine condensates and compositions thereof*, **1984**, US4433085.

84. G. Pope, P. Smewin, G. Stokes, *Carboxylation of unsatd polymers - by reaction with a carboxy-substd 4-phenyl-1,2,4-triazoline-3,5-dione*, **1974**, DE2342929.

85. C. Hilger, R. Stadler, *Makromol. Chem.* **1990**, *191*, 1347–1361.

86. U. Seidel, J. Hellman, D. Schollmeyer, C. Hilger, R. Stadler, *Supramol. Sci.* **1995**, *2*, 45–50.

87. S. Billiet, K. De Bruycker, F. Driessen, H. Goossens, V. Van Speybroeck, J. M. Winne, F. E. Du Prez, *Nat. Chem.* **2014**, *6*, 815–821.

88. V. P. Arya, S. J. Shenoy, *Indian J. Chem. Sect. B: Org. Chem. Incl. Med. Chem.* **1976**, *14*, 883–886.

89. A. R. Hajipour, S. E. Mallakpour, M. A. Zolfigol, H. Adibi, *Indian J. Chem. Sect. B: Org. Chem. Incl. Med. Chem.* **2002**, *41*, 2425–2427.

90. M. A. Zolfigol, E. Madrakian, E. Ghaemi, S. Mallakpour, *Synlett* **2002**, *2002*, 1633–1636.

91. S. E. Mallakpour, H. Nasr-Isfahani, *Iran. Polym. J.* **2002**, *11*, 57–61.

92. S. Mallakpour, Z. Rafiee, *J. Appl. Polym. Sci.* **2003**, *90*, 2861–2869.

93. S. Mallakpour, Z. Rafiee, *Iran. Polym. J.* **2004**, *13*, 225–234.

94. H. Mighani, H. N. Isfahani, S. Mighani, *Indian J. Chem. Sect. B: Org. Chem. Incl. Med. Chem.* **2012**, *51*, 366–369.

95. H. Nasr-Isfahani, S. Soldoozi, Z. Kalantar, H. Mighani, *Macromol.: Indian J.* **2012**, *8*, 7–11.

96. H. Nasr-Isfahani, M. Bakherad, Z. Kalantar, S. Yousefi, H. Mighani, *Macromol.: Indian J.* **2012**, *8*, 19–23.

97. O. Roling, K. De Bruycker, B. Vonhören, L. Stricker, M. Körsgen, H. F. Arlinghaus, B. J. Ravoo, F. E. Du Prez, *Angew. Chem. Int. Ed.* **2015**, *54*, 13126–13129.

98. S. Mallakpour, Z. Rafiee, *J. Appl. Polym. Sci.* **2004**, *91*, 2103–2113.

99. S. Dey, S. Purkayashtha, *Analysis of estrogens and analytes with phenolic OH using labeling chemistry and LC-MSMS workflow*, **2013**, WO2013108113.

100. J. F. W. Keana, A. P. Guzikowski, D. D. Ward, C. Morat, F. L. Van Nice, *J. Org. Chem.* **1983**, *48*, 2654–2660.

101. L. N. Goswami, Z. H. Houston, S. J. Sarma, S. S. Jalisatgi, M. F. Hawthorne, *Org. Biomol. Chem.* **2013**, *11*, 1116–1126.

102. J. L. Riebsomer, *Chem. Rev.* **1945**, *36*, 157–233.

103. M. Thiemann, E. Scheibler, K. W. Wiegand in *Nitric Acid, Nitrous Acid, and Nitrogen Oxides*, *Vol. 24*, Wiley-VCH Verlag GmbH and Co. KGaA, **2000**, book section 24, p. 177.

104. J. E. Herweh, R. M. Fantazier, *Tetrahedron Lett.* **1973**, *14*, 2101–2104.

105. A. G. Williams, *Ph.D. Thesis*, University of Florida, **1976**.

106. R. J. Pounder, M. J. Stanford, P. Brooks, S. P. Richards, A. P. Dove, *Chem. Commun.* **2008**, *2008*, 5158–5160.

107. B. H. Northrop, S. H. Frayne, U. Choudhary, *Polym. Chem.* **2015**, *6*, 3415–3430.

108. S. D. Fontaine, R. Reid, L. Robinson, G. W. Ashley, D. V. Santi, *Bioconjugate Chem.* **2015**, *26*, 145–152.

109. N. Roy, J.-M. Lehn, *Chem. - Asian J.* **2011**, *6*, 2419–2425.

110. A. Holleman, E. Wiberg, N. Wiberg, *Inorganic Chemistry*, Academic Press, **2001**, p. 1884.

111. P. S. Baran, C. A. Guerrero, E. J. Corey, *Org. Lett.* **2003**, *5*, 1999–2001.

112. W. Adam, O. De Lucchi, *Tetrahedron Lett.* **1981**, *22*, 929–932.

113. D. A. Singleton, C. Hang, *J. Am. Chem. Soc.* **1999**, *121*, 11885–11893.

114. A. G. Leach, K. N. Houk, *Chem. Commun.* **2002**, *2002*, 1243–1255.

115. C. J. Moody in *Azodicarbonyl Compounds in Heterocyclic Synthesis*, *Vol. 30* (Ed.: A. R. Katritzky), Academic Press, **1982**, pp. 1–45.

116. M. J. S. Dewar, S. Olivella, J. J. P. Stewart, *J. Am. Chem. Soc.* **1986**, *108*, 5771–5779.

117. F. Carey, R. J. Sundberg, *Advanced Organic Chemistry - Part B: Reactions and Synthesis*, Springer US, 5th ed., **2007**, p. 1322.

118. B. Rickborn in *The Retro–Diels–Alder Reaction Part II. Dienophiles with One or More Heteroatom*, John Wiley & Sons, Inc., **2004**, book section 2, pp. 223–629.

119. R. I. Yakhimovich, N. F. Fursaeva, V. E. Pashinnik, *Chem. Nat. Compd.* **1985**, *21*, 98–103.

120. M. Fernández-Herrera, J. Sandoval-Ramírez, S. Montiel-Smith, S. Meza-Reyes, *Heterocycles* **2013**, *87*, 571–582.

121. M. L. Poutsma, P. A. Ibarbia, *J. Am. Chem. Soc.* **1971**, *93*, 440–450.

122. A. P. Henderson, E. Mutlu, A. Leclercq, C. Bleasdale, W. Clegg, R. A. Henderson, B. T. Golding, *Chem. Commun.* **2002**, *2002*, 1956–1957.

123. J. Zhang, Y. Niu, C. Huang, L. Xiao, Z. Chen, K. Yang, Y. Wang, *Polym. Chem.* **2012**, *3*, 1390–1393.

124. X. Chen, M. A. Dam, K. Ono, A. Mal, H. Shen, S. R. Nutt, K. Sheran, F. Wudl, *Science* **2002**, *295*, 1698–1702.

125. D. P. Kjell, R. S. Sheridan, *J. Am. Chem. Soc.* **1984**, *106*, 5368–5370.

126. S. J. Hamrock, R. S. Sheridan, *Tetrahedron Lett.* **1988**, *29*, 5509–5512.

127. J. Dover, R. S. Sheridan, *Tetrahedron Lett.* **1990**, *31*, 1961–1964.

128. S. J. Hamrock, R. S. Sheridan, *J. Am. Chem. Soc.* **1989**, *111*, 9247–9249.

129. G. W. Breton, K. A. Newton, *J. Org. Chem.* **2000**, *65*, 2863–2869.

130. G. W. Breton, *Adv. Chem. Lett.* **2013**, *1*, 68–73.

131. K. Alder, F. Pascher, A. Schmitz, *Ber. Dtsch. Chem. Ges.* **1943**, *76*, 27–53.

132. K. Mikami, M. Shimizu, *Chem. Rev.* **1992**, *92*, 1021–1050.

133. M. L. Clarke, M. B. France, *Tetrahedron* **2008**, *64*, 9003–9031.

134. L. J. Watson, R. W. Harrington, W. Clegg, M. J. Hall, *Org. Biomol. Chem.* **2012**, *10*, 6649–6655.

135. A.-H. Gau, G.-L. Lin, B.-J. Uang, F.-L. Liao, S.-L. Wang, *J. Org. Chem.* **1999**, *64*, 2194–2201.

136. A. Pastor, W. Adam, T. Wirth, G. Tóth, *Eur. J. Org. Chem.* **2005**, *2005*, 3075–3084.

137. H. M. R. Hoffmann, *Angew. Chem. Int. Ed. Engl.* **1969**, *8*, 556–577.

138. L. J. Watson, *Ph.D. Thesis*, Newcastle University, **2013**.

139. Y. Hayashi, T. Shibata, K. Narasaka, *Chem. Lett.* **1990**, *19*, 1693–1696.

140. M. Squillacote, M. Mooney, J. De Felippis, *J. Am. Chem. Soc.* **1990**, *112*, 5364–5365.

141. M. M. Roubelakis, G. C. Vougioukalakis, Y. S. Angelis, M. Orfanopoulos, *Org. Lett.* **2006**, *8*, 39–42.

142. O. Acevedo, M. E. Squillacote, *J. Org. Chem.* **2008**, *73*, 912–922.

143. M. E. Squillacote, C. Garner, L. Oliver, M. Mooney, Y.-L. Lai, *Org. Lett.* **2007**, *9*, 5405–5408.

144. Z. Wang in *Retro-Ene Reaction*, John Wiley & Sons, Inc., **2010**, book section 534, pp. 2373–2377.

145. W. Oppolzer, V. Snieckus, *Angew. Chem. Int. Ed. Engl.* **1978**, *17*, 476–486.

146. H. Wamhoff, K. Wald, *Chem. Ber.* **1977**, *110*, 1699–1715.

147. A. Christoforou, G. Nicolaou, Y. Elemes, *Tetrahedron Lett.* **2006**, *47*, 9211–9213.

148. R. C. Cookson, I. D. R. Stevens, C. T. Watts, *Chem. Commun. (London)* **1966**, *1966*, 744a–744a.

149. L. H. Dao, D. Mackay, *Can. J. Chem.* **1979**, *57*, 2727–2733.

150. D. W. Borhani, F. D. Greene, *J. Org. Chem.* **1986**, *51*, 1563–1570.

151. M.-H. V. Huynh, M. A. Hiskey, E. L. Hartline, D. P. Montoya, R. Gilardi, *Angew. Chem. Int. Ed.* **2004**, *43*, 4924–4928.

152. A. Jacobs, *Understanding Organic Reaction Mechanisms*, Cambridge University Press, **1997**.

153. B. J. Gold, C. H. Hövelmann, C. Weiss, A. Radulescu, J. Allgaier, W. Pyckhout-Hintzen, A. Wischnewski, D. Richter, *Polymer* **2016**, *87*, 123–128.

154. J. Huang, L. Zhang, Z. Tang, S. Wu, N. Ning, H. Sun, B. Guo, *Macromol. Rapid Commun.* **2017**, *38*, 1600678.

155. E. Baumgartner, *Graft copolymers and process for producing the same*, **1990**, EP0390028A2.

156. B. Ostermayer, *Thermoplastic moulding compositions*, **1990**, EP0412414A2.

157. J. Blackborow, *Substituted azo-dicarbonylo derivatives*, **1996**, EP0728766A2.

158. K. Muehlbach, M. A. De Araujo, R. Stadler, *Modified polyphenylene ethers*, **1989**, EP0338425A1.

159. B. Ostermayer, K. Muehlbach, E. Baumgartner, H. Brandt, H. Feldmann, *Thermoplastic moulding compositions based on triazolindione-modified polyphenylene ethers*, **1989**, EP0370330A2.

160. K.-W. Leong, G. B. Butler, *J. Macromol. Sci. - Chem.* **1980**, *14*, 287–319.

161. T. C. S. Chen, G. B. Butler, *J. Macromol. Sci. Pure Appl. Chem.* **1981**, *16*, 757–768.

162. R. Stadler, M. M. Jacobi, W. Gronski, *Makromol. Chem. Rapid Commun.* **1983**, *4*, 129–135.

163. W. Gronski, R. Stadler, M. Maldaner Jacobi, *Macromolecules* **1984**, *17*, 741–748.

164. L. de Lucca Freitas, J. Burgert, R. Stadler, *Polym. Bull.* **1987**, *17*, 431–438.

165. L. de Lucca Freitas, R. Stadler, *Colloid. Polym. Sci.* **1988**, *266*, 1095–1101.

166. R. Wragg, J. Yardley, *Method of producing rubber-plastics composites*, **1973**, GB1456855.

167. R. Wragg, J. Yardley, *Method of producing rubber-plastics composites*, **1975**, US3899378.

168. C. Hilger, R. Stadler, *Macromolecules* **1990**, *23*, 2095–2097.

169. C. Hilger, R. Stadler, L. Liane, L. de Lucca Freitas, *Polymer* **1990**, *31*, 818–823.

170. C. Hilger, R. Stadler, *Makromol. Chem.* **1991**, *192*, 805–817.

171. C. Hilger, R. Stadler, *Macromolecules* **1992**, *25*, 6670–6680.

172. C. Hilger, M. Draeger, R. Stadler, *Macromolecules* **1992**, *25*, 2498–2501.

173. A. Dardin, R. Stadler, C. Boeffel, H. W. Spiess, *Makromol. Chem.* **1993**, *194*, 3467–3477.

174. A. Dardin, C. Boeffel, H. W. Spiess, R. Stadler, E. T. Samulski, *Acta Polym.* **1995**, *46*, 291–299.

175. S. Mallakpour, F. Rafiemanzelat, B. Sheikholeslami, *Iran. Polym. J.* **1997**, *6*, 235–241.

176. S. E. Mallakpour, A.-R. Hajipour, S. Khoee, B. Sheikholeslami, *Polym. Int.* **1998**, *47*, 193–197.

177. S. Rout, G. Butler, *Polym. Bull.* **1980**, *2*, 513–520.

178. L. L. de Lucca Freitas, M. M. Jacobi, R. Stadler, *Polym. Bull.* **1984**, *11*, 407–414.

179. R. Stadler, F. Bühler, W. Gronski, *Makromol. Chem.* **1986**, *187*, 1301–1312.

180. R. Stadler, L. L. D. L. Freitas, M. M. Jacobi, *Makromol. Chem.* **1986**, *187*, 723–729.

181. R. Stadler, M. Weber, *Polymer* **1986**, *27*, 1254–1260.

182. M. Weber, R. Stadler, *Polymer* **1988**, *29*, 1064–1070.

183. M. Weber, R. Stadler, *Polymer* **1988**, *29*, 1071–1078.

184. E. Cutts, G. Knight, *Surface treatment of polymers*, **1974**, US3966530.

185. S. van der Heijden, K. De Bruycker, R. Simal, F. Du Prez, K. De Clerck, *Macromolecules* **2015**, *48*, 6474–6481.

186. S. van der Heijden, L. Daelemans, K. De Bruycker, R. Simal, I. De Baere, W. Van Paepegem, H. Rahier, K. De Clerck, *Compos. Struct.* **2017**, *159*, 12–20.

187. Y. Zhao, J. Chen, W. Zhu, K. Zhang, *Polymer* **2015**, *74*, 16–20.

188. Z. Wang, L. Yuan, N. M. Trenor, L. Vlaminck, S. Billiet, A. Sarkar, F. E. Du Prez, M. Stefik, C. Tang, *Green Chem.* **2015**, *17*, 3806–3818.

189. V. D. Kiselev, D. A. Kornilov, I. I. Lekomtseva, A. I. Konovalov, *Int. J. Chem. Kinet.* **2015**, *47*, 289–301.

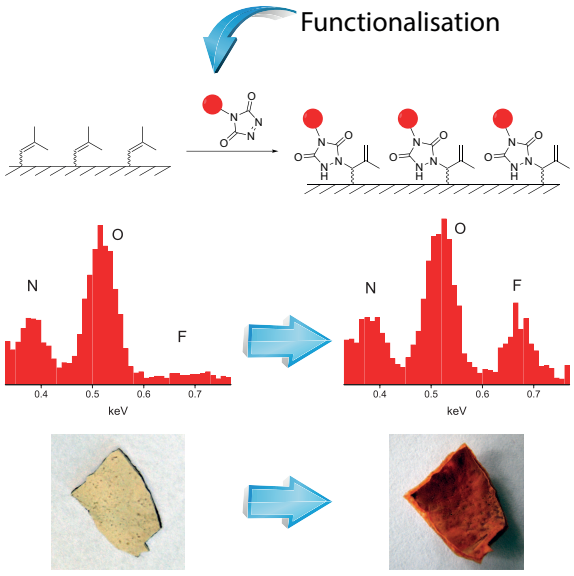

Abstract

For large scale adoption and further developments in the field of TAD-based click chemistry, the chemical community is in need of scalable and versatile synthesis methods for simple functionalised urazoles. In this aspect, this doctoral work is no exception, since tailored reagents are typically required to give an added value to TAD reactions at the interface. Therefore, using the concepts outlined in Chapter II, various functional triazolinediones and complementary reaction partners were targeted, of which the synthesis will be discussed in this chapter. After an initial assessment of their suitability for surface modifications, the obtained compounds were finally used in various polymer chemistry applications, which will be discussed in dedicated chapters.

Chapter III

General syntheses of functional triazolinediones and their applicability for surface modifications

III.1 Introduction

The main goal of this doctoral work has been the application of TAD chemistry in various interfacial systems. However, as discussed in Chapter II, very few triazolinediones or corresponding urazole precursors are commercially available, while only 'simple' TADs such as 4-phenyl- or 4-butyl-TAD and some bivalent cross-linkers are readily synthesised on a large scale from cheap starting materials, *i.e.* isocyanates. Moreover, isocyanate auxiliaries are typically not available for urazoles bearing an additional functionality, resulting in lengthy multistep procedures with a moderate to low overall yield. This limited versatility and chemoselectivity in the assembly of functional urazoles can be considered as the main reason for the absence of a general synthesis method for tailored triazolinediones.

While our research group already reported on the synthesis of some urazole compounds with a functional handle,[1–3] the aim of this chapter is the development of scalable syntheses for TADs that bring functionality to a material via a reaction at the solid-liquid interface, *e.g.* by impacting the wettability. However, for an initial assessment of the reactivity of

these triazolinediones in surface modifications, a cross-linked material containing TAD-complementary groups is required. Such a network might be obtained using TAD chemistry as well, since an excess of the polyunsaturated component in the monomer mixture will yield a material with residual unsaturations (Scheme III.1). Therefore, the first part of this research (section III.2) consists of the synthesis of suitable monomers that can be cross-linked with a bivalent triazolinedione, followed by an investigation of the reaction kinetics and the thermal properties of the materials as a function of the monomers.

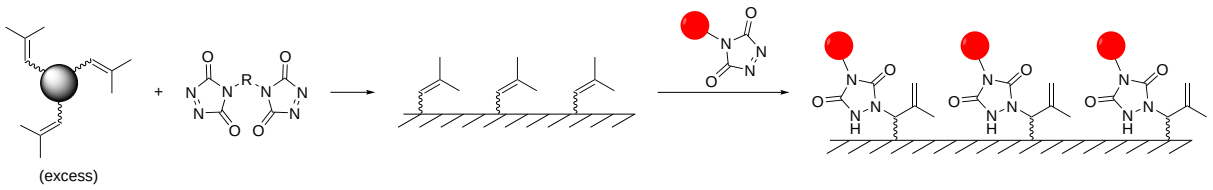

Scheme III.1: A network containing residual unsaturations can be synthesised by combining an excess of the polyunsaturated component and a TAD cross-linker. This material can then be used to assess the reactivity of functional triazolinediones for surface modifications.

The second part deals with the synthesis of various functional triazolinediones (section III.3), with scalability and versatility as main criteria when evaluating possible synthetic routes. Finally, after such TAD compounds are obtained, an initial proof of concept of their applicability for surface modifications is described (Scheme III.1).

III.2 Synthesis and characterisation of networks based on triazolinedione chemistry

As outlined above, the first part of this research consisted of the synthesis of an unsaturated model material to demonstrate the applicability of triazolinediones for surface modifications. In this context, our group previously demonstrated that bivalent triazolinediones can be used to cross-link crude, *i.e.* non-purified, readily available plant oils at room temperature (section II.4.2).[4] Indeed, a plant oil mainly consists of triglycerides of fatty acids, of which up to ~99 % is (mono-)unsaturated, giving the oil a theoretical functionality of three ($f = 3$) in its reaction with TAD. However, plant oils are never perfectly defined and are typically 'contaminated' with saturated chains, diglycerides and free fatty acids, which impact the overall functionality ($f < 3$). Therefore, problems will arise when networks are targeted with residual unsaturations, which are necessary for further TAD modifications.

Moreover, all the unsaturations in natural fatty acids are disubstituted, resulting in a similar reactivity for their Alder-ene reaction with triazolinediones (Figure II.10).

To overcome the issues with plant oils, this section will first discuss the synthesis of well-defined trivalent alkenes or dienes ($f = 3$). The main advantage of these compounds is that the monomer ratio can be easily varied to a certain extent, thereby yielding the targeted TAD-reactive materials. Moreover, by introducing different types of unsaturations, a significant impact on the cross-linking kinetics should be expected. Next, an equivalent amount of bivalent triazolinedione is added in order to investigate these reaction kinetics, as well as the thermal properties of the resulting networks.

III.2.1 Network synthesis

First, nine different trivalent alkenes or dienes were synthesised by reacting trivalent isocyanates with various unsaturated alcohols in the presence of dibutyltin dilaurate (DBTL) as catalyst (Figure III.1). On the one hand, isocyanurate-based trimers of hexamethylene diisocyanate (HDI_3, **78**), toluene diisocyanate (TDI_3, **79**) and isophorone diisocyanate ($IPDI_3$, **80**) were selected because of the stability of the isocyanurate group and an expected dependency of the thermal properties of the final materials on the exact core structure. Although the alcohols should also influence the thermal properties of the materials, *trans,trans*-2,4-hexadien-1-ol (HDEO, **81**), citronellol (**82**) and oleyl alcohol (**83**)

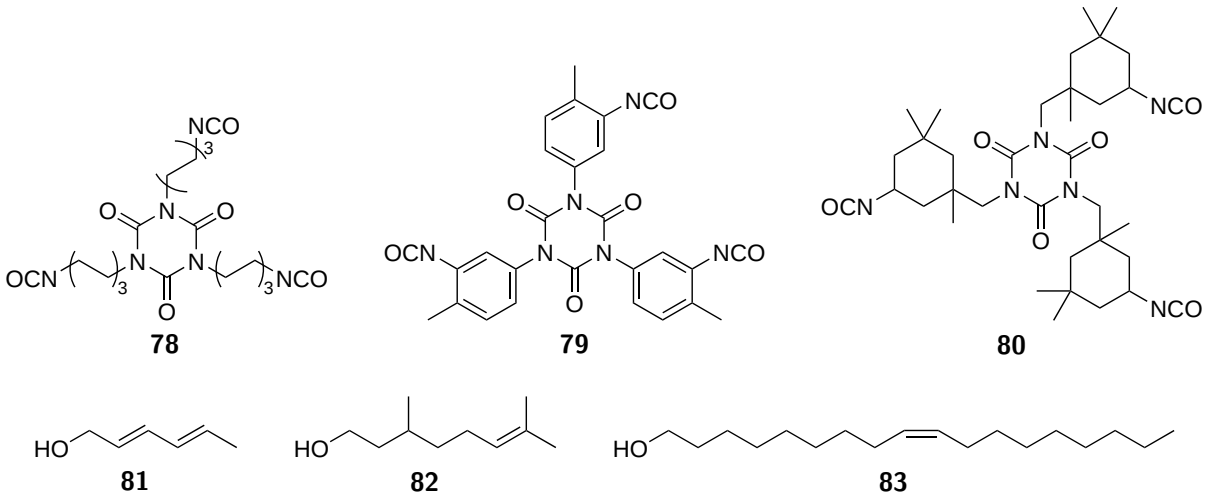

Figure III.1: Overview of the selected isocyanate trimers, *i.e.* HDI_3 (**78**), TDI_3 (**79**) and $IPDI_3$ (**80**), that were reacted with various unsaturated alcohols, *i.e.* HDEO (**81**), citronellol (**82**) and oleyl alcohol (**83**), to obtain a set of nine different trivalent alkenes or dienes. For TDI_3 and $IPDI_3$, only one isomer is shown.

were mainly chosen for their reactivity towards triazolinediones. Indeed, the conjugated diene, trisubstituted and disubstituted alkene, respectively, should have a significant effect on the cross-linking kinetics when the trimers are reacted with a bivalent TAD. Since the reaction kinetics are typically the most important experimental parameter, the notation (isocyanate$_3$)–alcohol, *e.g.* (HDI$_3$)–HDEO, will be used in this chapter for the trivalent alkenes or dienes to easily distinguish the nine different isocyanate-alcohol combinations.

In a next step, the trivalent alkenes or dienes were reacted with 4,4′-(4,4′-methylenediphenyl)-bis-(1,2,4-triazoline-3,5-dion) (MDI-TAD, **84**, Figure III.2) to form a cross-linked material. Similarly to our previous study on the cross-linking of plant oils,[4] acetone was selected for all cross-linking experiments since it readily evaporates from the material. 100 mg of MDI-TAD was dissolved in 1 mL of acetone, added to an equimolar amount of the complementary reaction partner in acetone, and subsequently mixed to obtain a homogeneous solution. The success of these polymerisations proved to be highly dependent on the solubility of the unsaturated reaction partners, as shown in Table III.1. While MDI-TAD is well soluble in acetone, some of the isocyanate-alcohol combinations were badly soluble or even completely insoluble in acetone. For example, the oleyl alcohol trimers were all badly soluble, which most likely resulted in a dilution that was too high to form a cross-linked material in the case of (TDI$_3$)–oleyl alcohol. (TDI$_3$)–HDEO, on the other hand, was only soluble in alcohols, which cannot be used as solvents for the cross-linking experiments because of the incompatibility with MDI-TAD (section II.3.3).

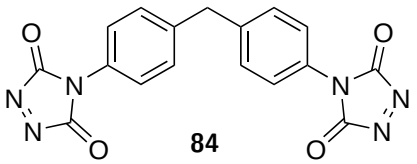

84

Figure III.2: Structure of the bivalent triazolinedione cross-linker (MDI-TAD).

Table III.1 also lists the gelation time and the time needed for the characteristic red colour of the TAD moieties to disappear, which indicates a full conversion, for every trivalent alkene or diene. As anticipated, the type of unsaturation has a high impact on the cross-linking kinetics, while no significant change in reaction speed is visible across the different isocyanate cores. In fact, the HDEO-based trimers reacted too fast with MDI-TAD to obtain a homogeneous mixture prior to gelation and are therefore less suited for the synthesis of polymeric materials. Nevertheless, these very fast kinetics sparked the idea to

Table III.1: Overview of the polymerisations with, for every isocyanate-alcohol combination, a qualitative indication of the solubility in acetone (top), the gelation time (middle) and the time needed for a full conversion, as judged by the disappearance of the characteristic red colour of the TAD moeities.

	HDI_3	TDI_3	$IPDI_3$	
	+	−−	+	solubility
HDEO	< 1 s	n.a.	< 1 s	gelation
	< 5 s	n.a.	< 5 s	fully reacted
	++	++	++	solubility
Citronellol	< 30 s	< 30 s	< 30 s	gelation
	< 1 h	< 1 h	< 1 h	fully reacted
	−	−	−	solubility
Oleyl alcohol	< 5 min	no gelation	< 5 min	gelation
	> 1 h	> 1 h	> 1 h	fully reacted

apply such a reactive pair in an alternating fashion, *i.e.* for the coating of surfaces, rather than in a homogeneous system. The details and results of this 'layer-by-layer' approach will be outlined in Chapter V. From a practical point of view, the citronellol-based trimers are preferred since they are very well soluble in a range of organic solvents while they are characterised by reaction kinetics that allow a fast gelation, yet provide enough time for shaping or moulding of the reaction mixture.

III.2.2 Characterisation of the synthesised networks

After the successful synthesis of the new TAD-based networks, thermogravimetric analysis (TGA) as well as differential scanning calorimetry (DSC) was performed on all materials in order to obtain more information about their thermal stability and phase behaviour. The resulting thermograms (Figure III.3) for the three (HDI_3)–alcohol combinations show a very similar degradation profile of the different materials. However, only the cross-linked (HDI_3)–HDEO loses approximately 5 % of its mass at a temperature around 180 °C, which might be explained by an incomplete reaction of the diene residues in the material. Indeed, because of the very fast reaction between the diene and MDI-TAD, gelation occurred before a homogeneous monomer mixture could be obtained (*vide supra*). Consequently, a significant amount of HDEO residues most likely remains unreacted in the final network structure, which can degrade according to the proposed mechanism shown in Scheme III.2. This mechanism could also explain the observed discolouration and decreased solubility of (HDI_3)–HDEO when it is stored at ambient conditions for a few weeks. Since the main

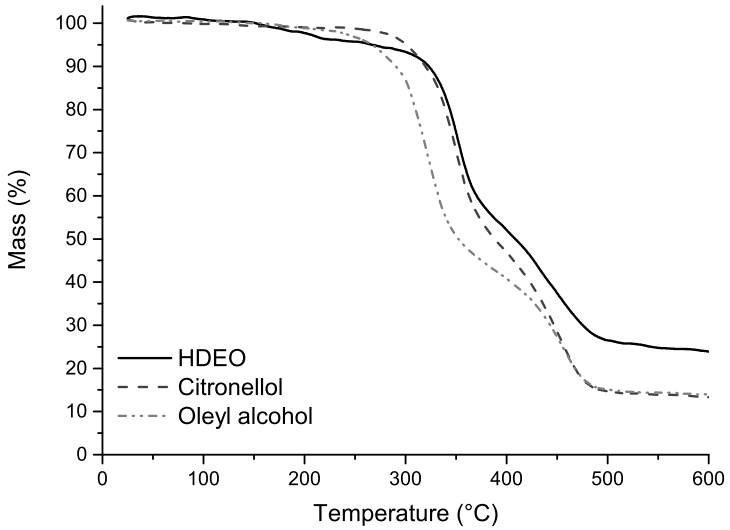

Figure III.3: Thermograms of the networks based on the three different (HDI_3)–alcohol monomers. TGA analyses were performed in a nitrogen atmosphere with a heating rate of 10 °C min^{-1}.

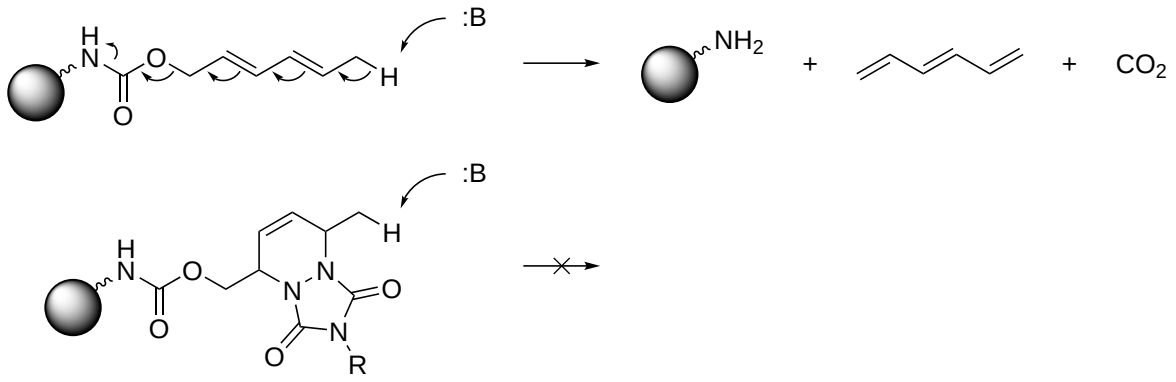

Scheme III.2: Proposed mechanism for the degradation of unreacted HDEO residues into volatile compounds, which can explain the small mass loss in the cross-linked materials at 180 °C as well as the observed slow degradation of the monomer at ambient conditions (top). After the Diels-Alder reaction with a TAD compound, this degradation can no longer occur (bottom).

degradation of the materials typically starts between 260 and 280 °C, it was not possible to identify a clear trend as a function of the exact isocyanate core or alcohol residue.

Once the degradation temperatures were determined, DSC analyses could be performed to measure the glass transition temperatures (T_gs) of the networks. Figure III.4 plots the second heating curves for the three HDI_3-based materials, all of which display a clear T_g with values between 20 and 200 °C. The onset temperatures for all the materials are summarised in Table III.2, showing that both the alcohols and the core structures greatly influence the T_g. In principle, these values could also be slightly impacted by residual monomers or soluble oligomers, which can be removed by a soxhlet extraction (not done).

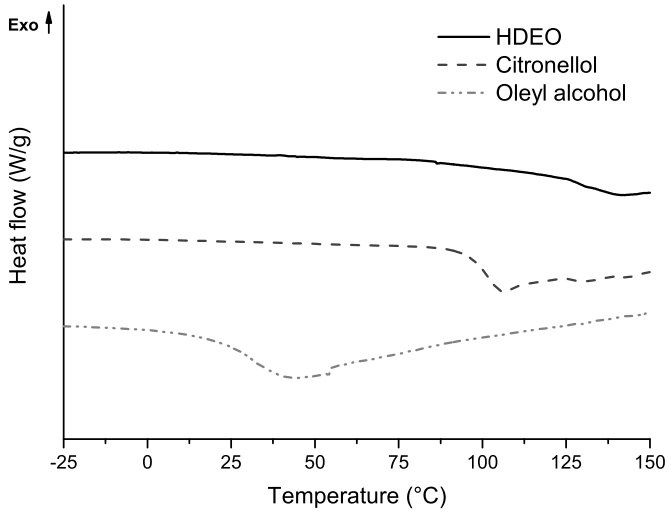

Figure III.4: DSC analysis of the (HDI_3)–alcohol-based networks (10 °C min^{-1}, N_2 atmosphere).

Table III.2: Glass transition temperatures (onset T_g in °C, determined via DSC) of the networks synthesised from the different isocyanate-alcohol combinations and MDI-TAD. No networks were obtained from (TDI_3)–HDEO or (TDI_3)–oleyl alcohol.

	HDI_3	TDI_3	$IPDI_3$
HDEO	124	-	198
Citronellol	96	151	168
Oleyl alcohol	24	-	89

Materials based on the trivalent diene are characterised by the highest T_gs, which can be rationalised by the short length of HDEO, as well as by the formation of a six-membered ring upon reaction with triazolinediones. In contrast, no rings are formed via an Alder-ene reaction with oleyl residues, which also introduce flexibility in the material because of the long dangling chains at each reactive site, resulting in the lowest T_g values. When comparing the different core structures, on the other hand, the higher flexibility of HDI_3 compared to TDI_3 and $IPDI_3$ is again reflected in the T_g of the network.

In conclusion, different trivalent TAD-complementary reaction partners could be synthesised by combining trivalent isocyanates with various unsaturated alcohols. These monomers were then reacted with a bivalent TAD, *i.e.* MDI-TAD, to obtain polymer networks with tunable thermal properties. Although both the core structure, originating from the trivalent isocyanate, and the alcohol residue significantly influenced the T_g of the materials, the cross-linking kinetics were solely dependent on the type of unsaturation and thus on the used alcohol.

By changing the monomer ratio, materials can be prepared with residual unsaturations, which can be applied in a later phase as heterogeneous reaction partners to assess the reactivity of triazolinediones for surface modifications (*vide infra*). For this application, no significant effect of the off-stoichiometry on the material properties is expected since only a slight excess of unsaturated monomer is required. Citronellol-based materials were selected, mainly because of their straightforward production and the well-balanced reaction kinetics. Furthermore, since the TAD modifications will be performed at room temperature, no preferential core structure was identified based on the thermal properties.

III.3 Synthesis of functional triazolinediones

Once the citronellol-based networks were identified as optimal model material to assess the reactivity of triazolinediones at the solid-liquid interface, multiple functional triazolinediones were targeted in the next phase of this research. As previously mentioned, our research group already reported on the synthesis of some urazole compounds with a functional handle,[1–3] some of which will be used herein for further modifications, while another was directly applied to modify glass or silicon supported self-assembled monolayers and will be discussed in a dedicated chapter (Chapter VI). Nevertheless, the compounds described in this section should bring functionality to a material via a reaction at the solid-liquid interface, while their synthesis is ideally scalable and versatile. To this end, the concepts outlined in section II.2 will be important for the evaluation of various possible synthetic routes.

First, two essentially different fluorinated triazolinediones were targeted (section III.3.1) that will be applied to alter the wettability of polymeric surfaces. After their synthesis, an initial proof of concept should demonstrate their applicability for surface modifications via a reaction with a previously obtained unsaturated material. However, because the modified and unmodified material were nearly indistinguishable in this case by traditional techniques, only surface analysis techniques providing information on the elemental composition were suitable to demonstrate a successful modification. Therefore, the next section (section III.3.2) will discuss the synthesis of triazolinedione-bearing dyes that can be used as probes for unsaturations, resulting in an easy and visual confirmation of a successful modification, without the need for advanced analytical techniques.

III.3.1 Synthesis of fluorinated triazolinediones

Two liquids that are mixed, and consequently form a biphasic system, are called 'orthogonal liquids'. A well-known example is the aqueous and organic phases, of which the immiscibility is typically exploited during the workup of reactions in organic chemistry, *e.g.* for removing certain side-products. However, as shown in Figure III.5, there is a third phase that is orthogonal to both the organic and aqueous phases, *i.e.* the fluorous phase.[5–7] Many fluorophilic molecules consist of a non-fluorinated and a fluorinated part, the latter typically being a so-called fluorinated ponytail. These tails are the most often used and investigated, are described by the general formula $-(CH_2)_m-(CF_2)_n-CF_3$ and are commonly abbreviated as $-(CH_2)_mR_{Fn}$.

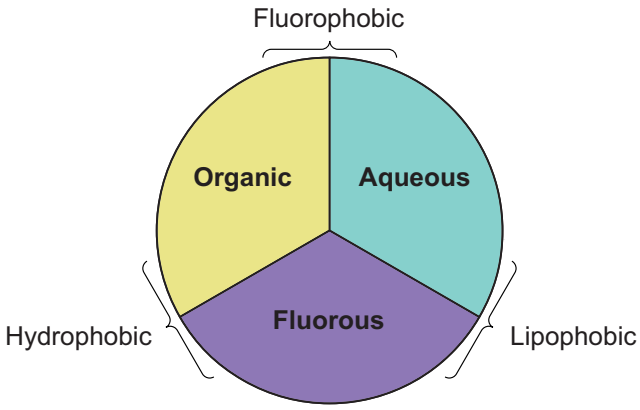

Figure III.5: Generic overview of three co-existent phases.

Not every molecule that contains fluorine atoms can be considered fluorous. Fluorinated aromatics, for example, are not included in this category, since they are characterised by a high polarity and polarisability.[5,7] In this context, the synthesis of fluorinated triazolinediones with either a fluorinated ponytail or a fluorinated aromatic group will be described in this section. Subsequently, after a first proof of concept of their reactivity in an interfacial system (section III.3.1.3), these compounds will be applied to functionalise various polydienes in Chapter IV, in which both the reactivity and the impact on the material properties of the 'real' fluorous component will be compared to its fluorinated aromatic counterpart.

III.3.1.1 Synthesis of a fluorinated alkyl-TAD

Werner and Curran previously reported on the successful synthesis of a urazole with a fluorinated ponytail by using 1*H*,1*H*,2*H*,2*H*-perfluorodecyl isocyanate in the straightforward Cookson method (section II.2.1.1).[8] A final oxidation step yielded the target fluorinated alkyl-TAD (R_FTAD, **85**, Scheme III.3). Nevertheless, since neither the isocyanate nor the precursor amine are nowadays readily available, 1*H*,1*H*,2*H*,2*H*-perfluorodecyl iodide (**86**) was used in this study as the auxiliary compound instead.

As depicted in Scheme III.3, two essentially different strategies were explored for the synthesis of the fluorinated alkylurazole. A first attempt consisted of the direct reaction between the iodide (**86**) and carboxyphenyl urazole (**87**), which was already available in our research group (Scheme III.3a). Because no evidence was found of a successful reaction, a more elaborate approach was investigated as well, using an amine (**88**) as intermediate for the synthesis of the corresponding urazole via an extended Cookson synthesis (Scheme III.3b and section II.2.1.3).

First, fluorinated iodide **86** was transformed into the corresponding azide (**89**) via a

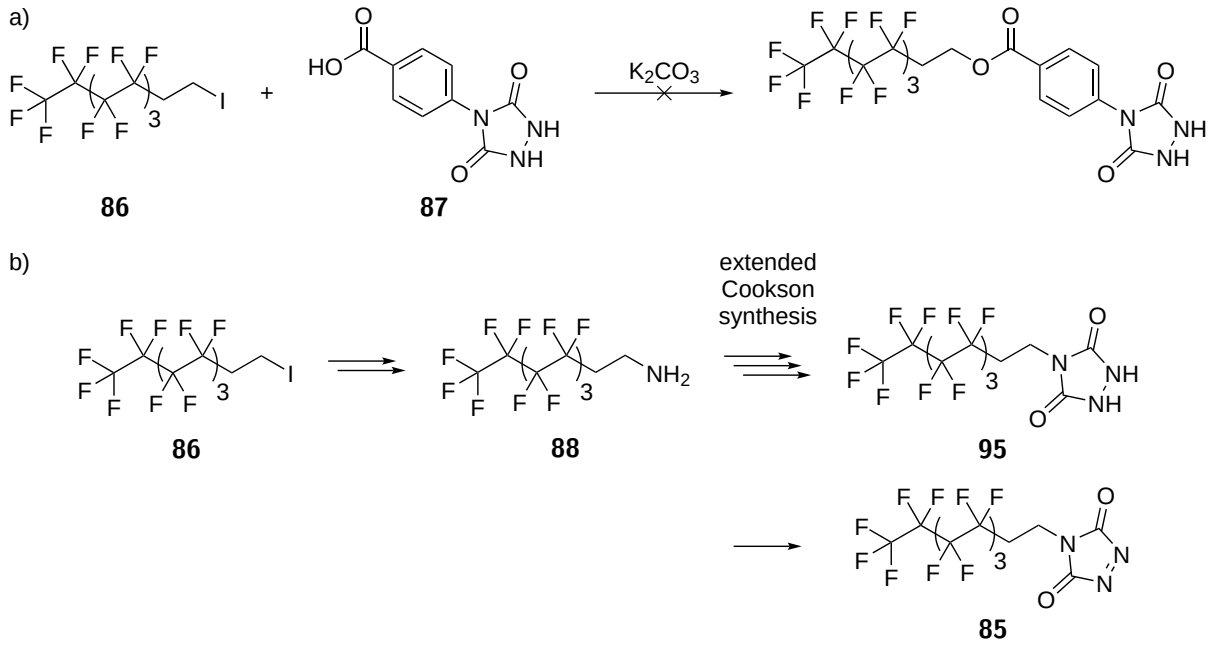

Scheme III.3: Overview of the different strategies to synthesise the fluorinated alkyl-urazole that is oxidised to R_FTAD in a final step. **(a)** First, an S_N2-reaction was tested between the iodide and carboxyphenyl urazole (**87**). **(b)** Alternatively, the iodide was transformed into an amine that can be used as an auxiliary for the extended Cookson synthesis.

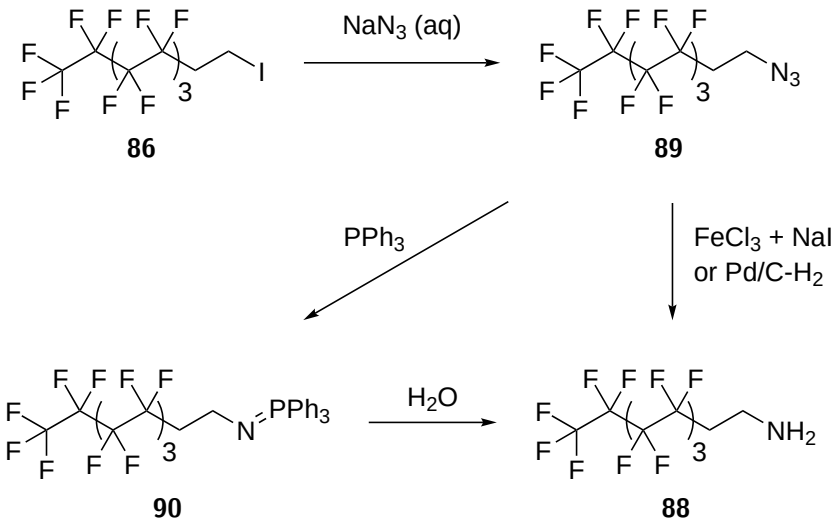

Scheme III.4: Overview of the different strategies to synthesise 1*H*,1*H*,2*H*,2*H*-perfluorodecyl amine (**88**).

procedure described by Szonyi and Cambon (Scheme III.4).[9] For this S_N2-reaction, an aqueous solution of NaN_3 was stirred with the iodide (**86**) at elevated temperatures using a quaternary ammonium salt as a phase transfer catalyst. By cooling the reaction mixture in a separation funnel, the fluorinated azide could easily be isolated in high yields (91 %).

The second step in the overall synthesis consisted of the reduction of the fluorinated azide to the corresponding amine (**88**). From the myriad of procedures that is available in literature for this type of reaction, three methods were selected that are known to be very robust. A first example is the well-known Staudinger reduction, in which the azide is reacted with a phosphine, *e.g.* triphenylphosphine, resulting in an iminophosphorane intermediate (**90**, Scheme III.4). Subsequent hydrolysis of this intermediate by the addition of water should readily yield the desired amine (**88**) and triphenylphosphine oxide. However, in this case, the expected product could not be obtained. Instead, next to triphenylphosphine oxide, an unidentified compound with a mass of 556 Da was detected in the mass spectrum of the crude mixture, which is 93 Da higher than the mass of the desired amine (463 Da). Because the same result was obtained both in ether and THF as solvents and the mass difference could not be explained by a predictable side reaction, the Staudinger reduction was judged unsuitable for the reduction of azide **89**.

An alternative method for the synthesis of the desired amine uses a combination of $FeCl_3$ and NaI. While this strategy is described in literature as a robust and fast technique for the reduction of azides,[10,11] no reaction could be observed in the case of azide **89**.

Therefore, also this procedure was not further investigated.

Finally, a simple hydrogenation was tested using hydrogen gas and palladium on carbon (Pd/C) as catalyst. No major issues were observed with this procedure, except for long reaction times of up to 72 hours, even when a fresh batch of Pd/C was added after 24 h. These long reaction times might be explained by the poisoning of the catalyst by the produced amine. Although the mass spectrum of the product suggests the presence of a side-product with a mass of 504 Da, next to the detected amine (463 Da), ^{1}H-NMR analysis showed the clean conversion of the fluorinated azide into the corresponding amine, without the presence of any unexplained resonances. While the reaction times might be improved by acidifying the reaction mixture or by using a pressurised vessel, we decided that a thorough optimisation is out of scope of this research, mainly because amine **88** used to be produced on a commercial scale.

Once the fluorinated amine was successfully obtained, it was transformed into the corresponding semicarbazide (**91**), *i.e.* the key intermediate in the (extended) Cookson synthesis. As discussed in section II.2.1.3, many different strategies are available to perform this reaction, either with an isocyanate or an activated carbonyl intermediate. First, triethylamine and triphosgene were sequentially added to a suspension of the amine in toluene, in an attempt to form the isocyanate intermediate (**92**, Scheme III.5a). However, subsequent addition of ethyl carbazate yielded a mixture of unreacted amine (**88**) and the target

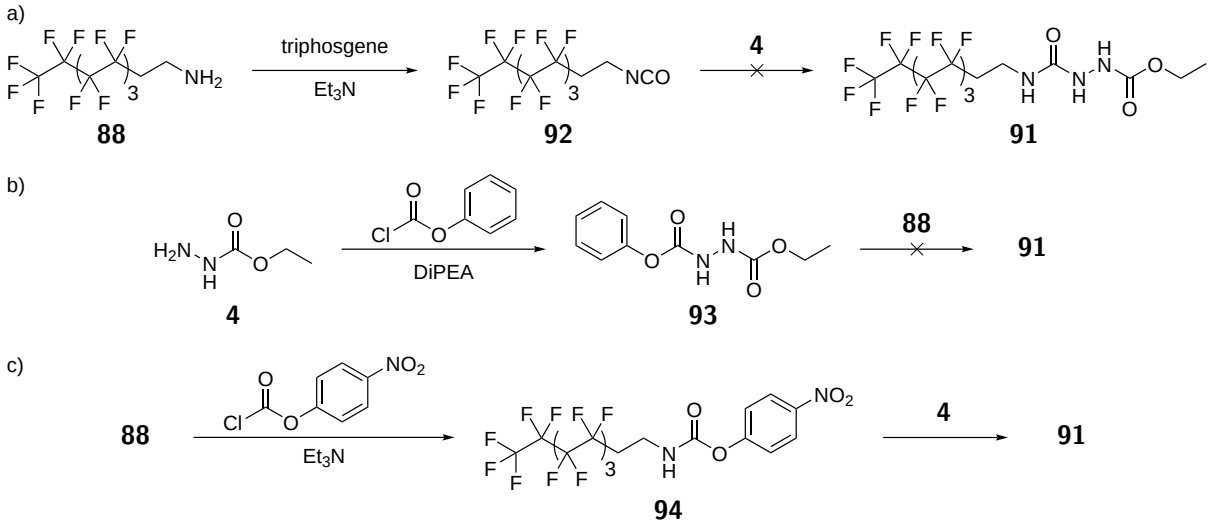

Scheme III.5: Overview of the different applied strategies to synthesise 1*H*,1*H*,2*H*,2*H*-perfluorodecyl semicarbazide (**91**), either with **(a)** an isocyanate or **(b, c)** an activated carbonyl intermediate.

semicarbazide (**91**), which might be explained by the limited solubility of the fluorinated compounds in the solvent. Moreover, some problems were encountered when trying to separate the formed triethylammonium chloride from the semicarbazide. For example, when water was added to the crude product to dissolve the salt, a gel-like substance was obtained which could not be filtered, most likely because of the combination of a hydrophobic ponytail and a polar semicarbazide. Therefore, this method was not further investigated for the synthesis of semicarbazide **91**.

Since the isocyanate-based route towards the fluorinated semicarbazide was unsuccessful, the reported isocyanate-free procedures were explored as well (Scheme II.7, section II.2.1.3). As a first example, the strategy developed by Breton and Turlington was applied, in which ethyl carbazate (**4**) was reacted with phenyl chloroformate to obtain ethyl phenyl hydrazine-1,2-dicarboxylate (**93**, Scheme III.5b).[12] This activated carbonyl derivative is a bench-stable solid that should readily react with aliphatic amines to form the corresponding semicarbazide. However, numerous attempts using different solvents such as toluene or acetonitrile, either at room temperature or at reflux, never resulted in the complete conversion of the amine into the semicarbazide, even after reacting for several days. Because the chromatographic purification of this type of fluorinated compounds is very tedious and the unreacted amine can react with the target triazolinedione (section II.3.3), a strategy using more reactive intermediates was investigated.

An alternative approach for the isocyanate-free synthesis of semicarbazides consists of the transformation of the amine, rather than ethyl carbazide, into an activated carbonyl derivative. In this strategy, the less reactive amine (**88**) was first treated with two equivalents of the highly reactive *p*-nitrophenyl chloroformate in the presence of triethylamine to yield the activated carbamate (**94**) as a synthetic equivalent of an isocyanate (Scheme III.5c). Next, an excess of ethyl carbazate was added, which resulted in a bright yellow reaction mixture caused by the formation of nitrophenol. Both ^{1}H-NMR and mass spectroscopy proved the successful formation of semicarbazide **91**, albeit in the presence of two side-products. The first originates from the reaction of the excess *p*-nitrophenyl chloroformate with two equivalents of ethyl carbazate, while the other is a small amount of fluorinated urea resulting from the reaction of amine **88** with activated carbamate **94**. Nevertheless, no extra purification steps were performed at this stage of the synthesis since neither of these

side-products were expected to negatively influence the following synthesis steps or to react with the final triazolinedione.

The final step of the urazole synthesis via the Cookson method generally consists of the cyclisation of the semicarbazide using alkaline conditions (section II.2.1.5). In a first attempt, this cyclisation was performed in 4 M aqueous potassium hydroxide solution at reflux temperature, as reported by Werner and Curran for this exact reaction.[8] Although the urazole (**95**, Scheme III.3) was indeed formed as expected, a significant amount of fluorinated amine (**88**) was found as a side-product. Since this amine was not present in the starting material, hydrolysis of the semicarbazide must occur as an important side reaction, next to the desired cyclisation. Therefore, milder cyclisation conditions were chosen by using a suspension of potassium carbonate in ethanol rather than the harsh potassium hydroxide solution. In this case, the urazole was successfully obtained while the amount of undesired amine was negligible.

Finally, the oxidation of urazole **95** to the target fluorinated alkyl-TAD (R_FTAD) proceeded by simply adding DABCO-Br, *i.e.* a heterogeneous oxidant (section II.2.3), to a suspension of the urazole in dichloromethane. Both the oxidant and unreacted urazole were readily filtered, yielding a solution of R_FTAD that can either be directly applied to modify unsaturated substrates or be concentrated *in vacuo* to switch solvents.

III.3.1.2 Synthesis of a fluorinated aryl-TAD

Next to the synthesis of a fluorinated triazolinediones with a so-called fluorinated ponytail, a TAD compound bearing a fluorinated aromatic group is targeted as well, in order to compare both the reactivity and the impact on the material properties of the 'real' fluorous compound to its fluorinated aromatic counterpart. Gilbertson and Ryan already reported on the synthesis of such a compound, *i.e.* 4-perfluorophenyl-TAD (PFPTAD),[13] which is undoubtedly the most simple fluorinated aryl-TAD suitable for this project. Similarly to this reported synthesis, pentafluoroaniline will be used as starting compound, mainly because it is readily available at a relatively low cost and thus applicable for the large-scale synthesis of triazolinediones.

The previous section already demonstrated multiple methods to synthesise triazolinediones from amines, using either an isocyanate or an activated carbonyl intermediate, albeit

with varying success. One of these methods uses ethyl phenyl hydrazine-1,2-dicarboxylate (**93**, Scheme III.5b) to transform an aliphatic amine into its corresponding semicarbazide, which is then converted to the TAD in two more steps. However, a more reactive hydrazine dicarboxylate is necessary to transform the less nucleophilic anilines. Indeed, Gilbertson and Ryan transformed ethyl carbazate into the very reactive carbonylchloride derivative using phosgene, which then reacted with pentafluoroaniline at elevated temperatures.[13] Nevertheless, rather than using the gaseous phosgene, we preferred to use triphosgene as a solid and safer alternative. Moreover, we found that the synthesis and isolation of the required ethyl carbazate derivative was very tedious, and therefore, we decided to react triphosgene with the aniline instead. The full synthetic scheme that was used to successfully synthesise 4-perfluorophenyl-TAD is shown in Scheme III.6.

First, the aniline (**96**) was transformed into the corresponding isocyanate (**97**). To this end, a solution of the aniline and Et_3N was added to a cooled solution of triphosgene in dry toluene. Once the reaction was complete, the semicarbazide (**98**) was easily obtained by filtering the reaction mixture, *i.e.* to remove the triethylammonium chloride, and by collecting the filtrate in a solution of ethyl carbazate (**4**) in toluene, after which **98** precipitated. The reaction conditions for the cyclisation of semicarbazide **98** to the corresponding urazole were adopted from literature,[13] which yielded pure perfluorophenyl

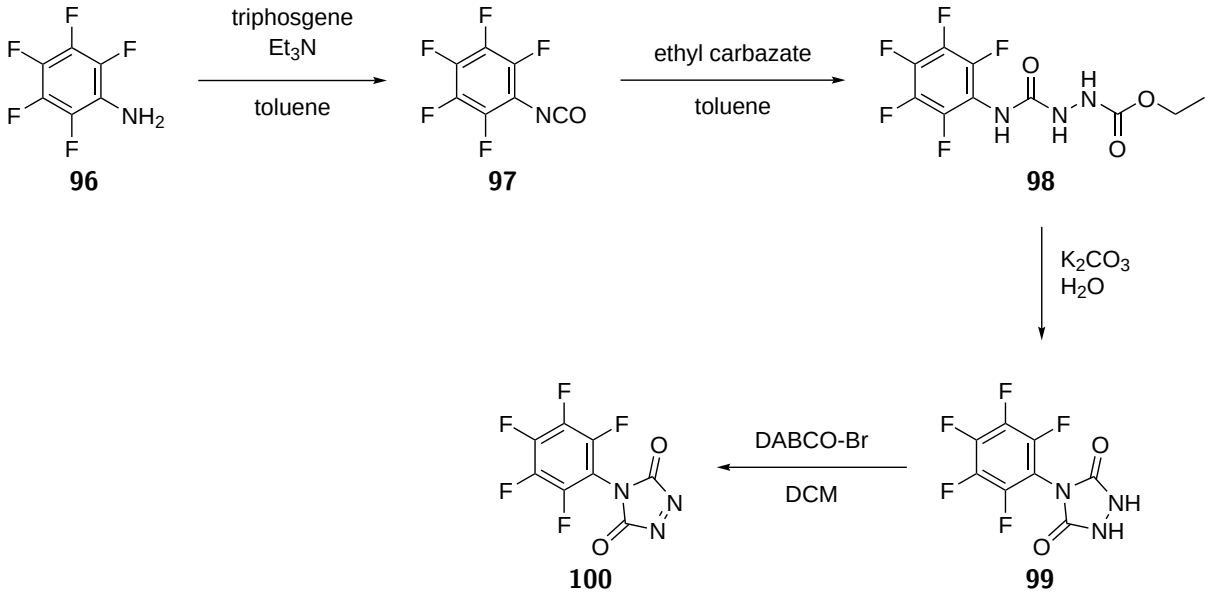

Scheme III.6: Overview of the synthesis of 4-perfluorophenyl-TAD using pentafluoroaniline as starting compound. First, **96** was transformed into the corresponding isocyanate (**97**), which was then converted into PFPTAD (**100**) via the Cookson method.

urazole (**99**) after recrystallisation. Again, the target fluorinated aryl-TAD (**100**, PFPTAD) was obtained by a final oxidation of the urazole using DABCO-Br in dichloromethane. It should be noted that PFPTAD proved to be too reactive to be isolated and was always applied immediately after the oxidation, either directly as filtered oxidation mixture or after a solvent switch by evaporating most of the solvent *in vacuo* and subsequently diluting with the desired solvent.

III.3.1.3 Reactivity assessment of the fluorinated triazolinediones for surface modifications

In this section, we describe a proof of concept that demonstrates the reactivity of the synthesised triazolinediones in an interfacial system by chemically modifying the surface of an unsaturated material with both R_FTAD and PFPTAD. To this end, a new batch of the previously described network based on ($IPDI_3$)–citronellol and MDI-TAD was prepared (section III.2), in which residual unsaturations were introduced by using an excess of the trivalent alkene during the polymerisation (alkene:TAD = 1.25). Different pieces of this material were then dipped for 30 minutes in a 55 mM solution of each of the triazolinediones, allowing the C=C bonds at the surface to react with the fluorinated TADs in solution. Finally, the samples were thoroughly rinsed with acetone and dried in a stream of nitrogen.

Because the synthesised networks are all characterised by a wrinkled surface, contact angle measurements cannot be performed on this kind of materials to confirm the modification. Nevertheless, since fluorine is an element unique to the introduced triazolinediones, a successful functionalisation can be verified by analysing the materials with a technique providing information on the elemental composition. Indeed, energy-dispersive X-ray spectroscopy with electron beam excitation (SEM-EDX) clearly shows the presence of fluorine in the modified samples while the signal is absent in the unmodified network, thereby proving the successful modification of the networks via a dip-coating approach (Figure III.6).

In conclusion, two essentially different fluorinated triazolinediones were successfully synthesised and subsequently applied for the surface modification of unsaturated materials. The potential of these compounds as reactive additives for various commercial polydienes, as well as their impact on the material properties, will be further explored in Chapter IV.

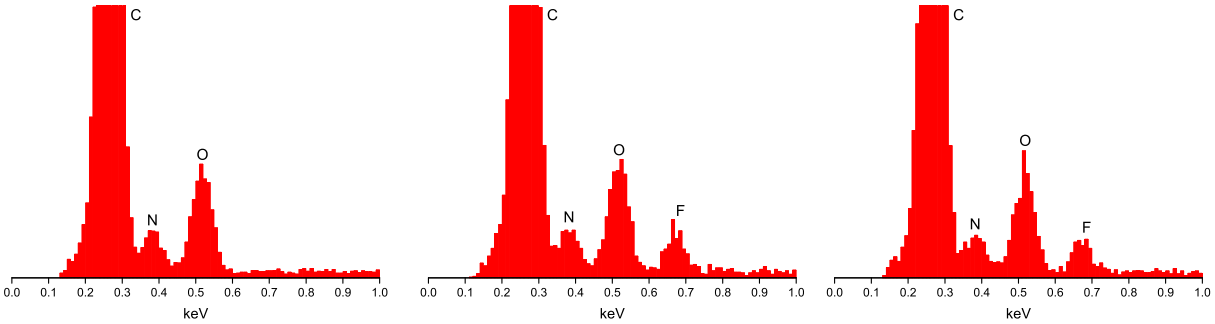

Figure III.6: Both **(a)** the unmodified network and the networks that were modified with either **(b)** R_FTAD or **(c)** PFPTAD were analysed via SEM-EDX. Fluorine is absent in the bare material while its signal is clearly visible for the modified materials, thereby proving the successful modification of the networks.

III.3.2 Synthesis of triazolinedione-modified dyes

While triazolinediones are in general characterised by a bright red colour, most Diels-Alder or Alder-ene adducts are colourless, which results in a visual feedback system to qualitatively judge when a homogeneous reaction is complete. Nevertheless, an excess of reagent is typically used in the case of surface modifications via the versatile dip-, spray- or spin coating techniques, rendering this visual feedback system useless.[14–17] Moreover, after the modification procedure, specialised surface characterisation techniques, such as time-of-flight secondary ion mass spectrometry (ToF-SIMS) or X-ray photoelectron spectroscopy (XPS), are generally required to prove that the compound is indeed covalently attached to the surface (*cf.* section III.3.1.3).

In this section, the synthesis of triazolinedione-modified dyes will be discussed, which can be used to visually confirm a successful surface modification after soxhlet extraction. To this end, some potential auxiliaries were selected from the myriad of commercially available dyes, since the compound should contain a functional group that can be transformed in a triazolinedione, while it should lack functionalities that are incompatible with the TAD chemistry. Therefore, the starting compounds described herein are not the only options, but were judged to have the highest chance of success with the length and scalability of the synthetic procedure in mind. Next to the easy visualisation of (irreversible) surface modifications, these dyes were anticipated to be useful for the visualisation of interfacial transclick processes, the covalent colouring of bulk materials or as a probe for unsaturations in screening applications.

III.3.2.1 TAD-functional Sudan II

As a first example of a TAD-modified dye, the dark red azo dye 'Sudan II' (**101**), containing a phenolic alcohol as functional handle, was selected as the starting compound. Despite the low solubility of Sudan II, it was successfully applied as a nucleophile in the S_N2-reaction with ethyl 4-bromobutyrate (**102**) using DMSO as the solvent (Scheme III.7). The resulting ethyl ester (**103**) was readily hydrolysed in a next step to obtain a carboxylic acid-functional Sudan II dye (**104**), which can be used as an auxiliary for the synthesis of urazoles via the extended Cookson synthesis (section II.2.1.2). Consequently, the acid was first stirred with diphenyl phosphoryl azide in the presence of triethylamine to form the corresponding acyl azide, which was then transformed into the isocyanate via a Curtius rearrangement by simply heating the reaction mixture. Addition of ethyl carbazate and an alkaline cyclisation step yielded the dye-functional urazole (**105**), which is oxidised in the final step to the target triazolinedione (Sudan II-TAD, **106**). It should be noted that this specific triazolinedione does not provide the aforementioned visual feedback because the colour of the attached azo dye is very similar to that of the TAD moiety.

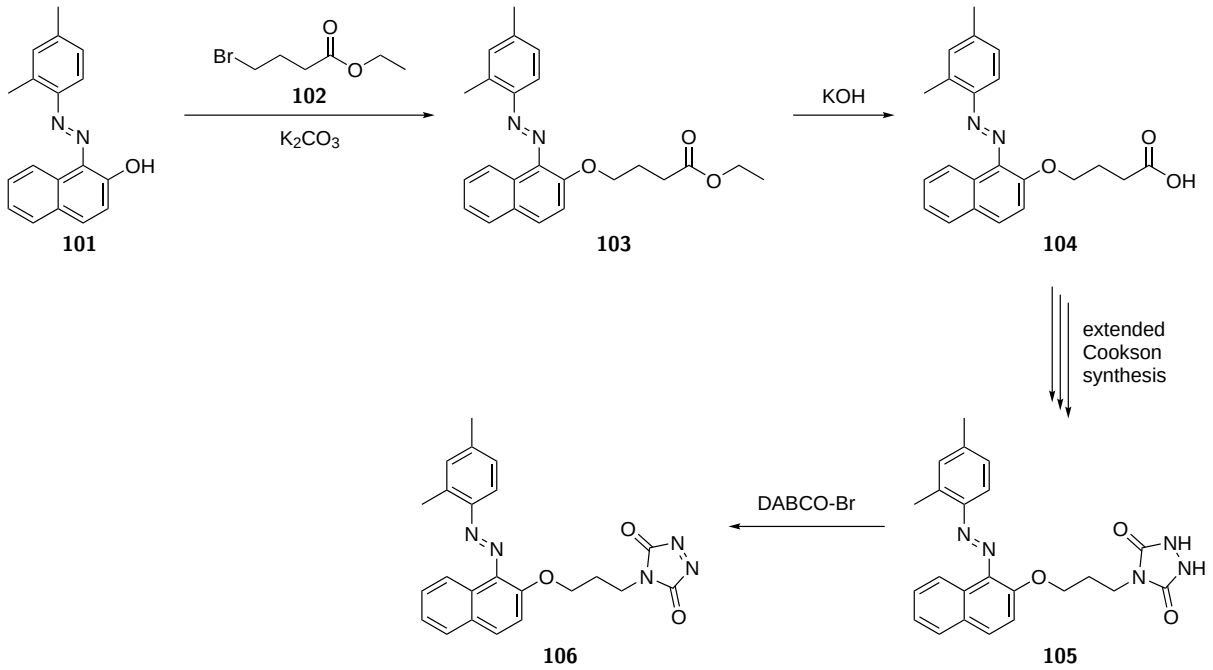

Scheme III.7: Overall reaction scheme for the synthesis of the TAD-modified Sudan II (**106**). First, an ethyl ester was attached to the Sudan II core (**103**), which could be hydrolysed in a next step. The Sudan II-urazole (**105**) was obtained from this carboxylic acid via an extended Cookson synthesis and finally oxidised to the target Sudan II-TAD.

Similar to the reactivity assessment of the fluorinated TADs (section III.3.1.3), the ($IPDI_3$)–citronellol-based network with residual unsaturations was submerged for 30 minutes in a 55 mM solution of the Sudan II-TAD in acetone. Moreover, this experiment was repeated with the non-reactive Sudan II (**101**) as a reference for the sample treated with the triazolinedione. Both the obtained samples are intensely coloured red, albeit with a slightly different tint (Figure III.7). Nevertheless, after a soxhlet extraction for 5 hours with acetone, the dye was almost completely leached out of the reference material, while the TAD-treated network partially retained the red colour.

Despite this successful chemical modification of a network with a dye-functional TAD, the result was not really convincing. As shown in Figure III.7, the soxhlet extraction significantly decreased the intensity of the colour, which indicates leaching of the dye in the chemically modified sample as well. Moreover, when this dye was used to modify the diene end-group of a polymer,[18] three equivalents of Sudan II-TAD were necessary to obtain a full conversion, while the polymer contained a significant amount of low molecular weight compounds after the modification, as determined by size exclusion chromatography. Because of these observations, we decided to verify the purity of urazole **105**, although the ^{1}H-NMR spectrum was interpreted as a mixture of *cis*- and *trans*-azo isomers. Indeed, column chromatography (80 % to 100 % ethyl acetate:hexane) combined with 2D NMR-analysis of the eluting fractions confirmed the presence of these two isomers, as well as two side-products that were identified as Sudan II and 4-(3-hydroxypropyl)urazole.

Since the semicarbazide-bearing dye (**107**) is purified prior to cyclisation, the aforemen-

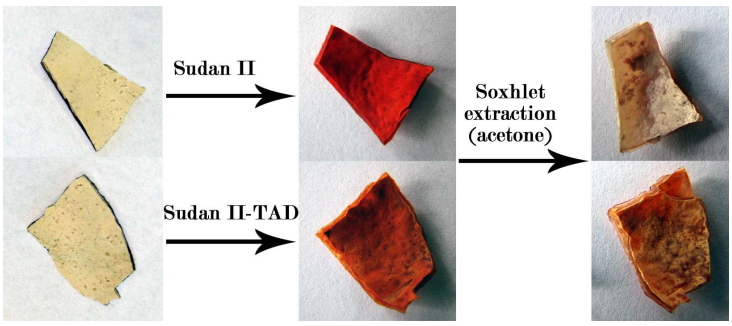

Figure III.7: When a network with residual unsaturations is dipped in a solution of either Sudan II (**101**, top, reference) or Sudan II-TAD (**106**, bottom), both materials are intensely coloured. This colour almost completely disappeared from the reference material after a soxhlet extraction, while the chemically modified material retained its colour to a certain extent.

tioned side-products must be generated during the urazole cyclisation step itself. A possible mechanism is depicted in Scheme III.8 and involves the decomposition of the initially formed urazolyl anion (**108**). Indeed, because of the low pK_a of the urazole moiety, the refluxing reaction mixture will contain the urazole salt (section II.2.1.5) and, after decomposition, cyclic intermediate **109** as well as the potassium salt of Sudan II (**110**). The acidic work-up finally yields the observed mixture of Sudan II-urazole (**105**), Sudan II (**101**) and 4-(3-hydroxypropyl)urazole (**111**).

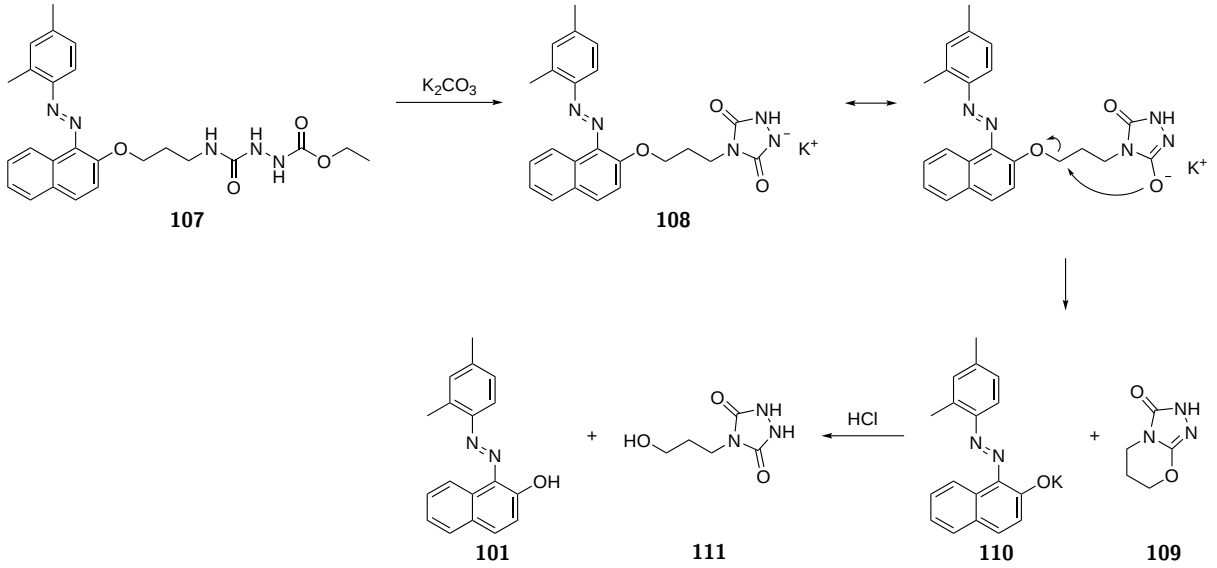

Scheme III.8: Proposed mechanism for the generation of Sudan II (**101**) and 4-(3-hydroxypropyl)urazole (**111**), two side-products that were identified after the cyclisation of the semicarbazide-bearing dye (**107**).

In conclusion, the synthesis of a TAD-bearing red dye and its application to covalently colour a material with residual unsaturations was demonstrated in this section. However, since the proposed decomposition mechanism of the urazole precursor (Scheme III.8) is also valid for the TAD-ene adducts and can – in theory – also occur under neutral or acidic conditions, many stability issues can be expected for applications with this reactive dye. Moreover, the overall synthetic procedure is long, low-yielding and requires multiple chromatographic purifications. Therefore, we decided to not further use this compound within the framework of this thesis and searched for a better alternative that avoids the aforementioned issues.

III.3.2.2 Synthesis of azobenzene-TAD

Because all the red Sudan-type dyes are based on the general 1-arylazo-2-naphthol scaffold, the same issues as discussed in the previous section will occur when a similar compound is used as an auxiliary for the TAD synthesis. Therefore, the orange-yellow 4-aminoazobenzene (**112**) was selected as alternative starting compound, which lacks this troublesome naphthol group, yet contains an amine that can be directly turned into a urazole via the extended Cookson synthesis. While the resulting TAD compound can be expected to be more reactive than PhTAD, for example, as a result of the electron-withdrawing azo substituent, generation of triazolinediones *in situ* is a common practice for the most reactive variants (sections II.1 and III.3.1.2).

Besides the generation of the isocyanate from the aniline using triphosgene, 4-(4-azobenzene)-urazole could be synthesised via the most straightforward variant of the Cookson synthesis (Scheme III.9). The isocyanate was separated from the triethylammonium salt by a simple filtration and collected in a solution of ethyl carbazate (**4**) to form the semicarbazide intermediate (**113**). This intermediate was then cyclised in an aqueous KOH solution to obtain the corresponding urazole (**114**) that was readily oxidised to the target triazolinedione

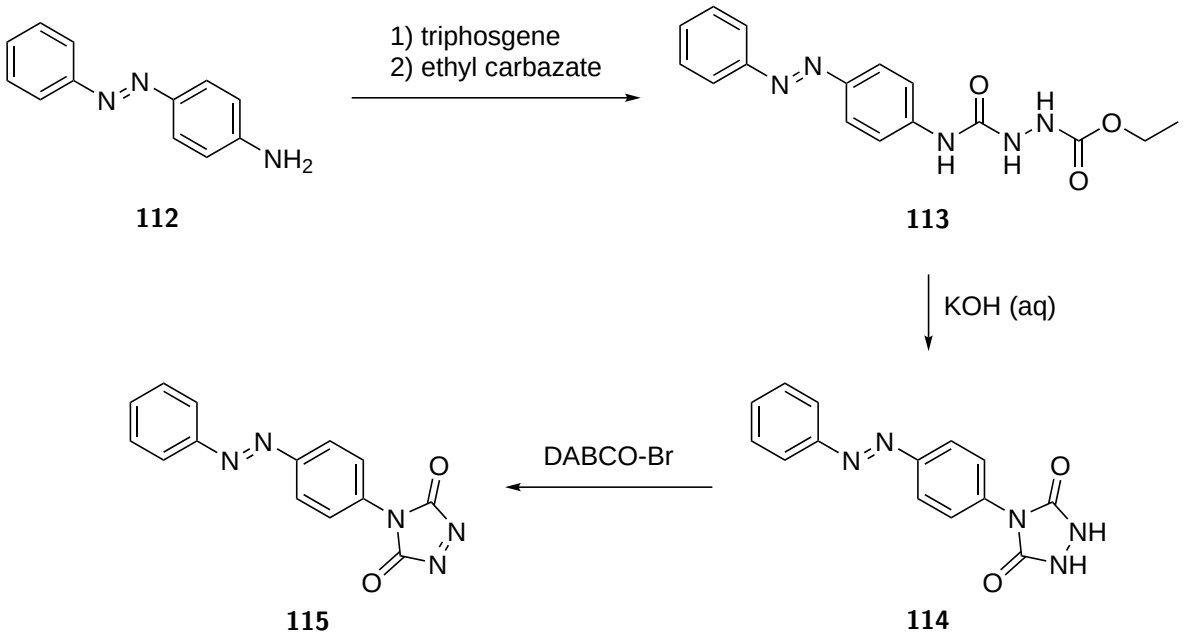

Scheme III.9: Overview of the synthesis of 4-(4-azobenzene)-TAD (**115**) using 4-aminoazobenzene (**112**) as starting compound. Once the isocyanate was generated, 4-(4-azobenzene)-urazole (**114**) was readily obtained via a standard Cookson synthesis.

(azobenzene-TAD, **115**). While the TAD is not isolated, the azobenzene-urazole synthesis easily outperforms that of the Sudan II-urazole in terms of experimental work and overall yield, *i.e.* 54 % for **114** compared to 26 % for **105**. Moreover, the reactions involving this dye can again be monitored visually since the orange and red colour of the azobenzene and TAD moeieties, respectively, are easily distinguishable.

Again, the applicability of the azobenzene-TAD for surface modifications was investigated by submerging a (HDI_3)–citronellol-based network with residual unsaturations for 30 minutes in a 55 mM solution of either the triazolinedione or 4-aminoazobenzene, *i.e.* the reference experiment. As displayed in Figure III.8, both the chemical and physical modifications yielded orange coloured materials, which were visually indistinguishable. However, after a soxhlet extraction for 5 hours with acetone, the difference between both substrates could be observed as a result of the leaching of the physisorbed dye. Moreover, because the colour of the TAD-modified material remained unchanged, this azobenzene-TAD clearly outperforms the previously discussed Sudan II-based triazolinedione for a chemical modification of unsaturated substrates.

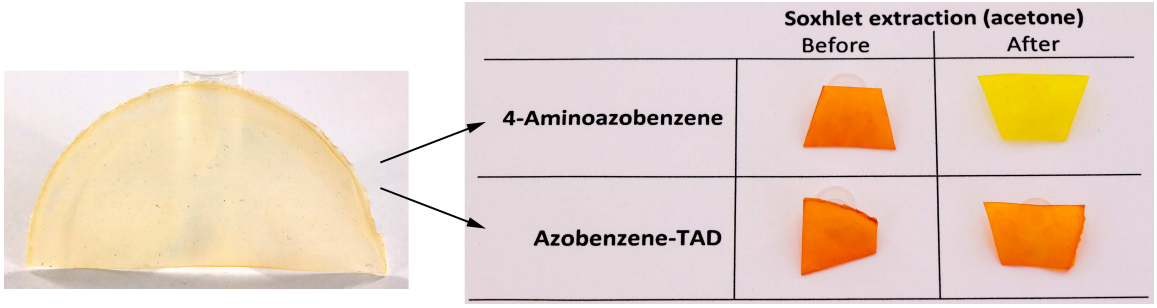

Figure III.8: Modification of a network with residual unsaturations using azobenzene-TAD (**115**). After a soxhlet extraction, the colour leached significantly from the reference material, submerged in 4-aminoazobenzene, whereas the colour did not fade in the case of the chemically modified material.

In summary, a versatile and scalable synthetic procedure for a TAD-bearing orange dye was discussed in this section. While a first proof of concept clearly showed its suitability for surface modifications, further applications in the framework of this thesis have not been explored. However, within the scope of another ongoing PhD dissertation in our group, it was successfully applied to visually demonstrate a transclick cascade reaction.[19]

III.3.2.3 Modification of Martius Yellow

While an orange triazolinedione-functional azo dye could eventually be synthesised via a scalable procedure, Martius Yellow (**116**) was investigated as a starting compound in order to obtain a yellow TAD-dye instead. In a similar approach compared to the modification of Sudan II (section III.3.2.1), this compound was first reacted with ethyl 4-bromobutyrate (**102**) to obtain an ethyl ester that could be further modified to the triazolinedione (Scheme III.10). However, the reaction was hampered by a low conversion, which could not be improved by varying the reaction temperature or equivalence of the reagents. Moreover, the isolation of the butyrate ester (**117**) via chromatography on silica gel proved to be impossible as a result of co-elution of the starting compound.

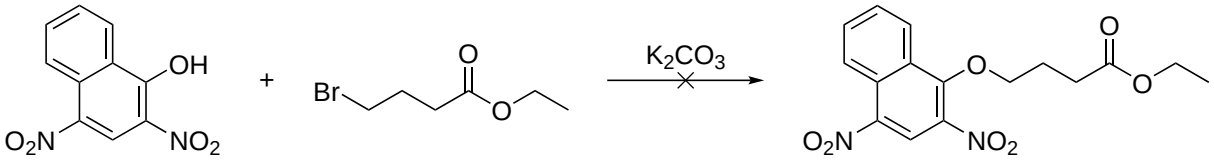

116 **102** **117**

Scheme III.10: Attempted modification of Martius Yellow via an S_N2-reaction with ethyl 4-bromobutyrate (**102**), similarly to the previously discussed modification of Sudan II (section III.3.2.1). The conversion proved to be low and the desired product (**117**) could not be isolated.

In an attempt to improve the alkylation of the alcohol in Martius Yellow, either α,α'-dibromo-*p*-xylene[20] or ethyl chloroacetate were used rather than ethyl 4-bromobutyrate in the previous synthesis, which were expected to react faster as a result of π^*-stabilisation of the LUMO. Nevertheless, similar problems were encountered for the xylene derivative, while only the reagents were recovered when the mixture with ethyl chloroacetate was heated to 120 °C for 4 days. Therefore, we assumed that the strong electron withdrawing effect of the nitro substituents resulted in a phenolate anion that was not nucleophilic enough for an efficient S_N2-reaction and decided to not further investigate this strategy.

III.3.2.4 Fluorescent TAD based on 4-chloro-7-nitro-1,2,3-benzoxadiazole

As a final example of the synthesis of TAD-bearing dyes, 4-chloro-7-nitro-1,2,3-benzoxadiazole (NBD-Cl, **118**) was investigated as a possible auxiliary for a triazolinedione. While this faint yellow compound is not useful as such, it is known to yield an orange compound with a green fluorescence when the chlorine is substituted by an amine.[21–23]

Initially, NBD-Cl was reacted with 4-(6-aminohexyl)-urazole hydrochloride (**119**),[2] in an attempt to synthesise a fluorescent urazole (**120**) in one step (Scheme III.11a). Although the reaction mixture quickly coloured dark brown after the addition of the functional urazole and the base, only the starting material was recovered from the reaction mixture after stirring for 16 hours. A possible explanation can be found in the acidity of the urazole moiety, which could result in the precipitation of a urazolyl ammonium salt from the basic solution in acetonitrile.

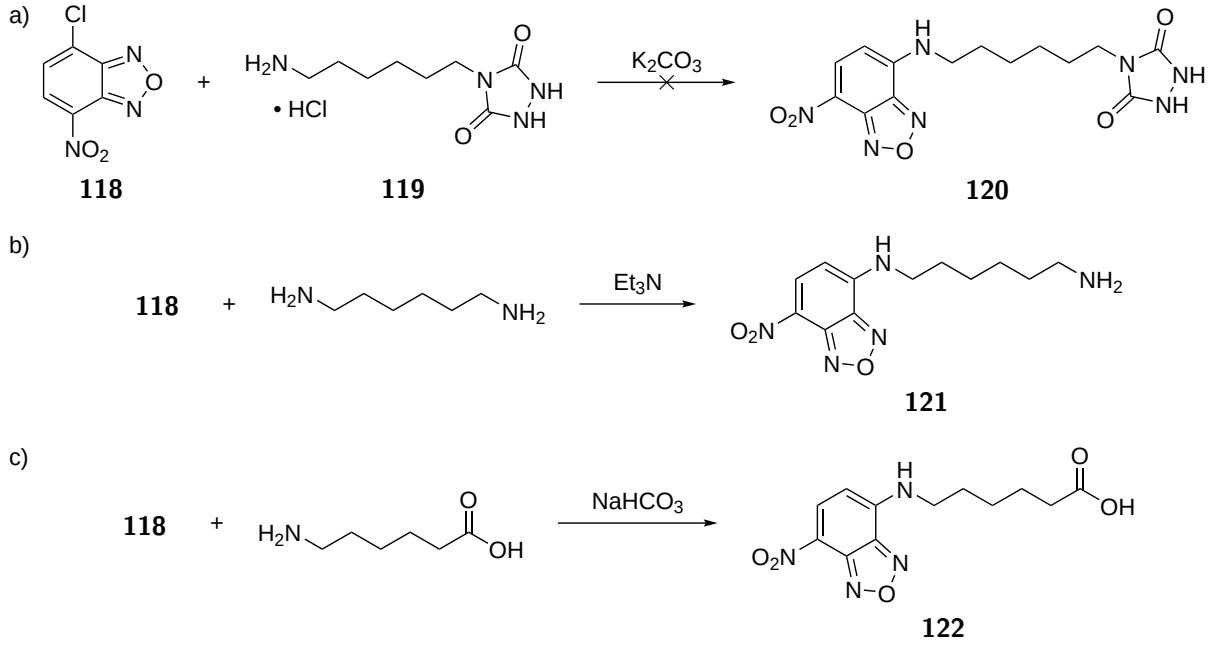

Scheme III.11: A nucleophilic aromatic substitution of the chlorine in **118** by an amine was tested for the production of a fluorescent urazole, either **(a)** by directly reacting an amine-functional urazole (**119**)[24] or by introducing a functional group that can be transformed to a urazole, *i.e.* **(b)** an amine[25] or **(c)** a carboxylic acid.[23]

Alternatively, a functional group may be attached on the nitrobenzoxadiazole (NBD) from which a urazole can be synthesised via an extended Cookson method. As demonstrated in the previous sections, both amines and carboxylic acids are readily transformed to the corresponding semicarbazide. Consequently, both an amine- (**121**) and a carboxylic acid-functional (**122**) NBD derivative were synthesised by reacting NBD-Cl (**118**) with 1,6-diaminohexane and 6-aminocaproic acid, respectively (Scheme III.11b and c). While both syntheses yielded the desired product, the amine (**121**) was contaminated with the double adduct, *i.e.* the product of this amine and another equivalent of NBD-Cl, whereas the acid (**122**) could be isolated by a simple precipitation in high yields and was therefore the preferred intermediate for further reactions.

Similarly to the synthesis of the TAD-bearing Sudan II dye (section III.3.2.1), the next step consisted of a Curtius rearrangement, allowing the conversion of the fluorescent carboxylic acid to its corresponding semicarbazide. Although this NBD semicarbazide was successfully produced, the low solubility of NBD derivatives not only troubled the synthesis, it also caused the separation of the semicarbazide from triethylammonium diphenyl phosphate, originating from DPPA (section II.2.1.2), to remain an unsolved issue until now. Nevertheless, we strongly believe that the solubility issues can be turned into an advantage for the purification by further optimising the procedure in future research, which should eventually lead to a versatile synthetic procedure for a fluorescent triazolinedione.

III.4 Conclusions and perspectives

This chapter first showed a straightforward strategy to obtain triazolinedione-based networks, in which a residual amount of unsaturations is easily introduced by using an excess of the corresponding monomer. By changing the structure of this monomer, both the cross-linking kinetics and the T_g of the final material could be greatly varied. From a practical point of view, citronellol-based networks were preferred as model materials for further TAD-modifications because of the reaction kinetics that allow for a fast gelation, yet provide enough time for moulding of the reaction mixture. While the thermal characteristics could be further tuned when necessary by varying the core structure of the monomer, the T_g of all the materials was well above the application temperature, resulting in no further preference on the exact composition for the intended application.

Next, two essentially different fluorinated triazolinediones were synthesised and successfully applied for the surface modification of unsaturated materials. A follow-up study on the potential of these compounds as functional and reactive additives for various commercial polydienes, will be discussed in a dedicated chapter (Chapter IV).

While the presence of most triazolinediones on a smooth surface can be demonstrated via contact angle goniometry, the successful modification of a rough surface can only be confirmed by advanced surface characterisation techniques. Therefore, this chapter also investigated the synthesis of various triazolinedione-bearing dyes, which allow a fast visual confirmation of a successful modification. Although both a red Sudan II-based and an

orange azobenzene-based dye were successfully functionalised with a TAD moiety, only the latter compound proved to be stable enough for further applications while it was obtained via a more versatile and scalable procedure.

Finally, a carboxylic acid bearing an NBD-group, *i.e.* a fluorescent tag, was synthesised in high yields, which could be transformed into the corresponding semicarbazide via a Curtius rearrangement. However, the purification of the latter intermediate proved to be problematic as a result of the low solubility of NBD derivatives. Therefore, more research will be needed to complete and to optimise this synthetic procedure. Nevertheless, the current promising results suggest an easily accessible TAD-bearing fluorescent dye that can be applied as a semi-quantitative indicator in polymer chemistry or biochemical research.

III.5 Experimental section

All materials, solvents and their corresponding purification are presented in appendix A.

III.5.1 Synthesis

III.5.1.1 Trivalent alkenes or dienes

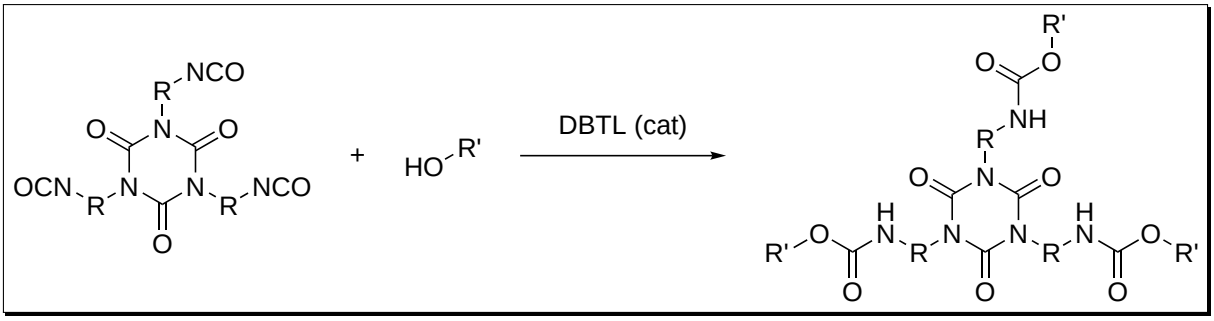

(HDI_3)–HDEO

In a 250 mL flask, 30 g HDI_3 (59.5 mmol, 1 eq) was dissolved in 150 mL ethyl acetate. To this solution, 17.5 g *trans,trans*-2,4-hexadien-1-ol (HDEO, 179 mmol, 3 eq) was added, followed by 100 µL dibutyltin dilaurate (DBTL) as catalyst. The mixture was stirred overnight under an inert atmosphere, after which the product was obtained by evaporating the solvent *in vacuo*.

Yield: 44.276 g yellow solid (55.41 mmol, 93 %).

Bruto formula: $C_{42}H_{66}N_6O_9$.

MW.: 799.02 g/mol.

Diene equivalent: 3.75 mmol/g.

ESI-MS (m/z): 857.5 $[MOAc]^-$.

^{1}H-NMR (300 MHz, $CDCl_3$): δ (ppm) = 1.34 (quint, 12 H, N−CH_2−CH_2−CH_2−CH_2), 1.49 (quint, 6 H, CO−NH−CH_2−CH_2), 1.63 (quint, 6 H, N−CH_2−CH_2), 1.75 (d, 9 H, CH_3−CH), 3.15 (q, 6 H, CO−NH−CH_2), 3.85 (t, 6 H, N−CH_2), 4.54 (d, 6 H, O−CH_2), 4.80 (br. t, 3 H, N−H), 5.61 (quint, 3 H, CH_3−CH), 5.73 (m, 3 H, CH_3−CH=CH), 6.04 (t, 3 H, CH_2−CH=CH), 6.23 (q, 3 H, CH_2−CH).

(TDI_3)–HDEO

In a 100 mL flask, 5.10 g TDI_3 (9.76 mmol, 1 eq) was dissolved in 50 mL toluene. To this solution, 2.87 g HDEO (29.3 mmol, 3 eq) was added, followed by 50 µL DBTL as catalyst. The mixture was stirred overnight under an inert atmosphere, after which the product was obtained by evaporating the solvent *in vacuo*. The product was not sufficiently soluble in common deuterated solvents to measure a ^{1}H-NMR spectrum.

Yield: 5.5 g yellow solid (6.73 mmol, 69 %).

Bruto formula: $C_{45}H_{48}N_6O_9$.

MW.: 816.91 g/mol.

Diene equivalent: 3.67 mmol/g.

ESI-MS (m/z): 815.3 $[M-H]^-$.

($IPDI_3$)–HDEO

In a 250 mL flask, 32.8 g $IPDI_3$ (49.2 mmol, 1 eq) was dissolved in 150 mL toluene. To this solution, 14.5 g HDEO (148 mmol, 3 eq) was added, followed by 100 µL DBTL as catalyst. The mixture was stirred overnight under an inert atmosphere, after which the product was obtained by evaporating the solvent *in vacuo*.

Yield: 41.079 g yellow solid (42.73 mmol, 87 %).

Bruto formula: $C_{54}H_{84}N_6O_9$.

MW.: 961.30 g/mol.

Diene equivalent: 3.12 mmol/g.

ESI-MS (m/z): 1019.6 $[MOAc]^-$.

^{1}H-NMR (300 MHz, $CDCl_3$): δ (ppm) = 6.23 (q, 3 H, CH_2-CH), 6.04 (t, 3 H, $CH_2-CH=CH$), 5.74 (m, 3 H, $CH_3-CH=CH$), 5.63 (m, 3 H, CH_3-CH), 4.54 (t, 6 H, $O-CH_2$), 1.76 (d, 9 H, CH_3-CH), 2.96 (m, 3 H, $NH-CH$), 3.73 (m, 6 H, $N-CH_2$), 0.81–1.00 (m, 18 H, $Cq-(CH_3)_2$), 1.06 (s, 9 H, $(CH_2)_3-Cq-CH_3$), 1.11 (s, 6 H, $Cq-CH_2-Cq$), 5.03 (m, 3 H, N−H), 1.17–1.46 (m, 12 H, $NH-CH-(CH_2)_2$).

(HDI_3)–citronellol

In a 50 mL flask, 5.20 g HDI_3 (9.91 mmol, 1 eq) was cooled to 0 °C under an inert atmosphere. 5.64 mL citronellol (29.7 mmol, 3 eq) was added, followed by 50 µL DBTL as catalyst, after which the mixture was homogenised. After a few minutes, the magnetic stirrer stopped

as a result of a rise in viscosity. The (HDI_3)–citronellol could be used as such for further reactions.

Yield: 8.39 g colourless viscous oil (8.62 mmol, 87 %).

Bruto formula: $C_{54}H_{96}N_6O_9$.

MW.: 973.40 g/mol.

Alkene equivalent: 3.08 mmol/g.

ESI-MS (m/z): 973.7 $[MH]^+$.

^{1}H-NMR (300 MHz, $CDCl_3$): δ (ppm) = 0.92 (d, 9 H, CH−CH_3), 1.19 (m, 3 H, CH_3−CH), 1.28–1.72 (m, 54 H, N−CH_2−CH_2−CH_2−CH_2−CH_2−CH_2−NH + O−CH_2−CH_2 + CH_2−CH_2−CH + Cq−(CH_3)$_2$), 1.98 (m, 6 H, CH_2−CH−Cq), 3.16 (q, 6 H, NH−CH_2), 3.86 (t, 6 H, N−CH_2), 4.09 (m, 6 H, O−CH_2), 4.69 (br. s, 3 H, N−H), 5.09 (t, 3 H, CH−Cq).

(TDI_3)–citronellol

In a 50 mL flask, 5.10 g TDI_3 (9.76 mmol, 1 eq) was cooled to 0 °C under an inert atmosphere. 5.35 mL citronellol (29.28 mmol, 3 eq) was added, after which the mixture solidified. 50 µL DBTL was added as catalyst and the blend was allowed to heat to room temperature to obtain a homogeneous mixture. The reaction was stirred overnight, after which the product was ready for further reactions *in vacuo*.

Yield: 7.8 g colourless viscous oil (7.87 mmol, 81 %).

Bruto formula: $C_{57}H_{78}N_6O_9$.

MW.: 991.28 g/mol.

Alkene equivalent: 3.03 mmol/g.

ESI-MS (m/z): 989.6 $[M-H]^-$.

^{1}H-NMR (300 MHz, $CDCl_3$): δ (ppm) = 0.93 (d, 9 H, CH−CH_3), 1.13–1.24 (m, 3 H, CH_3−CH), 1.32–1.45 (m, 6 H, O−CH_2−CH_2), 1.57 (t, 6 H, CH−CH_2−CH_2), 1.61 (s, 9 H, Cq−CH_3), 1.69 (s, 9 H, Cq−CH_3), 2.00 (m, 6 H, CH−CH_2), 2.27 (s, 9 H, Ar−CH_3), 3.69 (m, 6 H, O−CH_2), 5.11 (t, 3 H, Cq=CH), 7.02 (d, 3 H, Ar−H), 7.24 (d, 3 H, Ar−H), 7.39 (s, 3 H, Ar−H), 8.02 (s, 3 H, N−H).

($IPDI_3$)–citronellol

In a 50 mL flask, 3.61 g $IPDI_3$ (5.41 mmol, 1 eq) was cooled to 0 °C under an inert atmosphere. 2.96 mL citronellol (16.2 mmol, 3 eq) was added, followed by 50 µL DBTL as

catalyst, after which the mixture was homogenised. After a few minutes, the magnetic stirrer stopped as a result of a rise in viscosity. The ($IPDI_3$)–citronellol could be used as such for further reactions.

Yield: 5.65 g colourless viscous oil (4.98 mmol, 92 %).

Bruto formula: $C_{66}H_{114}N_6O_9$.

MW.: 1135.67 g/mol.

Alkene equivalent: 2.64 mmol/g.

ESI-MS (m/z): 1135.8 $[MH]^+$.

^{1}H-NMR (300 MHz, $CDCl_3$): δ (ppm) = 0.80–1.00 (m, 27 H, $(CH_2)_2$−Cq−$(CH_3)_2$ + CH_3−CH), 1.07 (s, 9 H, $(CH_2)_3$−Cq−CH_3), 1.12 (s, 6 H, Cq−CH_2−Cq), 1.17–1.46 (m, 15 H, O−CH_2−CH_2−CH−CH_2), 1.48–1.78 (m, 30 H, CH=Cq−$(CH_3)_2$ + NH−CH−$(CH_2)_2$), 1.97 (m, 6 H, Cq=CH−CH_2), 2.96 (m, 3 H, NH−CH), 3.73 (m, 6 H, N−CH_2), 4.07 (m, 6 H, O−CH_2), 5.09 (t, 3 H, CH=Cq), 8.42 (br. s, 3 H, N−H).

(HDI_3)–oleyl alcohol

In a 100 mL flask, 15.0 g HDI_3 (29.7 mmol, 1 eq) was dissolved in 50 mL toluene. To this solution, 23.9 g oleyl alcohol (89.1 mmol, 3 eq) was added, followed by 100 µL DBTL as catalyst. The mixture was stirred overnight under an inert atmosphere, after which the product was obtained by evaporating the solvent *in vacuo*.

Yield: 24.0 g white solid (18.32 mmol, 62 %).

Bruto formula: $C_{78}H_{144}N_6O_9$.

MW.: 1310.04 g/mol.

Alkene equivalent: 2.29 mmol/g.

^{1}H-NMR (300 MHz, $CDCl_3$): δ (ppm) = 0.89 (t, 9 H, CH_3−CH_2), 1.2–1.41 (br. m, 78 H, CH_2−CH_2−CH_2), 1.50 (t, 6 H, CO−NH−CH_2−CH_2), 1.62 (m, 12 H, N−CH_2−CH_2 + O−CH_2−CH_2), 1.92–2.07 (m, 12 H, CH_2−CH=CH−CH_2), 3.15 (q, 6 H, CO−NH−CH_2), 3.86 (t, 6 H, N−CH_2), 4.03 (t, 6 H, O−CH_2), 4.70 (br. s, 3 H, N−H), 5.29–5.41 (m, 6 H, CH=CH).

(TDI_3)–oleyl alcohol

In a 250 mL flask, 21.8 g TDI_3 (41.7 mmol, 1 eq) was dissolved in 100 mL toluene. To this solution, 33.6 g oleyl alcohol (125 mmol, 3 eq) was added, followed by 100 µL DBTL as

catalyst. The mixture was stirred overnight under an inert atmosphere, after which the product was obtained by evaporating the solvent *in vacuo*.

Yield: 51.99 g light yellow viscous oil (55.41 mmol, 94 %).

Bruto formula: $C_{81}H_{126}N_6O_9$.

MW.: 1327.93 g/mol.

Alkene equivalent: 2.26 mmol/g.

^{1}H-NMR (300 MHz, $CDCl_3$): δ (ppm) = 0.89 (t, 9 H, CH_3−CH_2), 1.20–1.42 (br. m, 66 H, 11 (CH_2−CH_2−CH_2)), 1.57 (m, 6 H, O−CH_2−CH_2), 2.03 (m, 12 H, 2 (CH_2−CH)), 2.27 (s, 9 H, CH_3−Ar), 4.15 (m, 6 H, O−CH_2), 5.37 (t, 6 H, CH=CH), 6.46 (s, 3 H, Ar−H), 7.01 (s, 3 H, Ar−H), 7.40 (s, 3 H, Ar−H), 8.02 (br. s, 3 H, N−H).

($IPDI_3$)–oleyl alcohol

In a 100 mL flask, 7.00 g $IPDI_3$ (10.5 mmol, 1 eq) was dissolved in 50 mL toluene. To this solution, 8.46 g oleyl alcohol (31.5 mmol, 3 eq) was added, followed by 100 µL DBTL as catalyst. The mixture was stirred overnight under an inert atmosphere, after which the product was obtained by evaporating the solvent *in vacuo*.

Yield: 3.127 g colourless viscous oil (2.12 mmol, 20 %).

Bruto formula: $C_{90}H_{162}N_6O_9$.

MW.: 1472.32 g/mol.

Alkene equivalent: 2.04 mmol/g.

^{1}H-NMR (500 MHz, $CDCl_3$): δ (ppm) = 0.87 (t, 9 H, CH_3−CH_2), 0.9–0.99 (m, 18 H, $(CH_2)_2$−Cq−(CH_3)$_2$), 1.06 (m, 9 H, $(CH_2)_3$−Cq−CH_3), 1.10 (m, 6 H, Cq−CH_2−Cq), 1.2–1.43 (m, 78 H, 11 (CH_2−CH_2−CH_2) + 2 (N−CH−CH_2)), 1.58 (m, 6 H, O−CH_2−CH_2), 2.00 (q, 12 H, 2 (=CH−CH_2)), 2.95 (m, 3 H, N−CH), 3.74 (m, 6 H, N−CH_2), 4.01 (m, 6 H, O−CH_2), 5.33 (m, 6 H, CH=CH), 8.35 (br. s, 3 H, N−H).

III.5.1.2 Tetrameric DABCO-bromine complex (DABCO-Br)

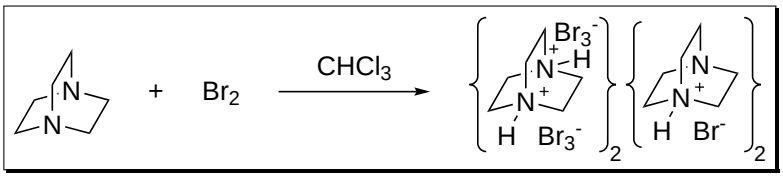

The synthesis of DABCO-Br was based on a literature procedure.[26] In a 500 mL two-neck flask, 1,4-diazabicyclo[2.2.2]octane (6.73 g, 60.0 mmol, 1 eq) was dissolved in chloroform (100 mL). In a next step, a solution of bromine (20.0 g, 0.125 mol, 2.1 eq) in chloroform (100 mL) was added dropwise using an addition funnel. The resulting mixture was stirred under inert atmosphere for 1 hour. The yellow precipitate was filtered off, washed with chloroform (50 mL) and dried overnight in a vacuum oven at 40 °C to obtain DABCO-Br.

Yield: 23.3 g yellow powder (14.8 mmol, 99 %).

Bruto formula: $C_{24}H_{54}Br_{14}N_8$.

MW.: 1573.40 g/mol.

III.5.1.3 4,4′-(4,4′-methylenediphenyl)-bis-(1,2,4-triazoline-3,5-dione) (84)

4,4′-(4,4′-methylenediphenyl)-bis-(1-(ethoxycarbonyl)semicarbazide)

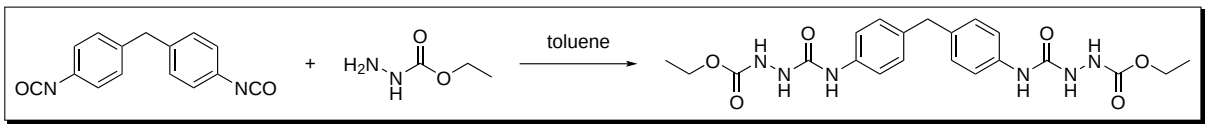

A mixture of ethyl carbazate (40.0 g, 0.384 mol, 2 eq) and toluene (300 mL) was placed in a three-neck flask (1 L) and cooled in an ice bath. The flask was equipped with an addition funnel, containing a solution of 48.0 g 4,4′-methylenebis(phenyl isocyanate) (0.192 mol, 1 eq) in 200 mL toluene, a mechanical stirrer and a bulb condenser. The mixture was put under inert atmosphere and the isocyanate was added slowly under vigorous stirring. After addition the mixture was stirred at room temperature for two hours, followed by 2 h at 90 °C. After cooling the reaction to room temperature, the desired product was filtered off, washed with toluene and dried overnight in a vacuum oven at 40 °C.

Yield: 86.2 g white powder (0.188 mol, 98 %).

Bruto formula: $C_{21}H_{26}N_6O_6$.

MW.: 458.48 g/mol.

^{1}H-NMR (300 MHz, DMSO−$\mathbf{d_6}$): δ (ppm) = 0.85 (t, 6 H, CH_3−CH_2−O), 3.78 (s, 2 H, C−CH_2−C), 4.05 (q, 4 H, CH_3−CH_2−O), 7.07 (d, 4 H, ArH), 7.35 (d, 4 H, ArH), 7.93 (br. s, 2 H, C−NH−CO), 8.62 (br. s, 2 H, NH−NH−CO), 8.88 (br. s, 2 H, NH−NH−CO).

4,4′-(4,4′-methylenediphenyl)-bis-(1,2,4-triazolidine-3,5-dione)

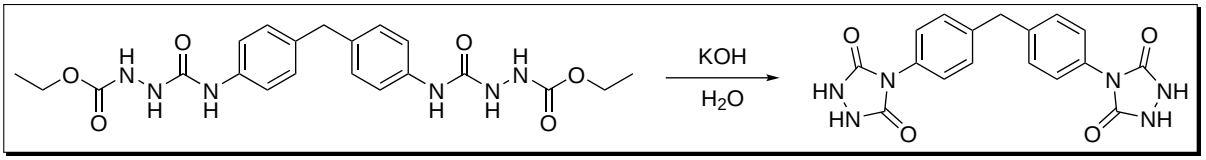

In a 1 L flask, bifunctional semicarbazide (86.2 g, 0.188 mmol) was dissolved in 330 mL of an aqueous potassium hydroxide solution (4 M) under inert atmosphere. This mixture was refluxed for 2 h (100 °C), filtered (hot), cooled to room temperature and acidified until pH 1 by the addition of aqueous hydrochloric acid. This mixture was cooled to room temperature to yield a solid white powder that was filtered off and dried overnight *in vacuo*.

Yield: 68.3 g white powder (0.186 mol, 99 %).

Bruto formula: $C_{17}H_{14}N_6O_4$.

MW.: 366.34 g/mol.

^{1}H-NMR (300 MHz, DMSO−$\mathbf{d_6}$): δ (ppm) = 4.03 (s, 2 H, C−CH_2−C), 7.35 (s, 8 H, ArH), 10.43 (s, 4 H, NH).

4,4′-(4,4′-methylenediphenyl)-bis-(1,2,4-triazoline-3,5-dione) (84)

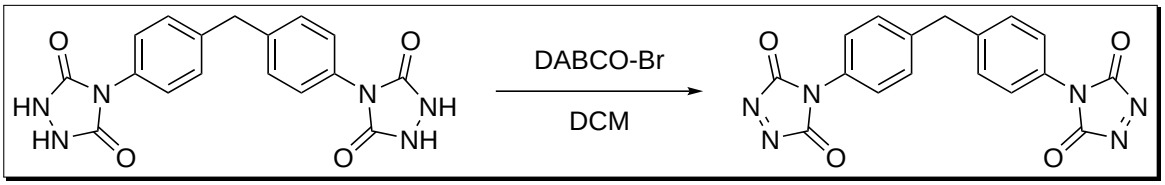

A mixture of bifunctional urazole (2.00 g, 5.46 mmol, 1 eq), DABCO-Br (5.00 g, 3.18 mmol, 0.58 eq) and dichloromethane (55 mL) was put in a flask (250 mL) under inert atmosphere and stirred for 5 h at room temperature. The reaction mixture was filtered off, the residue washed with dichloromethane (2 × 55 mL) and the filtrate was concentrated *in vacuo* to obtain 4,4′-(4,4′-methylenediphenyl)-bis-(1,2,4-triazoline-3,5-dione). For stability reasons, the temperature of the heating bath should preferably not exceed 30 °C.

Yield: 1.65 g pink powder (4.54 mmol, 83 %).

Bruto formula: $C_{17}H_{10}N_6O_4$.

MW.: 362.30 g/mol.

^{1}H-NMR (300 MHz, DMSO−d_6): δ (ppm) = 4.11 (s, 2 H, C−CH_2−C), 7.38 (d, 4 H, ArH), 7.48 (d, 4 H, ArH).

III.5.1.4 Networks from trivalent alkenes or dienes and MDI-TAD

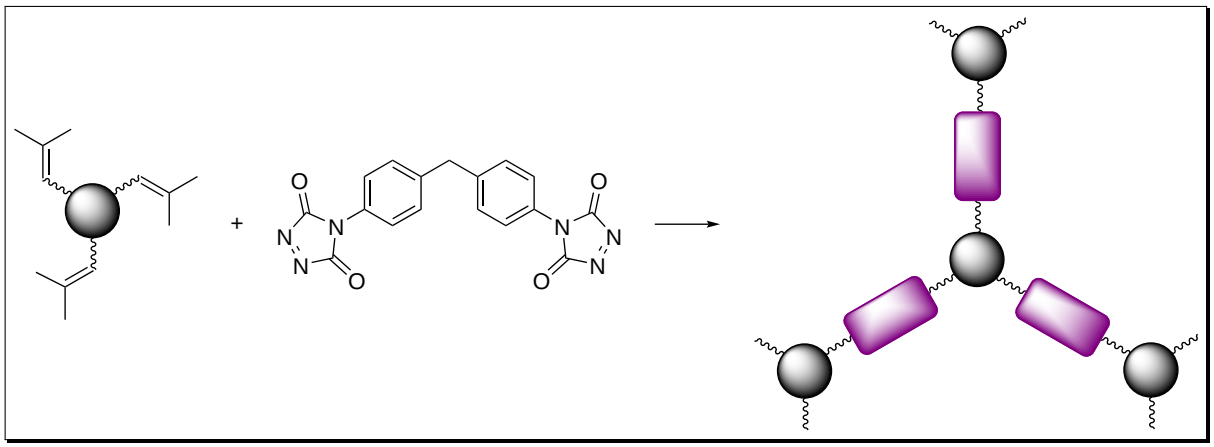

Network from (HDI_3)–HDEO

147 mg (HDI_3)–HDEO (0.551 mmol diene, 1 eq) and 100 mg MDI-TAD (0.276 mmol, 0.5 eq) were dissolved separately in 7 mL and 1 mL acetone, respectively. The solutions were combined and shaken. Gelation occurred within 1 s, *i.e.* before a homogeneous mixture could be obtained. The red colour of the TAD moieties faded in less than 5 s.

T_g (DSC): 124 °C. **T_{deg} (TGA):** 280 °C.

Network from ($IPDI_3$)–HDEO

177 mg ($IPDI_3$)–HDEO (0.552 mmol diene, 1 eq) and 100 mg MDI-TAD (0.276 mmol, 0.5 eq) were dissolved separately in 7 mL and 1 mL acetone, respectively. The solutions were combined and shaken. Gelation occurred within 1 s, *i.e.* before a homogeneous mixture could be obtained. The red colour of the TAD moieties faded in less than 5 s.

T_g (DSC): 198 °C. **T_{deg} (TGA):** 280 °C.

Network from (HDI_3)–citronellol

180 mg (HDI_3)–citronellol (0.554 mmol alkene, 1 eq) and 100 mg MDI-TAD (0.276 mmol, 0.5 eq) were dissolved separately in 4 mL and 1 mL acetone, respectively. The solutions

were combined and shaken to obtain a homogeneous mixture. Gelation occurred within 30 s while full conversion was obtained in less than 1 h.

T_g (DSC): 98 °C. **T_{deg} (TGA):** 260 °C.

Network from (TDI_3)–citronellol

182 mg (TDI_3)–citronellol (0.551 mmol alkene, 1 eq) and 100 mg MDI-TAD (0.276 mmol, 0.5 eq) were dissolved separately in 4 mL and 1 mL acetone, respectively. The solutions were combined and shaken to obtain a homogeneous mixture. Gelation occurred after approximately 20 s while full conversion was obtained in less than 1 h.

T_g (DSC): 151 °C. **T_{deg} (TGA):** 260 °C.

Network from ($IPDI_3$)–citronellol

209 mg ($IPDI_3$)–citronellol (0.552 mmol alkene, 1 eq) and 100 mg MDI-TAD (0.276 mmol, 0.5 eq) were dissolved separately in 4 mL and 1 mL acetone, respectively. The solutions were combined and shaken to obtain a homogeneous mixture. Gelation occurred within 30 s while full conversion was obtained in less than 1 h.

T_g (DSC): 168 °C. **T_{deg} (TGA):** 260 °C.

Network from (HDI_3)–oleyl alcohol

241 mg (HDI_3)–oleyl alcohol (0.552 mmol alkene, 1 eq) and 100 mg MDI-TAD (0.276 mmol, 0.5 eq) were dissolved separately in 5 mL and 1 mL acetone, respectively. The solutions were combined and shaken to obtain a homogeneous mixture. Gelation occurred within 5 min while full conversion was obtained after a few hours.

T_g (DSC): 24 °C. **T_{deg} (TGA):** 220 °C.

Network from (TDI_3)–oleyl alcohol

244 mg (TDI_3)–oleyl alcohol (0.551 mmol alkene, 1 eq) and 100 mg MDI-TAD (0.276 mmol, 0.5 eq) were dissolved separately in 5 mL and 1 mL acetone, respectively. The solutions were combined and shaken to obtain a homogeneous mixture. Although the red colour of the TAD moieties faded over a few hours, no gelation occurred.

Network from ($IPDI_3$)–oleyl alcohol

271 mg ($IPDI_3$)–oleyl alcohol (0.553 mmol alkene, 1 eq) and 100 mg MDI-TAD (0.276 mmol, 0.5 eq) were dissolved separately in 4 mL and 1 mL acetone, respectively. The solutions were combined and shaken to obtain a homogeneous mixture. Gelation occurred within 5 min while full conversion was obtained after a few hours.

T_g (DSC): 89 °C. **T_{deg} (TGA):** 260 °C.

III.5.1.5 Synthesis of ethyl phenyl hydrazine-1,2-dicarboxylate

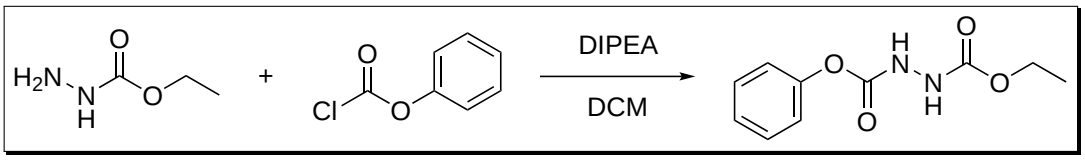

Ethyl phenyl hydrazine-1,2-dicarboxylate was synthesised according to a literature procedure.[12] In a 250 mL two-neck flask, 10.0 g ethyl carbazate (96.1 mmol, 1 eq) and 20.0 mL diisopropylethylamine (DIPEA, 115 mmol, 1.2 eq) were dissolved in 100 mL dichloromethane and cooled in an ice-bath under an inert atmosphere. 12.1 mL phenyl chloroformate (96.1 mmol, 1 eq) was added drop-wise and the reaction was stirred overnight at room temperature. The mixture was washed with a 0.5 M aqueous HCl-solution (3 × 30.0 mL) and 50.0 mL brine. The organic phase was dried on $MgSO_4$ and the solvent was evaporated *in vacuo*.

Yield: 19.6 g light yellow oil (87.4 mmol, 91 %).

Bruto formula: $C_{10}H_{12}N_2O_4$.

MW.: 224.22 g/mol.

^{1}H-NMR (300 MHz, $CDCl_3$): δ (ppm) = 1.27 (t, 3 H, O−CH_2−CH_3), 4.22 (q, 2 H, O−CH_2−CH_3), 7.01 (br. s, 1 H, N−H), 7.15 (d, 2 H, Ar−H), 7.21 (t, 1 H, Ar−H), 7.35 (t, 2 H, Ar−H), 7.42 (br. s, 1 H, N−H).

III.5.1.6 4-(1*H*,1*H*,2*H*,2*H*-perfluorodecyl)-1,2,4-triazoline-3,5-dione (85)

1*H*,1*H*,2*H*,2*H*-perfluorodecyl azide

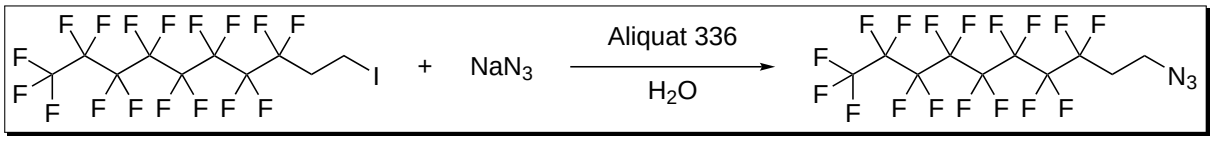

The synthesis of 1*H*,1*H*,2*H*,2*H*-perfluorodecyl azide was based on a literature procedure.[9] 45 g of a 25 wt% aqueous sodium azide solution (0.174 mol, 2 eq), 50 g 1*H*,1*H*,2*H*,2*H*-perfluorodecyl iodide (87.1 mmol, 1 eq) and 1.76 g trioctylmethylammonium chloride (Aliquat 336, 4.36 mmol, 0.05 eq) were mixed in a 250 mL flask and refluxed overnight at 100 °C under inert atmosphere. The mixture was transferred to a separation funnel and allowed to rest until the bottom phase was clear, which can take multiple hours. The azide was separated from the aqueous phase and if necessary filtered to remove solid contaminants.

Yield: 42.3 g light yellow liquid (86.5 mmol, 99 %).

Bruto formula: $C_{10}H_4F_{17}N_3$.

MW.: 489.14 g/mol.

^{1}H-NMR (300 MHz, CD_3OD): δ (ppm) = 2.47 (m, 2 H, CF_2-CH_2), 3.64 (t, 2 H, CH_2-N_3).

1*H*,1*H*,2*H*,2*H*-perfluorodecyl amine

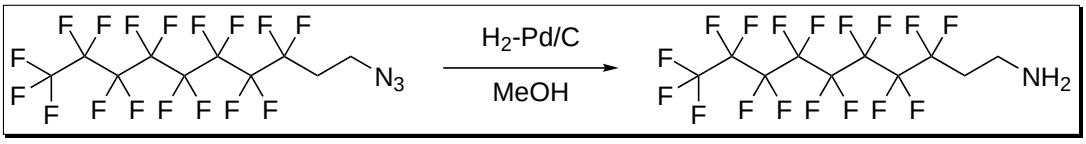

A mixture of 1*H*,1*H*,2*H*,2*H*-perfluorodecyl azide (20 g, 40.9 mmol) and 5 % palladium on carbon (approx. 0.5 g) in 200 mL methanol was vigorously stirred for 72 h at room temperature under a hydrogen atmosphere. The mixture was regularly saturated with hydrogen gas by alternatingly applying vacuum and hydrogen gas. Pd/C was removed by filtration over celite, and the solvent was evaporated *in vacuo* to obtain the desired amine.

Yield: 12.8 g off-white solid (27.6 mmol, 68 %).

Bruto formula: $C_{10}H_6F_{17}N$.

MW.: 463.14 g/mol.

ESI-MS (m/z): 464.0 $[M + H]^+$.

^{1}H-NMR (300 MHz, CD_3OD): δ (ppm) = 2.48 (m, 2 H, CF_2-CH_2), 3.10 (t, 2 H, CH_2-NH_2).

1*H*,1*H*,2*H*,2*H*-perfluorodecyl semicarbazide

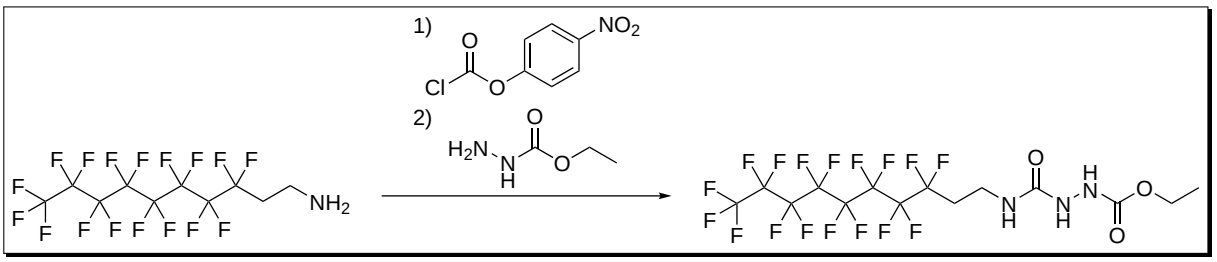

In a 100 mL two-neck flask, 7.50 g 1*H*,1*H*,2*H*,2*H*-perfluorodecyl amine (16.2 mmol, 1 eq) and 4.50 mL triethylamine (32.4 mmol, 2 eq) were dissolved in 50 mL tetrahydrofuran and cooled to 0 °C. 4-Nitrophenyl chloroformate (6.53 g, 32.4 mmol, 2 eq) was added portionwise and the resulting mixture was stirred for 3 hours at room temperature. Next, an extra 4.50 mL triethylamine (32.4 mmol, 2 eq) was added, followed by a solution of 4.38 g ethyl carbazate (42.1 mmol, 2.6 eq) in a minimal amount of THF. The mixture was stirred overnight at room temperature, after which the precipitate was removed by filtration and the solvent was evaporated *in vacuo*. Finally, addition of 20 mL of toluene to the concentrated filtrate resulted in the precipitation of the desired product, which was isolated by filtration.

Yield: 8.66 g off-white solid (14.6 mmol, 90 %).

Bruto formula: $C_{14}H_{12}F_{17}N_3O_3$.

MW.: 593.24 g/mol.

ESI-MS (m/z): 594.0 $[M + H]^+$, 1187.0 $[M_2 + H]^+$ (pos.); 592.0 $[M-H]^-$ (neg.).

^{1}H-NMR (300 MHz, Acetone$-d_6$): δ (ppm) = 1.19 (t, 3 H, CH_3), 2.35–2.57 (m, 2 H, CF_2-CH_2), 3.51 (quint, 2 H, CH_2-NH), 4.07 (q, 2 H, $O-CH_2$), 6.44 (br.s, 1 H, N*H*), 7.30 (br.s, 1 H, N*H*), 7.98 (br.s, 1 H, N*H*).

1*H*,1*H*,2*H*,2*H*-perfluorodecyl urazole

The synthesis of 1*H*,1*H*,2*H*,2*H*-perfluorodecyl urazole was based on a literature procedure.[27] In a 50 mL flask, a suspension of 1.00 g 1*H*,1*H*,2*H*,2*H*-perfluorodecyl semicarbazide (1.69 mmol, 1 eq) and 932 mg potassium carbonate (6.74 mmol, 4 eq) in ethanol was heated to 65 °C for 16 hours under an inert atmosphere. The reaction mixture was cooled to room temperature and the excess of potassium carbonate was removed by filtration. The filtrate was acidified with 4 M hydrochloric acid in dioxane to pH 4. The precipitated salts were removed by filtration and the urazole was finally obtained by concentrating the filtrate *in vacuo*.

Yield: 769 mg off-white solid (1.41 mmol, 83 %).

Bruto formula: $C_{12}H_6F_{17}N_3O_2$.

MW.: 547.17 g/mol.

ESI-MS (m/z): 546.0 $[M-H]^-$, 1092.9 $[M_2-H]^-$.

^{1}H-NMR (300 MHz, Acetone−d_6): δ (ppm) = 2.61–2.79 (m, 2 H, CF_2-CH_2), 3.85 (t, 2 H, CH_2-N), 8.97 (br.s, 2 H, N*H*).

1*H*,1*H*,2*H*,2*H*-perfluorodecyl triazolinedione

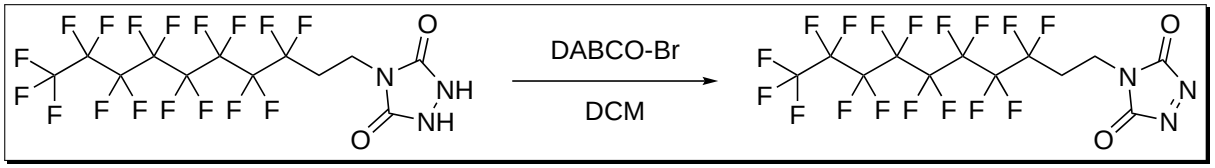

A suspension of 250 mg 1*H*,1*H*,2*H*,2*H*-perfluorodecyl urazole (0.457 mmol, 1 eq), 300 mg DABCO-Br (0.191 mmol, 0.42 eq) and a spatula tip of sodium sulphate in 9.75 g of dichloromethane was stirred for 4 hours at room temperature under an inert atmosphere. After filtration over a syringe filter, the solution should have a concentration of 2.5 wt% 1*H*,1*H*,2*H*,2*H*-perfluorodecyl triazolinedione (**85**) assuming 100 % conversion. This stock solution is either used as such for the modification in solution or evaporated *in vacuo* at a bath temperature of 30 °C and immediately dissolved in acetone for surface modification.

III.5.1.7 4-perfluorophenyl-1,2,4-triazoline-3,5-dione (100)

4-perfluorophenyl semicarbazide

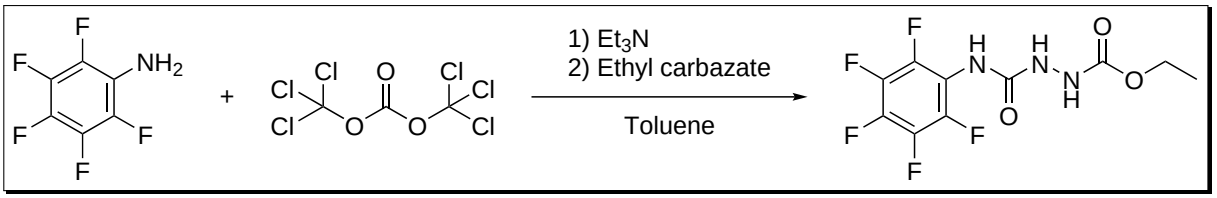

A solution of triphosgene (4.33 g, 14.6 mmol, 0.33 eq) in 30 mL dry toluene was cooled in an ice-bath under inert atmosphere. To this mixture, a solution of pentafluoroaniline (8.02 g, 43.8 mmol, 1 eq) and 4.47 mL triethylamine (32.1 mmol, 2.2 eq) in 20 mL dry toluene was slowly added. The reaction mixture was stirred overnight at room temperature. In a 250 mL flask, a solution of 4.56 g ethyl carbazate (43.8 mmol, 1 eq) in 50 mL toluene was prepared and cooled in an ice-bath. The isocyanate-containing reaction mixture was directly filtered in this ethyl carbazate solution. Immediately, the formation of a precipitate was observed, but the mixture was stirred overnight at room temperature to ensure complete reaction. The precipitated 4-perfluorophenyl semicarbazide was isolated by filtration and dried overnight in a vacuum oven.

Yield: 7.75 g white solid (24.7 mmol, 57 %).

Bruto formula: $C_{10}H_8F_5N_3O_3$.

MW.: 313.18 g/mol.

ESI-MS (m/z): 314.1 $[M + H]^+$, 331.1 $[M + NH_4]^+$.

^{1}H-NMR (300 MHz, DMSO−d_6): δ (ppm) = 1.19 (t, 3 H, CH_3), 4.06 (q, 2 H, O−CH_2), 8.53 (br.s, 1 H, NH), 8.70 (br.s, 1 H, NH), 9.07 (br.s, 1 H, NH).

4-perfluorophenyl urazole

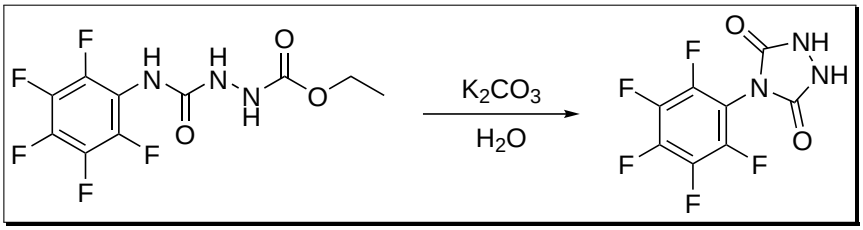

The synthesis of 4-perfluorophenyl urazole was based on a literature procedure.[13] 4-perfluorophenyl semicarbazide (6.75 g, 21.5 mmol, 1 eq) was mixed with a solution of potassium carbonate (14.0 g, 101 mmol, 4.7 eq) in 120 mL water. The mixture was heated

for 12 hours at 70 °C under an inert atmosphere. The hot mixture was filtered and, after cooling to room temperature, acidified to pH 2 using concentrated aqueous hydrochloric acid. The aqueous mixture was extracted with ethyl acetate (3 × 80 mL), after which the combined organic phases are dried ($MgSO_4$) and evaporated *in vacuo*. The crude urazole was recrystallised from toluene:ethyl acetate 3:1.

Yield: 3.63 g off-white solid (13.6 mmol, 63 %).

Bruto formula: $C_8H_2F_5N_3O_2$.

MW.: 267.12 g/mol.

ESI-MS (m/z): 265.9 $[M-H]^-$, 532.7 $[M_2-H]^-$.

^{1}H-NMR (300 MHz, DMSO−d_6): δ (ppm) = 11.15 (br.s, 2 H, N*H*).

4-perfluorophenyl triazolinedione

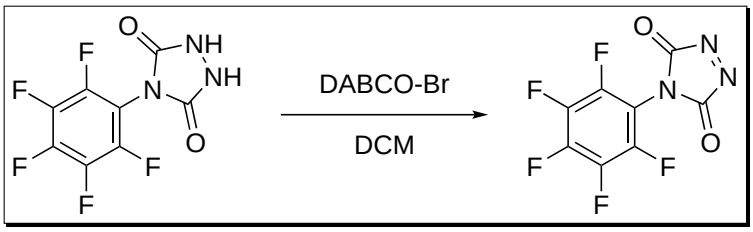

A suspension of 500 mg 4-perfluorophenyl urazole (1.87 mmol, 1 eq), 1.00 g DABCO-Br (0.636 mmol, 0.34 eq) and a spatula tip of sodium sulphate in 19.5 g of dichloromethane was stirred for 4 hours at room temperature under an inert atmosphere. After filtration over a syringe filter, the solution should have a concentration of 2.5 wt% 4-perfluorophenyl triazolinedione assuming 100 % conversion. This stock solution is either used as such for the modification in solution or evaporated *in vacuo* at a bath temperature of 30 °C and immediately dissolved in acetone for surface modification.

III.5.1.8 TAD-modified Sudan II dye (106)

This procedure was reported in the framework of a collaboration with our research group.[18]

Ethyl butyrate derivative of Sudan II

This S_N2-reaction is based on a literature procedure.[28] A mixture of 2.50 g Sudan II (9.05 mmol, 1 eq), 2.0 mL ethyl 4-bromobutyrate (13.6 mmol, 1.5 eq), 2.87 g potassium carbonate (18.1 mmol, 2 eq) and dimethyl sulfoxide (25 mL) was placed under inert atmosphere. The mixture was vigorously stirred for 24 hours at 65 °C and monitored by

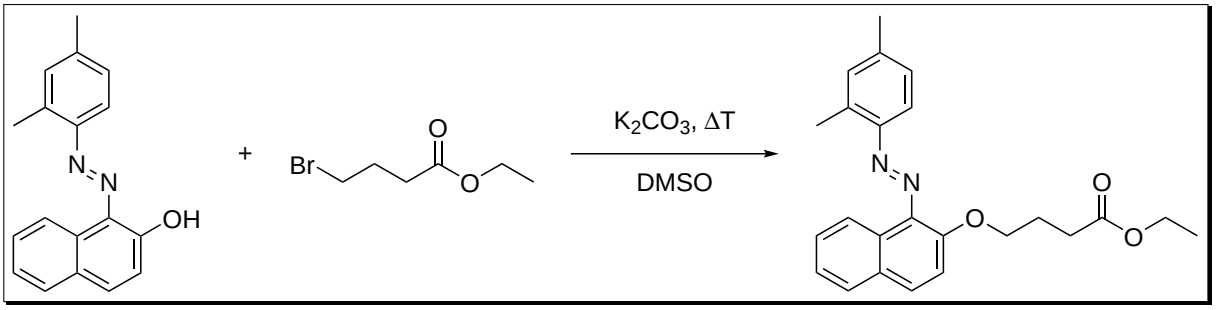

thin layer chromatography (hexane:ethylacetate 1:1). Water (120 mL) was added, followed by an extraction with ethyl acetate (3 × 50 mL). The combined organic layers were washed with brine (50 mL) and dried with magnesium sulphate. The organic layer was concentrated *in vacuo* to give the ethyl butyrate derivative of Sudan II.

Yield: 3.50 g red oil (9.0 mmol, 99 %).

Bruto formula: $C_{24}H_{26}N_2O_3$.

MW.: 390.48 g/mol.

^{1}H-NMR (300 MHz, DMSO−d_6): δ (ppm) = 1.13 (t, 3 H, O−CH_2−CH_3), 1.95 (quint, 2 H, CH_2−CH_2−CH_2), 2.37 (s, 3 H, Ar−CH_3), 2.44 (t, 2 H, CH_2−CO), 2.63 (s, 3 H, Ar−CH_3), 4.01 (q, 2 H, O−CH_2−CH_3), 4.21 (t, 2 H, Ar−O−CH_2), 7.17 (d, 1 H, Ar−H), 7.27 (s, 1 H, Ar−H), 7.45 (m, 1 H, Ar−H), 7.54 (d, 1 H, Ar−H), 7.59 (d, 2 H, Ar−H), 7.95 (d, 1 H, Ar−H), 8.00 (d, 1 H, Ar−H), 8.27 (d, 1 H, Ar−H).

Butyric acid derivative of Sudan II

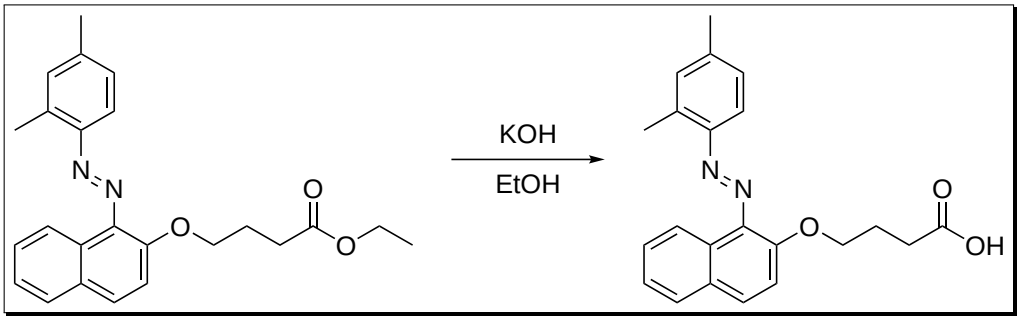

The hydrolysis of the ethyl ester to its carboxylic acid was based on a literature procedure.[29] The ethyl butyrate ester (3.50 g, 9.0 mmol, 1 eq) was dissolved in ethanol (45 mL), together with potassium hydroxide (6 g, 108 mmol, 12 eq) and placed under an inert atmosphere. 3 mL (166.8 mmol) of water was added and the mixture was stirred at a bath temperature of 100 °C for 1 hour. Water (120 mL) was added and the mixture was acidified with concentrated hydrogen chloride to a pH of 2, followed by an extraction with ethyl acetate

(4 × 150 mL). The combined organic layers were dried with $MgSO_4$ and concentrated *in vacuo* to give the desired product.

Yield: 3.2 g red solid (8.8 mmol, 98 %).

Bruto formula: $C_{22}H_{22}N_2O_3$.

MW.: 362.43 g/mol.

ESI-MS (m/z): 363.0 $[MH]^+$, 722.9 $[M_2{-}H]^-$.

^{1}H-NMR (300 MHz, DMSO$-$d$_6$): δ (ppm) = 1.93 (quint, 2 H, $CH_2{-}CH_2{-}CH_2$), 2.37 (m, 5 H, Ar$-$CH_3 + C$H_2{-}$CO), 2.63 (s, 3 H, Ar$-$CH_3), 4.21 (t, 2 H, Ar$-$O$-$CH_2), 7.17 (d, 1 H, Ar$-$H), 7.27 (s, 1 H, Ar$-$H), 7.45 (m, 1 H, Ar$-$H), 7.54 (d, 1 H, Ar$-$H), 7.59 (d, 2 H, Ar$-$H), 7.95 (d, 1 H, Ar$-$H), 8.01 (d, 1 H, Ar$-$H), 8.29 (d, 1 H, Ar$-$H).

Semicarbazide-modified Sudan II

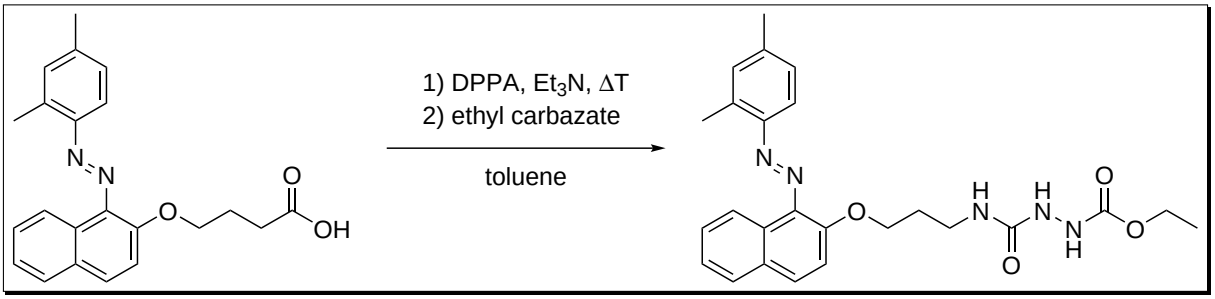

A solution of 3.2 g of the carboxylic acid (8.8 mmol, 1 eq), 2.43 g diphenyl phosphoryl azide (DPPA, 8.8 mmol, 1 eq) and 2.5 mL triethylamine (17.7 mmol, 2 eq) in 100 mL dry toluene, was placed under an inert atmosphere. The reaction was vigorously stirred at room temperature for 1 hour, followed by stirring at reflux for 3 hours. After the addition of a solution of ethyl carbazate (965 mg, 9.3 mmol, 1.05 eq) in 15 mL toluene at room temperature, the reaction was stirred overnight. The mixture was concentrated under reduced pressure, followed by chromatography over silica (ethyl acetate:hexane, 75 % to 100 % ethyl acetate) to give Sudan II-semicarbazide.

Yield: 2.35 g red solid (5.1 mmol, 57 %).

Bruto formula: $C_{25}H_{29}N_5O_4$.

MW.: 463.54 g/mol.

ESI-MS (m/z): 464.0 $[MH]^+$.

^{1}H-NMR (300 MHz, DMSO$-$d$_6$): δ (ppm) = 1.17 (t, 3 H, O$-$C$H_2{-}$CH_3), 1.85 (quint, 2 H, $CH_2{-}$C$H_2{-}CH_2$), 2.38 (s, 3 H, Ar$-$CH_3), 2.64 (s, 3 H, Ar$-$CH_3), 3.16 (q, 2 H, C$H_2{-}$NH), 4.01 (q, 2 H, O$-$C$H_2{-}$CH_3), 4.19 (t, 2 H, Ar$-$O$-$CH_2), 6.46 (br. s, 1 H,

N−H), 7.17 (d, 1 H, Ar−H), 7.27 (s, 1 H, Ar−H), 7.45 (m, 1 H, Ar−H), 7.54 (d, 1 H, Ar−H), 7.59 (d, 2 H, Ar−H), 7.67 (br. s, 1 H, N−H), 7.95 (d, 1 H, Ar−H), 8.01 (d, 1 H, Ar−H), 8.29 (d, 1 H, Ar−H), 8.73 (br. s, 1 H, N−H).

Urazole-modified Sudan II

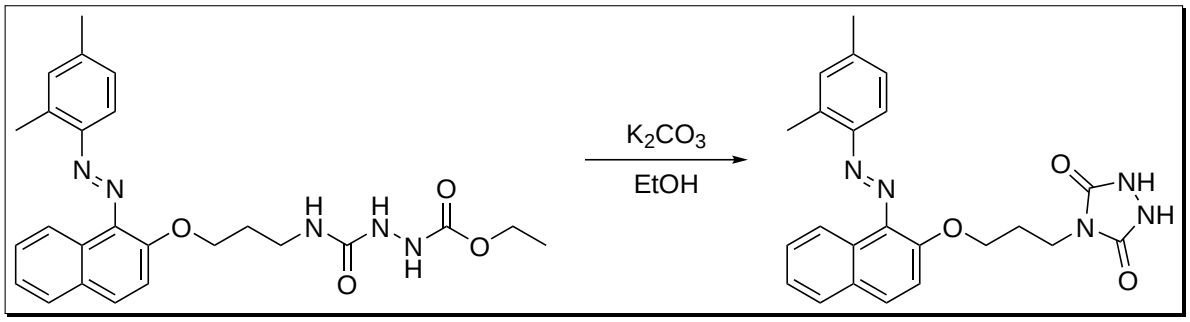

A suspension of Sudan II-semicarbazide (2.35 g, 5.1 mmol, 1 eq) and potassium carbonate (3.5 g, 25.4 mmol, 5 eq) in 40 mL ethanol was placed under an inert atmosphere and stirred at 75 °C for 24 hours. The excess of base was filtered off and the filtrate was acidified with hydrochloric acid (4 M in dioxane) to a pH of 4. The precipitate was filtered off and the filtrate was concentrated *in vacuo*, followed by chromatography over silica (ethyl acetate) to give Sudan II-urazole.

Yield: 1.00 g dark red solid (2.4 mmol, 47 %).

Bruto formula: $C_{23}H_{23}N_5O_3$.

MW.: 417.47 g/mol.

ESI-MS (m/z): 418.2 $[MH]^+$.

^{1}H-NMR (300 MHz, DMSO−d$_6$): δ (ppm) = 2.00 (quint, 2 H, CH_2−CH_2−CH_2), 2.38 (s, 3 H, Ar−CH_3), 2.64 (s, 3 H, Ar−CH_3), 3.54 (t, 2 H, CH_2−N), 4.21 (t, 2 H, Ar−O−CH_2), 7.17 (d, 1 H, Ar−H), 7.27 (s, 1 H, Ar−H), 7.46 (m, 1 H, Ar−H), 7.57 (m, 3 H, Ar−H), 7.95 (d, 1 H, Ar−H), 8.01 (d, 1 H, Ar−H), 8.33 (d, 1 H, Ar−H), 10.07 (s, 2 H, N−H).

TAD-modified Sudan II

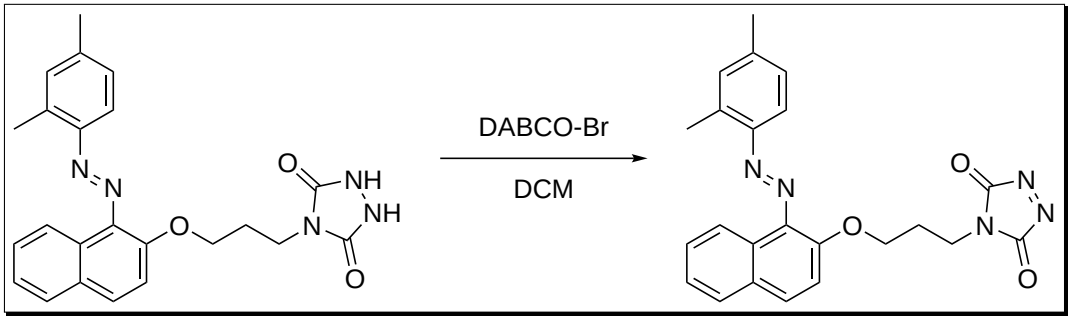

A suspension of 50.0 mg Sudan II-urazole (0.120 mmol, 1 eq) and 37.7 mg DABCO-Br (0.0240 mmol, 0.2 eq) was stirred at room temperature for 4 hours under an inert atmosphere. The mixture was filtered off to remove the heterogeneous oxidant and the filtrate was concentrated *in vacuo* to give Sudan II-TAD.

Yield: 15.9 mg dark red solid (0.0383 mmol, 31 %).

Bruto formula: $C_{23}H_{21}N_5O_3$.

MW.: 415.45 g/mol.

^{1}H-NMR (300 MHz, DMSO−d_6): δ (ppm) = 2.07 (m, 2 H, $CH_2-CH_2-CH_2$), 2.37 (s, 3 H, Ar−CH_3), 2.65 (s, 3 H, Ar−CH_3), 3.68 (t, 2 H, CH_2−N), 4.26 (t, 2 H, Ar−O−CH_2), 7.17 (d, 1 H, Ar−H), 7.27 (s, 1 H, Ar−H), 7.45 (m, 1 H, Ar−H), 7.57 (m, 3 H, Ar−H), 7.95 (d, 1 H, Ar−H), 8.02 (d, 1 H, Ar−H), 8.33 (d, 1 H, Ar−H).

III.5.1.9 4-(4-azobenzene)-1,2,4-triazoline-3,5-dione (115)

4-(4-azobenzene)-1-(ethoxycarbonyl)semicarbazide

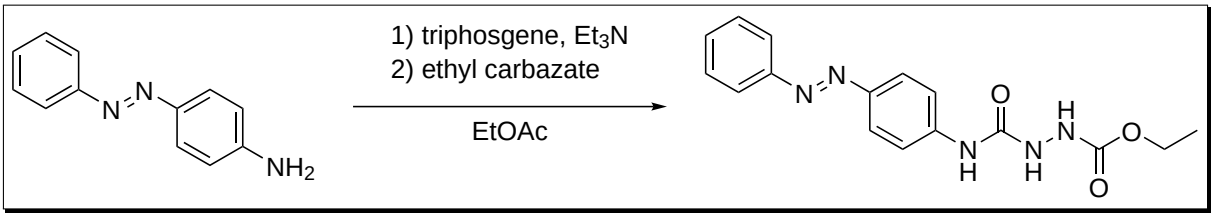

Triphosgene (5.70 g, 19.2 mmol, 0.35 eq) was dissolved in 100 mL ethyl acetate and cooled in an ice-bath. To this, a mixture of 4-aminoazobenzene (10.82 g, 55.0 mmol, 1 eq) and dry triethylamine (16.8 mL, 0.121 mol, 2.2 eq) in 40 mL ethyl acetate was slowly added. The ice-bath was removed and the solution was stirred overnight under inert atmosphere. The resulting reaction mixture was filtered directly into a mixture of ethyl carbazate (6.29 g, 60.4 mmol, 1.10 eq) in 20 mL ethyl acetate and the residue was washed with another

100 mL ethyl acetate. A precipitate is rapidly formed in the clear filtrate. After stirring for 5 minutes, the reaction mixture was evaporated *in vacuo*. To this crude, 200 mL toluene and 100 mL ethyl acetate were added and the resulting mixture was heated to reflux. Another 100 mL toluene was added, after which the mixture was cooled to room temperature and filtered. The residue was dried overnight in a vacuum oven to obtain 4-(4-azobenzene)-1-(ethoxycarbonyl)semicarbazide.

Yield: 10.2 g orange powder (31.2 mmol, 57 %).

Bruto formula: $C_{16}H_{17}N_5O_3$.

MW.: 327.34 g/mol.

HRMS (m/z for $[MH]^+$): calculated: 328.1404, found: 328.1395.

^{1}H-NMR (400 MHz, DMSO−d_6): δ (ppm) = 1.21 (t, 3 H, CH_3), 4.08 (q, 2 H, CH_2), 7.48–7.61 (m, 3 H, ArH), 7.64–7.78 (m, 2 H, ArH), 7.81–7.89 (m, 4 H, ArH), 8.21 (s, 1 H, Ar−NH), 8.63–9.01 (s, 1 H, Ar−NH−C(O)−NH), 9.20 (s, 1 H, Ar−NH−C(O)−NH−NH).

^{13}C-NMR (100 MHz, DMSO−d_6): δ (ppm) = 14.54, 60.59, 122.22, 123.72, 129.37, 130.78, 143.21, 146.66, 152.08.

4-(4-azobenzene)-1,2,4-triazolidine-3,5-dione

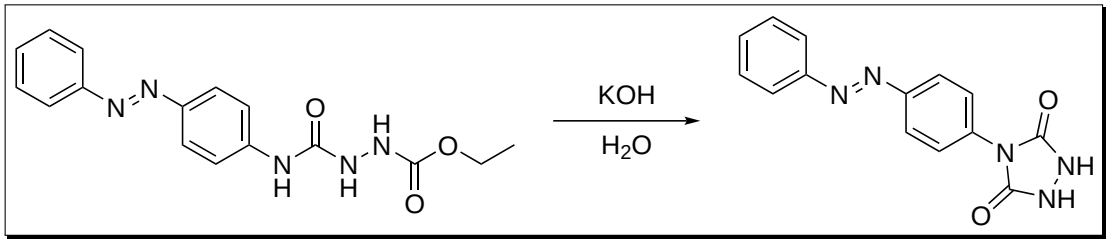

4-(4-azobenzene)-1-(ethoxycarbonyl)semicarbazide (1.00 g, 3.05 mmol, 1 eq) in 2.5 mL of a 4 M aqueous potassium hydroxide solution was placed under inert atmosphere and refluxed for 2.5 h at 100 °C. The resulting dark orange-brown solution was cooled to room temperature and acidified to pH= 1 with a 1 M aqueous hydrochloric acid solution. The obtained precipitate was filtered off, washed with water (3 × 5 mL) and dried in a vacuum oven overnight at 40 °C to yield 4-(4-azobenzene)-urazole.

Yield: 817 mg orange powder (2.90 mmol, 95 %).

Bruto formula: $C_{14}H_{11}N_5O_2$.

MW.: 281.28 g/mol.

LC-MS (m/z): 282.1 $[MH]^+$.

HRMS (m/z for $[MH]^+$): $[MH]^+$: calculated: 282.0986, found: 282.0994.

^{1}H-NMR (400 MHz, DMSO−d_6): δ (ppm) = 7.55–7.66 (m, 3 H, Ar*H*), 7.76 (dt, 2 H, Ar*H*), 7.92 (m, 2 H, Ar*H*), 8.00 (dt, 2 H, Ar*H*), 10.65 (s, 2 H, N*H*).
^{13}C-NMR (100 MHz, DMSO−d_6): δ (ppm) = 122.64, 122.89, 126.23, 129.51, 131.73, 134.63, 150.34, 151.88, 152.85.

4-(4-azobenzene)-1,2,4-triazoline-3,5-dione

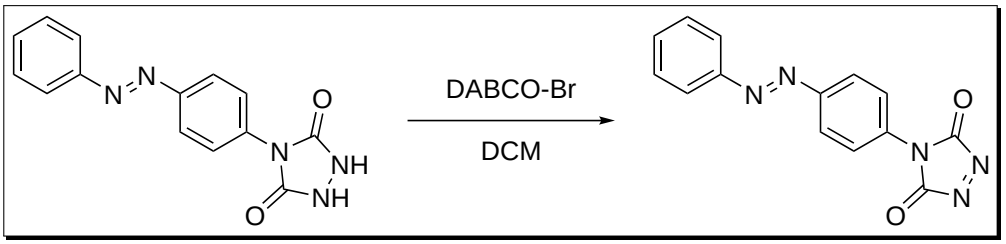

A mixture of 4-(4-azobenzene)-urazole (500 mg, 1.78 mmol, 1 eq) and DABCO-Br (559 mg, 0.356 mmol, 0.2 eq) in 25 mL dry dichloromethane was placed under inert atmosphere and stirred at room temperature for 4 h. The resulting dark red mixture was taken up with a syringe to remove the heterogenous oxidant with a syringe filter. The obtained dark red solution of 4-(4-azobenzene)-1,2,4-triazoline-3,5-dione was diluted to the desired concentration with dichloromethane and used without isolation, assuming 100 % conversion.

III.5.1.10 *N*-(5-carboxypentyl)-4-amino-7-nitro-1,2,3-benzoxadiazole (NBD-carboxylic acid, 122)

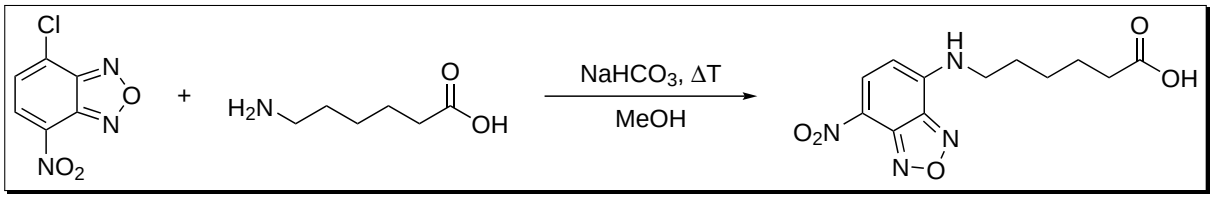

The synthesis of NBD-carboxylic acid was based on a literature procedure.[23] In a 250 mL flask, 3.07 g 6-aminocaproic acid (23.4 mmol, 1 eq) and 5.90 g sodium bicarbonate (70.2 mmol, 3 eq) were suspended in 150 mL methanol and cooled in an ice-bath. 4.67 g 4-chloro-7-nitro-1,2,3-benzoxadiazole (NBD-Cl, 23.4 mmol, 1 eq) was added in portions to obtain a light-yellow suspension. The mixture was stirred under an inert atmosphere for 30 min at 0 °C, 90 min at room temperature and 2.5 h at 55 °C. The black solution was cooled to room temperature and slowly poured in 600 mL 0.2 M aqueous hydrochloric

acid. The precipitate was filtered and dried overnight in a vacuum oven at 40 °C to obtain NBD-carboxylic acid.

Yield: 5.91 g orange solid (20.1 mmol, 86 %).

Bruto formula: $C_{12}H_{14}N_4O_5$.

MW.: 294.27 g/mol.

^{1}H-NMR (400 MHz, DMSO−d$_6$): δ (ppm) = 1.38 (quint, 2 H, CH_2−CH_2−CH_2), 1.55 (quint, 2 H, CH_2−CH_2−CH_2), 1.68 (quint, 2 H, CH_2−CH_2−CH_2), 2.22 (t, 2 H, CH_2−COOH), 3.46 (q, 2 H, NH−CH_2), 6.41 (d, 1 H, ArH), 8.51 (d, 1 H, ArH), 9.54 (t, 1 H, NH), 11.99 (s, 1 H, COOH).

III.5.1.11 4-(7-nitro-1,2,3-benzoxadiazol-4-yl)-1-(ethoxycarbonyl)-semicarbazide (NBD-semicarbazide)

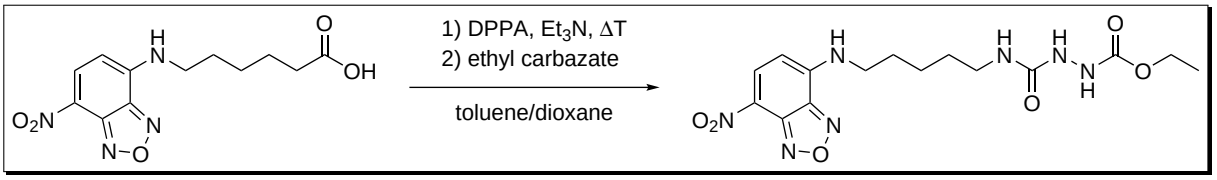

In a 50 mL two-neck flask, 242 mg NBD-carboxylic acid (0.822 mmol, 1 eq) was suspended in 10 mL toluene. Solutions of 166 mg triethylamine and 226 mg diphenyl phosphoryl azide, both in 2 mL toluene, were sequentially added, which resulted in the precipitation of a sticky residue. 5 mL dry dioxane was added to partially dissolve the residue, and the mixture was stirred under an inert atmosphere for 2 h at room temperature, followed by 3 h at 110 °C. The reaction was then cooled to room temperature, followed by the addition of 86 mg ethyl carbazate in 2 mL dry dioxane and stirring overnight. A precipitate formed that was filtered off, dried overnight in a vacuum oven at 40 °C and identified as a mixture of product (92 %) and triethylammonium diphenyl phosphate via ^{1}H-NMR. The filtrate was concentrated *in vacuo* and also identified as a mixture of product (22 %) and triethylammonium diphenyl phosphate. The latter crude could not be purified via column chromatography over silica gel and was finally discarded.

Purity (from ^{1}H-NMR): 92 %.

Yield: 214 mg orange solid (197 mg product, 0.498 mmol, 61 %).

Bruto formula: $C_{15}H_{21}N_7O_6$.

MW.: 395.38 g/mol.

LC-MS (m/z): 350.1 $[M - OEt]^+$, 396.1 $[MH]^+$, 791.2 $[M_2 + H]^+$.
^{1}H-NMR (300 MHz, DMSO−d_6): δ (ppm) = 1.16 (t, 3 H, CH_3), 1.28–1.50 (m, 4 H, CH_2−CH_2−CH_2), 1.68 (quint, 2 H, CH_2−CH_2−CH_2), 3.01 (q, 2 H, CO−NH−CH_2), 3.45 (q, 2 H, Ar−NH−CH_2), 4.01 (q, 2 H, O−CH_2), 6.32 (s, 1 H, NH), 6.41 (d, 1 H, ArH), 7.63 (s, 1 H, NH), 8.51 (d, 1 H, ArH), 8.71 (s, 1 H, NH), 9.54 (t, 1 H, Ar−NH).

III.5.2 Methods

III.5.2.1 Surface modification of citronellol-based networks

Networks were synthesised from (HDI_3)–citronellol or ($IPDI_3$)–citronellol as described in section III.5.1.4, albeit with 1.25 eq citronellyl residues relative to the TAD moieties, *i.e.* 224 mg or 261 mg trimer for 100 mg MDI-TAD, respectively.[19] After drying to the air overnight at room temperature, the network was cut in pieces of approximately 1 cm × 1 cm. A piece of this material was then submerged for 30 minutes in a 55 mM solution of the investigated triazolinedione in acetone or dichloromethane. Finally, the modified material was thoroughly rinsed with acetone and dried in a stream of nitrogen.

III.5.3 Instrumentation

Differential scanning calorimetry (DSC) Differential scanning calorimetry (DSC) analyses were performed with a Mettler-Toledo 1/700 under nitrogen atmosphere. The samples were analysed in aluminium sample pans which contained 5–15 mg of the sample. T_gs were determined from the midpoints in the second heating using the STARe software of Mettler-Toledo. Measurements were performed with a rate of 10 K min^{-1}.

Energy-dispersive X-ray spectroscopy (EDX) EDX with electron beam excitation (*i.e.* SEM-EDX) was performed on a Quanta 200 FEG FEI scanning electron microscope with an acceleration voltage of 5 kV, equipped with a Genesis 4000 EDX system.

Liquid chromatography - mass spectrometry (LC-MS) LC-MS analyses were performed on an Agilent Technologies 1100 series LC/MSD system with a diode array detector (DAD) and a single quad MS. Analytical reversed phase HPLC-analyses were performed with a Phenomex Luna C18 (2) column (5 µm, 250 mm × 4.6 mm) and a solvent

gradient (0 % to 100 % acetonitrile in H_2O in 15 min). The eluted compounds were analysed via UV detection (214 nm).

Nuclear magnetic resonance (NMR) NMR spectra were recorded on a Bruker Avance 300 (300 MHz) or a Bruker Avance 400 (400 MHz) FT-NMR spectrometer in the indicated solvent at room temperature. Chemical shifts are presented in parts per million (δ) with the residual solvent peak as an internal standard.[30] The resonance multiplicities are described as [br. (broad)] s (singlet), d (doublet), t (triplet), q (quadruplet), quint (quintuplet), sext (sextuplet) or m (multiplet). The obtained spectra were analysed with the ACD/NMR Processor Academic Edition of ACD/Labs.

Thermogravimetric analysis (TGA) All the TGA analyses were performed on a Mettler-Toledo TGA/SDTA 851e under N_2-atmosphere with a heating rate of 10 °C/ min from 25 °C to 800 °C. The thermograms were analysed with the STARe software from Mettler-Toledo.

III.6 Bibliography

1. S. Billiet, K. De Bruycker, F. Driessen, H. Goossens, V. Van Speybroeck, J. M. Winne, F. E. Du Prez, *Nat. Chem.* **2014**, *6*, 815–821.
2. S. Vandewalle, S. Billiet, F. Driessen, F. E. Du Prez, *ACS Macro Lett.* **2016**, *5*, 766–771.
3. L. Vlaminck, K. De Bruycker, O. Turunc, F. E. Du Prez, *Polym. Chem.* **2016**, *7*, 5655–5663.
4. O. Türünç, S. Billiet, K. De Bruycker, S. Ouardad, J. Winne, F. E. Du Prez, *Eur. Polym. J.* **2015**, *65*, 286–297.
5. I. T. Horváth, J. Rábai, *Science* **1994**, *266*, 72–75.
6. A. ur Rahman, K. K. Laali, *Advances in Organic Synthesis: Modern Organofluorine Chemistry-Synthetic Aspects*, *Vol. 2*, Bentham Science Publishers, **2005**.
7. I. T. Horváth, *Fluorous Chemistry*, Springer-Verlag Berlin Heidelberg, 1st ed., **2012**, p. 414.
8. S. Werner, D. P. Curran, *Org. Lett.* **2003**, *5*, 3293–3296.
9. F. Szonyi, A. Cambon, *J. Fluorine Chem.* **1989**, *42*, 59–68.
10. A. Kamal, K. V. Ramana, H. B. Ankati, A. V. Ramana, *Tetrahedron Lett.* **2002**, *43*, 6861–6863.
11. K. A. Kislyi, A. V. Samet, Y. A. Strelenko, V. V. Semenov, *J. Org. Chem.* **2008**, *73*, 2285–2291.
12. G. W. Breton, M. Turlington, *Tetrahedron Lett.* **2014**, *55*, 4661–4663.
13. T. J. Gilbertson, T. Ryan, *Synthesis* **1982**, *1982*, 159–160.
14. P. Kohli, G. J. Blanchard, *Langmuir* **2000**, *16*, 4655–4661.
15. J. J. Reisinger, M. A. Hillmyer, *Prog. Polym. Sci.* **2002**, *27*, 971–1005.
16. Z. Xue, M. Liu, L. Jiang, *J. Polym. Sci. Part B: Polym. Phys.* **2012**, *50*, 1209–1224.
17. C. Schulz, S. Nowak, R. Fröhlich, B. J. Ravoo, *Small* **2012**, *8*, 569–577.
18. J. Gaitzsch, M. Delahaye, A. Poma, F. Du Prez, G. Battaglia, *Polym. Chem.* **2016**, *7*, 3046–3055.
19. H. A. Houck, K. De Bruycker, S. Billiet, B. Dhanis, H. Goossens, S. Catak, V. Van Speybroeck, J. Winne, F. Du Prez, *Chem. Sci.* **2017**, *8*, 3098–3108.
20. A. Elkamhawy, J. Lee, B.-G. Park, I. Park, A. N. Pae, E. J. Roh, *Eur. J. Med. Chem.* **2014**, *84*, 466–475.
21. L. Tao, C. S. Kaddis, R. R. Ogorzalek Loo, G. N. Grover, J. A. Loo, H. D. Maynard, *Chem. Commun.* **2009**, 2148–2150.

22. W. Wan, M. Biyikal, R. Wagner, B. Sellergren, K. Rurack, *Angew. Chem. Int. Ed.* **2013**, *52*, 7023–7027.

23. G. Greco, N. D'Antona, G. Gambera, G. Nicolosi, *Synlett* **2014**, *25*, 2111–2114.

24. B. Moon, T. R. Hoye, C. W. Macosko, *Polymer* **2002**, *43*, 5501–5509.

25. Y. Chen, X. Zheng, M. P. Dobhal, A. Gryshuk, J. Morgan, T. J. Dougherty, A. Oseroff, R. K. Pandey, *J. Med. Chem.* **2005**, *48*, 3692–3695.

26. M. M. Heravi, F. Derikvand, M. Ghassemzadeh, B. Neumüller, *Tetrahedron Lett.* **2005**, *46*, 6243–6245.

27. R. Adamo, M. Allan, F. Berti, E. Danieli, Q.-Y. Hu, *Tyrosine ligation process*, **2013**, WO2013009564.

28. L. Séro, L. Sanguinet, S. Derbré, F. Boury, G. Brotons, S. Dabos-Seignon, P. Richomme, D. Séraphin, *Langmuir* **2013**, *29*, 10423–10431.

29. B. Vaisman, A. Shikanov, A. J. Domb, *J. Am. Oil Chem. Soc.* **2008**, *85*, 169–184.

30. H. E. Gottlieb, V. Kotlyar, A. Nudelman, *J. Org. Chem.* **1997**, *62*, 7512–7515.

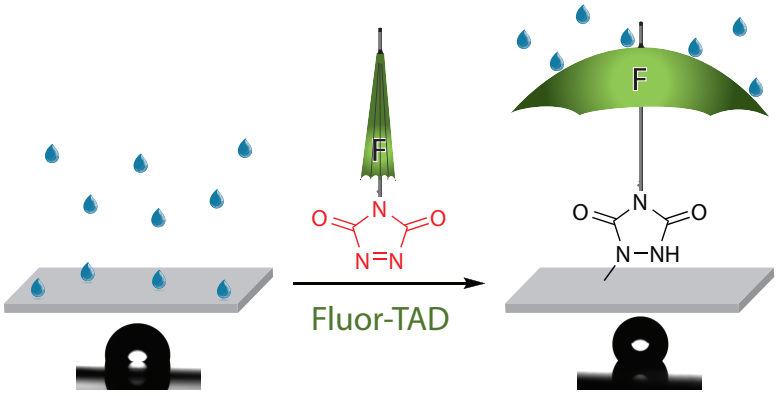

Abstract

Non-reactive additives are widely applied to enhance polymer properties but can leach out of the material over time. In this chapter, two essentially different fluorinated additives bearing a triazolinedione moiety were grafted on several polydiene backbones (acrylonitrile-butadiene-styrene, styrene-butadiene and styrene-isoprene-styrene copolymers), either by dip-coating or by reaction in solution. The resulting polymers were analysed by contact angle goniometry, size exclusion chromatography and NMR-, infrared- and X-ray photoelectron spectroscopy. Independent of the modification procedure, the fluorophilic perfluoroalkyl additive was found at the material surface, thereby yielding a more hydrophobic surface. For SIS thermoplastic elastomers for example, contact angles up to 125° have been obtained.

Published as

K. De Bruycker, M. Delahaye, P. Cools, J. Winne, F. E. Du Prez, *Macromolecular Rapid Communications* **2017**, *38*, 1700122.

Chapter IV

Fluorinated triazolinediones for the modification of polydienes

IV.1 Introduction

Polydienes are a very important class of polymers with everyday applications, ranging from rubber tires over suspension elements in cars to plastic toys and sports goods.[1,2] Nevertheless, these end-products rarely consist only of the neat polymer, but are typically a mixture of polymer and a range of additives such as fillers, plasticisers, stabilisers, dyes, cross-linkers and fire retardants to enhance the resulting material properties.[2,3] One problem that limits the use of these additives, however, is that they are typically added after the polymerisation, which implies that they must be compatible with the polymer matrix. Moreover, additives can volatilise or leach out through normal use or ageing, leading to a decrease in performance of the material over time.[2,4] These problems can be tackled by using reactive additives since they can be covalently grafted as side chains to the polymer backbone and thus remain effective for the life of product.

Apart from the widely applied chlorination or vulcanisation with sulphur or peroxides,[1] the scope of possible transformations on the unsaturated polydiene backbone is rather limited. Consequently, a typical functionalisation strategy consists of the introduction of functional handles, for example by hydroformylation,[5] epoxidation[6–12] or Alder-ene reactions,[6,12,13] that can subsequently be modified into the desired functionality. Nevertheless, these reactions often require very specific catalysts or harsh reaction conditions, which led

to the development of the radical[14,15] or light induced[16,17] thiol-ene addition as a much milder, one-step alternative for polydiene functionalisation. Recently, Barner-Kowollik and co-workers presented the use of a catalyst-free, N-bromosuccinimide initiated multi-component reaction, involving tetrahydrofuran and a functional carboxylic acid, to decorate polybutadiene with bromine and alkoxyether motifs in a few hours at room temperature (Scheme IV.1).[18]

Because of their high reactivity at room temperature, triazolinediones (TADs) have already been extensively studied for the modification of unsaturated polymers.[19–22] Depending on the substitution degree, TADs typically react with alkenes in seconds to minutes at room temperature via an Alder-ene reaction without the need for a catalyst (Scheme IV.2). While the reaction of TAD with a polybutadiene repeating unit can only result in one isomer (R_1=H), multiple isomers can be formed when polyisoprene is used. Nevertheless, in their reaction with trisubstituted alkenes, TADs show a high regioselectivity, resulting in the selective formation of only one regioisomer (R_1=CH_3), albeit as a mixture of two positional alkene isomers.[23,24] After the reaction, the very polar and acidic urazole moiety (pK_a(N−H) ≈ 5) will give rise to strong inter- and intramolecular hydrogen-bonding

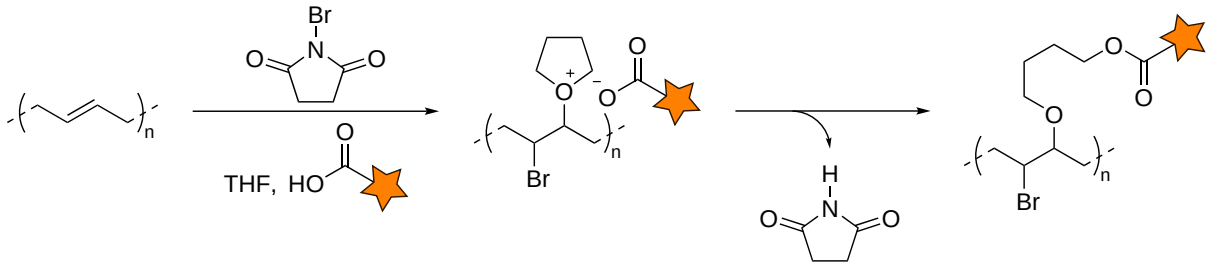

Scheme IV.1: Modification of polybutadiene via an electrophilic multi-component reaction, involving N-bromosuccinimide (NBS), tetrahydrofuran (THF) and a functional carboxylic acid.[18] Only the *trans*-1,4 polymer is shown.

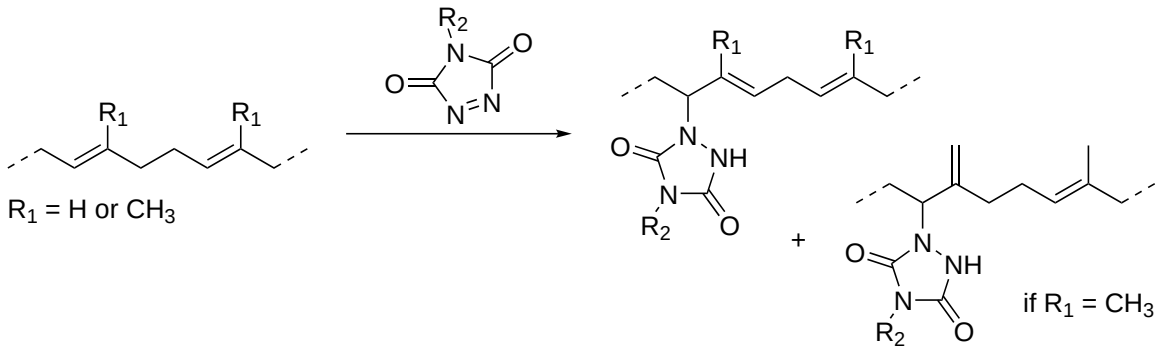

Scheme IV.2: Reaction of a triazolinedione with polybutadiene (R_1=H) or polyisoprene (R_1=CH_3). Only the trans isomers are shown.

interactions, thereby impacting the material properties.[25–28] Recently, this effect was applied in a collaboration with the research group of Prof. Karen De Clerck (not part of this PhD thesis) for tuning the delamination resistance of composite materials containing nanofibres of TAD-modified styrene-butadiene-styrene triblock copolymers (SBS).[29,30]

In this chapter, the impact of fluorinated triazolinediones on the wetting properties of various readily available bulk polymers was investigated. To this end, two essentially different fluorinated TAD compounds were selected and prepared for this research, *i.e.* 4-heptadecafluorodecyl-TAD (R_FTAD, **85**) and 4-perfluorophenyl-TAD (PFPTAD, **100**), as described in the previous chapter. Subsequently, they were reacted with either polybutadiene or polyisoprene copolymers (Scheme IV.2). Both a surface treatment, in which a solid material is dipped in a TAD-containing solution, and a homogeneous treatment in solution were applied, depending on the substrate. The influence of the reactive TAD-additive on the surface properties was determined by contact angle goniometry, and the modified polymers were further analysed via NMR, FT-IR, size exclusion chromatography (SEC) and X-ray photoelectron spectroscopy (XPS).

IV.2 Preparation of the fluorinated TADs

While Werner and Curran previously reported a synthesis of R_FTAD (**85**) from the corresponding isocyanate via the straightforward Cookson method (section II.2.1),[31] neither the isocyanate nor the precursor amine are nowadays readily available. Therefore, for this study, the amine was first synthesised from 1*H*,1*H*,2*H*,2*H*-perfluorodecyliodide

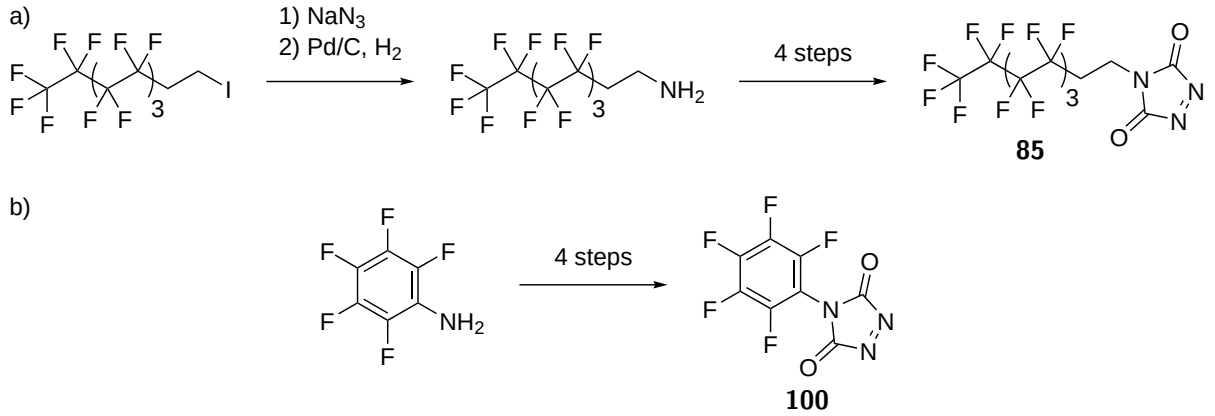

Scheme IV.3: **(a)** 1*H*,1*H*,2*H*,2*H*-Perfluorodecyl amine, obtained from the corresponding iodide, and **(b)** pentafluoroaniline were transformed to R_FTAD and PFPTAD, respectively, by an extended Cookson synthesis.

and then successfully transformed in the corresponding triazolinedione via an extended Cookson method without the need of chromatographic purifications, leading to a scalable production process (Scheme IV.3). PFPTAD (**100**), on the other hand, was synthesised via an altered literature procedure starting from pentafluoroaniline.[32] A more detailed discussion on the synthesis of these triazolinediones is provided in section III.3.1.

It should be noted that TADs are prone to hydrolysis upon prolonged exposure to water or moisture and are typically not bench stable, while no such issues occur with the precursor urazoles. Therefore, the fluorinated TADs were always freshly prepared before use by oxidation of the urazole, which can be stored without problems.

IV.3 Surface modification

With the two fluorinated TAD reagents in hand, the high reactivity of these TADs towards unsaturated carbon-carbon bonds was used to modify the surface of two polybutadiene-containing commercial polymers, *i.e.* acrylonitrile butadiene styrene terpolymer (ABS) and poly(styrene-*co*-butadiene) (SBC). Similarly to our previous study on the modification of SBS nanofibres,[29] the fluorinated TAD reagents were soluble in acetone, whereas the polydiene polymers swell yet do not dissolve in this common solvent. Therefore, samples of the materials were simply dipped for 10 minutes in a 55 mM solution of fluorinated TAD in acetone. As a result of the swelling behaviour of the polymers, the TAD reagents should be able to diffuse to a certain extent into the bulk of the material and react with the polybutadiene segments, while the macroscopic shape remains intact.

As expected, the static contact angle of treated samples rises significantly when the polymers are modified with R_FTAD (Figure IV.1). Interestingly, a decreased contact angle (and thus decreased hydrophobicity) is in fact observed for polymer surfaces treated with

(a) **(b)**

Figure IV.1: Static contact angles of the blank (left), R_FTAD modified (middle) and PFPTAD modified (right) polymers, *i.e.* acrylonitrile butadiene styrene terpolymer (ABS, **(a)**) and styrene-butadiene copolymer (SBC, **(b)**).

PFPTAD. Indeed, as discussed in section III.3.1, Horváth and Rábai reported on the 'fluorophilic' and thus hydrophobic behaviour of perfluoroalkyl groups (*cf.* R_FTAD) in contrast to the more polar fluorinated aryl groups (*cf.* PFPTAD).[33,34] However, apart from this initial proof of successful surface modification, a further analysis of the obtained materials, which might explain the remarkable difference in effect between R_FTAD and PFPTAD, proved rather troublesome, mainly because of the additives that are present in the commercial polymers. Nevertheless, these first results clearly showed the potential of fluorinated TADs to alter the wettability of unsaturated surfaces.

IV.4 Modification in solution

In order to facilitate the analysis of perfluoroTAD-modified polydiene materials, we next investigated these polymer conjugations under more controlled conditions with additive-free polymers in solution. Thus, styrene-isoprene-styrene triblock copolymer (SIS) was dissolved in chloroform, followed by the addition of varying amounts of R_FTAD and PFPTAD (from 2.5 to 50 wt%, relative to the polymer mass, Table IV.1). Because the reaction of polydienes with 4-phenyl-TAD (PhTAD) is well investigated in literature,[19,21,22,25,26] this triazolinedione was also included in this study as a non-fluorinated reference compound. Given a polystyrene content of 15 wt%, this procedure is expected to yield up to 7 %, 15 % and 23 % of modified unsaturations with R_FTAD, PFPTAD and PhTAD, respectively.

While solutions of either R_FTAD or PhTAD and the polydiene first give homogeneous

Table IV.1: Comparison of the expected and calculated amount of additive based on the NMR analysis, relative to the mass of SIS. While a quantitative modification can be obtained for both PFPTAD and PhTAD, the low yield of R_FTAD can be explained by suboptimal oxidation conditions for this specific class of perfluorinated TAD compounds. 50 wt% of additive corresponds to 7 mol % R_FTAD, 15 mol % PFPTAD or 23 mol % PhTAD, relative to the amount of unsaturations.

Additive added (wt%)	**Expected additive content (wt%)**	**Measured additive content (wt%), calculated from NMR (yield)**		
		R_FTAD	**PFPTAD**	**PhTAD**
2.5	2.4	0.9 (37 %)	1.7 (68 %)	2.4 (99 %)
5	4.8	1.5 (32 %)	4.1 (85 %)	4.6 (97 %)
10	9.1	3.1 (34 %)	8.9 (98 %)	8.4 (92 %)
20	16.7	5.8 (35 %)	15.5 (93 %)	15.6 (94 %)
35	25.9	9.3 (36 %)	25.8 (99 %)	23.3 (90 %)
50	33.3	13.2 (39 %)	33.0 (99 %)	30.8 (92 %)

mixtures upon mixing and then fully react in a few seconds, judged by the gradual disappearance of the red colour originating from the TAD moieties, the reactivity of PFPTAD was observed to be significantly higher, giving instantaneous reaction upon mixing. In this section, the remarkable difference in reactivity will first be rationalised via theoretical calculations, after which the obtained modified polymers will be analysed via NMR and FT-IR spectroscopy. Finally, the influence of the reactive additive on the surface properties was determined by contact angle goniometry and rationalised via XPS analysis.

IV.4.1 Theoretical rationalisation of the PFPTAD reactivity

As previously mentioned, PFPTAD reacted notably faster with SIS than PhTAD, *i.e.* its non-fluorinated reference, judged by the instantaneous disappearance of the characteristic red colour. Not unlike the well-known highly reactive 4-(4′-nitrophenyl)-TAD (NO_2PhTAD) reagent,[35] this higher reactivity might be explained by the inductive electron withdrawing effect of the perfluorophenyl group, which would make the electron deficient triazolinedione even more electron deficient. Therefore, the impact of this group on the electron density of the triazolinedione moiety is visualised by comparing the electrostatic potential maps (EPMs) of PFPTAD to those of PhTAD and NO_2PhTAD, respectively.

First, a conformational analysis was performed by calculating the energy (B3LYP/6-

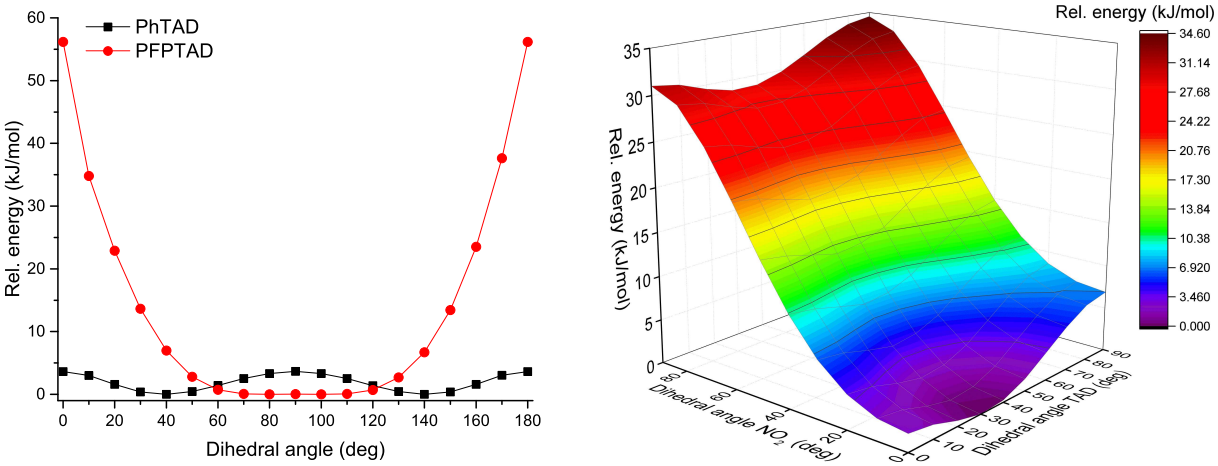

(a) **(b)**

Figure IV.2: Conformer energies (B3LYP/6-311G(d)) of **(a)** PhTAD and PFPTAD, as well as **(b)** NO_2PhTAD as a function of the dihedral angles defined by the planes of the triazolinedione-, phenyl- and nitro moieties. Energies are relative to the equilibrium conformer.

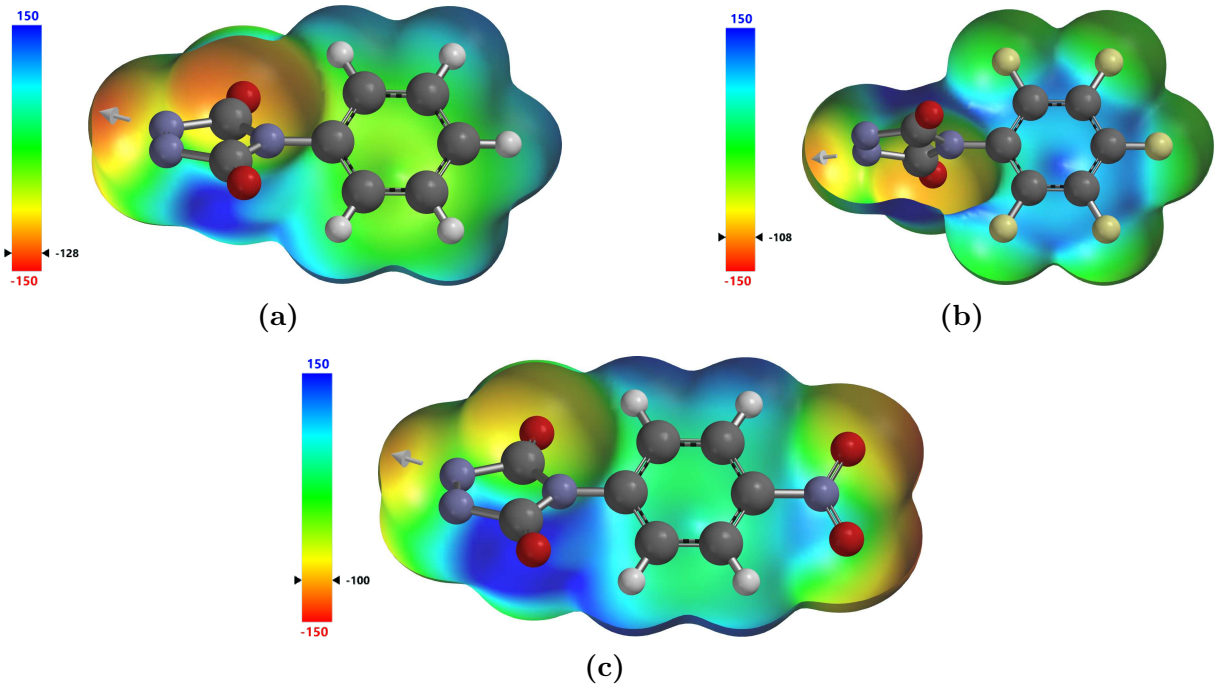

Figure IV.3: Electrostatic potential maps (0.002 isodensity surface) of **(a)** PhTAD, **(b)** PFPTAD and **(c)** NO_2PhTAD show that both the nitro and the perfluorophenyl group have a similar electron withdrawing effect, thereby explaining the high reactivity of PFPTAD.

311G(d)) as a function of the dihedral angle between the planar TAD moiety and the phenyl group for all compounds (Figure IV.2). The plane defined by the nitro substituent in NO_2PhTAD yielded a second scan coordinate. The resulting optimal geometries were further optimised (B3LYP/6-311G(d)) to obtain the equilibrium conformer.

The EPMs in Figure IV.3 for the three equilibrium conformers show a substantial influence of the fluorine atoms and the nitro group on the electron distribution in the corresponding TAD compounds. In both cases, the electron density around the triazolinedione moiety decreases significantly compared to PhTAD, thereby explaining the remarkably high reactivity of both PFPTAD and NO_2PhTAD. This effect can also be related to our difficulties encountered in attempts at isolating the PFPTAD reagent.

IV.4.2 Structural characterisation of the modified polydienes

After reacting the SIS polymers with triazolinedione reagents in solution, the resulting polymers were isolated by evaporation of the solvent and analysed in-depth by NMR and FT-IR spectroscopy as well as by size exclusion chromatography (SEC). All of these

indicated a successful modification. In particular, proton NMR analysis of the modified polymers proves that the additives are indeed covalently linked to the polymer (Figure IV.4). Moreover, Figure IV.5a shows a representative set of NMR spectra for the modified SIS, in which neither unreacted R_FTAD nor any of its known low molecular weight degradation products are visible, while a steady increase of the characteristic signals for the Alder-ene addition products can be clearly observed for an increasing additive content.

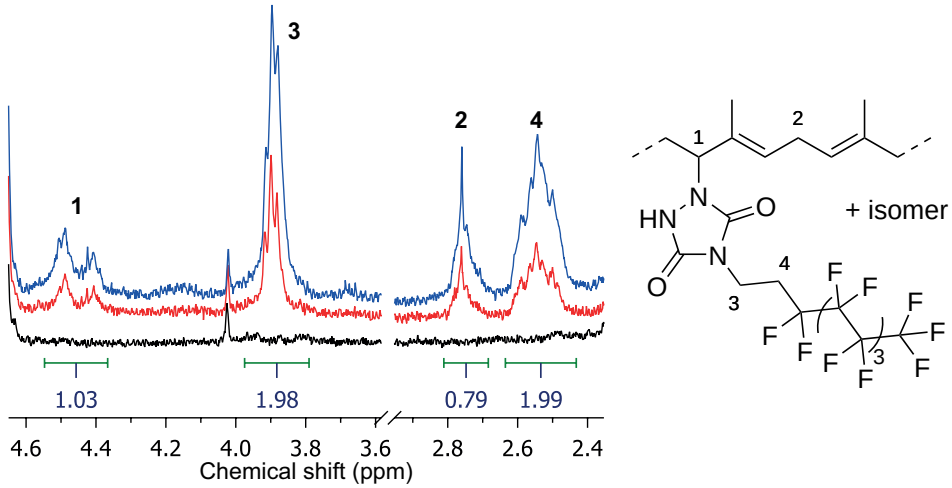

Figure IV.4: NMR spectra of SIS, modified with R_FTAD. The bottom curve shows the unmodified polymer, whereas the middle and the top curves show the modified polymers with resp. 20 wt% and 50 wt% R_FTAD, relative to the polymer weight.

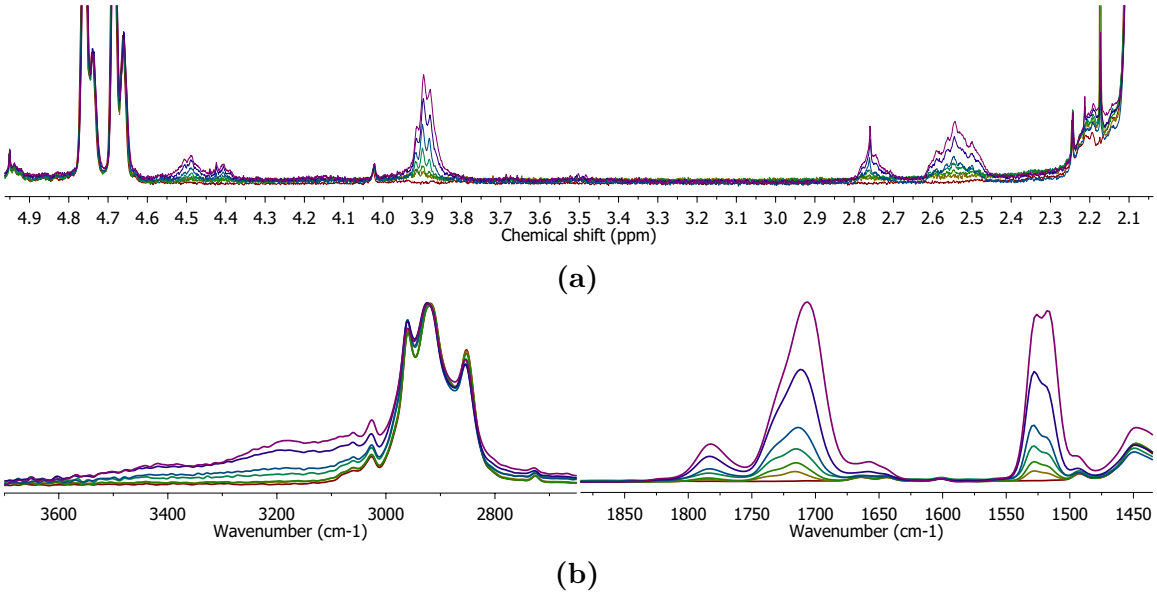

Figure IV.5: **(a)** Neither unreacted TAD nor related degradation products can be observed in the ^{1}H-NMR spectra of SIS with an increasing amount of R_FTAD. **(b)** IR spectroscopy on SIS with increasing amounts of PFPTAD shows an increasing intensity of the urazole C=O absorptions. Starting from an additive content of ~8 wt%, the presence of a hydrogen bonded urazole N−H is visible as well.

Using polystyrene as an internal standard, the NMR spectra of the modified polymers allow for the quantification of the urazole content and thus also of the actual amount of reacted additive. While this value corresponds well to the expected amount based on the amount of TAD reagent that was added for PFPTAD and PhTAD, showing typical yields between 85 % and 99 %, a consistently lower value of only 35 % was observed for the modification process with R_FTAD (Table IV.1). Nevertheless, as no other side reactions are observed here, the low urazole incorporation in the case of R_FTAD must be explained by a lower yield for the oxidation step for this specific class of perfluorinated TAD compounds, resulting in TAD solutions containing only about one third of the theoretical amount. While a further optimisation of this oxidation step might thus increase the overall efficiency, a thorough screening of the vast amount of possible urazole oxidants (section II.2.3) was out of the scope of this research. For our further analyses in this study, the experimentally determined yields were taken into account when evaluating the material properties as a function of the urazole content.

While infrared spectroscopy does not readily allow quantification of the amount of urazole, a representative set of spectra for the PFPTAD-modified polymers shows a steady increase in intensity of the absorptions around 1695 cm^{-1} and 1770 cm^{-1} as a function of the additive content, corresponding to the urazole C=O stretches (Figure IV.5b). Furthermore, a broad absorption corresponding to a hydrogen bonded urazole N−H (3150 cm^{-1}) is present in samples containing at least 8 wt% of additive (from NMR).[28]

Finally, the SEC elugrams show a significant influence on the apparent molecular weight and the dispersity of the resulting polymer (Figure IV.6). Nevertheless, since no degradation is observed in the NMR spectra, this apparent decrease in molecular weight as a function of additive content must be explained by the introduced hydrogen bonds, which lead to a decrease in hydrodynamic volume by self-aggregation of the polymer chains.

IV.4.3 Surface analysis of the modified polydienes

In the last phase of this project, the influence of the TAD modification on the surface properties of SIS was investigated by coating the different modified polymers on glass substrates. As already demonstrated by the initial surface modification experiments (*vide supra*), the perfluoroalkyl chain of R_FTAD was again found to have a huge influence on the

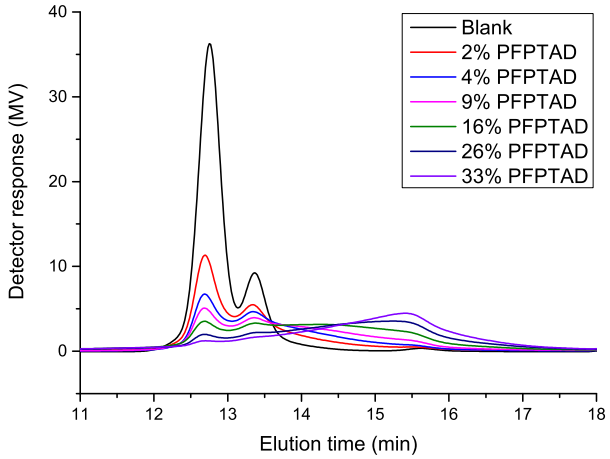

Figure IV.6: Representative set of SEC elugrams for the modified SIS. The apparent decrease in molecular weight as a function of the PFPTAD content can be explained by hydrogen bonding, which leads to a decrease in hydrodynamic volume.

hydrophobicity of the material (Figure IV.7a). An additive content of only 6 wt% (NMR-corrected) already increases its contact angle from 104° to 125° and thereby maximises the hydrophobicity, since a further increase in additive content has no significant effect on the wetting of the surface. Analysis of the fluorine content in the coatings via XPS confirms this trend observed in contact angles, as the fraction of fluorine detected at the surface rises quickly and above what is expected for a statistical distribution, levelling off when more than 6 wt% of additive is present (Figure IV.7b). The fact that the fluorine fraction is considerably higher than expected, based on a homogeneous distribution of the additive in the polymer, indicates that the fluorinated chains preferably assemble at the surface of the material, even when the modification is performed in solution.

Whereas modifications with R_FTAD in solution have a strong and remarkable effect on the surface characteristics of SIS, quite the opposite is true for PFPTAD. Indeed, only a modest increase in contact angle (3–4°) is observed at 5–10 wt% of additive content (Figure IV.7c). When even more TAD is added, the increasing importance of hydrogen bonds in the material, as evidenced by infrared analysis, results in a decrease in hydrophobicity, as initially observed in the surface modification experiments (Figure IV.1). At higher additive contents, PFPTAD actually leads to a constant contact angle, *i.e.* that of the unreacted SIS. Again, this behaviour can be further rationalised by XPS analysis of the corresponding coatings, which shows that the measured fluorine content, albeit below the quantification limit, is clearly lower than that expected for a homogeneous distribution of the additive in the polymer (Figure IV.7d). Therefore, in contrast to the surface modification in which the

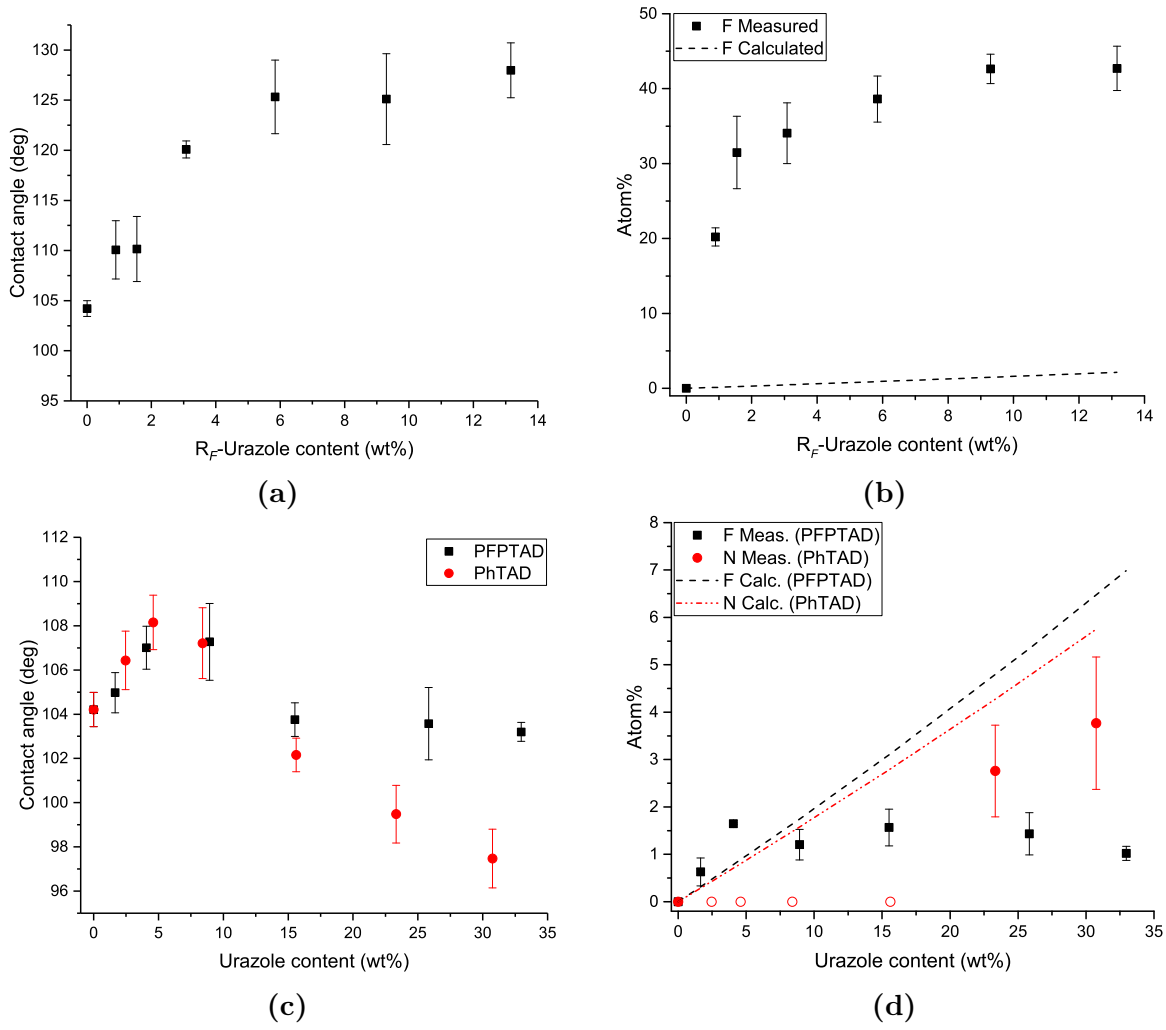

Figure IV.7: **(a)** Static water contact angles (SWCAs) for R$_F$TAD modified SIS as a function of the NMR-confirmed content of reacted additive: only 6 wt% of additive suffices to obtain a maximal hydrophobicity. **(b)** The corresponding XPS analysis clearly shows a higher fluorine content at the surface than expected for a homogeneous distribution of the additive. **(c)** SWCAs for PFPTAD and PhTAD modified samples as a function of the NMR confirmed wt% of reacted TAD show only a moderate effect on the wetting properties. Only a high amount of PhTAD decreases the hydrophobicity significantly. **(d)** The corresponding XPS analysis shows a fluorine or nitrogen content for PFPTAD resp. PhTAD that is, albeit below the quantification limit or even below the detection limit (open symbols), too low for a homogeneous distribution of both additives.

polar perfluorophenyl groups are introduced exclusively at the surface, the aromatic groups will preferably remain in the bulk of the material when the modification is performed in solution.

Finally, PhTAD proved to have a similar effect on the wettability of the surface compared to its fluorinated counterpart. Only at higher additive contents, *i.e.* >16 wt%, a significant decrease in hydrophobicity can be observed from the contact angle measurements

(Figure IV.7c), which is again explained by the corresponding XPS analysis. Nitrogen, originating from PhTAD, can only be detected at the surface as soon as the hydrophobicity of the material starts to decrease Figure IV.7d, which indicates that the wettability of the material is directly related to the appearance of polar and hydrogen-bonded urazole moieties at the surface (*cf.* Figure IV.5b).

IV.5 Conclusions and perspectives

Two fluorinated triazolinediones were investigated as reactive additives to modify the wetting properties of polydienes. Both heterogeneous modifications, *i.e.* submerging a solid polymer in a solution of TAD, and modifications in solution were performed. Despite the required synthetic effort to obtain the reactive additives, TAD chemistry outperforms all previously reported polydiene functionalisation strategies in terms of reaction conditions. For example, modifications in solution proved to be complete in a few of seconds at room temperature without the need for a catalyst. Moreover, compared to the multi-component reaction by Barner-Kowollik and co-workers (*vide supra*), TAD reactions are not limited to THF as solvent and do not introduce – thermally labile – halogens on the polymer chain.

While both the urazole moiety and the perfluorophenyl group, resulting from the modification with PFPTAD, introduce polarity in the polymer matrix, an influence on the wetting properties is only observed when a surface modification is performed. The aromatic substituents of both PFPTAD and its non-fluorinated analogue, *i.e.* PhTAD, are preferably located in the bulk of the material when the polymer is modified in solution, thereby limiting their effect on the surface properties.

Modifications using R_FTAD, on the other hand, unambiguously led to more hydrophobic materials with contact angles up to 125°. Even when the modification is performed in solution, an additive content of only 6 wt% is sufficient to have an optimal effect on the wetting properties since the fluorinated chains preferably assemble at the surface.

As a result of the high reactivity of triazolinediones, this research opens possibilities for the facile modification of other bulk or tailor-made polymers as well. By a similar assembly of fluorinated chains, a range of novel materials, of which the bulk is shielded with a covalently bound fluorophilic coating, could be easily obtained.

IV.6 Experimental section

All materials, solvents and their corresponding purification are presented in appendix A.

IV.6.1 Synthesis

The synthesis of R_FTAD is described in section III.5.1.6 while the synthesis of PFPTAD is described in section III.5.1.7.

IV.6.1.1 4-Phenyl-1,2,4-triazoline-3,5-dione (PhTAD)

4-Phenyl-1-(ethoxycarbonyl)semicarbazide

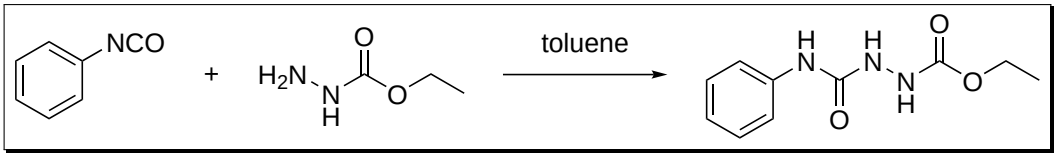

A mixture of ethyl carbazate (10 g, 96.1 mmol, 1 eq) and toluene (100 mL) was placed in a flask (250 mL) and cooled in an ice bath. The flask was equipped with an addition funnel, containing phenyl isocyanate (11.44 g, 96.1 mmol, 1 eq). The mixture was put under inert atmosphere and the isocyanate was added slowly under vigorous magnetic stirring. After addition, the mixture was stirred at room temperature for two hours, followed by two hours at 90 °C. After cooling to room temperature, 4-phenyl-1-(ethoxycarbonyl)semicarbazide was filtered off, washed with toluene and dried overnight in a vacuum oven at 40 °C.

Yield: 20.6 g white powder (92.3 mmol, 96 %).

Bruto formula: $C_{10}H_{13}N_3O_3$.

MW.: 223.23 g/mol.

4-Phenyl-1,2,4-triazolidine-3,5-dione

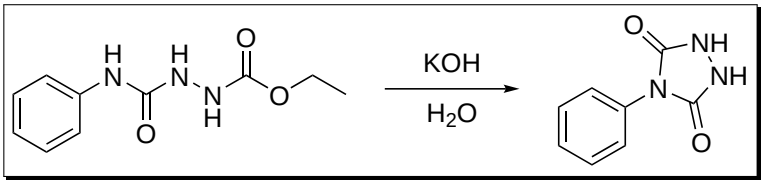

In a 100 mL flask, 4-phenyl-1-(ethoxycarbonyl)semicarbazide (20.6 g, 92.3 mmol) was dissolved in 50 mL (∼2 M semicarbazide) of an aqueous potassium hydroxide solution (4 M)

under inert atmosphere. 2 h (100 °C), filtered (hot), cooled to room temperature and acidified until pH 1 by the addition of aqueous hydrochloric acid. This mixture was cooled to room temperature to yield a solid white powder that was filtered off and dried overnight *in vacuo*.

Yield: 15.6 g white powder (88.1 mmol, 95 %).

Bruto formula: $C_8H_7N_3O_2$.

MW.: 177.16 g/mol.

^{1}H-NMR (300 MHz, DMSO−d_6): δ (ppm) = 7.33–7.53 (m, 5 H, Ar*H*), 10.46 (br.s, 2 H, N*H*).

4-Phenyl-1,2,4-triazoline-3,5-dione

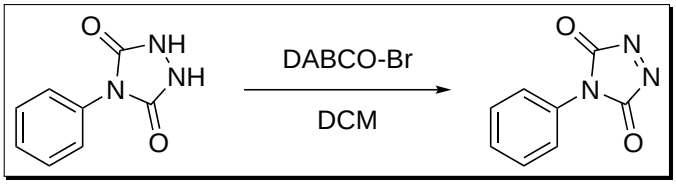

A mixture of 4-phenylurazole (1 g, 5.64 mmol, 1 eq), DABCO-Br (section III.5.1.2, 2.00 g, 1.27 mmol, 0.23 eq) and dichloromethane (30 mL) was put in a flask (100 mL) under inert atmosphere and stirred for 2 h at room temperature. The reaction mixture was filtered off, the residue washed with dichloromethane (2 × 30 mL) and the filtrate was concentrated *in vacuo* to obtain 4-phenyl-1,2,4-triazoline-3,5-dione. For stability reasons, the temperature of the heating bath should preferably not exceed 30 °C.

Yield: 819 mg dark red crystals (4.7 mmol, 83 %).

Bruto formula: $C_8H_5N_3O_2$.

MW.: 175.15 g/mol.

^{1}H-NMR (300 MHz, DMSO−d_6): δ (ppm) = 7.45–7.60 (m, 5 H, Ar*H*)).

IV.6.2 Methods

IV.6.2.1 Surface modification

Pellets of ABS and SBC were compression molded into plates of 70 × 40 × 2 mm for 2 min at 200 °C and a pressure of 4 metric tons using a pre-heated mold. The surface was modified by dipping the samples in a 55 mM solution of TAD in acetone for 10 minutes. The samples were then rinsed with acetone and dried under a stream of nitrogen gas. Finally, blank samples were obtained by the same treatment in the absence of TAD.

IV.6.2.2 Modification in solution

A 5 wt% stock solution of SIS in chloroform was prepared and used for all solution modifications. A sample of the SIS stock solution is mixed with a TAD solution of equal mass, containing either 2.5, 5, 10, 20, 35 or 50 wt% of TAD relative to the mass of the polymer. The latter TAD solutions were prepared by either dissolving the correct amount of PhTAD in the appropriate amount of dichloromethane, or by diluting the filtered oxidation mixtures (R_FTAD and PFPTAD) to the appropriate mass.

Example of a modification with 10 wt% PhTAD: 50 mg of PhTAD was dissolved in dichloromethane and diluted to a total mass of 10 g. This TAD solution was mixed with 10 g of the SIS stock solution (500 mg SIS). Example of a modification with 20 wt% R_FTAD: 1 g of the filtered oxidation mixture (2.5 wt% in R_FTAD, *i.e.* 25 mg TAD) was diluted to 2.5 g with dichloromethane. This TAD solution was mixed with 2.5 g of the SIS stock solution (125 mg SIS).

The resulting solutions of modified polymers were either evaporated and redissolved in $CDCl_3$ for NMR analysis, evaporated on the ATR crystal for FT-IR analysis, diluted with tetrahydrofuran for SEC analysis or spin coated on a glass substrate for contact angle goniometry and XPS analysis.

The additive yield was calculated from the ratio of the styrene signal (6.29–7.25 ppm, internal standard) and a representative TAD-adduct signal (PhTAD: 7.29–7.60 ppm, Ar−*H*; R_FTAD: 3.81–3.98 ppm, CF_2−CH_2−C*H*$_2$−N; PFPTAD: 4.27–4.81 ppm, [polymer]−C*H*−N−NH) in the ^{1}H-NMR spectra. The ratio of these signals was corrected for the number of protons and a constant contribution (*i.e.* signals corresponding with unreactive protons) of

the bare polymer and thus represents the molar ratio of styrene/TAD-adduct. Using this molar ratio, the molecular weights of styrene and the TADs, and a constant polystyrene content of 15 wt% in the supplied SIS, the actual additive content was determined together with the yield (*i.e.* by comparing the calculated additive content to the expected value). By calculating the yield in this way, a linear relation was obtained between the additive content and observed reacted additive for all experiments (Table IV.1), within the expected margins of error for such quantitative NMR measurements, as expected for a click reaction.

IV.6.3 Instrumentation

Computational methodology All energies and geometries were calculated at the ground state with the B3LYP/6-311G(d) level of theory in vacuum. The conformational analysis, in which the dihedral angles – defined by the planes of the planes of the different moieties – were varied in steps of 10° degrees, was performed with the Gaussian 09 software package. The final geometry optimisation and the generation of the electrostatic potential map on the 0.002 isodensity surface were performed with the Spartan '14 software package.

Fourier transform infrared spectroscopy (FT-IR) Infrared spectra were recorded with a Perkin Elmer FTIR SPECTRUM 1000 spectrometer, equipped with a PIKE Miracle attenuated total reflectance (ATR) unit. All spectra were recorded with a resolution of $4\,cm^{-1}$ and 8 scans were made for each measurement. ACD/Labs Spectrus Processor was used to analyse the obtained spectra.

Liquid chromatography - mass spectrometry (LC-MS) LC-MS analyses were performed on an Agilent Technologies 1100 series LC/MSD system with a diode array detector (DAD) and a single quad MS. Analytical reversed phase HPLC-analyses were performed with a Phenomex Luna C18 (2) column (5 µm, 250 mm × 4.6 mm) and a solvent gradient (0 % to 100 % acetonitrile in H_2O in 15 min). The eluted compounds were analysed via UV detection (214 nm).

Nuclear magnetic resonance (NMR) NMR spectra were recorded with a Bruker Avance 300 (300 MHz) FT-NMR spectrometer in the indicated solvent at room temperature. Chemical shifts are presented in parts per million (δ) with the residual solvent peak as an

internal standard.The resonance multiplicities are described as [br. (broad)] s (singlet), d (doublet), t (triplet), q (quadruplet), quint (quintuplet), sext (sextuplet) or m (multiplet).

Size exclusion chromatography (SEC) SEC was performed with an apparatus consisting of a Waters 1515 isocratic HPLC pump, a Waters 2410 Refractive Index detector and a Waters 2487 Dual λ Absorbance UV detector. The apparatus was equipped with two PLgel 5 µm MIXED-C 300 × 7.5 mm coupled in series at 35 °C. Polystyrene standards were used for calibration and THF as eluent at a flow rate of 1 mL min^{-1}. Samples were injected using a Waters 717plus autosampler.

Spin coating Polymer films were prepared by spin coating using the SPS Polos machine (SPIN150i/200i infinite). Glass cover slips (25 mm diameter) were used as substrate. A volume of 500 µL of polymer solution was deposited via micropipette and spin coated for 30 s, at a spin speed of 900 rpm and a spin acceleration of 400 rpm/s.

Static water contact angle goniometry A KRÜSS Easy Drop system was used to measure the static water contact angle (SWCA) values. Droplets of 1 µL were deposited onto the surface, after which a Laplace-Young fitting was applied. For each sample, a minimum of 15 drops were analysed. The outliers were identified using the IBM SPSS Statistics 24 software package.

X-ray photoelectron spectroscopy (XPS) The surface chemical composition of the spincoated polymer films were analysed by XPS (PHI 5000 Versaprobe II) employing an Al K_α X-ray source ($h\nu = 1486.6$ eV) operated at 50 W. All measurements were conducted in a vacuum of at least 10^{-6} Pa and the photoelectrons were detected with a hemispherical analyser positioned at an angle of 45° with respect to the normal of the sample surface. Survey scans 187.85 eV. The elemental composition was determined from the survey scans and quantified with Multipak software (V9.6.1) using a Shirley background and applying the relative sensitivity factors supplied by the manufacturer of the instrument.

IV.7 Bibliography

1. K. J. Saunders in *Polydienes*, Springer Netherlands, Dordrecht, **1973**, pp. 406–447.
2. D. J. Kind, T. R. Hull, *Polym. Degrad. Stab.* **2012**, *97*, 201–213.
3. G. Pritchard, *Plastics Additives: A Rapra Market Report*, iSmithers Rapra Publishing, United Kingdom, **2005**, p. 208.
4. D. Price, K. Pyrah, T. R. Hull, G. J. Milnes, J. R. Ebdon, B. J. Hunt, P. Joseph, C. S. Konkel, *Polym. Degrad. Stab.* **2001**, *74*, 441–447.
5. M. P. McGrath, E. D. Sall, S. J. Tremont, *Chem. Rev.* **1995**, *95*, 381–398.
6. D. N. Schulz, S. R. Turner, M. A. Golub, *Rubber Chem. Technol.* **1982**, *55*, 809–859.
7. A. Saffer, B. L. Johnson, *Ind. Eng. Chem.* **1948**, *40*, 538–541.
8. D. Derouet, F. Morvan, J.-C. Brosse, *Eur. Polym. J.* **2001**, *37*, 1297–1313.
9. D. Derouet, J.-C. Brosse, L. Cauret, F. Morvan, S. Mulder-Houdayer, *J. Appl. Polym. Sci.* **2003**, *87*, 47–60.
10. K. Brzezinska, K. B. Wagener, *Macromolecules* **1992**, *25*, 2049–2052.
11. A. Johnson, W. Nudenberg, *Halohydrin synthesis*, **1973**, US3733313A.
12. J. C. Brosse, I. Campistron, D. Derouet, A. El Hamdaoui, S. Houdayer, D. Reyx, S. Ritoit-Gillier, *J. Appl. Polym. Sci.* **2000**, *78*, 1461–1477.
13. Y. C. Bae, C. K. Ober, *Polym. Bull.* **2004**, *52*, 321–328.
14. J. Justynska, H. Schlaad, *Macromol. Rapid Commun.* **2004**, *25*, 1478–1481.
15. J. Justynska, Z. Hordyjewicz, H. Schlaad, *Polymer* **2005**, *46*, 12057–12064.
16. C. Decker, T. N. T. Viet, *Macromol. Chem. Phys.* **1999**, *200*, 1965–1974.
17. N. ten Brummelhuis, C. Diehl, H. Schlaad, *Macromolecules* **2008**, *41*, 9946–9947.
18. C. M. Geiselhart, J. T. Offenloch, H. Mutlu, C. Barner-Kowollik, *ACS Macro Lett.* **2016**, *5*, 1146–1151.
19. G. B. Butler, *Ind. Eng. Chem. Prod. Res. Dev.* **1980**, *19*, 512–528.
20. K. De Bruycker, S. Billiet, H. A. Houck, S. Chattopadhyay, J. M. Winne, F. E. Du Prez, *Chem. Rev.* **2016**, *116*, 3919–3974.
21. B. J. Gold, C. H. Hövelmann, C. Weiss, A. Radulescu, J. Allgaier, W. Pyckhout-Hintzen, A. Wischnewski, D. Richter, *Polymer* **2016**, *87*, 123–128.
22. J. Huang, L. Zhang, Z. Tang, S. Wu, N. Ning, H. Sun, B. Guo, *Macromol. Rapid Commun.* **2017**, *38*, 1600678.
23. C. C. Cheng, C. A. Seymour, M. A. Petti, F. D. Greene, J. F. Blount, *J. Org. Chem.* **1984**, *49*, 2910–2916.

24. Y. Elemes, M. Stratakis, M. Orfanopoulos, *Tetrahedron Lett.* **1989**, *30*, 6903–6906.

25. K.-W. Leong, G. B. Butler, *J. Macromol. Sci. - Chem.* **1980**, *14*, 287–319.

26. T. C. S. Chen, G. B. Butler, *J. Macromol. Sci. Pure Appl. Chem.* **1981**, *16*, 757–768.

27. C. Hilger, R. Stadler, *Macromolecules* **1990**, *23*, 2095–2097.

28. R. Stadler, L. de Lucca Freitas, *Polym. Bull.* **1986**, *15*, 173–179.

29. S. van der Heijden, K. De Bruycker, R. Simal, F. Du Prez, K. De Clerck, *Macromolecules* **2015**, *48*, 6474–6481.

30. S. van der Heijden, L. Daelemans, K. De Bruycker, R. Simal, I. De Baere, W. Van Paepegem, H. Rahier, K. De Clerck, *Compos. Struct.* **2017**, *159*, 12–20.

31. S. Werner, D. P. Curran, *Org. Lett.* **2003**, *5*, 3293–3296.

32. T. J. Gilbertson, T. Ryan, *Synthesis* **1982**, *1982*, 159–160.

33. I. T. Horváth, J. Rábai, *Science* **1994**, *266*, 72–75.

34. I. T. Horváth, *Fluorous Chemistry*, Springer-Verlag Berlin Heidelberg, 1st ed., **2012**, p. 414.

35. M. E. Burrage, R. C. Cookson, S. S. Gupte, I. D. R. Stevens, *J. Chem. Soc. Perkin Trans. 2* **1975**, *1975*, 1325–1334.

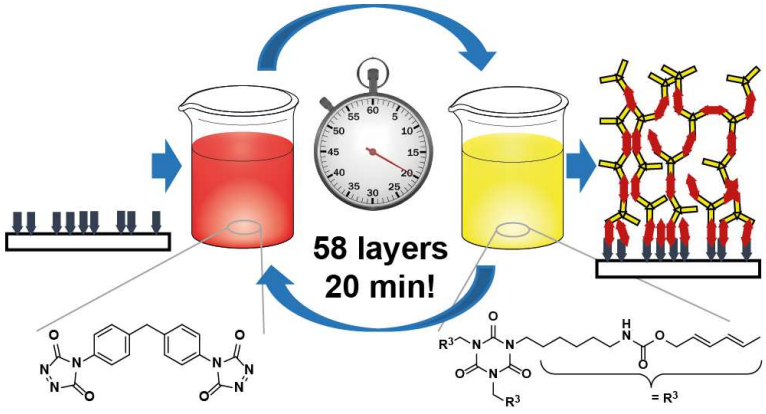

Abstract

Layer-by-layer deposition is a widely used method for surface functionalisation. It is shown here that up to 58 covalently linked molecular layers could be assembled in 20 minutes at room temperature on a silicon wafer by the highly efficient layer-by-layer reaction of a divalent triazolinedione and a trivalent diene. The layer growth was found to be linear. The multilayers were analysed by ellipsometry, atomic force microscopy, and X-ray photoelectron spectroscopy.

Adapted from

B. Vonhören, O. Roling, K. De Bruycker, R. Calvo, F. E. Du Prez, B. J. Ravoo, *ACS Macro Letters* **2015**, *4*, 331–334.

Chapter V

Triazolinedione-based layer-by-layer assembly

V.1 Introduction

Layer-by-layer (LbL) assembly is a popular and versatile technique for the deposition of thin films of controlled thickness on various substrates.[1–3] As the name suggests, it is a coating technique based on the alternating deposition of mutually attractive molecules. Shortly after the first examples, which required polyanions and polycations,[3] several systems based on other supramolecular interactions, such as hydrogen bonding[4,5] and host-guest interactions[6,7] were investigated as well. However, for applications in materials science and coatings, covalently linked multilayers are preferred over non-covalent LbL assemblies, mainly because of their solvent resistance and their higher stability in solutions of high ionic strength or extreme pH.[8–17]

The main reason for the popularity of the LbL technique is its experimental simplicity, which resulted in the widespread application of LbL depositions for the generation of functional surfaces. For example, LbL methods have been used to assemble stacked graphene anodes for organic solar cells,[18] to build healable polymer coatings[19] and to tune the wettability properties of a surface.[20,21] The multilayers are typically assembled by simply soaking a surface in two solutions that contain the mutually attractive molecules, thereby only requiring a set of tweezers and a couple of beakers as 'equipment'. Nevertheless, this experimental setup results in a highly time consuming LbL build-up, especially

for covalently cross-linked multilayers. Dipping times, *i.e.* the time required per layer, typically range from 20 minutes to several hours, resulting in a total assembly time of at least 6.5 hours for a 20-layer coating, excluding the washing steps in between each layer deposition.[9,11,13–16] Therefore, decreasing the time needed for the LbL assembly is of great interest to surface scientists.

One strategy to speed up the LbL process is by replacing the traditional dipping method by a more efficient experimental setup. A first example of such an optimised setup is the spray assisted LbL deposition, in which solutions containing molecules with complementary reactive groups are sprayed in a sequential manner on the surface rather than dipping the surface into the solutions.[22–25] Cho *et al.* reported on a second alternative by demonstrating that spin coating assisted LbL affords highly ordered polyelectrolite multilayers in a much shorter timespan compared to the direct dipping method.[26] Nevertheless, while either of these methods result in a decreased application time down to a few seconds per layer, a common drawback is the inefficient use of adsorbate solutions, which are rinsed off the substrate to a large extent.

Using a different and faster pair of reactants represents another possible strategy to improve the speed of the LbL deposition. As previously discussed (section II.3), Diels-Alder reactions between triazolinediones and dienes are typically complete within a timescale of seconds and proceed at room temperature without the need of a catalyst. Therefore, this chemistry should be well suited for the assembly of covalently linked multilayers if adsorbate molecules bearing multiple TAD and diene units, respectively, are reacted to a substrate. Moreover, because of their high reactivity, even at very low concentrations, LbL deposition should be possible by the traditional dipping method, thereby eliminating the previously discussed drawbacks of current LbL systems.

In this collaborative effort with the group of Prof. Bart Jan Ravoo (University of Münster), we first prepared a TAD-compatible substrate, *i.e.* a silicon wafer with a TAD-reactive monolayer. These substrates were then alternatingly dipped into solutions of a divalent TAD (MDI-TAD) and an isocyanurate derivative substituted with three diene moieties, respectively (Figure V.1). The choice for this reactive pair resulted from the study on homogeneous reactions of trivalent alkenes/dienes with MDI-TAD (section III.2.1), where the reaction kinetics and the solubility were the most important parameters for this project.

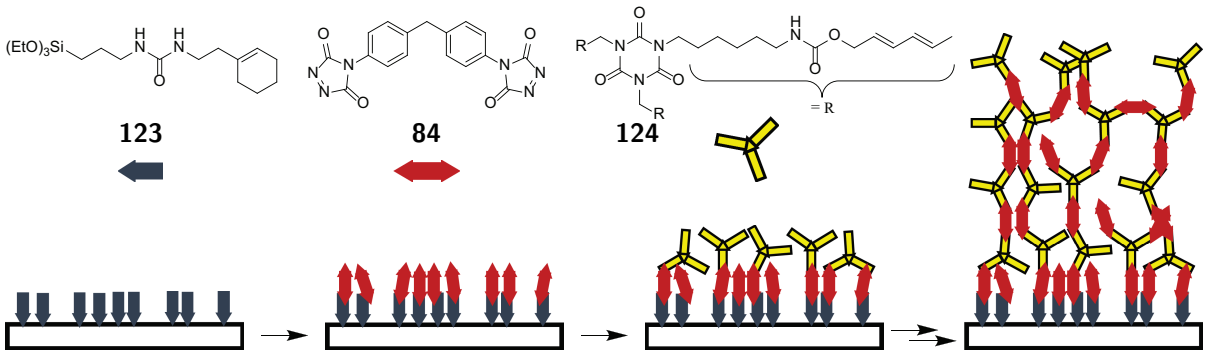

Figure V.1: Molecular building blocks used in this study and schematic representation of the layer-by-layer process. Silicon wafers were first covered with a layer of cyclohexene silane **123**. Multilayers were assembled by soaking the surface in solutions of divalent triazolinedione (TAD) **84** and trivalent diene **124** in an alternating fashion.

The layer thickness was monitored by ellipsometry and the samples were further analysed by atomic force microscopy (AFM) and X-ray photoelectron spectroscopy (XPS).

V.2 Preparation of TAD-compatible substrates

To start the layer-by-layer deposition of TAD- and diene-bearing molecules from solution, a complementary reaction partner for either of these molecules should first be chemically attached to the surface. While silicon wafers with an undecenyl-terminated self-assembled monolayer (SAM) were already available in the group of Ravoo and co-workers, these monosubstituted C=C bonds were especially useful for subsequent modifications using a radical hydrothiolation.[7,27] In the case of TAD chemistry, however, the unsaturations proved to react very slowly at the solid-liquid interface. Therefore, an alternative silane with a more suitable trisubstituted alkene (Figure II.10) was first obtained by reacting 2-(1-cyclohexenyl)ethylamine with 3-(triethoxysilyl)propyl isocyanate (Scheme V.1).

Next, silicon wafers were functionalised with a SAM of the synthesised cyclohexene-terminated silane (**123**) to yield surfaces that are reactive towards TAD (Figure V.1). As

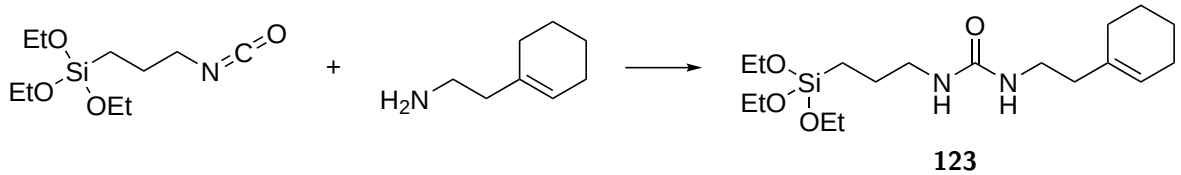

Scheme V.1: Synthesis of a TAD-reactive cyclohexene-terminated silane (**123**) that was subsequently used to functionalise silicon wafers.

a result of this modification, the static contact angle increased from less than 10° for the activated silicon surface to 67° for the coated surface (Figure V.2). While this increase in hydrophobicity is already an initial proof of the successful deposition of silane **123** on the silicon wafer, XPS analysis unambiguously showed the presence of nitrogen on the surface, as expected for a nitrogen-containing coating (*vide infra*).

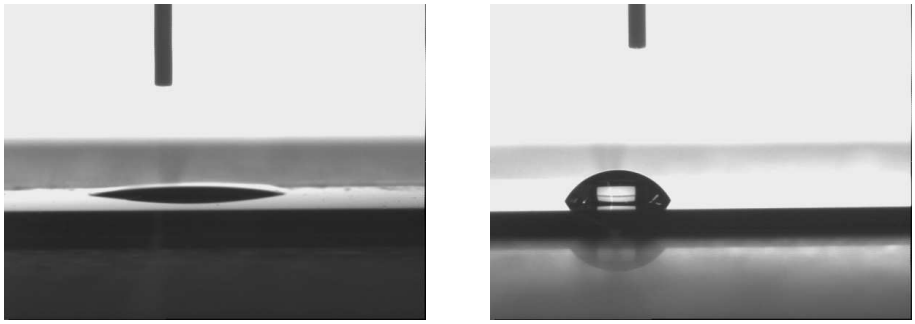

(a) **(b)**

Figure V.2: Static contact angles of a water droplet on **(a)** the activated silicon wafer (< 10°) and **(b)** the cyclohexene-functionalised monolayer (67°).

The thickness of the SAM was determined by ellipsometry and was found to be low in comparison to the length of the molecule, *i.e.* 1.0 nm and ∼2 nm, respectively. Therefore, we assume that a reactive coating with a lower density of cyclohexenes was obtained instead of a tightly packed SAM. This low coverage might be caused by the mild reaction conditions used for the monolayer preparation, *i.e.* stirring of the activated silicon wafers overnight at room temperature in a solution of a triethoxysilane rather than a trichlorosilane. Nevertheless, since TAD shows a good selectivity towards this kind of alkenes at short reaction times (section II.3.3), the surface modification should not be hampered by this lower density.

V.3 Layer-by-layer deposition

V.3.1 Traditional experimental setup

In general, any molecule that tolerates the reaction conditions and bears more than one TAD-reactive group could be used as building block for this LbL deposition. Nevertheless, the combination of a divalent TAD and a trivalent complimentary reaction partner should guarantee linear layer growth, even though some degree of 'back-bonding' to the surface

cannot be excluded.[9,10,12]

Section III.2.1 describes the synthesis of a range of trivalent alkenes/dienes from bulk chemicals, as well as their homogeneous reactions with MDI-TAD (**84**, Figure V.1). Based on this study, we decided to use the isocyanurate-based hexamethylene diisocyanate trimer (HDI_3) that was reacted with three equivalents of 2,4-hexadien-1-ol (HDEO). This diene trimer (**124**) was characterised by a good solubility and very high cross-linking kinetics when mixed with MDI-TAD. Moreover, because HDI_3 is supplied as a pure, highly viscous liquid, the diene trimer is readily synthesised either in bulk or in solution without the need for further purifications. Since the stability of TAD against moisture and heat is moderate while the corresponding urazole precursor is known to be very stable, we always prepared a fresh batch of TAD for the LbL deposition by oxidation of the urazole precursor.

Next, two solutions were prepared for the LbL deposition. MDI-TAD and the diene building block were each dissolved in dry THF under an argon atmosphere at concentrations of 150 mM and 75 mM, respectively. The coated silicon wafers (section V.2) were first immersed in the solution of TAD **84**, in which the cyclohexene on the monolayer reacted to yield a wafer with terminal TAD groups (Figure V.1). This layer could then be reacted with the diene building block **124** by immersion in the corresponding solution. These two soaking steps were repeated until the desired number of layers was deposited on the silicon wafer. In between each deposition step, the wafers were rinsed with acetone to remove unreacted molecules and dried in a stream of argon. When the reaction time was optimised, we found that soaking the sample for 10 seconds at each deposition step is sufficient, since longer dipping times of up to 5 minutes did not lead to a significant increase in multilayer thickness, as determined by ellipsometry.

Figure V.3 plots the layer thickness, determined by ellipsometry, as a function of the number of layers for a batch of samples with up to 20 layers. These analyses show a clear linear correlation between the thickness of the organic multilayer and the layer number with a slope of 1.8 nm/layer. The sample indicated by the red square shows a thickness that is lower than expected for the number of layers, because a blocking layer was assembled on this sample after five normal deposition steps. Instead of soaking this sample in a solution of building block **124** to assemble layer six, which could then again react with TAD, the sample was dipped in a solution of HDEO (500 mM) for five minutes

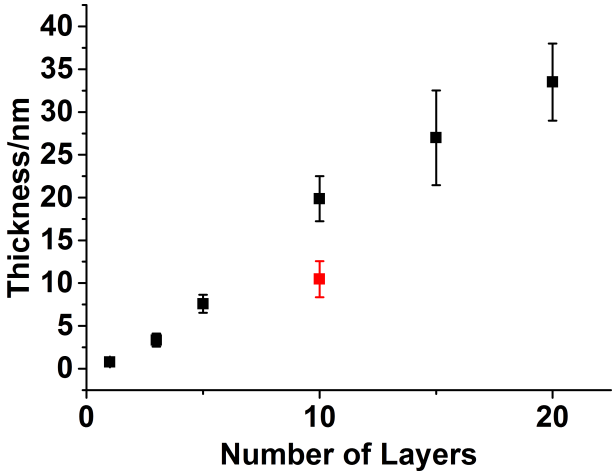

Figure V.3: Ellipsometry data for multilayer samples bearing up to 20 layers (black squares) show a linear increase of the thickness as a function of the number of layers. The red square describes a sample that was passivated after five regular dipping cycles, preventing further deposition of layers. Each sample was measured on ten spots. The error bars represent the standard deviation of these values.

in order to saturate all TAD moieties on the surface. Indeed, an attempted assembly of four more layers did not lead to a significant increase in layer thickness, which proves that the LbL process relies on covalent bonding and not on unspecific adsorption.

Apart from ellipsometry measurements, samples with 5 and 15 layers were further analysed by AFM to study the topography of the multilayer surfaces. Both samples show a granular polymer coating with a root-mean-square roughness of 2 and 5 nm, respectively (Figure V.4a and b). This observed increase in surface roughness with the number of layers can be ascribed to irregularities during the LbL process. As a reference, similar surface roughnesses of 4 and 6 nm were reported for eight- and sixteen-layer films, respectively, by Caruso and co-workers, who assembled multilayers of covalently linked polymers by azide-alkyne click chemistry.[11] Additionally, the multilayer coating was scraped off the silicon wafer with the cantilever, which allowed the measurement of the multilayer thickness by AFM. A thickness of around 6 nm was measured for the sample with 5 layers and around 27 nm for that with 15 layers (Figure V.4c and d). These values closely correspond to those obtained via ellipsometry (Figure V.3) and thus clearly confirm the linear increase in height with each deposition step.

Finally, the atomic composition of the multilayer was also determined by XPS for samples with up to eight layers. Carbon, nitrogen, silicon and oxygen can all be detected on the surface, which either derive from the organic multilayer coating or the underlying silicon

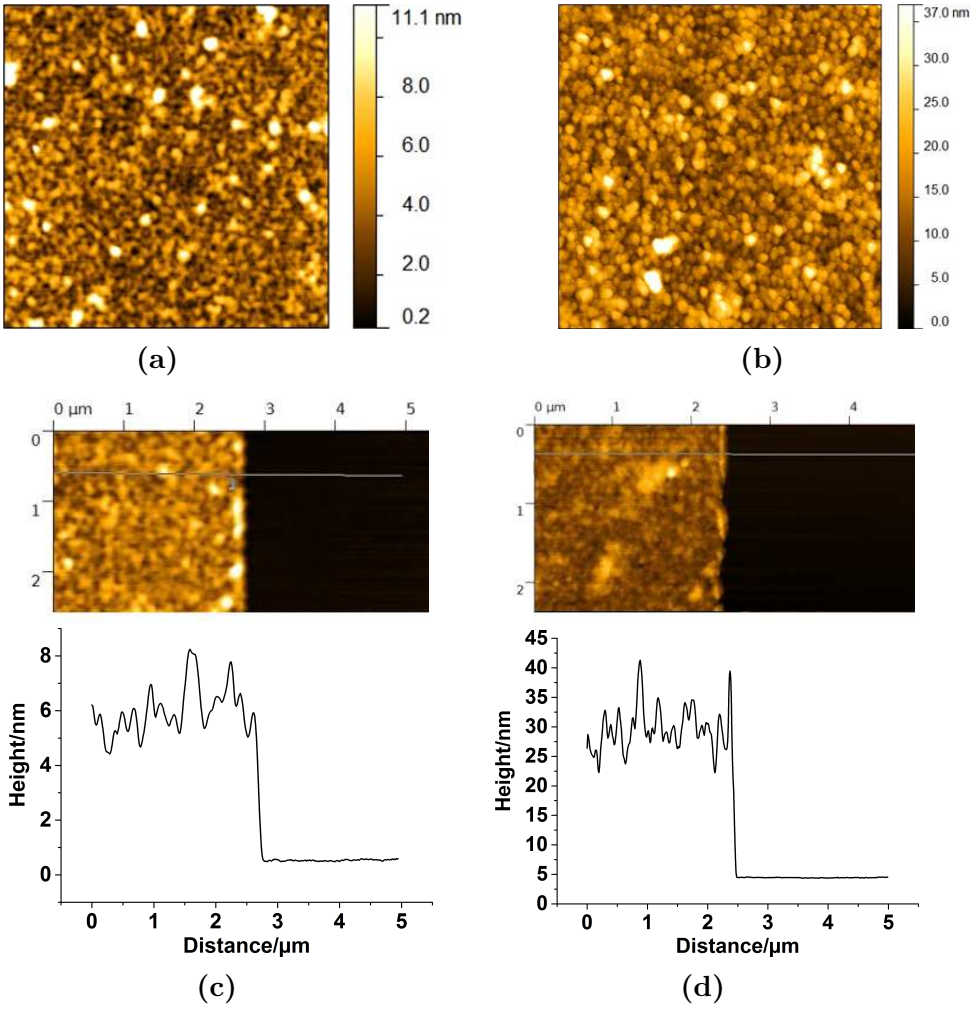

Figure V.4: AFM height images ($5 \times 5\,\mu m$) of **(a)** 5 layer sample and **(b)** 15 layer sample using the traditional washing method. Parts of these multilayer coating were then removed with the cantilever of the AFM in order to measure the height of the coating, as shown in **(c)** and **(d)**, respectively.

wafer that is oxidised under ambient conditions. Survey scans are shown in Figure V.5a, while Figure V.5b plots the calculated atomic concentrations as a function of the number of layers. These figures demonstrate that the intensities of the carbon and nitrogen signals, characteristic for the multilayers, increase with the number of layers, whereas the signals for silicon and oxygen show a steady decrease with the layer number. Indeed, the overlying organic multilayers prevent the photoelectrons of the silicon wafer from escaping the sample. High resolution spectra of the carbon and nitrogen signals of a selection of samples are shown in Figure V.5c and d, respectively. The monolayer shows the smallest carbon signal with shoulders that can be assigned to the higher oxidised carbon atom of the urea group in silane **123**. This urea group is also responsible for the small nitrogen signal in the SAM. Both intensities increase for the multilayer samples as a result of the larger

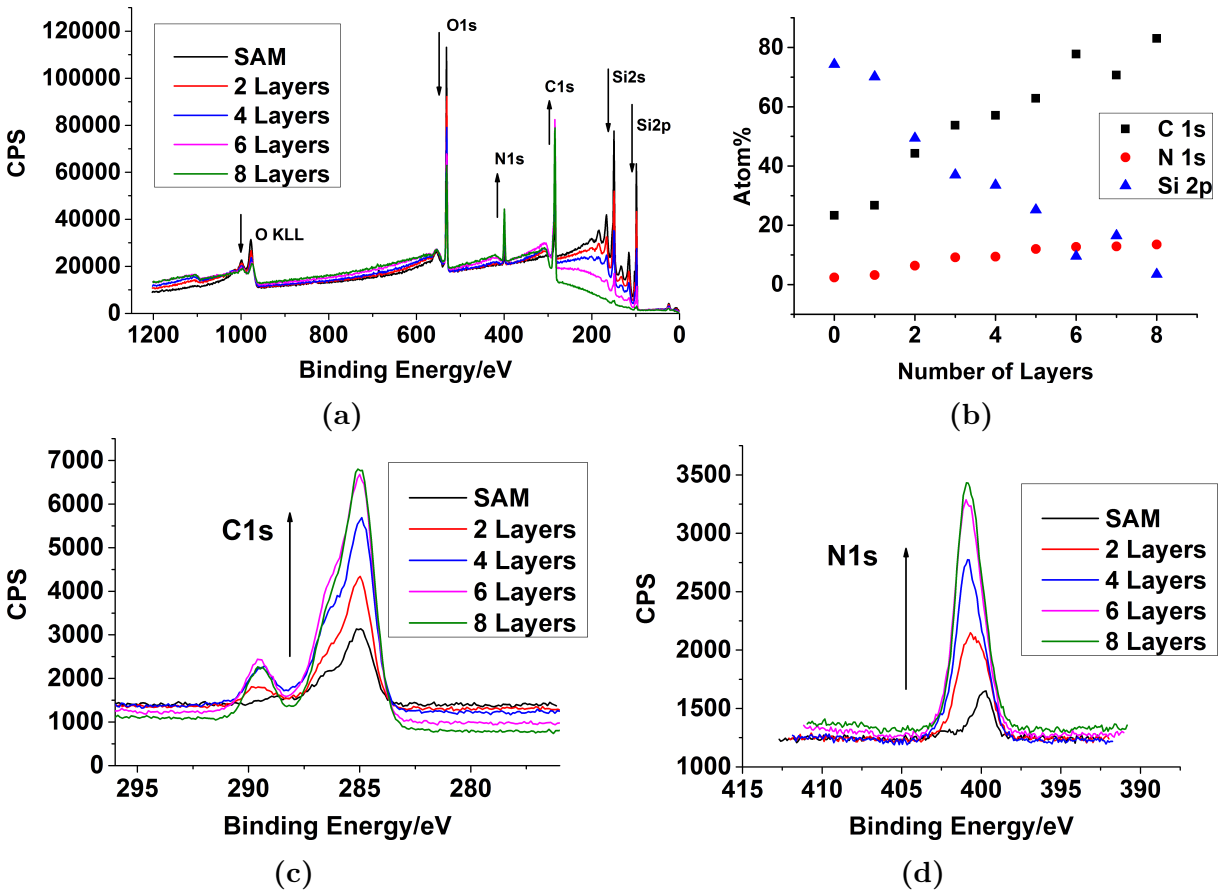

Figure V.5: X-ray photoelectron spectroscopy measurements. **(a)** Survey spectra and **(b)** atomic concentrations of C 1s, N 1s, and Si 2p for samples with up to eight layers. The intensities of the element being characteristic for the multilayer coating increase (C 1s and N 1s), whereas the Si 2p signal of the underlying wafer decreases with layer number. **(c)** High resolution scans of C 1s show significant shoulders as a result of higher oxidised carbon species in the molecular building blocks **84** and **124**, while **(d)** scans of the N 1s signal clearly show the increase in nitrogen content as a function of the number of layers.

amount of carbon and nitrogen from the polymer coating. Furthermore, the shoulders are more pronounced as the multilayer samples contain larger amounts of oxidised carbons, originating from the carbonyl carbon atoms in triazolinedione **84**, and the carbamate and isocyanurate functions in diene **124**.

V.3.2 Optimised washing step for LbL deposition

Since ellipsometry, AFM and XPS measurements provided consistent evidence that multilayers can be assembled based on TAD chemistry, the next objective consisted of further speeding up the LbL process. Indeed, with an optimal reaction time of 10 seconds, the rinsing and drying steps in between each layer deposition lasted about 1 minute and thus

became the remaining bottleneck that slowed down the LbL assembly. Nevertheless, it is important to remove unreacted molecules from the surface to prevent cross-contamination of the two adsorbate solutions. Therefore, the washing steps cannot be omitted.

Instead of skipping the washing step, we prepared an additional batch of samples using a simplified procedure. Rather than rinsing and drying the sample in between each soaking step, we simply dipped it consecutively for 3 seconds in both acetone and THF and immersed it in the other LbL solution. Overall, the drying step was thus skipped. Using this new dip washing method, the total assembly time for one layer, *i.e.* including the reaction time and the wasing, was decreased down to approximately 20 seconds. Consequently, 58 layers were successfully assembled in merely 20 minutes, which is in sharp contrast to previously reported deposition times of 20 minutes per layer (*vide supra*).

Similarly to the traditional method, the increase in layer thickness, as determined by ellipsometry, is directly proportional to the number of layers with the same slope as for the previously obtained samples (Figure V.6). Moreover, the obtained multilayer coatings display similar roughnesses as well (Figure V.7). Therefore, this optimised procedure allows an ultrafast LbL assembly without the loss of material that is inevitable in the spray assisted method, while still yielding equivalent coatings compared to the slower traditional LbL assembly.

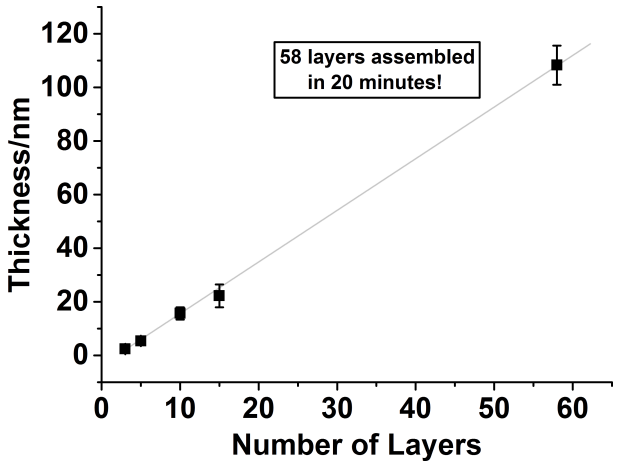

Figure V.6: Ellipsometry data for multilayers bearing up to 58 layers, prepared by the dip washing method, shows the same slope as the batch prepared by the traditional rinsing method (see Figure V.3).

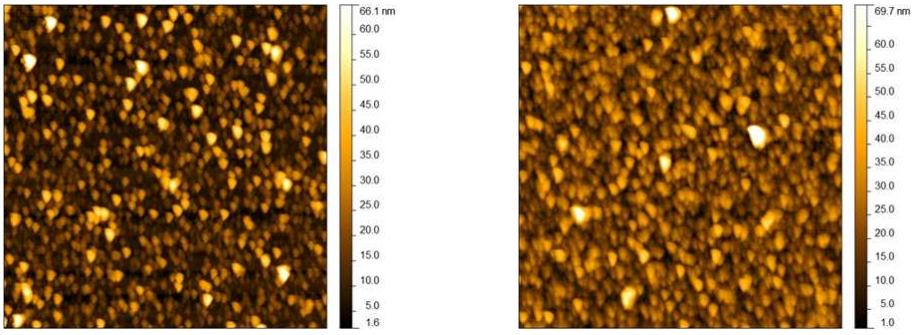

(a) **(b)**

Figure V.7: AFM height images ($5 \times 5\,\mu m$) of **(a)** 5 layer sample and **(b)** 15 layer sample by the optimised dip washing method.

V.4 Conclusions and perspectives

In this chapter, we presented an ultrafast LbL method utilising the highly efficient reaction between a divalent TAD and a trivalent diene molecule. Using ellipsometry, a linear increase of the layer thickness as a function of the layer number could be proven and further confirmed by AFM and XPS analyses. After optimisation of both the deposition and the washing steps, 58 layers could be assembled in merely 20 minutes.

Since the synthesis of the divalent TAD is straightforward and a variety of molecules can in theory be substituted with various dienes, we envision that this reaction can find application in numerous LbL systems. Nevertheless, in this system, the coatings cover the full surface as a result of the homogeneous cyclohexene-functional monolayer on the initial substrate. Alternatively, a patterned TAD-compatible substrate could be used to easily produce patterned coatings with a controllable thickness via this LbL process. While the next chapter will discuss the patterning of triazolinediones on similar, *i.e.* homogeneous, TAD-compatible substrates via microcontact chemistry, the proposed strategy requires the patterning of the TAD-complementary reaction partner. Although successful preliminary results were already obtained by our collaboration partner on this subject, further research will be necessary.

V.5 Notes on the collaboration

This chapter describes a collaboration with the group of Prof. Bart Jan Ravoo (University of Münster, Germany). Small molecules were synthesised by Kevin De Bruycker at Ghent University. Layer-by-layer depositions were performed and analysed by Benjamin Vonhören and Oliver Roling at the University of Münster. The collaborators discussed and commented on the results at all stages.

V.6 Experimental section

All materials, solvents and their corresponding purification are presented in appendix A.

V.6.1 Synthesis

The synthesis of 4,4′-(4,4′-methylenediphenyl)-bis-(1,2,4-triazoline-3,5-dione) (**84**) is described in section III.5.1.3.

V.6.1.1 1-(2-(cyclohexenyl)ethyl)-3-(3-(triethoxysilyl)propyl)urea (123)

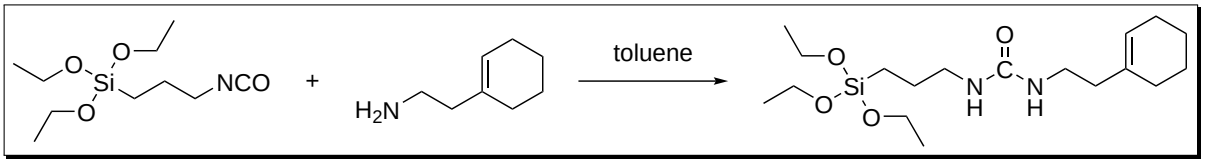

3-(Triethoxysilyl)propyl isocyanate (2 g, 8.09 mmol, 1 eq) was dissolved in toluene (10 mL) in a dry two neck flask under inert atmosphere. Then 2-(1-cyclohexenyl)ethylamine (1.013 g, 8.09 mmol, 1 eq) was added dropwise and the mixture was allowed to stir at room temperature overnight. The solvent was removed *in vacuo*, the flask heated to 60 °C and evacuated with an oil pump for several hours.

Yield: 2.52 g white powder (6.76 mmol, 84 %).

Bruto formula: $C_{18}H_{36}N_2O_4Si$.

MW.: 372.58 g/mol.

ESI-MS (m/z): 373.251 71 $[M + H]^+$.

^{1}H-NMR (300 MHz, $CDCl_3$): δ (ppm) = 0.64 (t, 2 H, Si−CH_2), 1.23 (t, 9 H, 3 × O−CH_2−CH_3), 1.49–1.69 (band, 6 H, 2 × CH_2(Ch) + Si−CH_2−CH_2), 1.92 (broad, 2 H, CH=C−CH_2), 1.99 (broad, 2 H, C=CH−CH_2), 2.13 (t, 2 H, CH=C−CH_2−CH_2−NH), 3.16 (q, 2 H, NH−CH_2), 3.23 (q, 2 H, NH−CH_2), 3.82 (q, 6 H, 3 × O−CH_2−CH_3), 4.28 (br. t, 1 H, NH), 4.51 (br. t, 1 H, NH), 5.47 (s, 1 H, C=CH).

^{13}C-NMR (75 MHz, $CDCl_3$): δ (ppm) = 158.31, 134.90, 123.63, 58.56, 43.06, 38.32, 38.29, 27.96, 25.36, 23.67, 22.94, 22.49, 18.42, 7.74.

V.6.1.2 Isocyanurate derivative 124

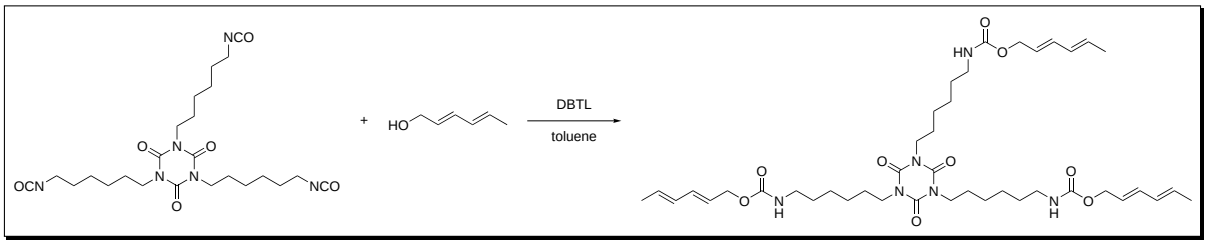

In a 250 mL flask, HDI_3 (**78**, 10.0 g, 19.8 mmol, 1 eq) was dissolved in 100 mL toluene under inert atmosphere. To this solution, 2,4-hexadiene-1-ol (5.84 g, 59.5 mmol, 3 eq) and dibutyltin dilaurate (100 µL) were sequentially added. The reaction mixture was stirred at room temperature for two hours. An exothermic reaction can be observed. After evaporation of the solvent *in vacuo*, the resulting oil solidified overnight in a vacuum oven at 40 °C.

Yield: 15.7 g off-white solid (19.7 mmol, 99 %).

Bruto formula: $C_{42}H_{66}N_6O_9$.

MW.: 799.02 g/mol.

ESI-MS (m/z): 857.5 $[M + OAc]^-$.

^{1}H-NMR (300 MHz, $CDCl_3$): δ (ppm) = 1.35 (broad, 12 H, $CH_2-CH_2-CH_2$), 1.50 (broad, 6 H, $CH_2-CH_2-CH_2$), 1.64 (broad, 6 H, $CH_2-CH_2-CH_2$), 1.76 (d, 9 H, CH=CH−CH_3), 3.16 (q, 6 H, NH−CH_2), 3.86 (t, 6 H, N−CH_2), 4.55 (d, 6 H, O−CH_2), 4.77 (br. s, 3 H, N*H*), 5.62 (m, 3 H, CH=C*H*−CH_3), 5.75 (m, 3 H, O−CH_2−C*H*), 6.05 (dd, 3 H, C*H*=CH−CH_3), 6.24 (dd, 3 H, CH_2−CH=C*H*).

^{13}C-NMR (75 MHz, $CDCl_3$): δ (ppm) = 156.50, 149.10, 134.42, 131.03, 130.66, 124.65, 65.32, 42.93, 40.96, 29.93, 27.80, 26.37, 26.31, 18.24.

V.6.2 Methods

V.6.2.1 Preparation of self-assembled monolayers

Silicon wafers were first cleaned by sonication for 3 min in pentane, acetone and water. Next, they were activated in piranha solution (H_2SO_4(*conc.*) : H_2O_2(30 %) = 2 : 1) for 30 min (danger!), rinsed with copious amounts of water, dried in a stream of argon and transferred into a solution of silane **123** (10 mM in toluene (analytical grade)) under a blanket of argon. After stirring the solution for 18 h at room temperature, the samples

were taken out and rinsed with dichloromethane, ethanol and water and dried in a stream of argon.

V.6.2.2 Layer-by-layer assembly of triazolinedione 84 and isocyanurate derivative 124

Two solutions were prepared for the layer-by-layer assembly of the active layer and kept in Schlenk flasks under an atmosphere of argon:

A) 150 mM triazolinedione **84** in dry THF.

B) 75 mM isocyanurate derivative **124** in dry THF.

The samples were initially placed in the solution A for 1 min, rinsed with acetone, dried in a stream of argon and then left alternatingly in the solutions A and B for 10 s. The samples were washed between each deposition step by rinsing with acetone and drying in an argon stream. The samples were typically rinsed for 5–10 s with 20–40 mL of acetone. Reaction times were the same for the last multilayer batch, but the rinsing and drying steps were omitted. Instead, the samples were simply dipped into beakers with acetone (300 mL) and THF (300 mL) for about 3 s each. The 2,4-hexadien-1-ol blocking layer was assembled by soaking the sample for 5 min in a 500 mM solution in dry THF.

V.6.3 Instrumentation

Atomic force microscopy (AFM) AFM imaging was performed using a Nanowizard 3 from JPK Instruments operated in tapping mode with Veeco RTESP-Tapping Mode Etched Silicon Probes. The AFM was typically operated with a setpoint of 0.900 V and a scan rate of 1.00 Hz with a resolution of 512×512 pixels. Scratching experiments were performed with the same set up operated in contact mode. 10 to 15 images were taken with a setpoint of 2.15 V and a line rate of 10.00 Hz in order to remove the organic material from the silicon wafers. The data was analysed with Gwyddion (version 2.22). The RMS roughness was measured over an area of $5 \times 5\,\mu m$.

Contact angle goniometry Water contact angles were measured by the sessile drop method on a DSA 100 goniometer (Krüss GmbH Wissenschaftliche Laborgeräte, Germany).

Ellipsometry Ellipsometry measurements were performed using 'The Multiskop' build by 'Optrel GBR' (Kleinmachnow, Germany). Measurements were performed at an angle of incidence of 55° with a laser of 632.8 nm wavelength. The built-in software of the machine was used to analyse the data. The refractive index of the organic materials was assumed to be 1.45. Every sample was measured on 10 different spots. The error bars in the graph represent the standard deviation of these measurements.

Mass spectrometry An Agilent technologies 1100 series LC/MSD system equipped with a diode array detector and single quadMSdetector (VL) with an electrospray source (ESI-MS) was used for MS analysis. ESI accurate masses were measured on a LTQ Orbitap LTQ XL (Thermo-Fisher Scientific, Bremen) with loop injection.

Nuclear magnetic resonance (NMR) NMR spectra were recorded at room temperature in deuterated solvents on a Bruker AVANCE 300 (300 MHz) FT-NMR spectrometer. Chemical shifts (δ) are reported in units of parts per million relative to tetramethylsilane. All ^{1}H spectra were referenced to proton signals of residual undeuterated solvents.

X-ray photoelectron spectroscopy (XPS) XPS measurements were performed with an Axis Ultra DLD (Kratos Analytical Ltd, UK). A monochromatic Al Kα source (hν = 1486.6 eV) at 10 mA filament current and 12 kV filament voltage source energies was used. The pass energy was set to 20 eV for high resolution scans and to 160 eV for survey scans. The charge neutraliser was used to compensate for sample charging. All measurements were carried out in the 'hybrid mode'. The data were evaluated with CasaXPS (version 2.3.15, Casa Software Ltd, UK) and the spectra were calibrated to aliphatic carbon (C1s = 285 eV). High resolution spectra were integrated to determine the atom fraction.

V.7 Bibliography

1. K. Ariga, J. P. Hill, Q. Ji, *PCCP* **2007**, *9*, 2319–2340.
2. K. Ariga, Y. Yamauchi, G. Rydzek, Q. Ji, Y. Yonamine, K. C.-W. Wu, J. P. Hill, *Chem. Lett.* **2014**, *43*, 36–68.
3. G. Decher, *Science* **1997**, *277*, 1232–1237.
4. W. B. Stockton, M. F. Rubner, *Macromolecules* **1997**, *30*, 2717–2725.
5. S. A. Sukhishvili, S. Granick, *J. Am. Chem. Soc.* **2000**, *122*, 9550–9551.
6. O. Crespo-Biel, B. Dordi, D. N. Reinhoudt, J. Huskens, *J. Am. Chem. Soc.* **2005**, *127*, 7594–7600.
7. O. Roling, C. Wendeln, U. Kauscher, P. Seelheim, H.-J. Galla, B. J. Ravoo, *Langmuir* **2013**, *29*, 10174–10182.
8. G. Rydzek, P. Schaaf, J.-C. Voegel, L. Jierry, F. Boulmedais, *Soft Matter* **2012**, *8*, 9738–9755.
9. C. Schulz, S. Nowak, R. Fröhlich, B. J. Ravoo, *Small* **2012**, *8*, 569–577.
10. J. F. Quinn, A. P. R. Johnston, G. K. Such, A. N. Zelikin, F. Caruso, *Chem. Soc. Rev.* **2007**, *36*, 707–718.
11. G. K. Such, J. F. Quinn, A. Quinn, E. Tjipto, F. Caruso, *J. Am. Chem. Soc.* **2006**, *128*, 9318–9319.
12. D. E. Bergbreiter, K.-S. Liao, *Soft Matter* **2009**, *5*, 23–28.
13. Y. Liu, M. L. Bruening, D. E. Bergbreiter, R. M. Crooks, *Angew. Chem. Int. Ed. Engl.* **1997**, *36*, 2114–2116.
14. W. J. Yang, D. Pranantyo, K.-G. Neoh, E.-T. Kang, S. L.-M. Teo, D. Rittschof, *Biomacromolecules* **2012**, *13*, 2769–2780.
15. R. Vestberg, M. Malkoch, M. Kade, P. Wu, V. V. Fokin, K. Barry Sharpless, E. Drockenmuller, C. J. Hawker, *J. Polym. Sci. Part A: Polym. Chem.* **2007**, *45*, 2835–2846.
16. P. Kohli, G. J. Blanchard, *Langmuir* **2000**, *16*, 4655–4661.
17. G. Rydzek, J.-S. Thomann, N. Ben Ameur, L. Jierry, P. Mésini, A. Ponche, C. Contal, A. E. El Haitami, J.-C. Voegel, B. Senger, P. Schaaf, B. Frisch, F. Boulmedais, *Langmuir* **2010**, *26*, 2816–2824.
18. Y. Wang, S. W. Tong, X. F. Xu, B. Özyilmaz, K. P. Loh, *Adv. Mater.* **2011**, *23*, 1514–1518.
19. X. Wang, F. Liu, X. Zheng, J. Sun, *Angew. Chem. Int. Ed.* **2011**, *50*, 11378–11381.
20. U. Manna, A. H. Broderick, D. M. Lynn, *Adv. Mater.* **2012**, *24*, 4291–4295.

21. S. G. Lee, H. S. Lim, D. Y. Lee, D. Kwak, K. Cho, *Adv. Funct. Mater.* **2013**, *23*, 547–553.

22. J. B. Schlenoff, S. T. Dubas, T. Farhat, *Langmuir* **2000**, *16*, 9968–9969.

23. A. Izquierdo, S. S. Ono, J. C. Voegel, P. Schaaf, G. Decher, *Langmuir* **2005**, *21*, 7558–7567.

24. M. Dierendonck, S. De Koker, R. De Rycke, B. G. De Geest, *Soft Matter* **2014**, *10*, 804–807.

25. M. Lefort, G. Popa, E. Seyrek, R. Szamocki, O. Felix, J. Hemmerlé, L. Vidal, J.-C. Voegel, F. Boulmedais, G. Decher, P. Schaaf, *Angew. Chem. Int. Ed.* **2010**, *49*, 10110–10113.

26. J. Cho, K. Char, J. D. Hong, K. B. Lee, *Adv. Mater.* **2001**, *13*, 1076–1078.

27. B. Oberleitner, A. Dellinger, M. Deforet, A. Galtayries, A.-S. Castanet, V. Semetey, *Chem. Commun.* **2013**, *49*, 1615–1617.

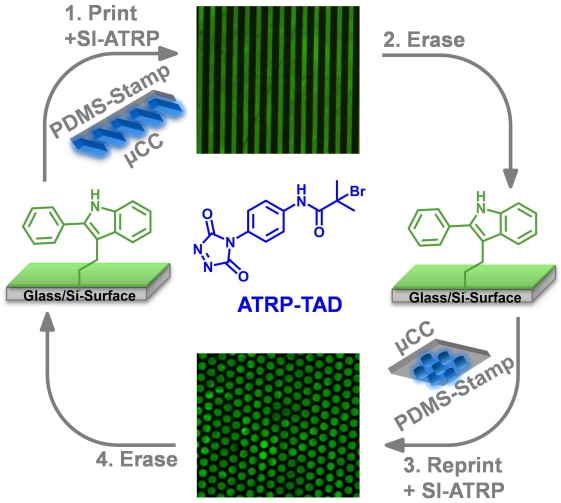

Abstract

Triazolinedione (TAD) click and transclick reactions were combined with microcontact chemistry to print, erase, and reprint polymer brushes on surfaces. By patterning substrates with a TAD-tagged atom-transfer radical polymerisation initiator (ATRP-TAD) and subsequent surface-initiated ATRP, it was possible to graft micropatterned polymer brushes from both alkene- and indole-functionalised substrates. As a result of the dynamic nature of the Alder-ene adduct of TAD and indole at elevated temperatures, the polymer pattern could be erased while the regenerated indole substrate could be reused to print new patterns. To demonstrate the robustness of the methodology, the write-erase cycle was repeated four times.

Adapted from

O. Roling, K. De Bruycker, B. Vonhören, L. Stricker, M. Körsgen, H. F. Arlinghaus, B. J. Ravoo, F. E. Du Prez, *Angewandte Chemie International Edition* **2015**, *54*, 13126–13129.

Chapter VI

Writing and rewriting on surfaces via triazolinedione chemistry

VI.1 Introduction

The fabrication of micro- and nanostructured polymer substrates is a key focus of materials science, leading to devices with potential applications in information storage,[1] electronic devices,[2,3] biosensing and anti-fouling coatings.[4–11] In this context, polymer brushes grown by the 'grafting from' approach are especially attractive since an excellent control of film thickness is given and high grafting densities are accessible. Moreover, any chemical function can be incorporated into the brushes since a wide variety of monomers is available. To date, many different polymer materials have been used in combination with various lithography techniques in order to tailor surface properties, thereby yielding substrates with enhanced functions.[12–15]

One type of soft lithography that has been frequently used for the generation of patterned self-assembled monolayers (SAMs) is microcontact printing (μCP).[16,17] In this technique, a SAM is patterned by means of a selective transfer of an ink from a patterned stamp to a substrate, exclusively in the area of contact. μCP features a set of advantageous properties such as low cost and low consumption of material, large and fast area patterning, high pattern resolution, high versatility, preparative ease and simplicity. For example, μCP has been used to form patterned SAMs of polymerisation initiators on gold surfaces employing thiols as anchoring moieties, after which a surface initiated polymerisation

results in microstructured polymer brushes.[18,19]

A wide range of materials can be applied as stamps for μCP, such as polyurethanes, styrene-butadiene-styrene triblock copolymers, agarose gels and even various hydrogels, which were each developed for specific applications.[20] Nevertheless, poly(dimethylsiloxane) (PDMS) is still the most commonly used polymer because it has multiple properties that are ideal in the context of μCP. Most importantly, a patterned PDMS stamp can easily be obtained by curing a commercially available prepolymer on a non-adhesive structured master.[21] Moreover, this cross-linking yields a flexible elastomer that is able to make conformal contact even with rough surfaces, yet is strong enough to reproduce micrometre-scale patterns.[20] Finally, while the unmodified stamps are hydrophobic, the polymer surface is readily oxidised by UV ozone or an oxygen plasma, thereby increasing its compatibility with polar inks as well.[17]

Microcontact chemistry (μCC) is a variation of μCP in which a substrate, coated with a reactive layer, is brought into close conformal contact with an elastomeric stamp. This stamp is soaked with an ink containing a complementary reactive group, which leads to surface functionalisation by a chemical reaction in the area of contact. Because of the previously mentioned advantages, PDMS is typically used as stamp material for μCC as well. Additionally, a wide range of photochemical reactions are possible as a result of the optical transparency of this polymer, while its chemical inertness and high thermal stability allow reactions at elevated temperatures.[21,22] Nevertheless, because of their compatibility with various functional groups and typically milder reaction conditions, especially 'click' reactions were found to be versatile for the surface functionalisation via μCC.[21,23]

While most of the examples cited above aim at a robust and irreversible surface functionalisation, only very few reactions offer stable (*i.e.* covalent) yet dynamic grafting with switchable surface properties. A first example is the elegant photo-click system reported by Arumugam and Popik, which works very well for small molecules.[24] The reversible nature of Diels-Alder reactions between reversible addition fragmentation transfer (RAFT) agents and cyclopentadienyl moieties serves as a second example. Using this reactive pair, Barner-Kowollik and co-workers demonstrated the grafting of polymer brushes onto silicon substrates in a non-patterned fashion, which could subsequently be detached at elevated temperatures and thus switch the surface properties.[25]

In our research group, we already demonstrated that Diels-Alder and Alder-ene reactions of various reactive triazolinediones (TAD) with a range of dienes and alkenes could be used to produce block copolymers, cross-linked plant oil-based materials as well as the covalently linked layer-by-layer assemblies discussed in the previous chapter.[26,27] These reactions all proceed at room temperature with high reaction rates and are often complete within seconds without the need for a catalyst, irradiation or other external stimuli, and thus comply to many characteristics of a click reaction. Moreover, if an indole is used instead of a simple alkene, reversibility of the Alder-ene adduct is observed at elevated temperatures, which led to the development of so-called transclick reactions, in analogy to a transesterification reaction (Scheme VI.1). A more detailed explanation of this transclick concept is provided in section II.4.3, while a study of the reaction mechanism will be discussed in this chapter (section VI.3.2.1).

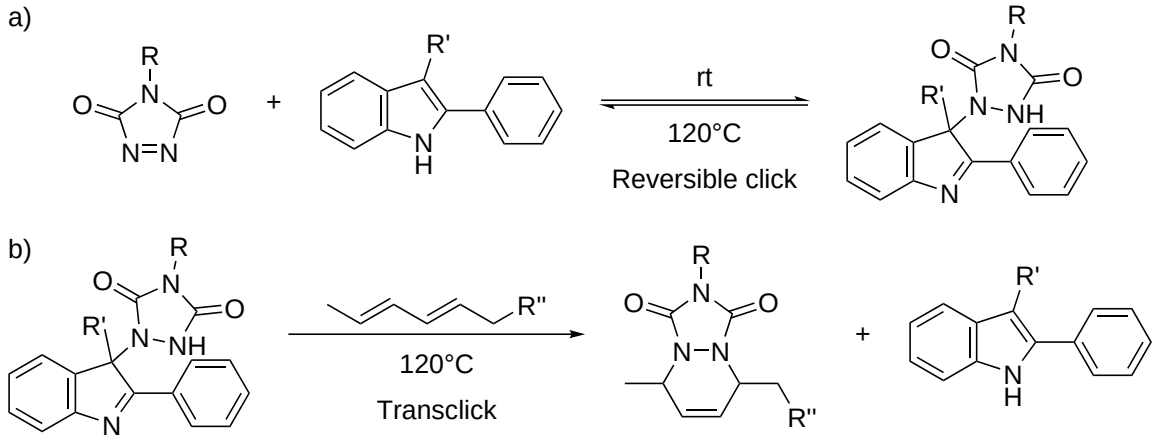

Scheme VI.1: **(a)** The TAD click reaction with an indole, which is reversible at elevated temperatures. **(b)** If another reaction partner (*e.g.* a diene) for TAD is introduced in this reversible regime, a transclick reaction takes place.

The interesting characteristics of the TAD-based chemistry, together with the possibility to generate adducts that are stable at room temperature and dynamic at elevated temperatures, were the inspiration for this chapter. In this second collaboration with the group of Prof. Bart Jan Ravoo (University of Münster), we developed the first truly rewritable surfaces by combining TAD-based μCC with transclick reactions from a surface-bound indole to a diene in solution (Figure VI.1). To this end, we synthesised both irreversibly and reversibly reacting TAD-compatible substrates, after which the different steps in the overall writing-erasing-rewriting process were developed separately.

In a first step, the irreversible patterning of a TAD-bearing initiator for atom transfer

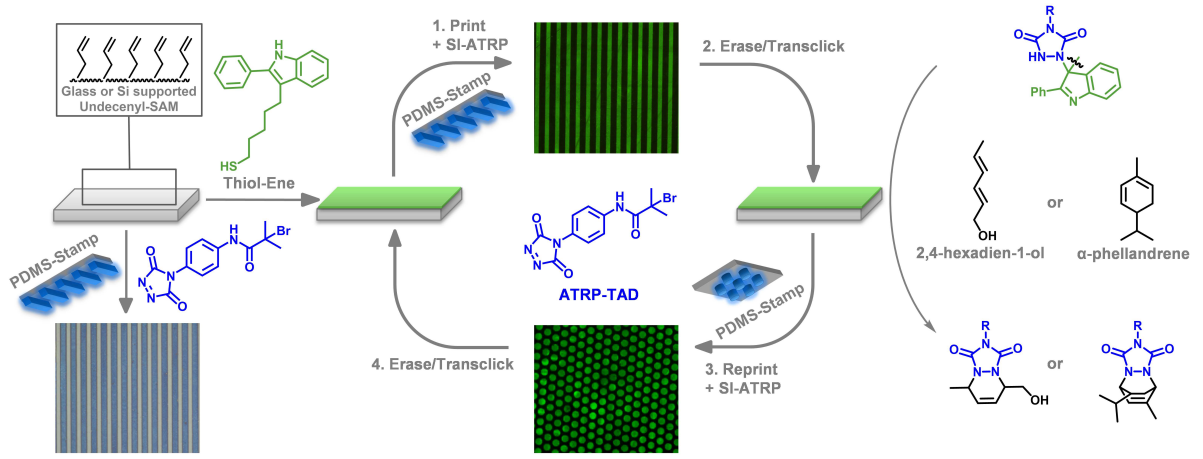

Figure VI.1: Schematic representation of the functionalisation of alkene-modified substrates by TAD click chemistry and generation of rewritable surfaces employing the transclick approach using either 2,4-hexadien-1-ol or α-phellandrene.

radical polymerisation (ATRP-TAD) on alkene-modified substrates is shown, followed by surface-initiated ATRP (SI-ATRP) which affords substrates functionalised with micropatterned poly(methyl acrylate) (PMA) brushes. Since ascorbic acid was added during every polymerisation, atom transfer radical polymerisation with activators regenerated by electron transfer (ARGET-ATRP) is formally used. However, an in-depth discussion of copper-mediated polymerisations and the many different variants is out of the scope of this dissertation. Then, reversibility was introduced into the system and the transclick reaction was demonstrated both with small molecules and polymer brushes. Finally, this reversible system was further optimised to enable multiple write-erase-rewrite cycles on the same surface, which creates the possibility to reversibly graft polymers in any desired micropattern and with any desired functional group.

VI.2 Preparation of TAD-compatible substrates

Similarly as described in section V.2, both glass and silicon supported 10-undecenyl trichlorosilane SAMs were already available in the group of Ravoo and co-workers. However, for the production of substrates that yield dynamic TAD-adducts, an indole-terminated SAM is required.

While in theory an indole-functional silane could be synthesised, we already encountered issues with the packing density of a tailored silane before (section V.2). Moreover, in this project, a low packing density of the SAM could hamper a well-defined patterning of the

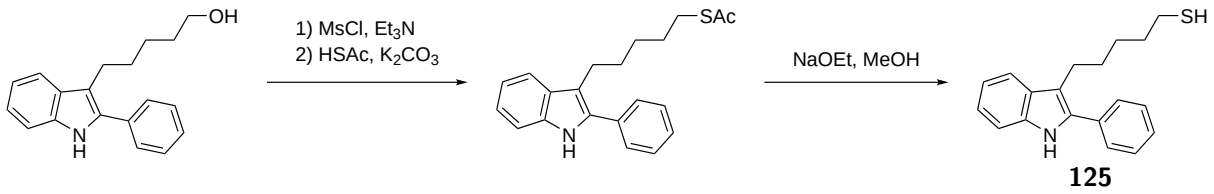

Scheme VI.2: Synthesis of an indole-bearing thiol (**125**) that was subsequently used to functionalise glass or silicon substrates.

surface and consequently negatively influence the ability to grow polymer brushes from the substrate. Nevertheless, the monosubstituted C=C bonds in the available undecenyl-terminated SAMs are perfectly suitable for radical hydrothiolations.[28,29] Therefore, we first synthesised an indole-bearing thiol (**125**) in three steps from the corresponding alcohol that was already available in our group (Scheme VI.2).[26]

Next, the indole-terminated surfaces were prepared by printing the newly synthesised indole-thiol (**125**) on the alkene-terminated SAM with a flat unstructured PDMS stamp via a UV-initiated radical thiol-ene reaction (Figure VI.1). As a result of this modification, the static water contact angle decreased from 99° for the initial substrate to 81° for the indole-functional surface (Figure VI.2a and b). Moreover, the covalent immobilisation of the indole was proven by XPS analysis, which indicated the presence of nitrogen on the surface (Figure VI.2c).

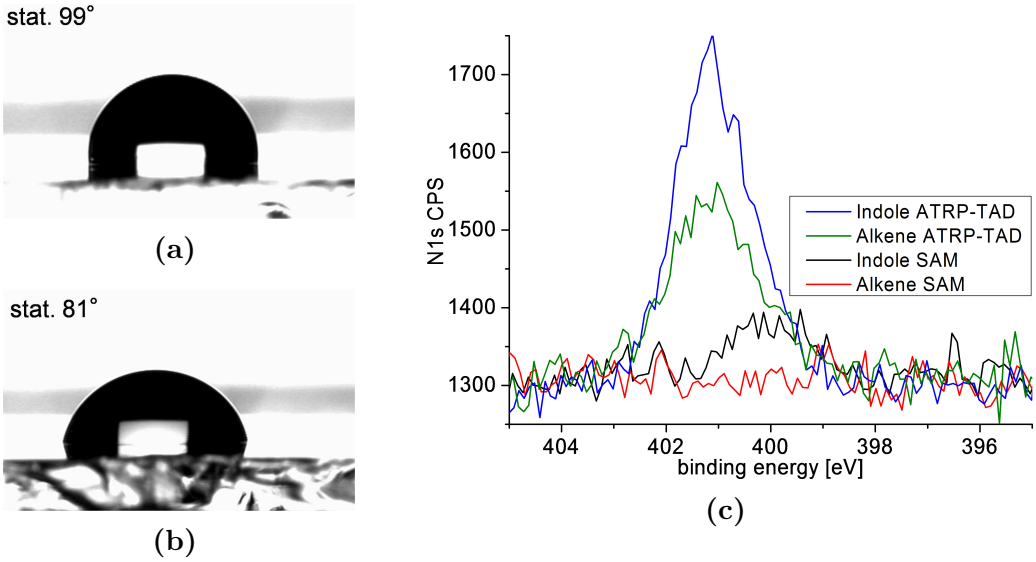

Figure VI.2: Static contact angles of a water droplet on **(a)** an undecenyl-terminated SAM and **(b)** a surface functionalised with indole-thiol **125**. **(c)** N1s signal of XPS measurements for the 10-undecenyl trichlorosilane SAM, indole functionalised SAM and the respective surfaces reacted with ATRP-TAD (bottom to top).

VI.3 Triazolinedione reactions in the field of μCC

Once the required indole-functional substrates were obtained, a TAD-tagged atom-transfer radical polymerisation initiator (ATRP-TAD, Figure VI.1) was synthesised according to a procedure developed in our group.[26] Then, we immediately started printing the ATRP-TAD on a silicon-supported SAM in 5 μm stripes that were spaced by 3 μm using commonly applied μCC conditions,[28] followed by the growing of poly(methyl acrylate) (PMA) brushes via surface-initiated ATRP (SI-ATRP) and transclick experiments by heating the resulting substrates in a solution of 2,4-hexadien-1-ol (HDEO).

The results of these initial printing and transclick experiments were not quite positive, but very informative nonetheless. First, the outcome of the patterning procedure, *i.e.* the combination of printing the initiator and growing polymer brushes, was fairly random and seemed to be dependent on the time needed to load the stamp with the triazolinedione, which could be attributed to the solvent. Indeed, methanol or ethanol are the typical solvents used to prepare the ink solutions, which are known to react with TADs (section II.3.3). Therefore, the reactive ink degrades over the time needed to dissolve the TAD and incubate the stamp. Moreover, in the rare cases that AFM analysis showed the successful functionalisation of the substrates with micropatterned PMA brushes, the pattern was clearly broadened (Figure VI.3a). This observation is a result of diffusion of the ink during

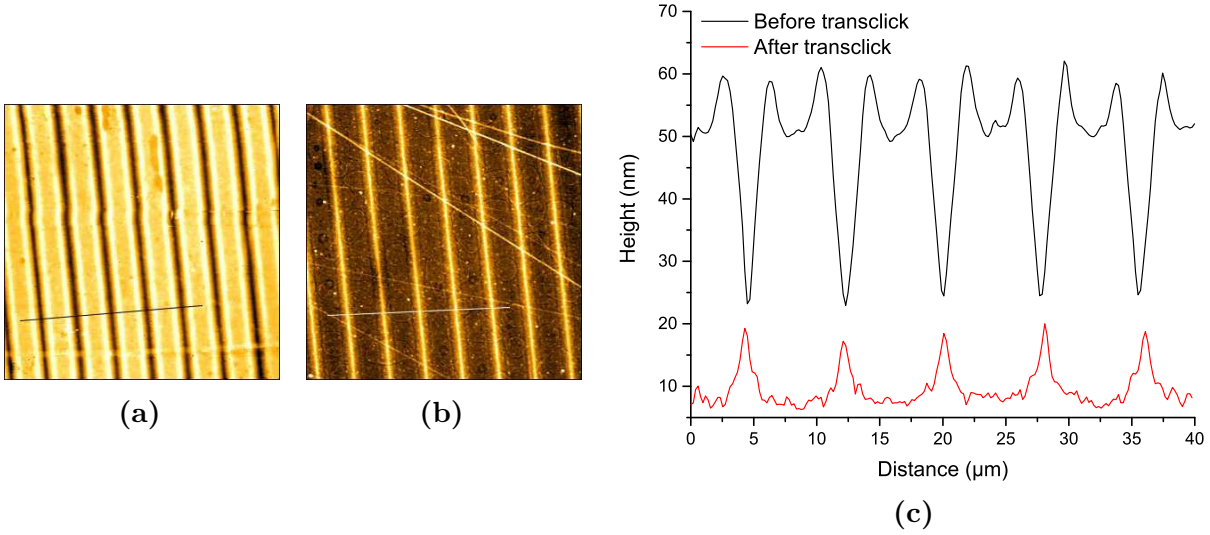

Figure VI.3: AFM analysis (60×60 μm) of the first triazolinedione-based μCC experiments with **(a)** the polymer brushes obtained after μCC of the ATRP-TAD in 5 μm stripes spaced by 3 μm and subsequent SI-ATRP, **(b)** the surface after an attempted transclick reaction and **(c)** the corresponding height profiles.

the printing process and could again be related to a bad choice of solvent. Additionally, after an attempt to remove the obtained brushes via a transclick reaction, AFM analysis suggested that an inversion of the pattern occurred (Figure VI.3b and c). In conclusion, several issues needed to be solved while the procedure that introduces a new click chemistry in the field of μCC *and* a new interfacial transclick reaction is rather complex. Therefore, we simplified the problem by optimising each step separately.

VI.3.1 Irreversible surface pattering

As a first step, simple 10-undecenyl trichlorosilane SAMs were applied as irreversible TAD-reactive surfaces, while the solvent that is used for loading the stamp with the ATRP-TAD was varied. Indeed, the solvent should only dissolve the reactive ink without swelling the PDMS stamp to ensure a faithful reproduction of the pattern on the surface.[17,30] The choice of these monosubstituted olefins as reactive substrates seems somewhat counterintuitive at first, especially since this kind of substrates was found to react very slowly in the case of layer-by-layer depositions (section V.2). Nevertheless, as a result of a local concentration effect, combined with a higher affinity of the ink for the substrate than for the stamp, reaction kinetics at the solid-liquid interface (*cf.* layer-by-layer assembly) are not directly comparable to those in a μCC approach.[21]

The best results were obtained when either a glass or a silicon supported alkene-modified surface was brought into conformal contact with a PDMS stamp that was soaked with a 50 mM solution of ATRP-TAD in acetonitrile. After contacting stamp and substrate for 10 minutes, the stamp was lifted off and the surfaces cleaned by rinsing with acetone, dichloromethane (DCM) and subsequent sonication. The success of the immobilisation of the triazolinedione via μCC was verified by X-ray photoelectron spectroscopy (XPS), since the presence of a pronounced N1s signal (green line in Figure VI.2c) indicates the presence of the ATRP-TAD-adduct on the surface. Moreover, the faithful reproduction of the micropattern was visualised via time-of-flight secondary ion mass spectrometry (ToF-SIMS), where the detected fragments of the ATRP-TAD in the 2D images mirror the pattern of the stamp (Figure VI.4).

Following the successful patterning of the triazolinedione, surface-initiated ATRP using methyl acrylate as the monomer afforded substrates functionalised with micropatterned

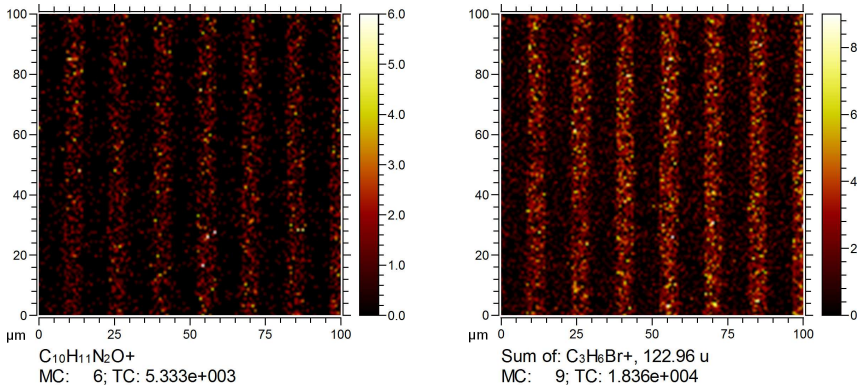

Figure VI.4: ToF-SIMS analysis of 10-undecenyl trichlorosilane SAMs patterned with ATRP-TAD in 5 µm stripes spaced by 10 µm.

PMA brushes, which could be seen using an optical microscope (Figure VI.5a). Furthermore, AFM imaging provided evidence of a high edge resolution, as well as the growth of polymer brushes of up to around 100 nm (Figure VI.5b and c). Finally, XPS analysis of the substrate proved the growth of polymer brushes, since the C1s peak in the spectrum shows characteristic shoulders for the oxidised carbons in the PMA layer (Figure VI.5d).

In conclusion, by changing the solvent from methanol to acetonitrile, the ATRP-TAD

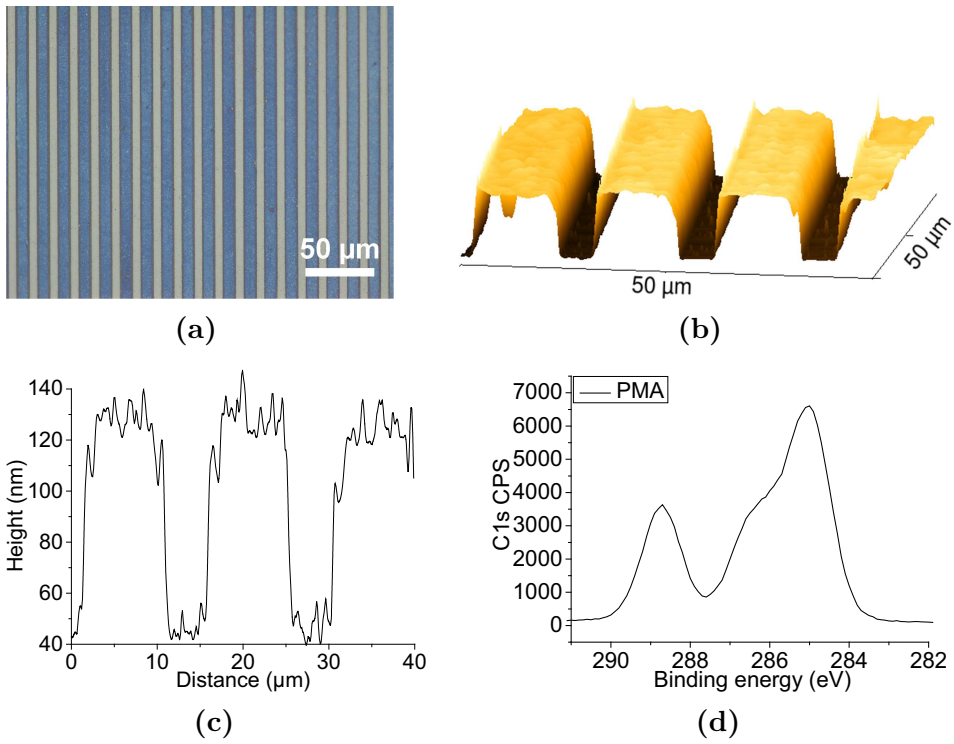

Figure VI.5: PMA brushes grown from an undecenyl-terminated SAM, patterned with ATRP-TAD in 10 µm stripes spaced by 5 µm. **(a)** Optical microscopy image, **(b)** AFM 3D image, **(c)** AFM height profile and **(d)** C1s signal of the XPS analysis.

could be printed on an undecenyl-terminated substrate and subsequently used to grow polymer brushes of ∼100 nm with a well-defined pattern and high edge resolution. Because acetonitrile is an inert solvent in the context of triazolinedione chemistry, no reproducibility issues were encountered.

VI.3.2 Reversible patterning on indole-terminated surfaces

VI.3.2.1 Mechanistic study of the transclick reaction

The next phase of this project consisted of the substitution of the irreversibly reacting undecenyl-terminated SAMs by the reversible indole-functional substrates. However, besides the development of an interfacial transclick reaction that works, we were also interested in *how* it works. Our research group, in collaboration with the group of Prof. Veronique Van Speybroeck (UGent), previously reported an *in silico* mechanistic study of the reversible TAD-indole reaction, which suggested a stepwise route via an iminium-urazolide zwitterionic intermediate (IZ, Figure VI.6) that is readily converted into the Alder-ene adduct by a simple proton transfer.[26] Assuming the same pathway for the backward reaction, an activation energy of ∼140 kJ mol^{-1} was obtained for the transclick process, *i.e.* an unclick-click cascade that transfers a TAD moiety at elevated temperatures from its indole adduct to a different reaction partner such as (*e.g.* HDEO, **81**), and thereby quantitatively regenerates the parent indole compound (**126**, Figure VI.6).

Additional research by our group on the TAD-based transclick reactions introduced structural variability in the indole compound in order to gain control over the temperature at which reversibility is observed.[31] Consequently, the theoretical model was updated to include these new experimental data as well as a correction for the high polarity of DMSO, *i.e.* the solvent in which the (experimental) transclick studies are typically performed. This optimised model resulted in Gibbs free activation energies for the backward TAD-indole reaction of 130 to 140 kJ mol^{-1}, depending on the indole substitution pattern, and thereby closely reproduced the trend in experimentally obtained activation energies for the transclick reactions.

Besides the previously described *in silico* simulations, which focused on explaining the tunable reversibility of the Alder-ene adduct via the forward TAD-indole reaction mechanism, we decided to investigate possible alternative transclick mechanisms that seem reasonable

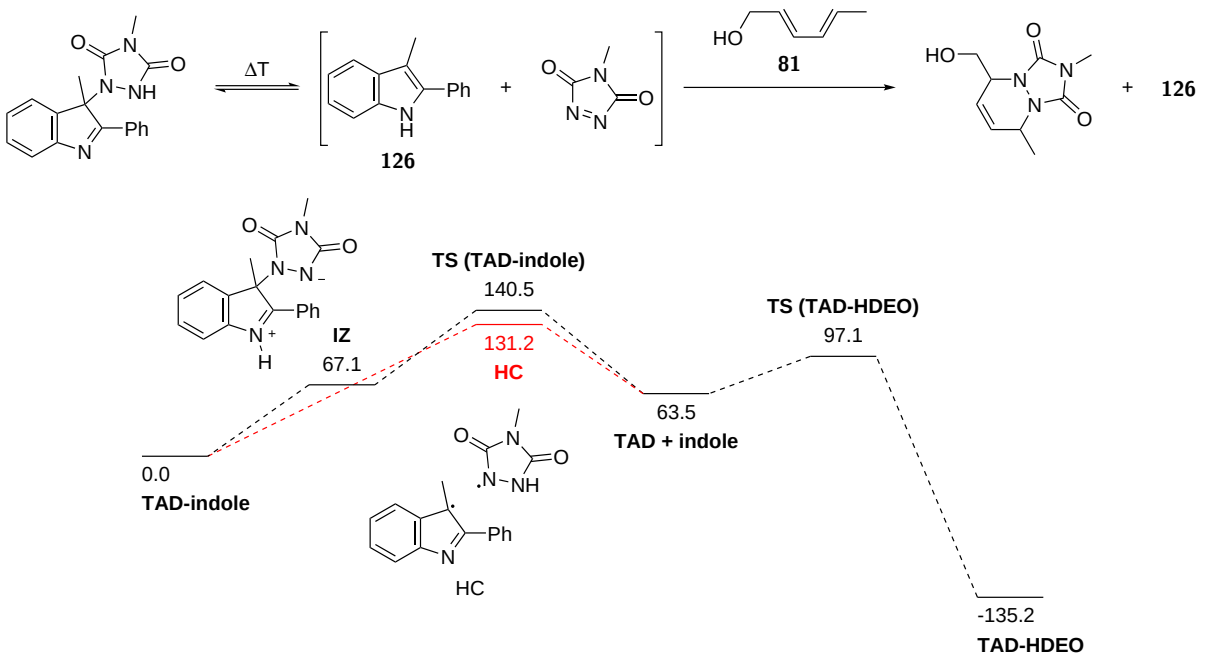

Figure VI.6: Reported mechanism and corresponding Gibbs free energy profile (black) of the transclick reaction between a TAD-indole adduct and a diene, involving the backward Alder-ene reaction via an iminium-urazolide zwitterion (IZ) and subsequent addition of the released triazolinedione to the diene.[26,31] Additional *in silico* experiments suggested a possible alternative mechanism involving the homolytic cleavage (HC) of the indole-urazole bond (red). All energies were obtained via DFT calculations (M06-2X/6-31+G(d,p)).

at these elevated temperatures. One of the possible mechanisms involves the homolytic cleavage of the TAD-indole adduct, generating an indolyl and a urazolyl radical (HC, Figure VI.6). In fact, the calculated dissociation energy of this bond is indeed quite low (*i.e.* 130 kJ mol^{-1}) compared to that of a typical C−N bond (∼300 kJ mol^{-1}).[32] Consequently, these calculations suggest an alternative pathway for the transclick mechanism, involving radical species rather than the previously reported ionic intermediates (Figure VI.6).

Because the difference in activation energy for the aforementioned competitive pathways is within the error margin of DFT calculations (∼10 kJ mol^{-1}), an experiment was designed that would allow unambiguous differentiation between an ionic and a radical pathway. First, an unsaturated indole (**127**, Scheme VI.3) was synthesised that can be applied as a 'radical clock', *i.e.* a compound that will undergo a very rapid intramolecular radical addition (cyclisation) if any radical intermediate is formed out of it.[33] As a result of the good kinetic selectivity of triazolinediones, 4-butyl-TAD (BuTAD) could be selectively reacted with the electron-rich 2,3-π-bond of indole **127** in the presence of the monosubstituted alkene, yielding the corresponding reversible adduct (**128**).

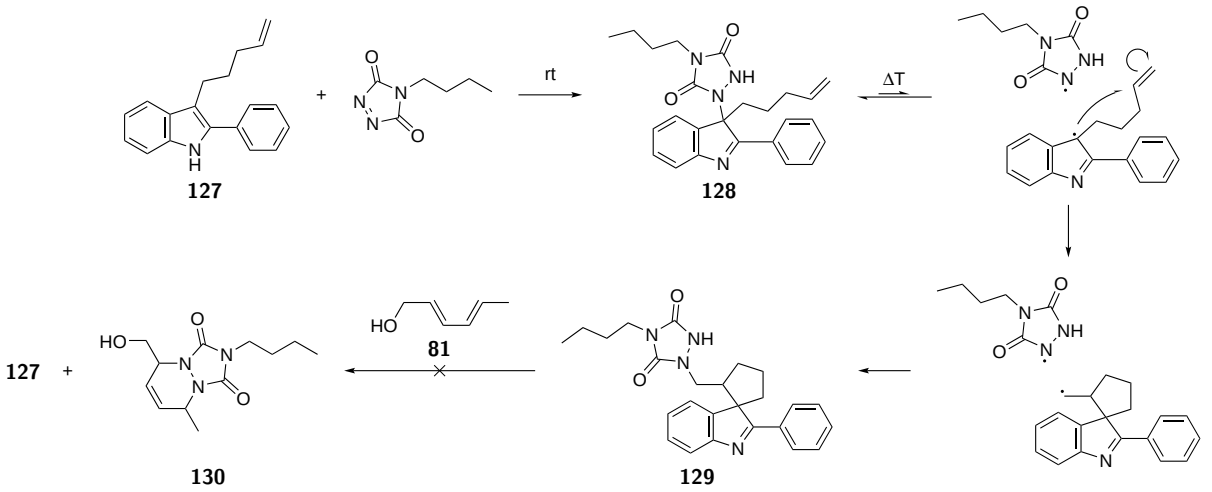

Scheme VI.3: Concept of the radical clock (indole **127**) for a mechanistic elucidation of the transclick reaction. When a homolytic cleavage occurs upon heating of TAD-indole adduct **128**, the generated indolyl radical can cyclise and recombine with the urazolyl radical to yield compound **129**. Since the latter TAD-adduct is irreversible, no transclick reaction occurs.

Finally, the BuTAD-adduct of the radical clock (**128**) was heated in the presence of HDEO for 15 minutes at 150 °C, *i.e.* conditions at which a full conversion is expected for this transclick reaction.[26,31] In the case of a radical mechanism instead of an ionic one, homolytic cleavage of this adduct will unavoidably result in indolyl radicals that undergo an intramolecular addition to the alkene before they recombine with the urazolyl radical to generate urazole **129** (Scheme VI.3). In contrast to adduct **127**, the latter compound is irreversibly formed and will thus remain in the solution as an indicator for a radical pathway. However, ^{1}H-NMR analysis of the different intermediates, as well as the reaction mixture before and after heating, shows a clean conversion of the BuTAD-indole adduct (**128**) into the BuTAD-HDEO adduct (**130**) together with the quantitative regeneration of the parent indole compound (**127**, Figure VI.7).

In conclusion, although suggested by theoretical calculations, a possible radical mechanism for the transclick reaction, involving indolyl and urazolyl radicals, is shown experimentally to be very unlikely. Even when an indole is used that should generate a significant amount of side-product when radical species are formed, a clean transclick reaction is observed. Therefore, the originally reported ionic mechanism still stands for both the forward and backward TAD-indole reaction.

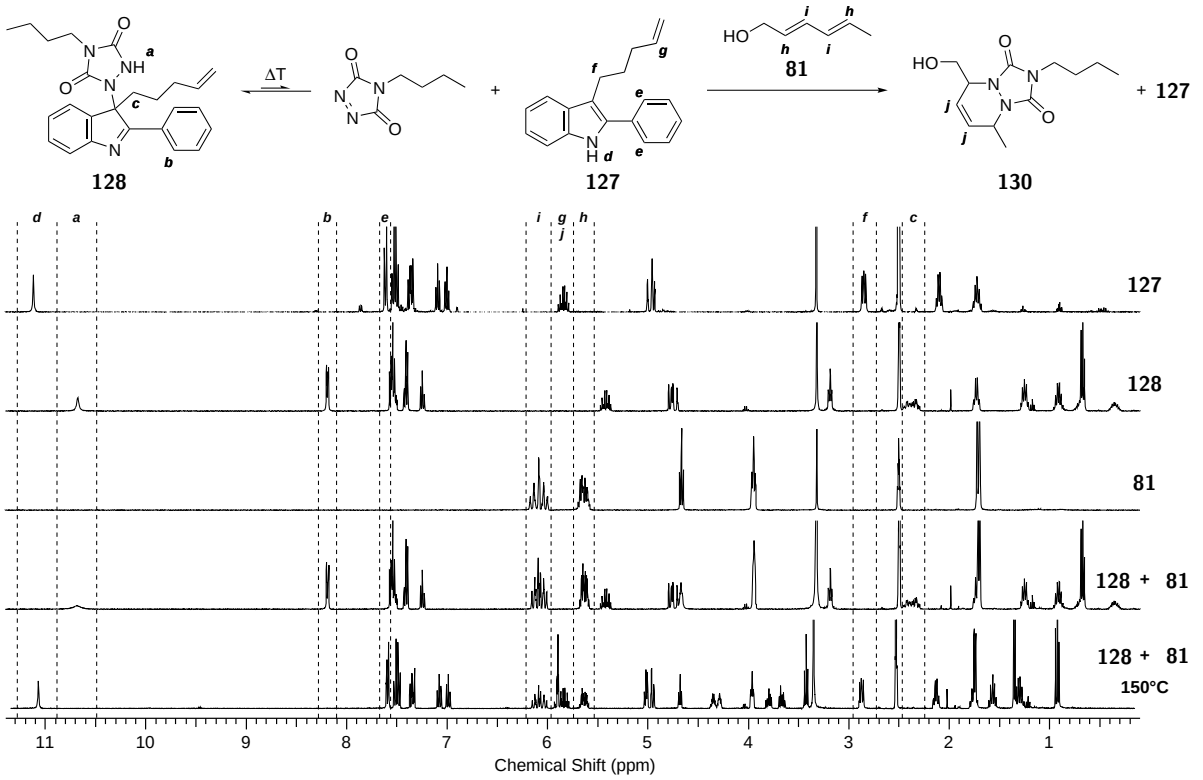

Figure VI.7: Transclick experiment with a radical clock. If the mechanism involves a homolytic cleavage of the TAD-indole adduct, side-products are expected when heating **128** in the presence of HDEO (Scheme VI.3). ^{1}H-NMR analysis shows a clean conversion, which supports an ionic mechanism.

VI.3.2.2 Click and transclick of low molecular weight components

After the very first transclick experiment from a surface-bound indole to a diene in solution (*vide supra*), AFM analysis suggested that an inversion of the pattern occurred (Figure VI.3). Without over-analysing this observation, it made us realise that the radical thiol-ene addition, which was used to immobilise indole **125** on the substrate (section VI.2), most likely did not consume all available undecenyl residues. Indeed, while an indole reacts faster during the initial printing step, the alkene residues can also react with triazolinediones. This might result in TAD moieties 'walking' over the surface at elevated temperatures, *i.e.* via an indole-to-indole transclick, until an irreversible reaction with a surface-bound alkene occurs. Therefore, after immobilising the indole-thiol on the SAM via μCC, all the residual alkene groups were passivated by an additional UV-initiated thiol-ene reaction with Boc-cysteamine in a next step.

Using the passivated substrates, high edge resolutions were observed after printing times of only 5 minutes from a 50 mM solution of ATRP-TAD, while DMSO was used for

acetonitrile because of the higher compatibility of this solvent with the indole-terminated SAMs. Similarly as in section VI.3.1, the success of the immobilisation was evidenced by XPS analysis of the patterned surface (blue curve in Figure VI.2c). Again, the faithful reproduction of the pattern, *i.e.* 5 µm stripes that are spaced by 10 µm, was verified by ToF-SIMS analysis, in which the characteristic secondary ions reflect the chemical composition of the ATRP-TAD-adduct (Figure VI.8a).

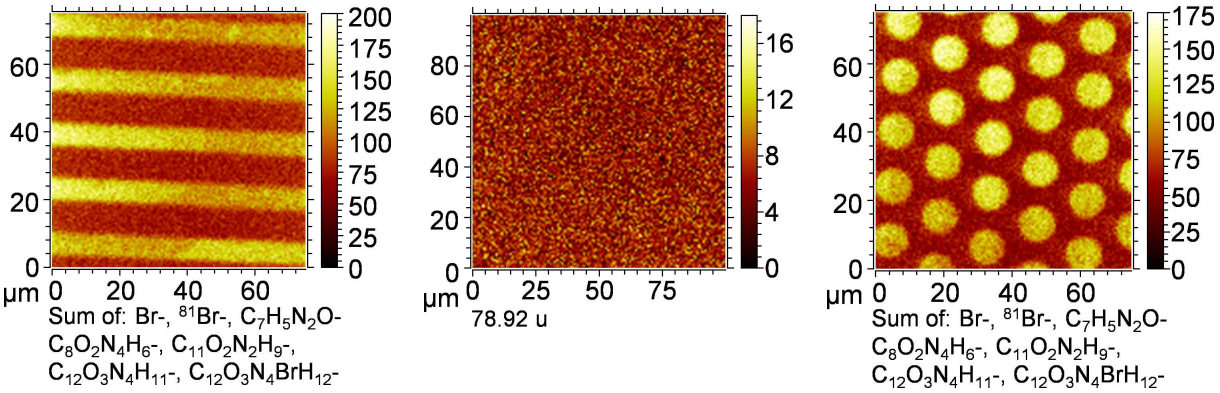

(a) **(b)** **(c)**

Figure VI.8: ToF-SIMS data (negative ion mode, field of view: 75 × 75 mm^2) of **(a)** ATRP-TAD printed in 5 µm stripes spaced by 10 µm, **(b)** the regenerated indole surface after transclick, where no bromide is detectable and **(c)** reprinted ATRP-TAD in 10 µm dots spaced by 5 µm.

Next, the modified substrates were immersed into a 1 M solution of HDEO in DMF for 1 hour at 150 °C, which should result in the transclick reaction of the ATRP-TAD from the surface-bound indole to the diene in solution. After performing this reaction, the substrates were subjected to ToF-SIMS measurements again. This time, no fragments corresponding to the ATRP-TAD-adduct could be detected, as exemplified by the absence of the bromine signal (Figure VI.8b), clearly showing the dynamic nature of TAD-indole adducts on surfaces and consequently the successful detachment of the initiator.

Finally, to demonstrate that not only the initiator could be erased from the surface, but that also the surface-bound indole groups are properly regenerated, ATRP-TAD was reprinted in 10 µm dots spaced by 5 µm on the same substrates. Again, ToF-SIMS analysis proved the presence of the expected surface pattern without any defects (Figure VI.8c). Therefore, a first proof for the application of TAD click and transclick chemistry for truly rewritable surfaces via µCC was presented.

VI.3.2.3 Writing, erasing and rewriting polymer brushes

Once the dynamic nature of the TAD-indole adducts on the surface was proven with the low molecular weight ATRP-TAD, these substrates were subjected to SI-ATRP, again using methyl acrylate as the monomer. The outcome of the polymerisation was analysed with AFM and infrared (FTIR) spectroscopy. On the one hand, the AFM image and corresponding height profile in Figure VI.9a show the presence of polymer brushes with a high edge resolution, grown to a height of approximately 40 nm. The corresponding FTIR spectrum (Figure VI.10), on the other hand, displays significant absorptions at wavenumbers of around 1740 cm^{-1}, originating from the methyl esters, and 1440 cm^{-1}, caused by the aliphatic polymer backbone.

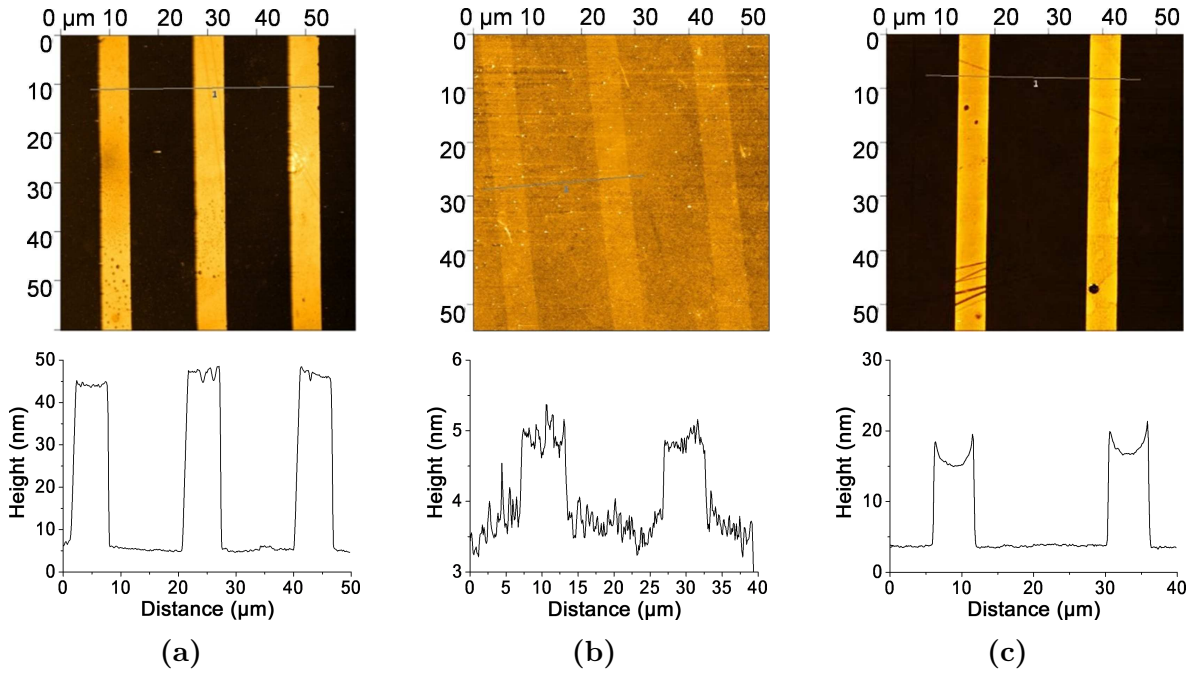

Figure VI.9: AFM analysis of **(a)** PMA brushes structured in 5 µm stripes spaced by 15 µm, **(b)** the same substrate after the regeneration of indole moieties via a transclick reaction and **(c)** PMA brushes structured in 5 µm stripes spaced by 20 µm on a regenerated and cleaned substrate, each with their corresponding height profiles.

Next, a transclick reaction was performed on the polymeric surface to regenerate the indole substrate. The same reaction conditions were applied as for the non-polymerised surfaces, *i.e.* immersion in a 1 M solution of HDEO in DMF at 150 °C, albeit with a longer reaction time. However, when the polymer brushes were too long, *i.e.* longer than 60 nm, they could not be removed reliably, probably as a result of hindered diffusion of the diene to the anchoring points of the polymer brushes. This limited diffusion could also account for

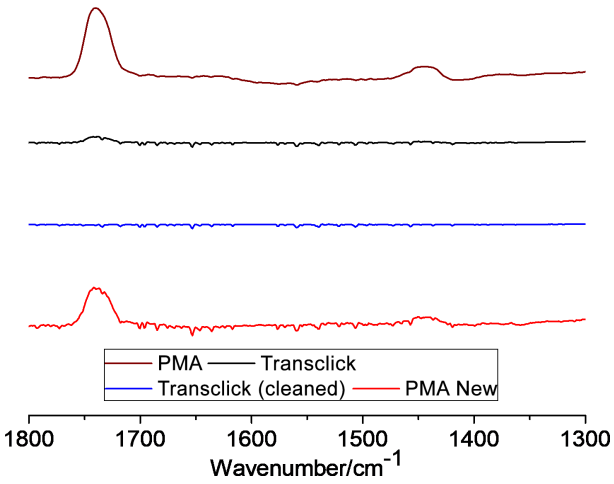

Figure VI.10: ATR-FTIR spectra of a substrate after SI-ATRP, transclick, cleaning and rewriting (top to bottom).

the need of longer transclick reaction times for polymer brush functionalised substrates, in comparison to substrates that are only functionalised with the ATRP-TAD species (section VI.3.2.2).

For shorter brushes, a reaction time of 5 hours was sufficient to remove all polymer brushes. While AFM and FTIR spectroscopy on the resulting substrates (Figure VI.9b and Figure VI.10, respectively) suggest that the detachment of the brushes is not complete yet, this observation can be caused by PMA that adheres to the surface to a small extent as a result of non-specific physisorption, rather than an incomplete transclick reaction. Indeed, when the surfaces were additionally cleaned by sonication in acetone, acetonitrile and DCM and finally carefully wiped with a tissue, the adhering polymeric material was completely removed, as evidenced by the infrared analysis (Figure VI.10).

Finally, reprinting of ATRP-TAD in 5 µm stripes spaced by 20 µm and subsequent SI-ATRP yielded polymer brushes that reproduce the expected pattern, as confirmed by AFM imaging (Figure VI.9c). FTIR measurements, on the other hand, again feature peaks originating from the methyl ester groups and aliphatic polymer backbone (Figure VI.10). Therefore, these results unambiguously prove the possibility to write, erase and rewrite polymer brush microstructures on indole-functionalised surfaces.

VI.3.2.4 Optimisation of the rewriting process

Although the previous sections describe the successful application of TAD click and transclick reactions for the generation of rewritable surfaces, the overall erasing and rewriting process, in the case of polymer brush micropatterns, is rather cumbersome. Indeed, in addition to the transclick reaction time of 5 hours, growing the brushes consumed at least 14 hours, and multiple cleaning steps in between were necessary. Therefore, the final phase of this project consisted of the optimisation of the individual steps, thereby reducing the overall processing time.

First, the accessibility of the TAD-indole adduct was improved by decreasing the steric bulk around the reactive site, since the transclick reaction seemed to be hampered by the limited diffusion of the diene (*vide supra*). In theory, printing a mixture of ATRP-TAD and a dummy compound, such as 4-phenyl-TAD, can be used to obtain a lower density of polymer brushes after SI-ATRP. However, this strategy was not investigated because the initiator density is easily over-diluted, leading either to a collapse of the brushes, resulting in a similar steric hindrance, or island formation rather than a faithful reproduction of the pattern. Therefore, the length of the polymer brushes was decreased instead, since a similar effect on the diffusion of the diene was expected compared to a lower polymer density. Moreover, decreasing the targeted length of the brushes shortens the required polymerisation time as well.

Secondly, because of its high boiling point and ability to dissolve both the TAD-adduct and the typically used diene (HDEO), DMF is in general a good solvent for transclick reactions. Nevertheless, the high polarity of the solution in combination with the quite apolar poly(methyl acrylate) brushes on the surface[34] might also contribute to the lower reaction kinetics for the erasing step. Therefore, rather than the polar HDEO, α-phellandrene was selected as an apolar and even more reactive alternative (Figure VI.1). Moreover, because the latter diene has a boiling point of $\sim$170 °C, it can directly be used as the solvent.

Lastly, in addition to methyl acrylate, 1 mol % of the green fluorescent nitrobenzoxadiazole acrylate (NBDA) was co-polymerised into the PMA brushes. While this co-monomer has no influence on the overall processing time, it allows a facile visualisation of the polymer brush growth, erasing and rewriting via fluorescence microscopy.

Figure VI.11a shows AFM and fluorescence microscopy images of a substrate functionalised with 10 µm stripes of PMA-NBDA copolymer brushes, spaced by 5 µm. Compared to the previous samples (section VI.3.2.3), the height of the brushes was reduced from ∼40 nm to ∼10 nm by shortening the polymerisation time from 14 h to 3.5 h. When the substrates were subsequently immersed in α-phellandrene at 150 °C, the brushes were completely removed in merely 45 minutes. Moreover, instead of a tedious cleaning procedure, carefully wiping the surface with a tissue and sonicating in DCM sufficed to remove all the physisorbed polymer. The success of both the transclick reaction and cleaning procedure was confirmed by the absence of any fluorescence on the substrate (Figure VI.12a).

Finally, the regenerated indole substrates were used to implement new patterns following the procedure explained above (Figure VI.11b). Moreover, two more of these erase-write cycles were performed on the same surface (Figure VI.11c–d). Figure VI.12b shows the fluorescence microscopy data of the fourth pattern (*cf.* Figure VI.11d), verifying the high quality of the pattern over a large area. In conclusion, substrates could be successfully rewritten up to four times without observing a reduced brush quality or significant defects.

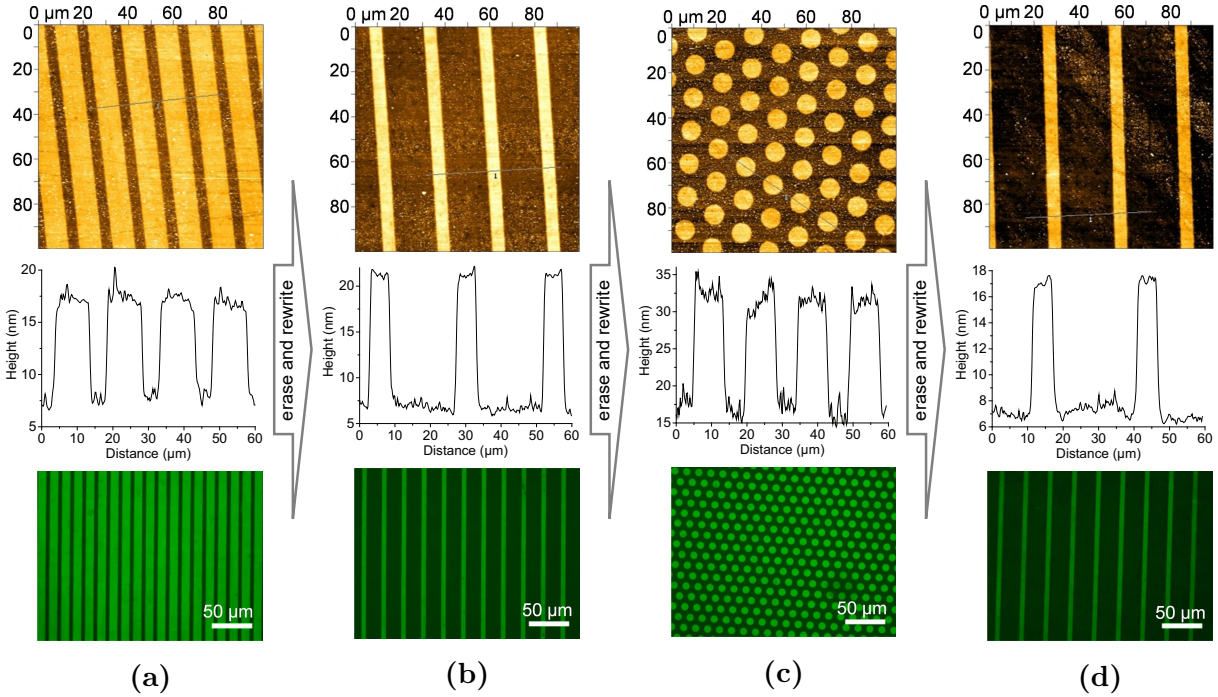

Figure VI.11: Four consecutive write and erase cycles of polymer brushes visualised by AFM with corresponding height profile (top and middle) and fluorescence microscopy imaging (bottom). **(a)** PMA-NBDA copolymer brushes patterned in 10 µm stripes spaced by 5 µm, **(b)** rewritten copolymer brushes on the same surface patterned in 5 µm stripes spaced by 20 µm, **(c)** repeated rewriting in 10 µm dots spaced by 5 µm and **(d)** final rewriting in 5 µm stripes with spacing of 25 µm.

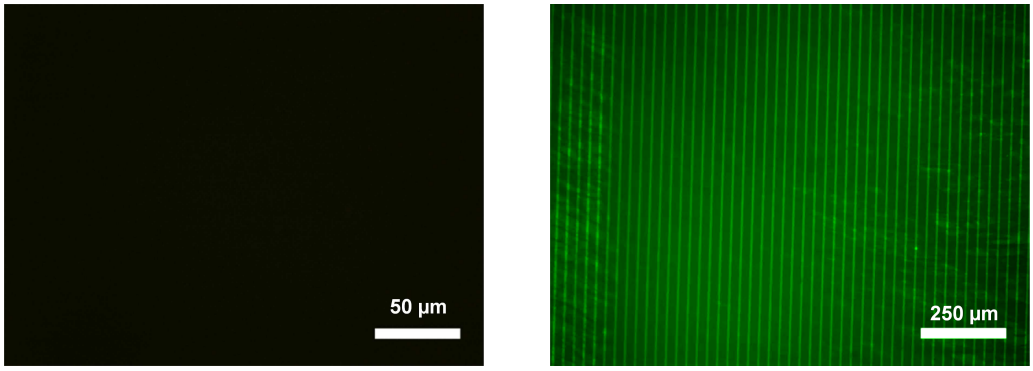

(a) **(b)**

Figure VI.12: **(a)** Representative image of a substrate after transclick and cleaning, where no fluorescent patterns were detected. **(b)** Fourth writing of PMA-NBDA copolymer brushes structured in 5 µm stripes with spacing of 25 µm on a single substrate visualised by fluorescence microscopy imaging. Both images were taken with an irradiation time of 50 ms.

VI.4 Conclusions and perspectives

In this chapter, the application of triazolinedione chemistry as a highly efficient reaction for the reliable patterning of surfaces with an ATRP-initiator and polymer brushes, grown via the grafting from approach, was demonstrated. It was possible to immobilise the initiator in a permanent manner, *i.e.* via a traditional TAD-based Alder-ene reaction. Additionally, the reversibility of the TAD-indole Alder-ene adduct could be exploited to generate substrates with dynamic covalent bonds, which led to the development of the first truly rewritable surfaces. Consequently, we were able to write and erase micropatterned polymer nanofilms using subsequent grafting and degrafting reactions up to four times on the same substrate.

After this initial report on rewritable surfaces, Ravoo and co-workers also investigated the reversible hetero-Diels-Alder reaction between cyclopentadiene and a RAFT agent for the production of rewritable surfaces.[35] Nevertheless, the erasing step required an overnight treatment at 150 °C and was thus significantly harsher than the optimised transclick procedure. Zhou and co-workers, on the other hand, reported on an initiator-embedded polystyrene that allows for a repeated grafting of polymer brushes from a polished surface.[36] However, both the patterning and erasing procedures are based on a mechanical surface treatment to expose 'fresh' underlying initiator for the subsequent writing step. Therefore, to the best of our knowledge, the reversible TAD-indole chemistry still represents the

fastest and mildest strategy to (chemically) write and rewrite patterned polymer brushes on a substrate.

This chapter already provides multiple optimisations to the different processing steps compared to the initial procedure, allowing multiple erase and rewriting cycles within a reasonable timeframe. Nevertheless, further research should include additional optimisations to this system, for example a decrease in temperature required for erasing the pattern. In the current system, the transclick reaction requires a temperature of 150 °C, which is mainly dictated by the indole reaction partner. Recent advances in our research group resulted in a significant decrease of this transclick temperature,[31] which might allow for an erasing step at approximately 80 °C – or even lower – in the future.

VI.5 Notes on the collaboration

This chapter describes a collaboration with the group of Prof. Bart Jan Ravoo (University of Münster, Germany). Kevin De Bruycker and Oliver Roling conceived and designed the experiments. Synthesis of small molecules and mechanistic studies were performed by Kevin De Bruycker at Ghent University. Writing and erasing experiments were performed by Oliver Roling, initially at Ghent University and continued at the University of Münster. The collaborators discussed and commented on the results at all stages.

VI.6 Experimental section

All materials, solvents and their corresponding purification are presented in appendix A.

VI.6.1 Synthesis

VI.6.1.1 2-Phenyl-3-(5-hydrothiopentyl)-indole (125)

2-Phenyl-3-(5-hydroxypentyl)-indole

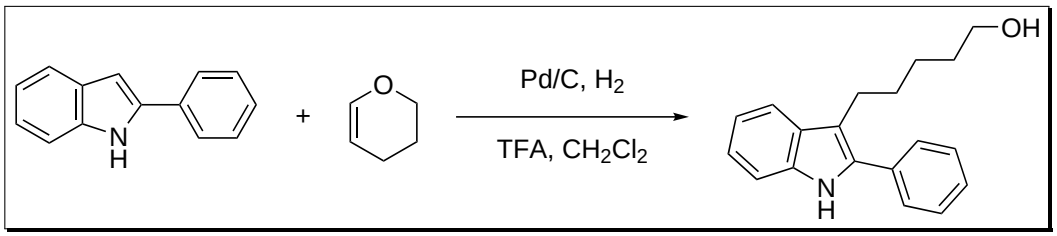

A mixture of trifluoro acetic acid (31.6 g, 0.277 mol, 1.5 eq), palladium (5 % on activated carbon, 2.8 g) and dichloromethane (380 mL) was put under hydrogen atmosphere in a 2 L two neck flask and cooled in an ice bath. To this mixture, 2-phenyl-1*H*-indole (35.7 g, 0.185 mol, 1 eq) and 3,4-dihydro-2*H*-pyran (17.2 g, 51.1 mmol, 1.1 eq) in dichloromethane (560 mL) was added dropwise. This solution was vigorously stirred in a water bath for 48 hours, regularly flushing with hydrogen gas. With the help of TLC (ethyl acetate:hexane 1:9) the reaction was followed until completion. The mixture was filtered over celite and washed with saturated aqueous sodium carbonate solution (400 mL). The organic phases are dried over magnesium sulphate and concentrated *in vacuo* to obtain a yellow brown oil. To this oil methanol was added until a dilution of ∼10 wt%, followed by the addition of potassium carbonate until saturation of the solution. After stirring for 15 minutes, water was added to double the volume. The obtained mixture was concentrated until half volume under reduced pressure and extracted with dichloromethane (2 × 400 mL). The obtained organic phases were collected, dried on magnesium sulphate and concentrated *in vacuo*.

Yield: 51.3 g yellow brown oil (0.184 mol, 99 %).

Bruto formula: $C_{19}H_{21}NO$.

MW.: 279.38 g/mol.

^{1}H-NMR (300 MHz, $CDCl_3$): δ (ppm) = 1.46 (m, 2 H, CH_2), 1.59 (m, 2 H, CH_2), 1.77 (quint., 2 H, CH_2), 2.92 (t, 2 H, C=C−CH_2), 3.62 (t, 2 H, CH_2−OH), 7.11–7.26 (m, 2

H, Ar*H*), 7.34–7.42 (m, 2 H, Ar*H*), 7.44–7.52 (m, 2 H, Ar*H*), 7.53–7.59 (m, 2 H, Ar*H*), 7.62–7.68 (d, 1 H, Ar*H*), 8.04 (br. s, 1 H, N*H*).

2-Phenyl-3-(5-mesyloxypentyl)-indole

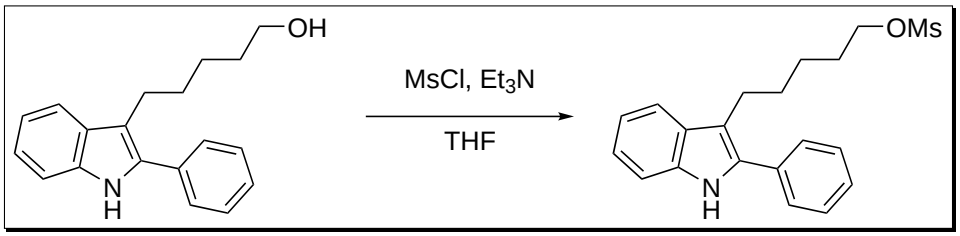

Indole alcohol (51.3 g, 0.184 mol, 1 eq) was added to a two neck 1 L flask and dissolved in dry THF (500 mL). After addition of dry triethylamine (55 mL, 0.367 mol, 2 eq), the mixture was cooled in an ice bath. Then mesyl chloride (22 mL, 0.275 mol, 1.5 eq) was added dropwise and the mixture stirred overnight under inert atmosphere. The mixture was washed with water (240 mL) and the aqueous phase extracted with THF (240 mL). The combined organic layers were then washed with saturated aqueous sodium bicarbonate solution (2 × 240 mL) and brine (240 mL). After drying over $MgSO_4$ the mesylated indole was acquired by evaporation of the solvent.

Yield: 52.5 g black oil (0.147 mol, 80 %).

Bruto formula: $C_{20}H_{23}NO_3S$.

MW.: 357.47 g/mol.

^{1}H-NMR (300 MHz, $CDCl_3$): δ (ppm) = 1.48 (m, 2 H, CH_2), 1.75 (m, 4 H, CH_2), 2.94 (m, 5 H, SO_2−CH_3 + C=C−CH_2), 4.17 (t, 2 H, CH_2−OMs), 7.10–7.25 (m, 2 H, Ar*H*), 7.34–7.42 (m, 2 H, Ar*H*), 7.45–7.59 (m, 4 H, Ar*H*), 7.59–7.66 (m, 1 H, Ar*H*), 8.08 (br. s, 1 H, N*H*).

2-Phenyl-3-(5-acetylthiopentyl)-indole

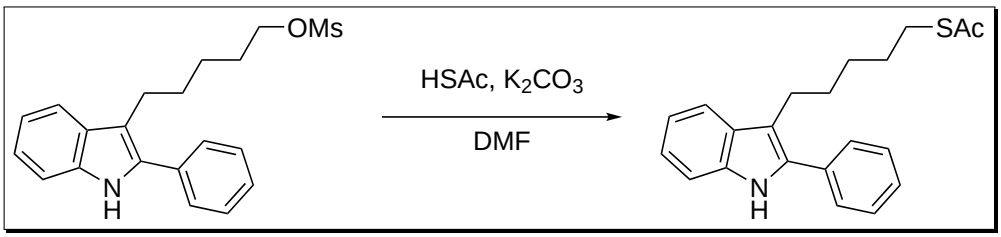

Potassium carbonate (1.93 g, 14.0 mmol, 1 eq) was suspended in DMF (10 mL) under inert atmosphere. Then thioacetic acid (1.07 g, 14.0 mmol, 1 eq) and indole mesylate (5.00 g,

14.0 mmol, 1 eq) dissolved in DMF (10 mL) were added while cooling with an ice bath. After the addition of DMF (120 mL), the reaction was allowed to stir at room temperature overnight. DMF was evaporated, the residue taken up in ethyl acetate and filtered. The solvent was removed *in vacuo* and the crude product purified via column chromatography (ethyl acetate:heptane 1:9) in order to yield the desired product.

Yield: 2.17 g off-white solid (6.42 mmol, 46 %).

Bruto formula: $C_{21}H_{23}NOS$.

MW.: 337.48 g/mol.

^{1}H-NMR (300 MHz, $CDCl_3$): δ (ppm) = 1.48 (m, 2 H, CH_2), 1.59 (m, 2 H, CH_2), 1.75 (quint., 2 H, CH_2), 2.33 (s, 3 H, SAc), 2.85 (t, 2 H, CH_2−S), 2.90 (t, 2 H, C=C−CH_2), 7.11–7.26 (m, 2 H, ArH), 7.34–7.43 (m, 2 H, ArH), 7.49 (m, 2 H, ArH), 7.56 (m, 2 H, ArH), 7.66 (d, 1 H, ArH), 8.02 (br. s, 1 H, NH).

2-Phenyl-3-(5-hydrothiopentyl)-indole

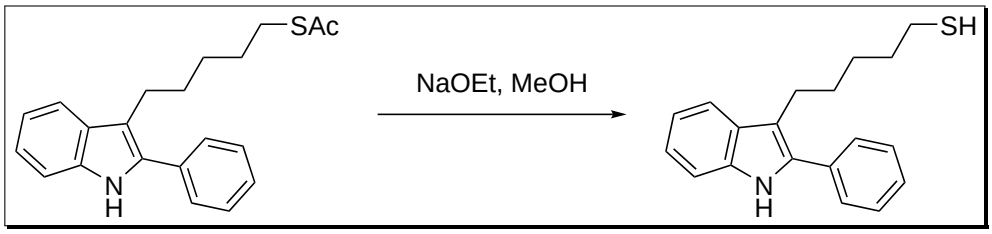

Indole thioacetate (0.50 g, 1.48 mmol, 1 eq) was dissolved in MeOH (5 mL) and the solution was degassed by bubbling nitrogen through it for 30 min. Sodium ethanolate (0.30 g, 4.44 mmol, 3 eq) was dispersed in MeOH (4 mL) and degassed by bubbling nitrogen through it for 30 min. The solutions were combined in a nitrogen flushed 2 neck flask and stirred for 3 h. The reaction was controlled via TLC. Then 1 M HCl (40 mL) was added, the aqueous phase was extracted with EtOAc (4x75 mL) and the combined organic phases were dried over MgSO4. After evaporation of the solvent, the product was obtained.

Yield: 0.42 g off-white solid (1.42 mmol, 96 %).

Bruto formula: $C_{19}H_{21}NS$.

MW.: 295.44 g/mol.

ESI-HRMS (m/z): $[C_{19}H_{21}NNaS]^+$: calculated: 318.1287, found: 318.1293.

^{1}H-NMR (300 MHz, $CDCl_3$): δ (ppm) = 1.30 (t, 1 H, SH), 1.47 (m, 2 H, CH_2), 1.61 (m, 2 H, CH_2), 1.74 (quint., 2 H, CH_2), 2.49 (q, 2 H, CH_2−SH), 2.91 (t, 2 H, C=C−CH_2), 7.10–7.25 (m, 2 H, ArH), 7.34–7.43 (m, 2 H, ArH), 7.49 (m, 2 H, ArH), 7.56 (m, 2 H, ArH),

7.63 (d, 1 H, Ar*H*), 8.01 (br. s, 1 H, N*H*).

^{13}C-NMR (75 MHz, $CDCl_3$): δ (ppm) = 136.0, 133.5, 129.3, 129.0, 128.1, 127.7, 122.4, 119.6, 119.3, 113.8, 110.9, 34.0, 30.5, 28.6, 24.8, 24.50.

VI.6.1.2 4-(4-(2-Bromo-2-methylpropanamido)phenyl)-1,2,4-triazoline-3,5-dione

4-(4-Nitrophenyl)-1-(ethoxycarbonyl)semicarbazide

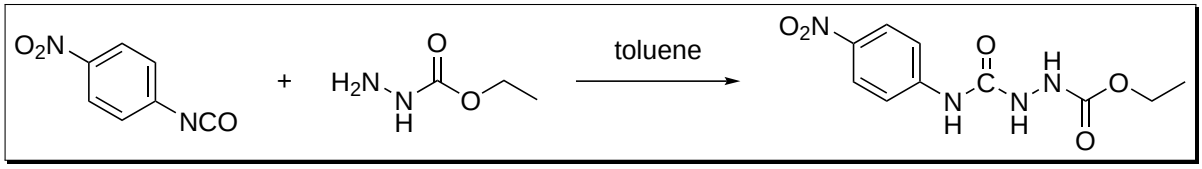

In a 50 mL two-neck flask, 4-nitrophenyl isocyanate (1 g, 6.1 mmol) was dissolved in dry toluene (15 mL). This mixture was cooled on an ice batch for 30 min. Then ethyl carbazate (0.634 g, 6.1 mmol) dissolved in dry toluene (15 mL) was added dropwise over 10 minutes. The reaction mixture was brought to room temperature and allowed to stir for 8 hours, after which it was cooled in an ice batch. The desired product was filtered off and used without any further purification in the next step.

Yield: 1.56 g bright yellow powder (5.8 mmol, 95 %).

Bruto formula: $C_{10}H_{12}N_4O_5$.

MW.: 268.23 g/mol.

^{1}H-NMR (300 MHz, DMSO$-$$d_6$): δ (ppm) = 1.20 (t, 3 H, C$H_3$$-CH_2$), 4.07 (q, 2 H, C$H_2$$-CH_3$), 7.73 (d, 2 H, Ar*H*), 8.17 (d, 2 H, Ar*H*), 8.40 (br. s, 1 H, N*H*), 9.04 (br. s, 1 H, N*H*), 9.52 (br. s, 1 H, N*H*).

4-(4-Nitrophenyl)-1,2,4-triazolidine-3,5-dione

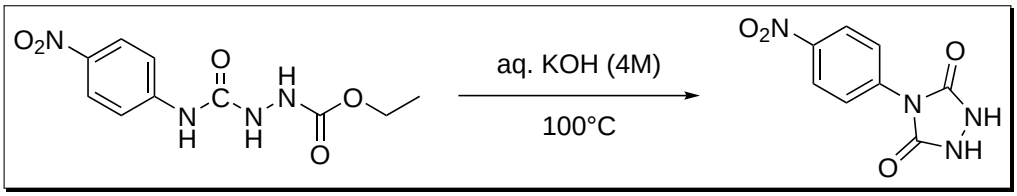

In a 5 mL flask, 4-(4-nitrophenyl)-1-(ethoxycarbonyl)semicarbazide (1 g, 3.7 mmol) was dissolved in 2.5 mL of an aqueous potassium hydroxide solution (4 M) under inert atmosphere. This mixture was refluxed for 4 hours (100 °C), warm filtered, cooled to room

temperature and acidified until pH1 by the addition of hydrogen chloride. This mixture was cooled to room temperature to yield a solid white powder that was filtered off.

Yield: 0.77 g (3.5 mmol, 95 %).

Bruto formula: $C_8H_6N_4O_4$.

MW.: 222.16 g/mol.

^{1}H-NMR (300 MHz, DMSO−d_6): δ (ppm) = 7.89 (d, 2 H, Ar*H*), 8.36 (d, 2 H, Ar*H*), 10.82 (br. s, 2 H, N*H*).

4-(4-Aminophenyl)-1,2,4-triazolidine-3,5-dione

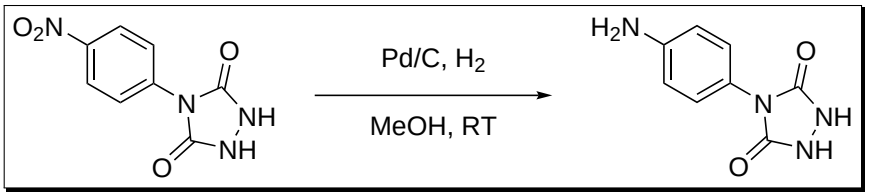

In a 25 mL flask, 4-(4-nitrophenyl)-1,2,4-triazolidine-3,5-dione (0.5 g, 2.6 mmol) was dissolved in 10 mL of methanol. A catalytic amount of palladium (5 % on activated carbon) was added. Then a balloon containing hydrogen gas was placed on the reaction, this mixture was stirred vigorously for 24 hour at room temperature. The solution was filtered over a plug of celite to remove the palladium and then concentrated under reduced pressure to give the desired product.

Yield: 0.48 g (2.5 mmol, 96 %).

Bruto formula: $C_8H_8N_4O_2$.

MW.: 192.17 g/mol.

^{1}H-NMR (300 MHz, DMSO−d_6): δ (ppm) = 5.29 (br. s, 2 H, NH_2), 6.59 (d, 2 H, Ar*H*), 6.98 (d, 2 H, Ar*H*), 10.17 (br. s, 2 H, N*H*).

4-(4-(2-Bromo-2-methylpropanamido)phenyl)-1,2,4-triazolidine-3,5-dione

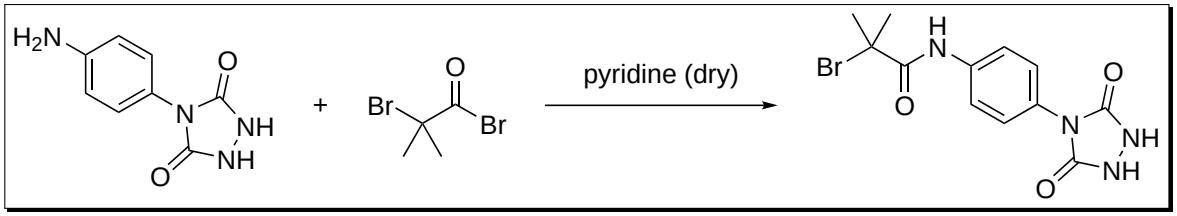

In a 25 mL flask, 4-(4-aminophenyl)-1,2,4-triazolidine-3,5-dione (1 g, 5.2 mmol) was dissolved in 10 mL of dry pyridine. After cooling this mixture to ice, α-bromoisobutyryl

bromide (1.20 g, 5.2 mmol, 0.65 mL) was added dropwise. The mixture was slowly brought to room temperature and stirred overnight. Then 15 mL of water was added and the mixture was separated 3 times with ethyl acetate. The organic phase was washed once with a 1 M aqueous HCl solution and concentrated *in vacuo*. The product was dissolved in methanol and concentrated on silica *in vacuo*. Then a flash chromatography was conducted: (ethyl acetate:methanol:acetic acid 95:5:1):(petroleum ether) 2:1 (rf = 0.25).

Yield: 1.3 g (3.8 mmol, 73 %).

Bruto formula: $C_{12}H_{13}N_4O_3$.

MW.: 341.16 g/mol.

^{1}H-NMR (300 MHz, DMSO−d_6): δ (ppm) = 2.08 (s, 6 H, 2 × CH_3), 7.45 (d, 2 H, ArH), 7.79 (d, 2 H, ArH), 10.01 (s, 1 H, Ar−NH), 10.50 (br. s, 2 H, NH).

4-(4-(2-Bromo-2-methylpropanamido)phenyl)-1,2,4-triazoline-3,5-dione

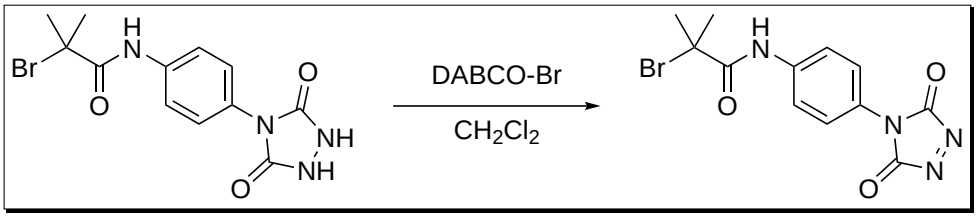

A mixture of ATRP-urazole (100 mg, 0.295 mmol, 1 eq), DABCO-Br (see section III.5.1.2, 93 mg, 0.059 mmol, 0.2 eq) and dichloromethane (3 mL) was put in a flask (10 mL) under inert atmosphere and stirred for 2 hours at room temperature. The reaction mixture was filtered off, the residue washed with dichloromethane (2 × 3 mL) and the filtrate was concentrated *in vacuo* to obtain ATRP-1,2,4-triazoline-3,5-dione. The temperature of the heating bath cannot exceed 50 °C due to the stability of the obtained compound.

Yield: 81 mg bright pink crystals (0.238 mmol, 81 %).

Bruto formula: $C_{12}H_{11}BrN_4O_3$.

MW.: 339.15 g/mol.

^{1}H-NMR (300 MHz, DMSO−d_6): δ (ppm) = 2.01 (s, 6 H, 2 × CH_3), 7.39 (d, 2 H, ArH), 7.86 (d, 2 H, ArH), 10.07 (s, 1 H, Ar−NH).

VI.6.1.3 2-Phenyl-3-(4-pentenyl)-indole (radical clock, 127)

4-Pentenal

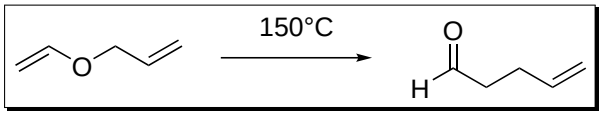

4-Pentenal was synthesised via a reported procedure.[37] In a pressure tube, 5 g allyl vinyl ether (59.4 mmol) was stirred at 150 °C. According to NMR analysis, full conversion was obtained after 8 hours. The product was used in the next step without further purifications.

Bruto formula: C_5H_8O.

MW.: 84.12 g/mol.

^{1}H-NMR (300 MHz, $CDCl_3$): δ (ppm) = 2.40 (m, 2 H, CH−CH_2), 2.55 (m, 2 H, C(O)−CH_2), 4.98–5.12 (m, 2 H, CHH_2=CH), 5.84 (m, 1 H, CH_2=CH), 9.79 (t, 1 H, HCO).

2-Phenyl-3-(4-pentenyl)-indole

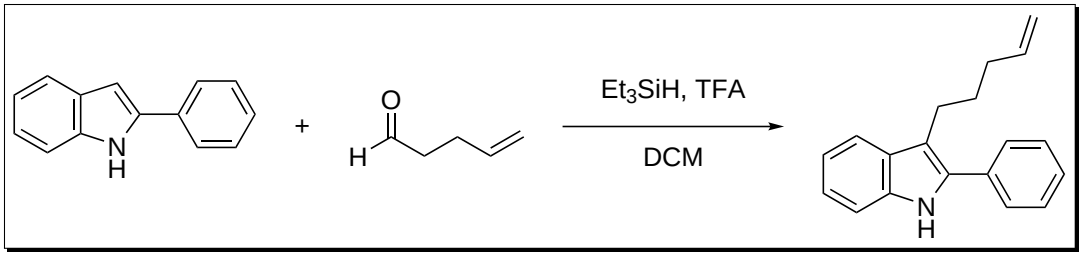

The synthesis of 2-phenyl-3-(4-pentenyl)-indole was based on a reported procedure.[38] 942 mg triethylsilane (8.10 mmol, 3 eq) and 462 mg trifluoroacetic acid (4.05 mmol, 1.5 eq) were each dissolved separately in 2.5 mL dichloromethane, mixed in a 50 mL two-neck flask under an inert atmosphere and cooled in an ice-bath. Next, a solution of 522 mg 2-phenylindole (2.70 mmol, 1 eq) and 261 mg 4-pentenal (3.11 mmol, 1.15 eq) in 11 mL dichloromethane was added drop-wise. During the addition, the colour of the reaction mixture changed from colourless over orange and green to blue. The reaction was stirred overnight at room temperature and controlled for complete conversion by TLC (ethyl acetate:heptane 1:7). Then, the pH was adjusted to ∼11 by the drop-wise addition of 2 M aqueous sodium hydroxide (approx. 10 mL), which also changed the colour of the mixture to yellow-orange. The aqueous phase was separated and extracted with 10 mL dichloromethane. The combined organic phases were washed with 30 mL brine and dried

over $MgSO_4$. After evaporating the solvent *in vacuo*, the crude product was purified via column chromatography over silica gel (5 % ethyl acetate in heptane).

Yield: 571 mg brown waxy solid (2.18 mmol, 81 %).

Bruto formula: $C_{19}H_{19}N$.

MW.: 261.37 g/mol.

LC-MS (m/z): 262.2 $[MH]^+$.

HRMS (m/z for $[MH]^+$): $[MH]^+$: calculated: 262.1590, found: 262.1585.

^{1}H-NMR (400 MHz, DMSO−d_6): δ (ppm) = 1.72 (quint, 2 H, CH_2−CH_2−CH_2), 2.10 (q, 2 H, CH_2=CH−CH_2), 2.85 (t, 2 H, Indole−CH_2), 4.92 (m, 2 H, CH_2=CH), 5.84 (m, 1 H, CH_2=CH), 7.00 (t, 1 H, ArH), 7.09 (t, 1 H, ArH), 7.36 (m, 2 H, ArH), 7.52 (m, 3 H, ArH), 7.61 (dd, 2 H, CH_2−C=C−C=CH), 11.12 (s, 1 H, NH).

VI.6.1.4 4-Butyl-TAD adduct of 2-phenyl-3-(4-pentenyl)-indole (128)

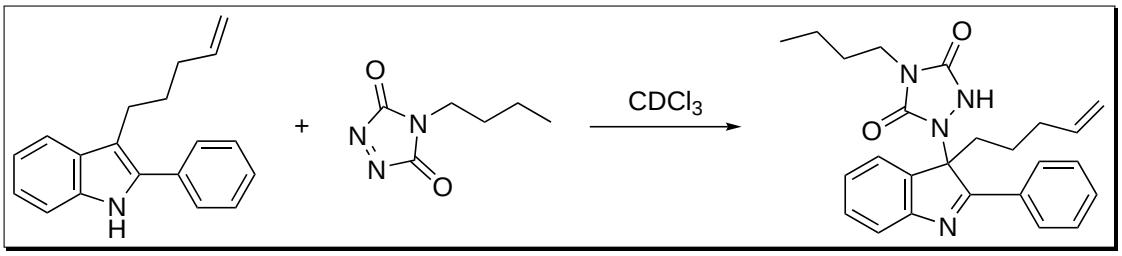

122.5 mg 2-phenyl-3-(4-pentenyl)-indole (469 µmol, 1 eq) and 72.7 mg 4-butyl-1,2,4-triazoline-3,5-dione (469 µmol, 1 eq) were weighed in separate vials and each dissolved in 1 mL deuterated chloroform. Both solutions were combined, the vials were washed with 0.5 mL deuterated chloroform after which the characteristic red colour of the TAD faded in less than 10 min. The reaction mixture was stirred overnight and the completion of the reaction was confirmed via NMR analysis by diluting an aliquot with deuterated chloroform. After evaporation of the solvent *in vacuo*, the product was purified by column chromatography over silica gel (ethyl acetate:hexane 1:2; RF ≈ 0.16).

Yield: 109 mg white solid (262 µmol, 56 %).

Bruto formula: $C_{25}H_{28}N_4O_2$.

MW.: 416.53 g/mol.

LC-MS (m/z): 417.2 $[MH]^+$.

HRMS (m/z for $[MH]^+$): $[MH]^+$: calculated: 417.2285, found: 417.2299.

^{1}H-NMR (400 MHz, DMSO−d_6): δ (ppm) = 0.36 (m, 1 H, CH_2−CH_2−CH_2), 0.67 (t,

4 H, CH_3 + CH_2−CH_2−CH_2), 0.92 (m, 2 H, CH_3−CH_2), 1.25 (quint, 2 H, N−CH_2−CH_2), 1.73 (q, 2 H, CH_2=CH−CH_2), 2.38 (m, 2 H, N−C−CH_2), 3.19 (t, 2 H, N−CH_2), 4.69–4.81 (m, 2 H, CH_2=CH), 5.42 (m, 1 H, CH_2=CH), 7.25 (t, 1 H, ArH), 7.41 (m, 2 H, ArH), 7.54 (m, 4 H, ArH), 8.19 (dd, 2 H, N=C−C=CH), 10.68 (s, 1 H, NH).

VI.6.1.5 *N*-(2-Acryloxyethyl)-*N*-methyl-4-amino-7-nitrobenzofurazan (152)

***N*-(2-Hydroxyethyl)-*N*-methyl-4-amino-7-nitrobenzofurazan**

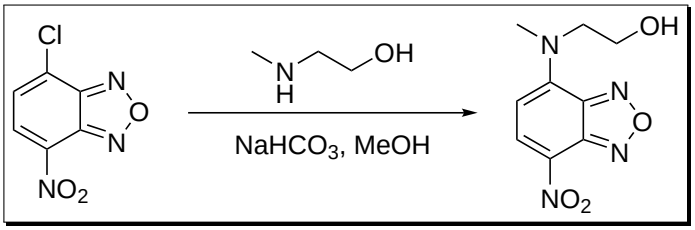

Hydroxyl terminated NBD (NBD-OH) was synthesised in analogy to a published procedure.[39] In a 250 mL flask, 2-(methylamino)ethanol (753 mg, 10.0 mmol, 1 eq) was dissolved in 100 mL methanol, to which 2.53 g sodium bicarbonate (30.1 mmol, 3 eq) was added. Then, 2.00 g 4-chloro-7-nitrobenzofurazan (NBD-Cl, 10.0 mmol, 1 eq) was added in portions at room temperature. The mixture was heated to 55 °C for three hours. During heating, a bright orange precipitate was formed. After cooling to room temperature, the reaction mixture was gently poured in a solution of 200 mL water, 200 mL brine and 100 mL 1 M aqueous hydrochloric acid. The solids were filtered and dried overnight in a vacuum oven at 40 °C in order to yield *N*-(2-hydroxyethyl)-*N*-methyl-4-amino-7-nitrobenzofurazan.

Yield: 2.28 g bright orange solid (9.57 mmol, 95 %).

Bruto formula: $C_9H_{10}N_4O_4$.

MW.: 238.20 g/mol.

LC-MS (m/z): 239.1 $[MH]^+$.

^{1}H-NMR (300 MHz, DMSO−d_6): δ (ppm) = 8.47 (d, 1 H, ArH), 6.44 (d, 1 H, ArH), 4.96 (t, 1 H, OH), 4.19 (br.s, 2 H, CH_2−N), 3.75 (q, 2 H, CH_2−OH), 3.53 (br.s, 3 H, CH_3−N).

***N*-(2-Acryloxyethyl)-*N*-methyl-4-amino-7-nitrobenzofurazan**

NBD-acrylate (NBDA) was synthesised in analogy to a published procedure.[40] NBD-OH (500 mg, 2.1 mmol, 1 eq) was suspended in 18 mL dry acetonitrile, triethylamine (1.50 g,

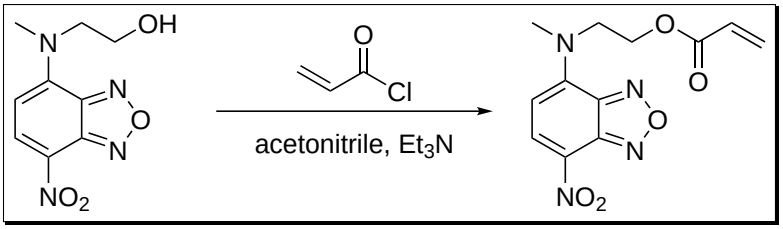

14.7 mmol, 7 eq) was added and the mixture cooled to 0 °C. Then, a solution of acryloyl chloride (950 mg, 10.5 mmol, 5 eq) in 2 mL dry acetonitrile was added drop-wise. The mixture was stirred at 0 °C for two hours and then stirred at room temperature overnight. The solvent was evaporated and the crude product was purified via column chromatography (dichloromethane) in order to yield the desired product.

Yield: 391 mg bright orange solid (1.34 mmol, 64 %).

Bruto formula: $C_{12}H_{12}N_4O_5$.

MW.: 292.25 g/mol.

ESI-HRMS (m/z): $[C_{12}H_{12}N_4NaO_5]^+$: calculated: 315.0700, found: 315.0707.

^{1}H-NMR (400 MHz, $CDCl_3$): δ (ppm) = 3.48 (s, 3 H), 4.45–4.51 (m, 2 H), 4.52–4.56 (m, 3 H), 5.82 (dd, 1 H), 6.00 (dd, 1 H), 6.18 (d, 1 H), 6.30 (dd, 1 H), 8.45 (d, 1 H).

^{13}C-NMR (100 MHz, $CDCl_3$): δ (ppm) = 165.8, 145.4, 144.8, 144.7, 135.3, 132.1, 127.6, 102.0, 62.0, 54.3, 42.1.

VI.6.2 Methods

VI.6.2.1 Stamp preparation

Poly(dimethyl siloxane) (PDMS) stamps were prepared from Sylgard 184 provided by Dow Corning. PDMS and curing agent are mixed in a 10:1 ratio (v/v) and thoroughly stirred by hand for 10 minutes. The precursor mixture is casted onto a structured silicon master, degassed and cured in an oven at 80 °C overnight. The cured stamps were cut out with a knife and treated with a UV ozonizer (PSD-UV, Novascan Technologies Inc.) for 55 min—or 25 min in the case of the optimised transclick procedure. If not used immediately, the PDMS stamps were stored in distilled water.

VI.6.2.2 Preparation of alkene and indole surfaces

Glass slides were cut into pieces of approximately $1.4 \times 1.4\,cm^2$ and cleaned by sonication in pentane, acetone and deionised water. The substrates were dried in a stream of argon and

immersed into a freshly prepared piranha solution ($H_2SO_4(conc.) : H_2O_2(30\,\%) = 3 : 1$). After 30 minutes the substrates were thoroughly washed with deionised water, dried in a stream of argon and put into a freshly prepared solution of 10-undecenyl trichlorosilane in toluene (0.1 vol%). The surfaces were taken out of this solution after 45 min, washed with ethanol and deionised water and dried in a stream of argon. These substrates were ready for TAD reactions or further functionalisation with indole via radical thiol-ene addition.

The indole thiol was immobilised via μCC with freshly oxidised flat unstructured PDMS stamps. Therefore, flat stamps were incubated with a solution containing 50 mM indole thiol and 25 mM 2,2-dimethoxy-2-phenylacetophenone (DMPA) in MeOH for 1 min. After drying of the stamp with a stream of argon, the soaked stamps were brought into conformal contact with the alkene substrates and irradiated with a 365 nm high-power UV-LED, which was placed approximately 2 cm above the contact area between stamp and substrate. After 5 min, the reaction was stopped, the substrates washed with ethanol and sonicated in acetone and DCM. A droplet of a 3 w% solution of DMPA in Boc-cysteamine was put onto these substrates, a microscopy cover slide put on top and then irradiated with a wavelength of 365 nm for 10 min again in order to make sure that no residual alkene groups remain on the surface. After rinsing with ethanol and sonication with acetone and DCM, these substrates were ready for μCC with ATRP-TAD.

VI.6.2.3 μCC procedure

Oxidised PDMS stamps were covered with approximately 30 μL of a 50 mM solution of ATRP-TAD in acetonitrile or dry DMSO. After an incubation time of 1 min, the stamps were dried in a stream of argon and placed on 10-undecenyltrichlorosilane SAMs or indole functionalised surfaces. After reaction times of 10 min or 5 min respectively, the stamps were lifted off and the substrates washed with acetone and DCM. After sonication in acetone and DCM these substrates were ready for SI-ATRP.

VI.6.2.4 General polymerisation procedures

Methyl acrylate (3.8 g, 44.1 mmol) and ethyl-α-bromo isobutyrate (1.8 mg, 9.4 μmol) were added to a Schlenk tube containing initiator functionalised substrates. Then a vortexed solution (100 μL) of Cu (II)Br_2 (0.5 mg, 2.2 μmol) and tris[2-(dimethylamino)ethyl]amine (3.6 mg, 11 μmol) in acetone (1 mL) was added. The tube was purged with argon and

subjected to three freeze/thaw circles with intermediate argon purges. Then ascorbic acid (24 mg, 141 µmol) was added and the tube placed in an oil bath for 14–24 h. In the case of ATRP-TAD-functionalised alkene substrates, the oil bath was heated to 75 °C, while ATRP-TAD-functionalised indole surfaces were heated to 50 °C. The polymer grown in solution was dissolved in DCM and precipitated from MeOH. The precipitation was repeated three times in order to remove unreacted monomers. Polymerisations at 75 °C gave polymers with an M_n around 210 kg mol^{-1} and a dispersity of 1.5. Based on this data, the grafting density of polymer brushes can be estimated to be 0.34 nm^{-2}. In the case of polymerisations at 50 °C, polymers with an M_n between 127 kg mol^{-1} and 184 kg mol^{-1} were obtained – depending on reaction times – with dispersities between 1.1 and 1.2. Based on these data, grafting densities between 0.09 nm^{-2} and 0.16 nm^{-2} were calculated. For the polymerisation of NBDA-containing brushes, 1 mol % of the monomer feed was substituted with NBDA. The polymerisations were performed at 50 °C overnight or at 75 °C for 3.5 hours. For the latter conditions, copolymers with an M_n of 169 kg mol^{-1} and a grafting density of 0.06 nm^{-2} were obtained.

VI.6.2.5 Radical clock experiment

An NMR sample was prepared of the BuTAD adduct of 2-phenyl-3-(4-pentenyl)-indole (**128**, 10.3 mg, 24.8 µmol, 1 eq) and *trans*,*trans*-2,4-hexadiene-1-ol (4.8 mg, 49.5 µmol, 2 eq) in 0.75 mL DMSO-d_6. This sample was submerged for 15 min in a pre-heated oil-bath at 150 °C. NMR analysis demonstrated a full transclick reaction with a fully intact terminal alkene. Next, the same experiment was repeated without the diene, *i.e.* 10.0 mg **128** (24.8 µmol) in 0.75 mL DMSO-d_6. In this case, the radical clock (**127**) is again recovered with a fully intact terminal alkene. The disappearance of the TAD-adduct and thus of the TAD moieties can be explained by a combination of TAD dimerisation at elevated temperatures in the absence of a suitable (irreversibly reacting) partner and hydrolysis by traces of water in the solvent (section II.3.3). In neither of these experiments, a significant cyclisation of the indole 4-pentenyl substituent is observed, which suggests that no radicals are formed at the indole C-3 position during the retro-Alder-ene reaction.

VI.6.2.6 Original transclick procedure (sections VI.3.2.2 and VI.3.2.3)

For the regeneration of indole functionalities, the clicked surfaces were immersed into a 1 M solution of 2,4-hexadien-1-ol in DMF and heated to 150 °C. In order to ensure that the transclick reaction led to a complete detachment of TAD groups, the reaction was allowed to proceed for 1 h (for ATRP-TAD, section VI.3.2.2) to 5 h (for polymer brushes, section VI.3.2.3). Unpolymerised substrates were sonicated in acetone and DCM for 5 min, dried in a stream of argon and were then ready for rewriting. Substrates with detached polymer brushes were sonicated in acetone, acetonitrile and DCM for 15 min each, carefully wiped with a tissue and dried in a stream of argon in order to remove all polymeric material sticking to the surface unspecifically. After sonicating these substrates in DCM again, the surfaces were ready for rewriting with ATRP-TAD.

VI.6.2.7 Optimised transclick procedure (section VI.3.2.4)

For faster regeneration of indole moieties from brush functionalised substrates, surfaces were immersed into α-phellandrene at 150 °C for 45 min. Substrates with detached polymer brushes were rinsed with DCM, carefully wiped with a tissue, sonicated in DCM for 10 min and were then ready for rewriting with ATRP-TAD.

VI.6.3 Instrumentation

Atomic force microscopy (AFM) AFM imaging was done with a NanoWizard 3 from JPK Instruments operated in tapping mode using Veeco RTESP-Tapping Mode etched silicon probes. The AFM was typically operated with a scan rate of 1.00 Hz and a set point of 0.900 V while images were recorded with a resolution of 512 × 512 pixels. Data evaluation was done with gwyddion version 2.36.

Computational methodology Similarly our previous theoretical rationalisations of TAD-based chemistry,[26,31] the M06-2X/6-31+G(d,p) level of theory, which has been shown successful to describe thermochemistry, was used for the calculation of the bond dissociation energy of the TAD-indole adduct. The stationary points were characterized as minima (ground states) or first order saddle points (transition states) by normal modes analysis. Since the reactions under study take place in CH_2Cl_2 or DMSO, which cannot form hydrogen bonds with the reactive substrate, the solvent environment was taken

into account by means of a polarisable continuum model. All computations were carried out by Hannelore Goossens (Center for Molecular Modeling, Ghent University) using the Gaussian 09 program package.

Contact angle goniometry Water CA measurements were performed using the sessile drop method on a DSA 100 goniometer (Krüss GmbH Wissenschaftliche Laborgeräte). Contact angle measurements were performed on glass substrates by applying a water droplet of 7 µL to the surface. Evaluation of the recorded data was performed using the software Drop Shape Analyses, which takes approximately 100 data points for each measurement.

Fourier transform infrared spectroscopy (FT-IR) FTIR spectra were recorded on a Digilab TFS 4000 equipped with a MKII Golden Gate Single reflection ATR system with diamond crystal 45° top plate P/N 10563. This top plate can be fitted to the Golden Gate optical unit to provide a single reflection 45° specular reflectance measurement of microsamples. The top plate slot aperture is 5 mm × 2.5 mm.

Nuclear magnetic resonance (NMR) NMR spectra were recorded with a Bruker Avance 300 (300 MHz) FT-NMR spectrometer in the indicated solvent at room temperature. Chemical shifts are presented in parts per million (δ) with the residual solvent peak as an internal standard.The resonance multiplicities are described as [br. (broad)] s (singlet), d (doublet), t (triplet), q (quadruplet), quint (quintuplet), sext (sextuplet) or m (multiplet).

Optical and fluorescence microscopy For fluorescence microscopy imaging an Olympus BX 53 microscope was operated with an Olympus XC 10 camera and a X-Cite® Series 120Q by Lumen Dynamics as the irradiation source. Data processing was carried out with the software OLYMPUS Stream Start 1.8. Images were taken at 50-fold magnification with an exposure time of 50 ms.

Size exclusion chromatography (SEC) SEC was performed using a Varian PL-GPC 50 Plus instrument, using a refractive index detector, equipped with two PL-gel 5 µm MIXED-D columns 40 °C. Polystyrene standards were used for calibration and THF as eluent at a flow rate of 1 mL min^{-1}. Samples were injected using a PL AS RT autosampler.

Time-of-flight secondary ion mass spectrometry (ToF-SIMS) ToF-SIMS imaging was performed using an instrument that is widely compatible to the commercial ION-TOF ToF-SIMS V instrument (Münster, Germany). A pulsed 30 kV liquid metal ion source (LMIG, ION-TOF) was used for imaging the samples under static conditions with Bi^{3+} primary ions and an analysis current of 0.05 pA (pulse width 100 ns). The beam spot size was approximately 200 nm. To increase the mass resolution delayed extraction for secondary ions was applied. All samples were analysed with the detection mode for negative secondary ions.

X-ray photoelectron spectroscopy (XPS) XPS measurements were performed with an Axis Ultra DLD (Kratos Analytical Ltd, UK). A monochromatic Al Kα source (hν = 1486.6 eV) at 10 mA filament current and 12 kV filament voltage source energies was used. The pass energy was set to 20 eV for high resolution. The charge neutraliser was used to compensate for sample charging. All measurements were carried out in the 'hybrid mode'. The data were evaluated with CasaXPS (version 2.3.15, Casa Software Ltd, UK) and the spectra were calibrated to aliphatic carbon (C1s = 285 eV).

VI.7 Bibliography

1. A. Halperin, M. Tirrell, T. P. Lodge in *Tethered chains in polymer microstructures*, *Vol. 100*, Springer Berlin Heidelberg, Berlin, Heidelberg, **1992**, pp. 31–71.

2. T. K. Tam, J. Zhou, M. Pita, M. Ornatska, S. Minko, E. Katz, *J. Am. Chem. Soc.* **2008**, *130*, 10888–10889.

3. Z. B. Zhang, S. J. Yuan, X. L. Zhu, K. G. Neoh, E. T. Kang, *Biosens. Bioelectron.* **2010**, *25*, 1102–1108.

4. C. Rodriguez-Emmenegger, C. M. Preuss, B. Yameen, O. Pop-Georgievski, M. Bachmann, J. O. Mueller, M. Bruns, A. S. Goldmann, M. Bastmeyer, C. Barner-Kowollik, *Adv. Mater.* **2013**, *25*, 6123–6127.

5. M. Zamfir, C. Rodriguez-Emmenegger, S. Bauer, L. Barner, A. Rosenhahn, C. Barner-Kowollik, *J. Mater. Chem. B* **2013**, *1*, 6027–6034.

6. O. Roling, A. Mardyukov, J. A. Krings, A. Studer, B. J. Ravoo, *Macromolecules* **2014**, *47*, 2411–2419.

7. H. Wagner, Y. Li, M. Hirtz, L. Chi, H. Fuchs, A. Studer, *Soft Matter* **2011**, *7*, 9854–9858.

8. N. Zhang, T. Pompe, I. Amin, R. Luxenhofer, C. Werner, R. Jordan, *Macromol. Biosci.* **2012**, *12*, 926–936.

9. A. Synytska, E. Svetushkina, N. Puretskiy, G. Stoychev, S. Berger, L. Ionov, C. Bellmann, K.-J. Eichhorn, M. Stamm, *Soft Matter* **2010**, *6*, 5907–5914.

10. M. F. Delcroix, G. L. Huet, T. Conard, S. Demoustier-Champagne, F. E. Du Prez, J. Landoulsi, C. C. Dupont-Gillain, *Biomacromolecules* **2013**, *14*, 215–225.

11. I. Cringus-Fundeanu, J. Luijten, H. C. van der Mei, H. J. Busscher, A. J. Schouten, *Langmuir* **2007**, *23*, 5120–5126.

12. O. Azzaroni, *J. Polym. Sci. Part A: Polym. Chem.* **2012**, *50*, 3225–3258.

13. T. Chen, I. Amin, R. Jordan, *Chem. Soc. Rev.* **2012**, *41*, 3280–3296.

14. Z. Nie, E. Kumacheva, *Nat. Mater.* **2008**, *7*, 277–290.

15. J. E. Poelma, B. P. Fors, G. F. Meyers, J. W. Kramer, C. J. Hawker, *Angew. Chem. Int. Ed.* **2013**, *52*, 6844–6848.

16. Y. Xia, G. M. Whitesides, *Angew. Chem. Int. Ed.* **1998**, *37*, 550–575.

17. A. Perl, D. N. Reinhoudt, J. Huskens, *Adv. Mater.* **2009**, *21*, 2257–2268.

18. F. Zhou, Z. Zheng, B. Yu, W. Liu, W. T. S. Huck, *J. Am. Chem. Soc.* **2006**, *128*, 16253–16258.

19. T. Chen, R. Jordan, S. Zauscher, *Small* **2011**, *7*, 2148–2152.

20. T. Kaufmann, B. J. Ravoo, *Polym. Chem.* **2010**, *1*, 371–387.

21. C. Wendeln, B. J. Ravoo, *Langmuir* **2012**, *28*, 5527–5538.

22. J. M. Spruell, M. Wolffs, F. A. Leibfarth, B. C. Stahl, J. Heo, L. A. Connal, J. Hu, C. J. Hawker, *J. Am. Chem. Soc.* **2011**, *133*, 16698–16706.

23. C. Wendeln, S. Rinnen, C. Schulz, H. F. Arlinghaus, B. J. Ravoo, *Langmuir* **2010**, *26*, 15966–15971.

24. S. Arumugam, V. V. Popik, *J. Am. Chem. Soc.* **2012**, *134*, 8408–8411.

25. J. P. Blinco, V. Trouillet, M. Bruns, P. Gerstel, H. Gliemann, C. Barner-Kowollik, *Adv. Mater.* **2011**, *23*, 4435–4439.

26. S. Billiet, K. De Bruycker, F. Driessen, H. Goossens, V. Van Speybroeck, J. M. Winne, F. E. Du Prez, *Nat. Chem.* **2014**, *6*, 815–821.

27. O. Türünç, S. Billiet, K. De Bruycker, S. Ouardad, J. Winne, F. E. Du Prez, *Eur. Polym. J.* **2015**, *65*, 286–297.

28. O. Roling, C. Wendeln, U. Kauscher, P. Seelheim, H.-J. Galla, B. J. Ravoo, *Langmuir* **2013**, *29*, 10174–10182.

29. B. Oberleitner, A. Dellinger, M. Deforet, A. Galtayries, A.-S. Castanet, V. Semetey, *Chem. Commun.* **2013**, *49*, 1615–1617.

30. J. N. Lee, C. Park, G. M. Whitesides, *Anal. Chem.* **2003**, *75*, 6544–6554.

31. H. A. Houck, K. De Bruycker, S. Billiet, B. Dhanis, H. Goossens, S. Catak, V. Van Speybroeck, J. Winne, F. Du Prez, *Chem. Sci.* **2017**, *8*, 3098–3108.

32. S. J. Blanksby, G. B. Ellison, *Acc. Chem. Res.* **2003**, *36*, 255–263.

33. M. Newcomb in *Radical Kinetics and Clocks*, John Wiley and Sons, Ltd, **2012**, pp. 107–124.

34. A. Barton, *Handbook of Polymer-Liquid Interaction Parameters and Solubility Parameters*, Taylor and Francis, **1990**, p. 768.

35. B. Vonhören, M. Langer, D. Abt, C. Barner-Kowollik, B. J. Ravoo, *Langmuir* **2015**, *31*, 13625–13631.

36. T. Du, B. Li, X. Wang, B. Yu, X. Pei, W. T. S. Huck, F. Zhou, *Angew. Chem. Int. Ed.* **2016**, *55*, 4260–4264.

37. I. Coldham, A. J. M. Burrell, H. D. S. Guerrand, N. Oram, *Org. Lett.* **2011**, *13*, 1267–1269.

38. Q. Cai, C. Zheng, S.-L. You, *Angew. Chem. Int. Ed.* **2010**, *49*, 8666–8669.

39. R. S. Jardine, P. Bartlett, *Colloids Surf. A* **2002**, *211*, 127–132.

40. L. Tao, C. S. Kaddis, R. R. Ogorzalek Loo, G. N. Grover, J. A. Loo, H. D. Maynard, *Chem. Commun.* **2009**, 2148–2150.

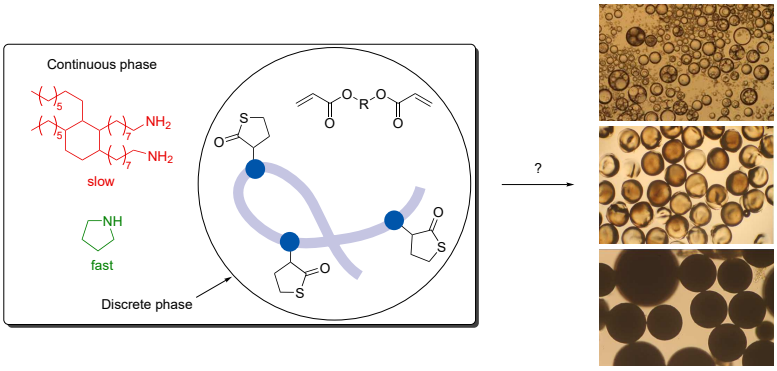

Abstract

Similarly to other fast and efficient ligation methods, the high reactivity of triazolinedione chemistry can present a problem for the development of specific applications. This chapter will give a short overview of the problems that are encountered when the TAD chemistry is applied in liquid-liquid biphasic systems. Next, a brief discussion of thiolactone chemistry will demonstrate that a thiolactone-based one-pot multi-component reaction can be applied as a TAD-complementary alternative, which is not hampered by these limitations. Finally, the applicability of this thiolactone ligation method for the synthesis of polymeric particles will be demonstrated. To this end, both water-in-oil and oil-in-water interfacial polymerisations will be investigated, in which a multivalent thiolactone is combined with an acrylic cross-linker in the discrete phase.

Chapter VII

Triazolinedione-complementary ligation method: Thiolactone chemistry

VII.1 Introduction

The very high reaction rates are typically the main advantage of triazolinediones over alternative ligation chemistries, both in homogeneous and in interfacial systems, as demonstrated by the various examples in the previous chapters. Moreover, the reaction kinetics can be further tailored to the needs of specific applications. For example, readily available undecenyl-bearing substrates were efficiently functionalised via microcontact printing (Chapter VI), although these monosubstituted alkenes are known to react relatively slowly with TADs in solution. The layer-by-layer assembly of a coating, on the other hand, could be realised in a matter of minutes by using a trivalent conjugated diene as TAD-reactive monomer (Chapter V), which represents the other extreme on the reactivity scale (Figure II.10).

While all the discussed interfacial reactions with triazolinediones were performed at the solid-liquid interface, we also envisioned that the fast yet tunable reaction kinetics would allow for the synthesis and functionalisation of polymeric beads and microcapsules. Indeed, polymer beads could in principle be produced when both the TAD cross-linker and the complementary reaction partner are dissolved in the same solvent, which is then dispersed

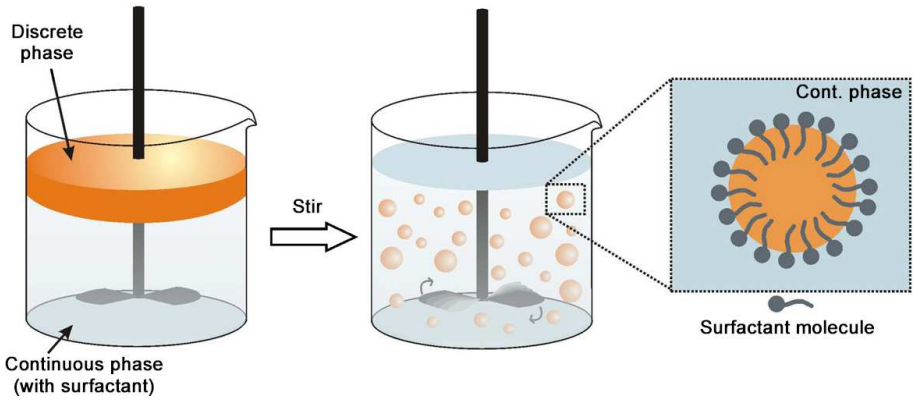

Figure VII.1: General strategy for the production of TAD-based particles via an interfacial polymerisation. When the discrete phase contains both monomers, polymer beads should be generated, whereas microcapsules are expected when a TAD-solution is dispersed in a continuous phase containing the complementary reaction partner. Figure adapted from Gokmen *et al.*[1]

in a continuous phase (Figure VII.1). On the other hand, when both reagents are dissolved in the separate phases, they can only react at the interface, yielding microcapsules instead. However, multiple time-consuming problems were encountered when the TAD cross-linking was applied in such a liquid-liquid biphasic system.

In this chapter, the limitations of the TAD chemistry in the context of an interfacial polymerisation will first be highlighted, together with the resulting – sometimes contradicting – requirements for the TAD-complementary reaction partners. Next, thiolactone chemistry will be introduced as a possible alternative ligation method that is not hampered by these limitations. Finally, the first applications of this thiolactone strategy in a liquid-liquid biphasic system will be discussed.

VII.2 Limitations of triazolinedione chemistry for interfacial polymerisations

For interfacial polymerisations, water is typically the solvent of choice for one of the liquid phases because of the immiscibility with many organic solvents (Figure VII.1). Nonetheless, the presence of water can cause issues with the TAD platform, of which the reported orthogonality is mainly based on a very good kinetic selectivity between desired and undesired reactions.[2] In fact, water will not hamper a fast TAD reaction such as the well-investigated tyrosine ligation, which is often performed in an aqueous buffer,[3–5]

while side reactions or hydrolysis of the TAD moieties cannot be excluded when a slower reacting alkene is used.[6–8] Therefore, the choice of a fast reacting unsaturated reaction partner is key for a successful interfacial polymerisation.

Secondly, for the production of polymeric beads via TAD chemistry, two complementary monomers are necessary that both dissolve in the discrete phase. Moreover, they should react slow enough to prevent gelation before the mixture is completely dispersed in the continuous phase. For example, initial tests using the citronellol-based trivalent alkenes, *i.e.* trisubstituted unsaturations (section III.2.1), were unsuccessful because of their fast cross-linking kinetics. Further attempts to slow down the reaction, by reducing the concentration of the reagents or by using monomers based on oleyl alcohol instead, rather promoted the aforementioned hydrolysis than the production of polymeric beads.

Finally, the synthesis of microcapsules was mainly hampered by the solubility of the unsaturated reaction partners. Indeed, to prevent hydrolysis of the TAD moieties, the cross-linker should be dissolved in the organic phase, which implies that a multivalent 'fatty' alkene should dissolve in the aqueous phase. To this end, water-soluble polymers were targeted in which unsaturated side-chains were introduced by adding an appropriate compound to the monomer mixture.

For the synthesis of water-soluble unsaturated polymers that are reactive to TAD-compounds, prenyl acrylate (**131**) and (cyclohexenyl)ethylacrylamide (**132**) were identified as suitable co-monomers. These compounds were first synthesised and subsequently polymerised with 2-hydroxyethyl acrylate and *N*,*N*-dimethylacrylamide, respectively, via a reversible addition-fragmentation chain transfer (RAFT) polymerisation. Nevertheless, no (co-)polymers could be isolated, even after a reaction time of up to 24 hours. This observation can be explained by an intramolecular cyclisation of the propagating radical (Scheme VII.1), similarly to the cyclopolymerisation of allyl acrylate,[9,10] yielding a tertiary radical that reacts irreversibly with the chain transfer agent and thus generates a deactivated chain. While this side reaction might be avoided by introducing a longer aliphatic spacer in the unsaturated monomer, the water-solubility of the resulting polymer will be impacted as well. Moreover, the large-scale synthesis of a polymer with unsaturated side-chains via a reversible-deactivation or free radical polymerisation will remain problematic because of the limited stability of C=C bonds in the presence of radicals.

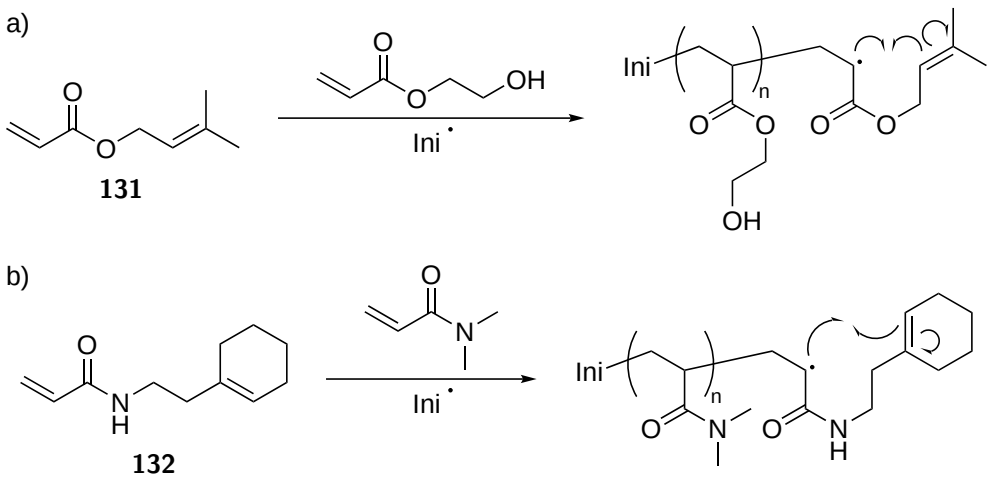

Scheme VII.1: For both monomers, an intramolecular cyclisation of the propagating radical will yield a tertiary radical that reacts irreversibly with the chain transfer agent. This proposed side reaction explains the absence of polymer in the mixture, even after a reaction time of up to 24 h. Ini = initiating radical.

In summary, this section provided a short overview on the encountered problems when developing a liquid-liquid biphasic system with triazolinedione chemistry. The main limitation is the presence of water in these systems, which results in a competitive hydrolysis next to the desired polymerisation process and thus cancels out the versatility of the TAD cross-linking to a certain extent. Therefore, the application of triazolinedione chemistry for the synthesis of polymeric beads or microcapsules was not further investigated in this doctoral work.

VII.3 Brief introduction to thiolactone chemistry

Besides triazolinedione chemistry, conjugation and modification reactions involving a thiol recently gained a lot of interest as well. This group is known to react with a wide variety of substrates, while many of these so-called 'thiol-X' reactions possess some of the 'click' requirements.[11–13] However, the main difference with triazolinediones is that thiols are electron-rich and thus preferentially react with electrophilic species such as epoxides and isocyanates. Unsaturations such as terminal alkenes and electron-deficient acrylates are also included in the substrate scope, while internal alkenes or conjugated diene exhibit a much lower reaction rate.[14,15] In this perspective, thiols can be seen as moieties with a complementary reactivity to the previously applied triazolinediones.

Despite the positive characteristics of thiol-X conjugations, applications are often hampered

by the limited commercial availability and shelf life of thiols as a result of their oxidative sensitivity.[16] Moreover, they are usually associated with a very strong and unpleasant odour. To avoid some of these drawbacks, our group introduced a γ-thiolactone (TLa, Scheme VII.2) as a latent thiol functionality.[17] These cyclic thioesters react with a wide variety of nucleophiles such as water, alcohols or amines, and thereby release a thiol that can subsequently react in one of the thiol-X reactions.[18]

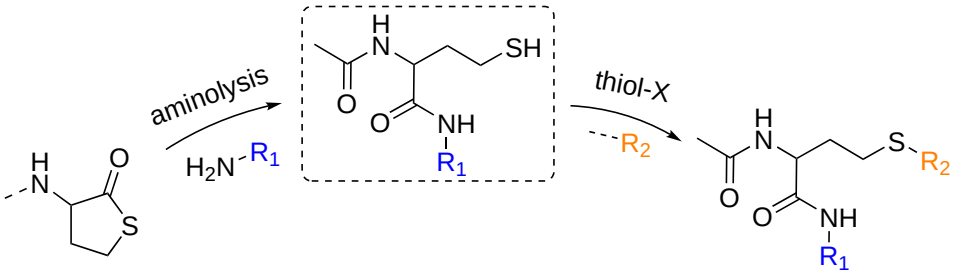

Scheme VII.2: Thiolactone-based chemistry in which the thiolactone group functions as a latent thiol functionalitity that is released upon aminolysis. Subsequently, the free thiol can react in a 'thiol-X' conjugation.

Hydrolysis or alcoholysis of thiolactone units only proceeds rapidly in an alkaline environment or in the presence of a catalyst, while no additives are required in the case of amines.[16] Therefore, an aminolysis is often preferred as the first step in the overall thiolactone strategy. Moreover, this step can be carried out in an aqueous environment, although hydrolysis is an important side reaction as a result of the basicity of the amine.[19,20] Finally, in some cases, both the ring opening with an amine and the subsequent thiol-X reaction can even be performed in a one-pot fashion.[16]

This section aims to provide a brief overview of the features of the thiolactone concept that are relevant for this doctoral work. First, the impact of the specific amine on the aminolysis will be discussed, followed by two thiol-X reactions that were demonstrated to be particularly compatible with these latent thiols. Finally, the possibility to use thiolactone units as a 'one-pot double modification' tool will be highlighted by a selection of applications in polymer science. For a more elaborate review of the applications of thiolactone chemistry or specific thiol-X ligations, the reader is referred to one of the dedicated review articles[16,21–23] or the theoretical sections of certain PhD manuscripts by our research group.[24,25]

VII.3.1 Thiolactone aminolysis

As previously discussed, ring opening of TLa units with amines is characterised by several advantages over the alternative hydrolysis or alcoholysis to produce the latent thiol functionality. Nevertheless, this aminolysis was found to be the rate determining step in the overall thiolactone ligation strategy for multiple subsequent thiol-X reactions.[17,26] Therefore, Espeel *et al.* performed a kinetic screening of the TLa ring opening in the presence of various amines.[16,26]

The secondary amine pyrrolidine (**133**) reacts faster than the primary propyl amine (**134**), which can be explained by the higher electron density and thus nucleophilicity of the former amine (Figure VII.2). Moreover, the reaction speed decreases when an inductive electron withdrawing group is present, *cf.* glycine *tert*-butyl ester (**135**) or benzylamine (**136**). Steric effects play an important role as well, as evidenced by the hindered nucleophilic attack of Jeffamine M-600 (**137**) as a result of the α-branching. Finally, secondary or tertiary amines, such as diethyl- or trimethylamine, can be considered unreactive towards thiolactones, with the aforementioned cyclic secondary amine as a remarkable exception.

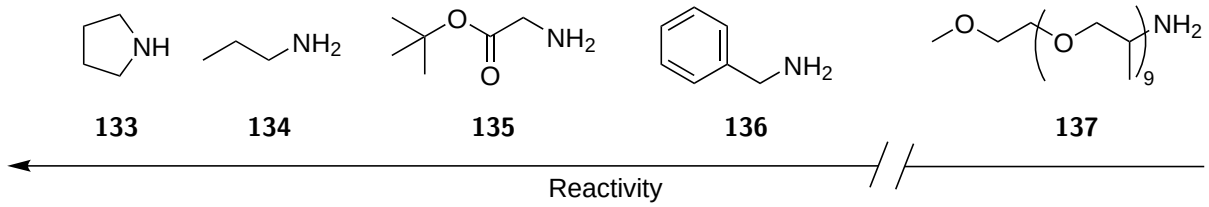

Figure VII.2: Empirical reactivity order of various amines for the TLa aminolysis in THF.[26]

In summary, similarly to triazolinedione chemistry, the reaction kinetics of the thiolactone strategy can also be tuned to a certain extent. Whereas the reactivity of triazolinediones is highly dependent on the electron density of the π-cloud type reaction partner, the kinetics of the rate determining aminolysis in the two-step TLa protocol can be explained and predicted by the nucleophilic properties of the amine.

VII.3.2 Radical amine-thiol-ene conjugation

Thiol groups react very efficiently with a wide variety of substrates, which originates from the nature of the sulphur atom. The relatively large size leads to an increased polarisability, which makes the thiol a better nucleophile compared to amines and alcohols in alkylation

reactions. Moreover, thiyl radicals are generated easily because of the weak S−H bond. In the context of polymer chemistry, the reaction between thiols and a C=C bond, *i.e.* a so-called 'thiol-ene' reaction, is the most important.[21,22] Depending on the nature of this alkene, the reaction mechanism is generally accepted to proceed via a radical or a nucleophilic pathway (Scheme VII.3). This section will discuss the radical hydrothiolation, whereas the nucleophilic variant will be addressed in the next section.

The radical hydrothiolation (Scheme VII.3a) proceeds via a chain process that is often initiated using either a thermal or a photoinitiator (Scheme VII.4).[11,12] Nevertheless, Bowman and co-workers as well as Schlaad and co-workers demonstrated that an initiator is not always required, since UV-light and even sunlight can generate the necessary thiyl radicals.[27–29] After the initiation phase, the hydrothiolation propagates via the addition of a thiyl radical to a double bond, generating an intermediate carbon-centered radical that

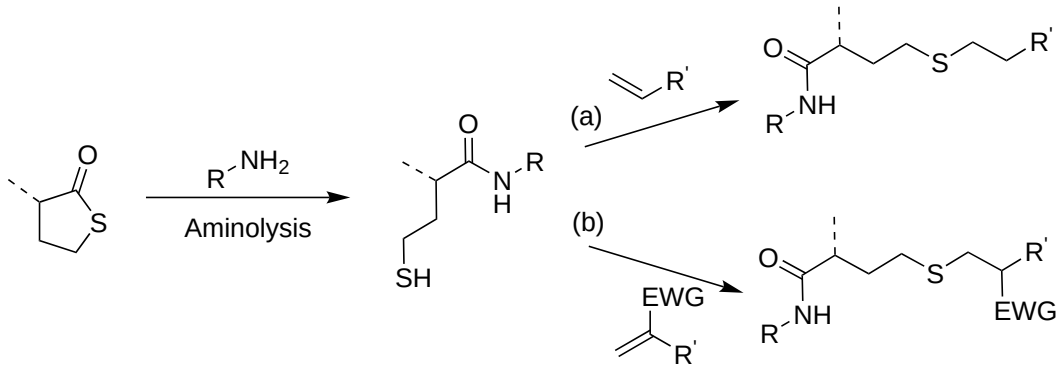

Scheme VII.3: Aminolysis of the TLa unit generates a free thiol that can react in a 'thiol-ene' reaction. Depending on the nature of the alkene, the mechanism is either (**a**) radical or (**b**) nucleophilic. EWG = electron withdrawing group.

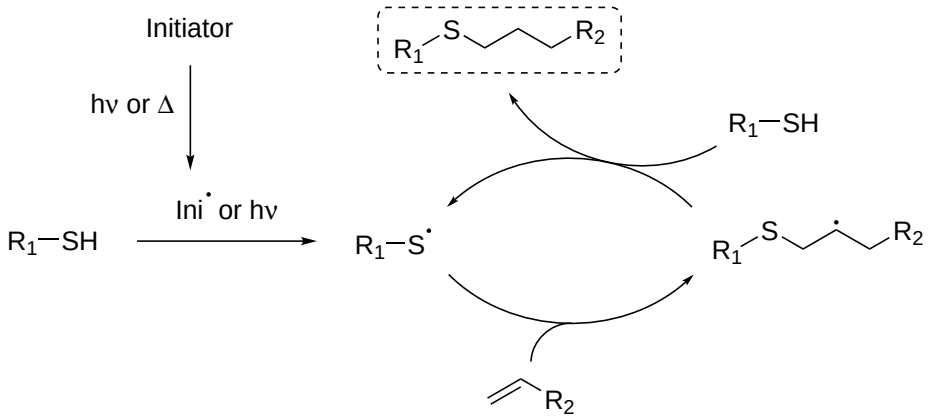

Scheme VII.4: Mechanism of the radical hydrothiolation. Thiyl radicals are generated by treating a thiol with an initiating radical (Ini) or by illumination with UV- or sunlight. Addition of this thiyl radical to the alkene yields a carbon radical that maintains the propagation by abstracting a hydrogen of another thiol.

rapidly abstracts a hydrogen of another thiol. This cycle is repeated until termination occurs by recombination of two radicals. Depending on the exact reagents, the overall reaction is very fast, *i.e.* it can result in near-quantitative yields in only a few seconds, and very robust because of its high tolerance towards oxygen and water.

Despite the robustness of the thiol-ene reaction, some orthogonality issues might occur when it is combined in a one-pot fashion with the aminolysis of the overall thiolactone strategy, *i.e.* the 'radical amine-thiol-ene conjugation'. For example, benzylamine (**136**) can react with the radicals originating from typical photoinitiators such as 2,2-dimethoxy-2-phenylacetophenone (DMPA). While this problem can be circumvented by avoiding the use of a photoinitiator,[17] some functional amines are not inert in the radical environment of the hydrothiolation (*e.g.* allylamine or propargylamine). Nevertheless, various other functional amines were proven to be compatible with this amine-thiol-ene conjugation.[16]

VII.3.3 Nucleophilic amine-thiol-ene conjugation

Next to the isolated α-olefins that were discussed in the previous section, thiols also react with Michael acceptors, *i.e.* α,β-unsaturated carbonyl compounds (Scheme VII.3b). In contrast to the previously discussed radical mechanism, the addition to these activated alkenes is generally accepted to proceed via a nucleophilic pathway. This reaction is well-known as a highly specific bioconjugation for cysteine residues in peptides and proteins, and has been investigated more recently in the context of polymer chemistry.[16,30–33] It proceeds very efficiently, both in bulk and in solution, when catalysed by amines or phosphines and is often referred to as a thia-Michael addition.[12,21,22]

When applying this hydrothiolation as part of a one-pot thiolactone strategy, *i.e.* the 'nucleophilic amine-thiol-ene conjugation', both the amine and the generated thiol can

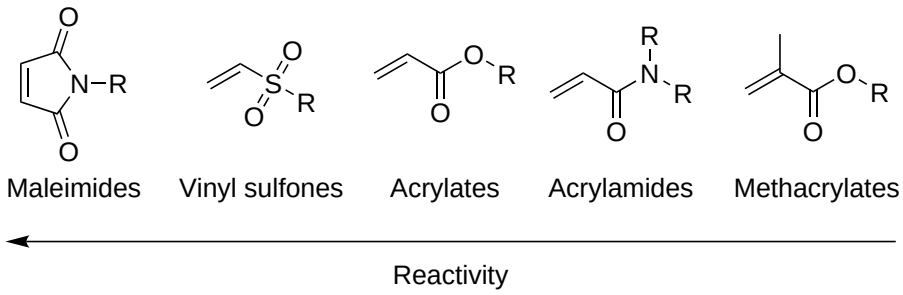

Figure VII.3: Reactivity order of the commonly used substrates in the thia-Michael addition.[34]

react with the activated alkene. Therefore, a kinetic selectivity in the reactivity of the Michael acceptor (Figure VII.3), similar to the triazolinedione chemistry, will dictate the outcome of this ligation method. Indeed, Mather *et al.* showed that the competition between an amine and a thiol is important when maleimides are used,[35] while Wu *et al.* reported that only secondary amines readily react with the less reactive acrylates at room temperature and without a catalyst.[36] Because these secondary amines are in general not suitable for TLa aminolysis (*vide supra*), a good kinetic selectivity is obtained when mixing a thiolactone with different acrylates (or less reactive substrates) and primary amines in one pot.[17] Moreover, a slight excess of amine is beneficial for the overall process, since it also catalyses the Michael addition after full conversion of the thiolactone.[17,34,37]

VII.3.4 Applications of TLa chemistry in polymer science

Because of the versatility of the amine-thiol-ene conjugation, this strategy was already thoroughly investigated by our research group, resulting in many applications in the field of synthetic polymer science. As a first example, Espeel *et al.* synthesised various AB′-type monomers bearing both a reactive double bond and a thiolactone unit (Scheme VII.5). After release of the thiol through aminolysis, the reactive AB monomer is produced that can be polymerised via a step-wise polyaddition.

Apart from the requirement of a full conversion of the thiolactones to obtain high molecular weight polymers, *i.e.* the ratio thiol:ene should equal one, this polymerisation method is very straightforward and allows a large structural freedom. Firstly, varying the functional group that links the thiolactone to the double bond, such as a carbamate[17,26] or an amide,[38] will influence the final properties of the synthesised polymers. Secondly, by changing the nature of the double bond in the monomer from an α-olefin to an acrylate, the polymerisation that needs a source of radicals[17,38] can be switched to a spontaneous process. Finally,

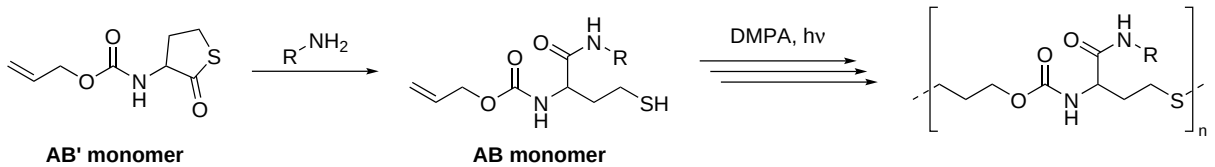

Scheme VII.5: Stepwise (radical) polymerisation of an AB′-type monomer bearing a thiolactone and alkene moiety in a one-pot process, yielding the corresponding polymer with a polythioether-urethane backbone.

because the amine is also incorporated into the final polymer structure, numerous chemical functionalities can be introduced without the need for protection/de-protection strategies, as long as they are compatible with the amine-thiol-ene conjugation.[16,17,26]

Similarly to the synthesis of functional linear polymers described above, polymers can also be grown from a solid support when a thiolactone moiety is immobilised on a cross-linked bead. Moreover, by carefully selecting a set of bifunctional molecules, a two-step process can be developed that allows both the introduction of a functionality in the polymer backbone and the recovery of a thiolactone chain end, *i.e.* the start of the next iteration in the sequential polymer growth (Scheme VII.6).[16] This solid-supported synthesis of sequence defined oligomers represents the second application where the thiolactone chemistry eliminates the need for any protecting groups, in contrast to alternative systems such as the established protocols for peptide synthesis.[39]

Two essentially different procedures were developed in our research group, introducing the desired functionality via either the aminolysis or the hydrothiolation of the amine-thiol-ene conjugation. In the former case (Scheme VII.6, left), an AB′-type monomer (**138**) is used as a chain extender, which implies that the generated thiol must be isolated from the amine to prevent an uncontrolled polyaddition (*vide supra*).[40] Consequently, this first step is hampered by the formation of disulfides, of which the formation is promoted

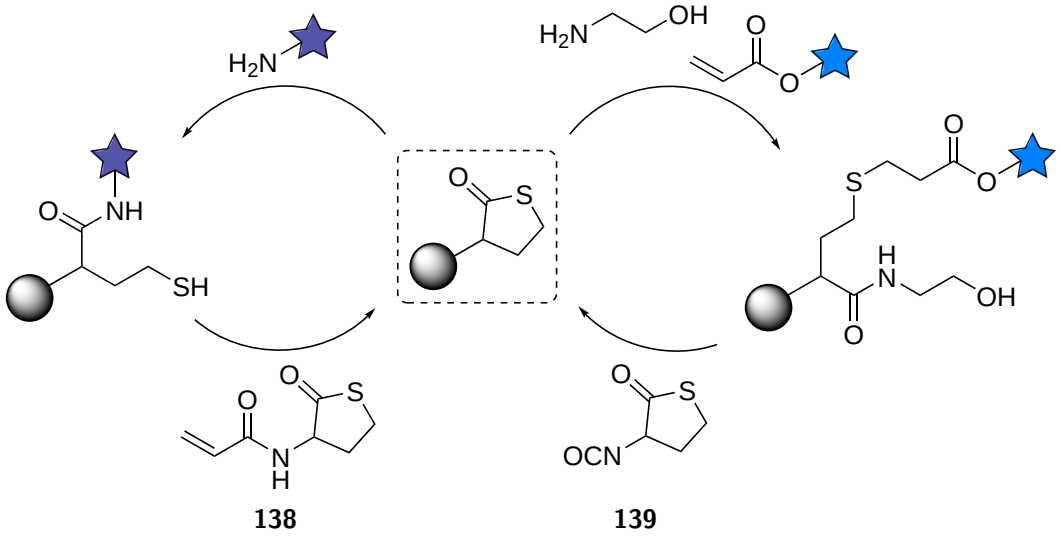

Scheme VII.6: Concept of the synthesis of sequence-defined oligomers via thiolactone chemistry. The two-step iterative protocol includes the introduction of a functionality in the backbone using a functional amine (left)[40] or a functional acrylate (right),[41] followed by a chain extension to recover the thiolactone chain end.

by the absence of a thiol-complementary reaction partner and the alkaline medium.[26,42] Moreover, because the aminolysis is the rate determining step in the overall thiolactone strategy, a variation in the functionality of the amine will also result in a variation of the reaction kinetics. Therefore, Martens *et al.* developed an alternative protocol that uses an invariable alkanolamine to obtain reproducible kinetics, whereas the functionality is introduced via different acrylates (Scheme VII.6, right).[41] Since this protocol allows an amine-thiol-ene conjugation in a one-pot fashion, no issues were encountered with disulfide formation, while the thiolactone chain end is readily recovered by reacting the alcohol, introduced via the amine, with an isocyanate-functional thiolactone (**139**).

The final example of TLa chemistry in polymer science that will be discussed in this section uses thiolactone moieties for post polymerisation modifications. In fact, because each of these units chemically binds both the amine and the thiol-complementary reaction partner, thiolactones allow a double modification or a simultaneous functionalisation and cross-linking when they are introduced as side-chains in a polymer.[16] To this end, Du Prez and co-workers prepared various polymers via a random co-polymerisation of an acrylic (**138**) or a styrenic (**140**) TLa-containing monomer with *N*-isopropylacrylamide or styrene, respectively (Scheme VII.7).[43–45] Addition of an amine to these TLa-containing polymers yields a polythiol that is directly reacted with an acrylate[44,46] or a functional bromide[45] in a one-pot fashion. Alternatively, the polythiol can be isolated to perform thiol-X

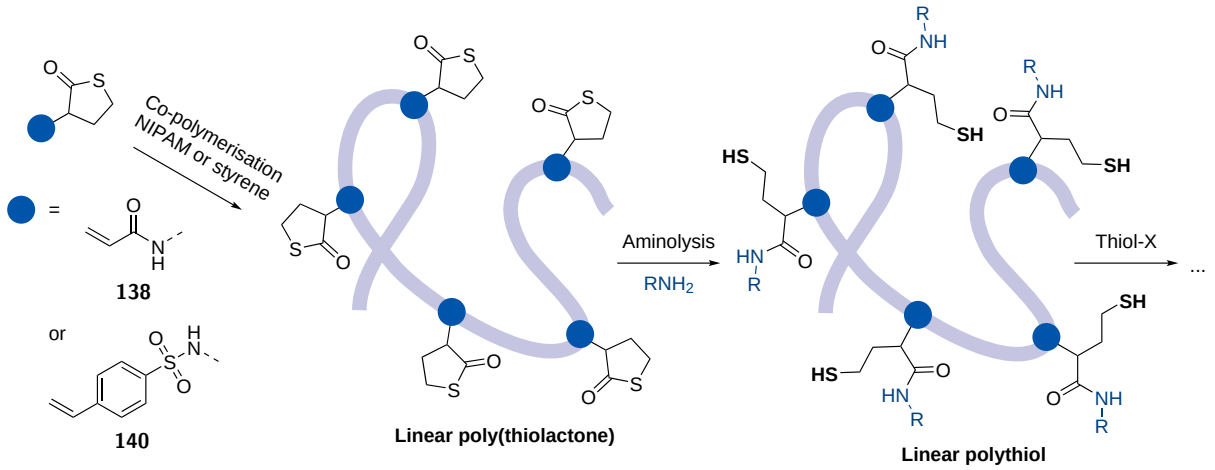

Scheme VII.7: Co-polymerisation of a TLa-containing monomer yields a linear poly(thiolactone) that allows a double post polymerisation modification. Aminolysis generates a polythiol that is either reacted directly with the complementary partner in a one-pot fashion, or purified prior to the thiol-X reaction. NIPAM = *N*-isopropylacrylamide.

reactions that are not compatible with the aminolysis process, such as a thiol-maleimide conjugation.[43]

VII.3.5 Conclusions for the theoretical introduction

Thiolactone-based chemistry is a very versatile strategy for the synthesis and modification of functionalised polymers. A thiolactone unit is essentially a protected thiol that can be released via a ring opening with an amine and subsequently react in one of the many thiol-X reactions, thereby circumventing the limited shelf-life of thiols. Moreover, when the desired thiol-X reaction is compatible with the aminolysis, both steps can be performed in a one-pot fashion where all the reagents are present from the start. For example, in the case of amine-thiol-ene conjugations, two (functional) residues can be introduced at the same time with an atom efficiency of 100 %.

It should be noted that the reactivity of thiolactones (or thiols) is to a certain extent complementary to the previously applied triazolinediones, while both chemistries also share some advantages. In fact, hydrothiolations are typically limited to mono- or disubstituted alkenes and Michael acceptors, of which the former react rather slowly with triazolinediones, while the latter typically show no affinity for TADs at all. Moreover, the amine-thiol-ene conjugation shows a high tolerance towards water, which proved to cause hydrolysis of triazolinediones. Nevertheless, depending on the exact reaction partners, both chemistries are very fast, while the kinetics can be further tailored by varying the amine or the unsaturated compound for the thiolactone or triazolinedione strategy, respectively.

VII.4 Application of thiolactone chemistry for interfacial polymerisations

As outlined in section VII.2, the application of triazolinediones in a liquid-liquid biphasic system is hampered by a competitive hydrolysis next to the desired polymerisation process. In contrast, both the aminolysis and the subsequent hydrothiolation of the two-step thiolactone strategy show a high tolerance towards water. Moreover, because the thiol-ene addition requires a simple α-olefin or an acrylate rather than a 'fatty' trivalent alkene or conjugated diene (section VII.3), no major issues are expected when the TLa-

complementary reagents must be dissolved in an aqueous phase. Therefore, the focus of this section has been to apply this TAD-complementary ligation method for the synthesis of polymeric particles via an interfacial polymerisation.

To avoid the need for an additional radical initiator or UV irradiation, the nucleophilic amine-thiol-ene conjugation was selected for the development of a TLa-based interfacial system. In fact, the presence of an amine can be considered as a chemical trigger for the spontaneous addition of the thiol to an acrylate, since these thiols are generated *in situ* via the aminolysis of the thiolactone units. Consequently, a discrete phase containing a mixture of a multivalent thiolactone and an acrylic cross-linker will not react until an amine reaches the liquid-liquid interface. Therefore, two distinct strategies will be discussed: firstly, an aqueous solution of a multivalent thiolactone and an acrylic cross-linker is dispersed in an organic solvent to obtain a water-in-oil emulsion. Secondly, the polarity of the poly(thiolactone) is decreased, resulting in an oil-in-water emulsion instead. This research was conducted in collaboration with Jiaojun Tan, a visiting PhD candidate under the supervision of Prof. Qiuyu Zhang (Northwestern Polytechnical University, Xi'an, China).

VII.4.1 Water-in-oil emulsions

The first strategy for the application of thiolactone chemistry in a biphasic system required the synthesis of a water-soluble multivalent thiolactone, which can be applied for water-in-oil emulsions. To this end, the commercially available D,L-homocysteine thiolactone hydrochloride was transformed to an acrylamide monomer (TLaAm, **138**) and subsequently polymerised with *N*,*N*-dimethylacrylamide (DMA, Scheme VII.8).[47] As the water-soluble cross-linker, a commercially available poly(ethylene glycol) (PEG) diacrylate was selected.

Once the polymer was obtained, an initial model experiment was performed to demonstrate

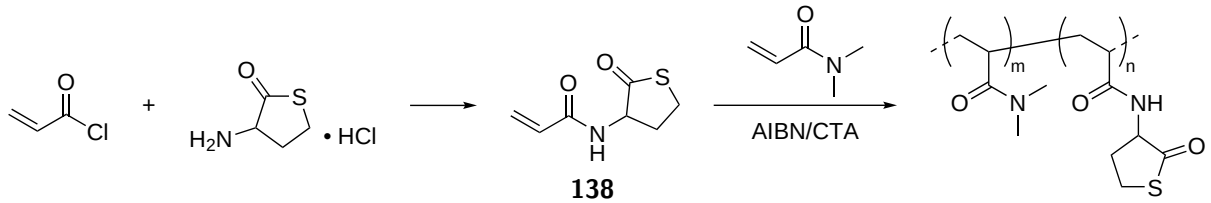

Scheme VII.8: Synthesis of a water-soluble poly(thiolactone) ($M_n = 12 \times 10^3\,g\,mol^{-1}$ and $Đ = 1.19$ (SEC)) from the commercially available D,L-homocysteine thiolactone hydrochloride. CTA = chain transfer agent.

the compatibility of the thiolactone-based cross-linking with an aqueous environment. Indeed, mixing the poly(thiolactone) with the PEG diacrylate (M_n = 700 g mol^{-1}) in distilled water yielded a clear and stable solution. However, as soon as an amine is added, the curing is triggered because of the aminolysis of thiolactone units, which generates thiols that quickly react with the cross-linker. Moreover, because the aminolysis is the rate determining step in the overall curing mechanism, the gelation kinetics should be tunable by varying the nature of the amine (section VII.3.1).

Addition of pyrrolidine was found to result almost instantaneously in a cross-linked gel, whereas the reaction mixture remained liquid for over one hour when 3-aminopropanol was used, finally yielding a very weak network (Table VII.1). Although both the kinetics and the mechanical stability could be improved by using an aliphatic diamine, which introduces extra cross-links in the material, the gelation times remained rather long. Therefore, pyrrolidine was selected as the most suitable reagent for the following interfacial polymerisations. Finally, the reactivity of the amines in water was expected to be pH-dependent. Nevertheless, because no significant changes in gelation time were observed when the experiments were repeated in an aqueous buffer (*i.e.* pH 7 or 10), distilled water was used for all further experiments.

Table VII.1: Qualitative gelation times of a mixture of poly(DMA-*co*-TLaAm) and PEG diacrylate to which different amines are added. [a]A very weak gel is obtained.

Amine	Time
Pyrrolidine	<10 s
1,4-Butanediamine	55 min
1,6-Hexanediamine	55 min
3-Aminopropanol	>1 h[a]

Next, an aqueous solution of poly(thiolactone) and acrylic cross-linker (M_n = 250 g mol^{-1}) was dispersed in various organic solvents to determine the most suitable oil phase for this interfacial polymerisation. Because of its favourable hydrophilic-lipophilic balance (HLB) for water-in-oil emulsions, Span 80 was selected as oil-soluble surfactant.[48,49] From the range of tested organic solvents (section VII.7.2.2), toluene was found to produce the most stable emulsions and was consequently used for all further experiments (Figure VII.4a). However, as soon as pyrrolidine (**133**) was added to initiate the cross-linking, the droplets were destroyed and no polymeric particles could be obtained (Figure VII.4b).

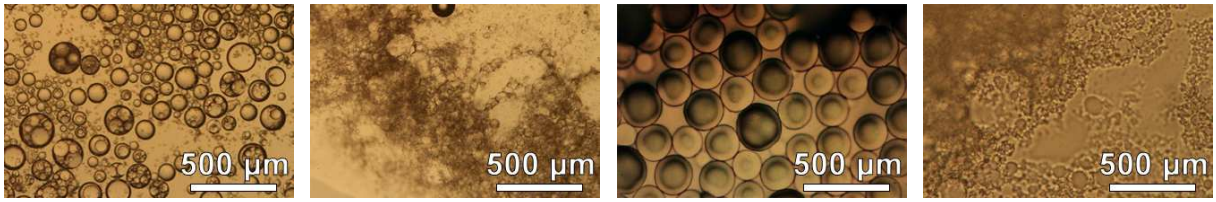

(a) **(b)** **(c)** **(d)**

Figure VII.4: Stable droplets could be formed by dispersing the aqueous phase in toluene, both **(a)** in an emulsion polymerisation or **(c)** a microfluidic setup. **(b, d)** The droplets were destroyed rather than solidified upon addition of pyrrolidine.

Multiple experimental parameters were varied in an attempt to solidify the dispersed droplets prior to the destruction of the emulsion. Firstly, the amount of pyrrolidine was decreased from the initial 5 %, relative to the oil phase, down to 1 %. However, in each case, the emulsion was destroyed in less than 10 minutes and no polymeric particles could be obtained. Secondly, the fraction of TLaAm (**138**, Scheme VII.8) in the copolymer was varied from 10 wt% to 50 wt% to accelerate the gelation process. Nevertheless, the content of this hydrophobic monomer mainly impacted the solubility of the polymer, *i.e.* the TLa-content should be limited to 30 wt% for the production of stable emulsions, while no particles could be isolated. Finally, the surfactant concentration was increased up to 10 % albeit with similar results.

Because of the unsuccessful interfacial polymerisation via a classical emulsion polymerisation approach, a simple T-junction microfluidic setup was applied instead. In this setup, homogeneous droplets are produced by pumping the discrete phase in a flow of the continuous phase, after which they are collected in a stirred solution of pyrrolidine in toluene, thereby triggering the cross-linking (Figure VII.5).[50] The main advantage of this microfluidics approach is that the amine can also be added from the start, *i.e.* to the syringe containing the continuous phase. Therefore, the polymerisation will already start while the droplets are spatially separated, which should prevent the previously encountered coagulation. Nevertheless, while this approach indeed allows the formation of homogeneous droplets (Figure VII.4c), their solidification remained an issue. Independent from the presence of pyrrolidine in the continuous phase, the droplets coagulated as soon as they were collected (Figure VII.4d).

In a final effort to produce particles from the water-soluble poly(thiolactone), priamine (**141**) was selected as a more hydrophobic alternative for pyrrolidine. Using this fatty

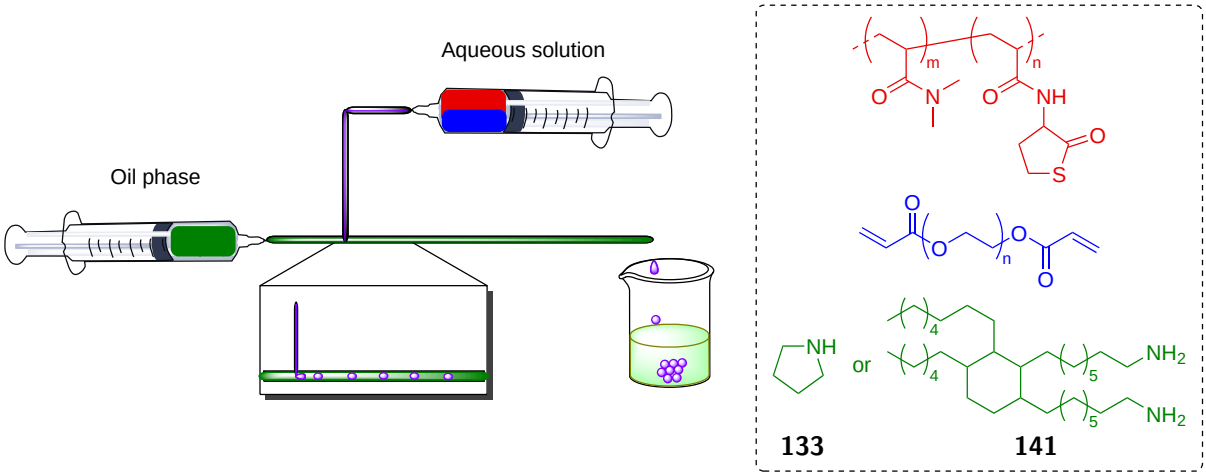

Figure VII.5: Schematic overview of the microfluidic setup. The discrete phase, *i.e.* an aqueous solution of TLa-containing polymer and PEG diacrylate, is pumped in a flow of the continuous phase (5 % Span 80 in toluene) to produce spatially separated droplets. The amine that triggers the cross-linking can be present either in the continuous phase or the collection vessel.

diamine, droplets were obtained that could be solidified, although long reaction times were necessary. Nevertheless, even after stirring for two days, the solidified particles remained very soft and formed an aggregated gel as soon as they they were collected.

In conclusion, the cross-linking of TLa-containing polymer via an amine-thiol-ene conjugation was shown to be compatible with an aqueous environment, while the reactivity of the amine was reflected in the gelation time. However, this reaction was troubled by multiple problems when the aqueous solution is dispersed in an organic phase. Firstly, the most reactive amine for the thiolactone ring-opening, *i.e.* pyrrolidine, destabilised the emulsions and prevented the production of polymeric particles. This problem could not be solved by varying the amine concentration, the TLaAm content in the water-soluble polymer, the amount of surfactant or by using a microfluidic device rather than a classical emulsion polymerisation approach. Secondly, while an alternative amine, *i.e.* the hydrophobic priamine, allowed the production of stable emulsions, the obtained particles remained soft and sticky, even after a reaction time of up to two days. Finally, because of the organic backbone and the hydrophobic co-monomer, the water-soluble polyacrylamide will also be (partially) soluble in the continuous phase, which is assumed to impact the stability of the produced droplets as well. Therefore, we decided to not further pursue the synthesis of polymeric particles via a water-in-oil emulsion in this doctoral work.

VII.4.2 Oil-in-water emulsions

For the alternative strategy to the problematic water-in-oil emulsions described above, an oil-soluble multivalent thiolactone was synthesised. First, 4-vinylbenzenesulfonic acid was transformed into the corresponding sulfonyl chloride, which was subsequently reacted with D,L-homocysteine thiolactone hydrochloride to generate a styrenic TLa-containing monomer (TLaSt, **140**, Scheme VII.9).[43,51] This monomer was then co-polymerised with styrene to obtain a suitable polymer for oil-in-water emulsions.

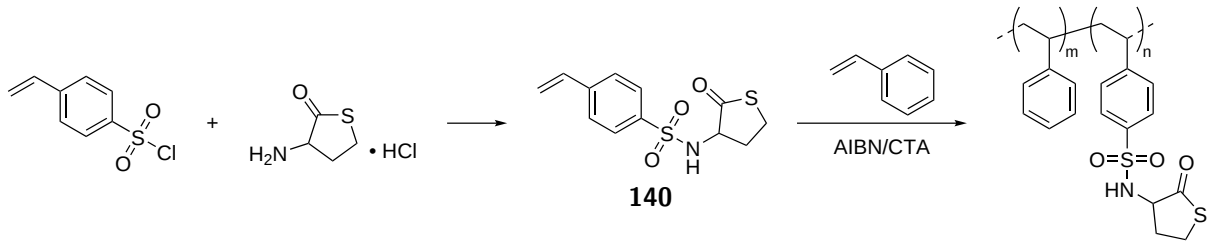

140

Scheme VII.9: Synthesis of an oil-soluble poly(thiolactone) ($M_n = 17.3 \times 10^3\,g\,mol^{-1}$ and $Đ = 1.28$ (SEC)) from the commercially available D,L-homocysteine thiolactone hydrochloride. CTA = chain transfer agent.

The synthesised polymer proved to be well soluble in chloroform, which is also a suitable discrete phase for interfacial polymerisations. Moreover, this polystyrene was insoluble in the continuous phase, *i.e.* water, in contrast to the polyacrylamide described above. Similarly to the previously discussed model experiment, a network is obtained in less than 10 seconds after the addition of pyrrolidine when the commercially available trimethylolpropane triacrylate is used as a chloroform-soluble cross-linker. Next, this curable mixture was dispersed in an aqueous solution of poly(vinyl alcohol) (PVA), a commonly applied non-ionic surfactant for oil-in-water emulsions.[49,52] In contrast to the water-in-oil emulsions, stable droplets could be produced that successfully solidified upon addition of pyrrolidine (Figures VII.6a and VII.6b, respectively).

Finally, by swapping the discrete and continuous phases in the microfluidic setup as depicted in Figure VII.5, droplets with a size in the order of 200 µm were produced that could also be solidified when pyrrolidine is added to the aqueous surfactant solution (Figures VII.6c and VII.6d, respectively). Unfortunately, a thorough study of the droplet size as a function of the experimental parameters, as well as an in-depth characterisation of the produced polymeric particles, could not be completed within the time-frame of this

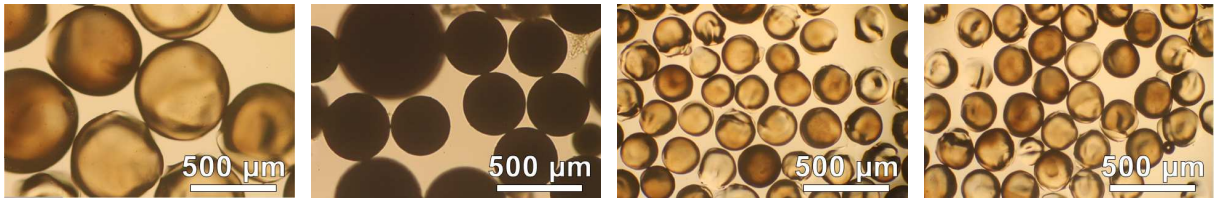

(a) **(b)** **(c)** **(d)**

Figure VII.6: Stable droplets could be formed by dispersing the chloroform solution of poly(styrene-*co*-TLaSt) and trivalent acrylate in water, both **(a)** in an emulsion polymerisation or **(c)** a microfluidic setup. **(b, d)** The droplets were solidified to produce polymeric particles upon addition of pyrrolidine.

doctoral work. This ongoing research project will thus be finished by our collaboration partner at the Northwestern Polytechnical University of Xi'an, China.

VII.5 Conclusions and perspectives

Just like many other versatile, fast and efficient 'click-like' ligation methods, the applicability of triazolinedione chemistry is not without limits. While water can be used as a solvent for certain fast TAD-based reactions, hydrolysis becomes a major problem when triazolinediones are used in a liquid-liquid biphasic system. Therefore, this chapter introduced thiolactones as an alternative for TAD chemistry that should not be hampered by this issue.

The commonly applied one-pot thiolactone strategy includes two distinct steps, *i.e.* the aminolysis of the cyclic thio-ester and the subsequent hydrothiolation with the generated thiol. For this thiol-ene addition, monosubstituted alkenes or electron-deficient acrylates are typically preferred, which are inferior substrates for the electron-poor triazolinediones. Moreover, both steps in the overall amine-thiol-ene conjugation show a high tolerance towards water. Consequently, the thiolactone chemistry can be considered as a complementary ligation method for the TAD-based reactions.

Next, a water-soluble poly(thiolactone) was synthesised and cross-linked in an aqueous environment by the subsequent addition of a PEG diacrylate cross-linker and pyrrolidine as amine. Despite the very fast gelation kinetics and the compatibility of this nucleophilic amine-thiol-ene reaction with water, problems occurred when this reaction was performed in a biphasic system. Although multiple experimental parameters were varied, the presence

of pyrrolidine in the oil phase consistently destabilised the emulsions and thus prevented the production of polymeric particles. Moreover, when the hydrophobic priamine was used as an alternative amine, the gelation kinetics become too slow for practical applications, while the obtained particles remain soft and sticky and could not be isolated.

Finally, a TLa-functional polystyrene was synthesised that is soluble in chloroform. Consequently, the discrete and the continuous phases were swapped, resulting in an oil-in-water approach with pyrrolidine in the aqueous phase. Using this strategy, solidified particles were successfully obtained via both an emulsion polymerisation and a microfluidic setup.

Future studies should include a thorough characterisation of the polymeric particles, as well as a further optimisation of the experimental parameters. For example, one of the advantages of a microfluidic setup is the ability to produce particles with a narrow yet tunable size distribution by varying the flow rates of the immiscible phases. Moreover, addition of a functional amine or acrylate to the continuous or the discrete phase, respectively, should allow the facile functionalisation of the synthesised particles. These functionalities can be either chemical or physical in nature, such as carboxylic acids for selective interactions or dyes for screening applications, as long as they are compatible with the thiolactone platform.

VII.6 Notes on the collaboration

Part of this chapter describes a collaboration with the group of Prof. Qiuyu Zhang (Northwestern Polytechnical University, Xi'an, China). The research was performed at Ghent University. Kevin De Bruycker and Jiaojun Tan, an exchange PhD student who was guided on a daily basis, conceived and designed the experiments. Small molecule synthesis and triazolinedione-related research was performed by Kevin De Bruycker. Synthesis of thiolactone-containing polymers as well as interfacial polymerisations were performed by Jiaojun Tan. The collaborators discussed and commented on the results at all stages.

VII.7 Experimental section

All materials, solvents and their corresponding purification are presented in appendix A.

VII.7.1 Synthesis

VII.7.1.1 Prenyl acrylate (131)

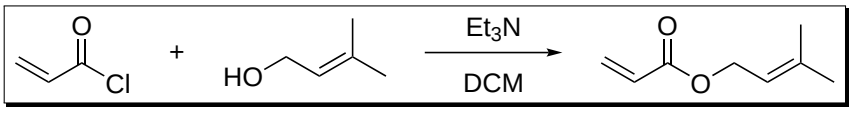

In a 1 L flask, a solution was prepared of 50.0 g prenol (580 mmol, 1 eq) and 70.5 g triethylamine (697 mmol, 1.2 eq) in 300 mL dichloromethane. This mixture was cooled in an ice-bath, after which a solution of 52 mL acryloyl chloride (639 mmol, 1.1 eq) in 100 mL dichloromethane was added drop-wise using an addition funnel. The reaction was stirred overnight under an inert atmosphere. Potassium carbonate was added until the solution was saturated, the salts were filtered and the solution was concentrated *in vacuo*. Finally, the crude product was further purified by a vacuum distillation: a spoonful of phenothiazine was added, followed by the collection of the fraction with a boiling point of 60 °C (10 mbar).

Yield: 66.1 g colourless liquid (471 mmol, 81 %).

Bruto formula: $C_8H_{12}O_2$.

MW.: 140.18 g/mol.

^{1}H-NMR (400 MHz, $CDCl_3$): δ (ppm) = 1.73 (s, 3 H, CH_3), 1.77 (s, 3 H, CH_3), 4.66 (d, 2 H, O−CH_2), 5.38 (m, 1 H, O−CH$_2$−CH), 5.81 (dd, 1 H, CH_2=CH), 6.13 (dd, 1 H, CH$_2$=CH), 6.41 (dd, 1 H, CH_2=CH).

VII.7.1.2 2-(1-Cyclohexenyl)ethylacrylamide (132)

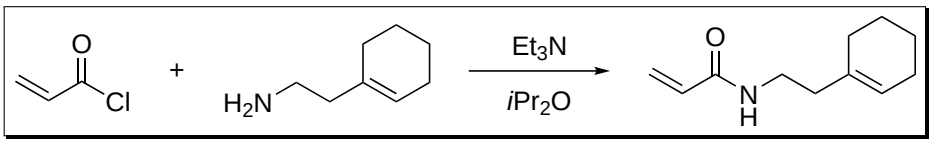

In a 1 L flask equipped with an addition funnel, a solution was prepared of 43.54 g 2-(1-cyclohexenyl)ethylamine (348 mmol, 1 eq) and 42.22 g triethylamine (417 mmol, 1.2 eq) in 200 mL isopropyl ether. This mixture was cooled in an ice-bath, after which a solution

of 34.61 g acryloyl chloride (382 mmol, 1.1 eq) in 200 mL isopropyl ether was added over a period of 25 min under vigorous stirring. The addition funnel was rinsed with 50 mL isopropyl ether. The reaction was stirred overnight under an inert atmosphere and filtered to remove the triethylammonium chloride precipitate. The filtrate was concentrated *in vacuo* and purified by column chromatography over silica gel (40 % ethyl acetate in petroleum ether).

Yield: 51.5 g white solid (287 mmol, 83 %).

Bruto formula: $C_{11}H_{17}NO$.

MW.: 179.26 g/mol.

LC-MS (m/z): 180.2 $[MH]^+$.

HRMS (m/z for $[MH]^+$): $[MH]^+$: calculated: 180.1383, found: 180.1385.

^{1}H-NMR (300 MHz, $CDCl_3$): δ (ppm) = 1.49–1.69 (band, 4 H, 2 × CH_2(Ch)), 1.88–1.97 (band, 2 H, CH=C−CH_2), 1.97–2.04 (band, 2 H, C=CH−CH_2), 2.17 (t, 2 H, NH−CH_2−CH_2), 3.41 (q, 2 H, N−CH_2), 5.48 (m, 1 H, C=CH), 5.62 (dd + br.s, 1 H, CH_2=CH + NH), 6.08 (dd, 1 H, CH_2=CH), 6.26 (dd, 1 H, CH_2=CH).

VII.7.1.3 Thiolactone acrylamide (TLaAm, 138)

The synthesis of TLaAm was synthesised using a literature procedure.[40] D,L-homocysteine thiolactone hydrochloride (7.0 g, 45.6 mmol, 1 eq) was dissolved in a mixture of 50 mL dioxane and 50 mL water. 19.1 g sodium bicarbonate (228 mmol, 5 eq) was added in portions and the mixture was stirred for 30 min at 0 °C. Next, 7.4 mL acryloyl chloride (91.1 mmol, 2 eq) was added drop-wise and the reaction was stirred overnight at room temperature under an inert atmosphere. Brine (100 mL) was added, followed by an extraction with ethyl acetate (3 × 200 mL. The combined organic phases were dried with $MgSO_4$ and the solvent was removed *in vacuo*. The crude product was purified by column chromatography over silica gel (dichloromethane to dichloromethane:acetone 95:5).

Yield: 6.3 g white solid (36.8 mmol, 81 %).

Bruto formula: $C_7H_9NO_2S$.

MW.: 171.21 g/mol.

LC-MS (m/z): 172.1 $[MH]^+$.

^{1}H-NMR (400 MHz, DMSO−d_6): δ (ppm) = 2.10 (m, 1 H, S−CH_2−CH_2), 2.46 (m, 1 H, S−CH_2−CH_2), 3.30 (m, 1 H, S−CH_2), 3.42 (m, 1 H, S−CH_2), 4.70 (m, 1 H, NH−CH), 5.66 (dd, 1 H, CH_2=CH), 6.13 (dd, 1 H, CH_2=CH), 6.23 (dd, 1 H, CH_2=CH), 8.45 (d, 1 H, NH).

VII.7.1.4 Poly[(*N*,*N*-dimethylacrylamide)-*co*-TLaAm]

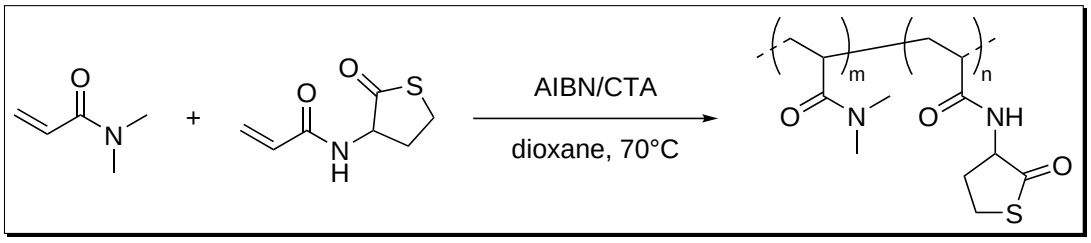

The statistical co-polymerisation of TLaAm with *N*,*N*-dimethylacrylamide (DMA) is based on a reported procedure.[47] For the preparation of a copolymer containing 20 wt% TLaAm (∼13 mol%), 2.00 g DMA (20.2 mmol), 0.500 g TLaAm (2.91 mmol), 22.0 mg 2-{[(butylsulfanyl)-carbonothioyl]sulfanyl}propanoic acid[44] as chain transfer agent (CTA, 0.092 mmol) and 1.5 mg α,α'-azoisobutyronitrile (AIBN, 0.009 mmol) were dissolved in 20 mL of dioxane ($[M]_0/[CTA]/[AIBN] = 250/1/0.1$). The solution was transferred into a Schlenk tube and degassed by 4–5 freeze-pump-thaw cycles. After that, the tube was immersed in a thermostatted oil bath set to 70 °C and the solution was stirred for 24 h. The polymerisation was stopped by immersing the Schlenk tube in an ice/water bath followed by exposure of the polymerisation solution to air. The final polymer was obtained by precipitation into diethyl ether. Different poly(DMA-*co*-TLaAm) copolymers containing various amounts of TLaAm can be synthesised by varying the initial DMA:TLaAm monomer ratio. The solubility of this polymer was approximately 40 wt% in water.

TLa equivalent: 1.17 mmol/g.

M_n (theoretical): 27 000 g/mol.

M_n (SEC): 12 000 g/mol.

$Đ$ (SEC): 1.19.

Conversion (SEC): 44 %.

VII.7.1.5 Styrenic thiolactone-containing monomer (TLaSt, 140)

TLaSt was synthesised via the following reported procedure.[43] An ice-cooled solution of D,L-homocysteine thiolactone hydrochloride (16.38 g, 106.7 mmol, 1 eq) in a 1:1 mixture of dioxane and H_2O (240 mL) was treated with sodium bicarbonate (44.8 g, 533.3 mmol, 5 eq). After 30 min, a solution of crude 4-vinylbenzenesulfonyl chloride[53] (25.9 g, 128 mmol, 1.2 eq) in 1,4-dioxane (20 mL) was added at 0 °C and the mixture was stirred overnight at room temperature. The reaction mixture was diluted with brine (500 mL) and extracted with ethyl acetate (3 × 1 L). The organic phase was dried ($MgSO_4$). The drying agent was filtered and the resulting clear solution was evaporated under reduced pressure. The residue was purified by flash column chromatography on silica gel (dichloromethane:acetone 98:2 to 95:5) to provide the title compound.

Yield: 25.3 g white solid (89.2 mmol, 83 %).

Bruto formula: $C_{12}H_{13}NO_3S_2$.

MW.: 283.36 g/mol.

LC-MS (m/z): 282.0 $[M-H]^-$.

^{1}H-NMR (300 MHz, DMSO−d_6): δ (ppm) = 1.83 (m, 1 H, S−CH_2−CH_2), 2.20 (m, 1 H, S−CH_2−CH_2), 3.25 (m, 2 H, S−CH_2), 4.27 (m, 1 H, NH−CH), 5.44 (d, 1 H, CH=CH_2), 6.01 (d, 1 H, CH=CH_2), 6.82 (dd, 1 H, Ar−CH), 7.66 (d, 2 H, ArH), 7.79 (d, 2 H, ArH), 8.25 (d, 1 H, NH).

VII.7.1.6 Poly(styrene-*co*-TLaSt)

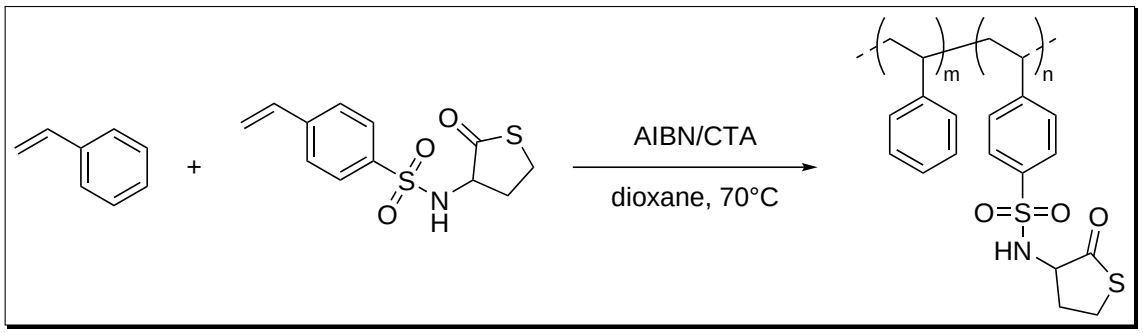

The statistical co-polymerisation of TLaSt with styrene is based on a reported procedure.[43] For the preparation of a copolymer containing 20 wt% TLaSt (∼8 mol%), 2.00 g styrene (19.2 mmol), 0.500 g TLaSt (1.76 mmol), 38.2 mg *S*-1-dodecyl-*S*′-(α,α′-dimethyl-α′′-acetic acid)trithiocarbonate[51] (DDMAT) as chain transfer agent (CTA, 0.105 mmol) and 1.7 mg α,α′-azoisobutyronitrile (AIBN, 0.010 mmol) were dissolved in 20 mL of dioxane ($[M]_0/[CTA]/[AIBN] = 200/1/0.1$). The solution was transferred into a Schlenk tube and degassed by three freeze-pump-thaw cycles. After that, the tube was immersed in a thermostatted oil bath set to 70 °C and the solution was stirred for 24 h. The polymerisation was stopped by immersing the Schlenk tube in an ice/water bath followed by exposure of the polymerisation solution to air. The final polymer was obtained by precipitation in a 10-fold excess of cold methanol. The solubility of this poly(styrene-*co*-TLaSt) was approximately 30 wt% in chloroform.

TLa equivalent: 0.706 mmol/g.

M_n (theoretical): 24 000 g/mol.

M_n (SEC): 17 300 g/mol.

$Đ$ (SEC): 1.28.

Conversion (SEC): 72 %.

VII.7.2 Methods

VII.7.2.1 Qualitative cross-linking experiments

The poly(thiolactone) (1 eq of TLa units) and cross-linker (1 eq of acrylate functions) were mixed in an appropriate solvent, *i.e.* either water (polyTLa:water = 1:3 by mass) or chloroform (polyTLa:chloroform = 3:7 by mass) for the water- or oil soluble polymer, respectively. Then, the amine was weighed and added, which starts the thiolatone aminolysis and thus the cross-linking. The gelation time was defined as the time after which the stirring stopped as a result of the viscosity increase.

For example, poly(DMA-*co*-TLaAm) (250 mg, 0.293 mmol TLa moieties, 1 eq) was mixed with 102 mg PEG diacrylate (M_n = 700 g mol^{-1}, 0.146 mmol, 0.5 eq) in 750 mg water to form a clear solution. 15.5 mg 1,4-diaminobutane (0.176 mmol, 0.6 eq) was added. Gelation occurred, *i.e.* the magnetic stirring stopped, after 55 minutes.

VII.7.2.2 Interfacial polymerisations

For the emulsion polymerisations, poly(DMA-*co*-TLaAm) or poly(styrene-*co*-TLaSt) was first dissolved in water (37 wt%) or chloroform (30 wt%), respectively. To this solution, the multivalent acrylate, *i.e.* PEG diacrylate (M_n = 250 g mol^{-1}) resp. trimethylolpropane triacrylate, was added to obtain an equivalent amount of acrylate groups, relative to the TLa units. The continuous phase, containing either 5 wt% Span 80 (oil-soluble) or 2 wt% poly(vinyl alcohol) (water-soluble) as surfactant, was weighed and added to the discrete phase. The mass ratio of the discrete and the continuous phase was approximately 1:10 for every experiment. After stirring the heterogeneous mixture for 10 min to create droplets, the amine was added to solidify the droplets overnight.

For the preparation of particles via microfluidics, a T-junction setup was used as depicted in Figure VII.5. For the discrete and continuous phases, the same solutions were prepared as described above. The amine (5 wt%) was added either to both the continuous phase and the collection vessel, or only to the collection vessel. Pumping rates of the continuous and discrete phases could be varied from 0.025–0.6 mL min^{-1} and 0.06–0.9 mL h^{-1}, respectively.

For example, 1.0 g poly(DMA-*co*-TLaAm) (1.17 mmol TLa units, 1 eq) was dissolved in 1.7 g water (37 wt%), to which 146 mg PEG diacrylate (1.17 mmol acrylate groups, 1 eq)

was added. This aqueous phase was dispersed in 28 g of a 5 wt% solution of Span 80 in toluene, after which 1.4 g pyrrolidine (5 wt%, relative to the oil phase) was added.

In the case of water-in-oil emulsions, various organic solvents were tested as potential oil phases, *i.e.* butyl acetate, cyclohexane, ethyl acetate, light mineral oil, silicon oil and toluene. Silicon oil proved to be incompatible with Span 80, while toluene was found to produce the most stable emulsions. No significant difference in stability of the emulsions was observed when 5 wt% of Hypermer B246 was used as an alternative oil-soluble surfactant with a similar hydrophilic-lipophilic balance (HLB).[48]

Addition of 5 wt% of pyrrolidine, as described above, was found to destabilise the water-in-oil emulsion. Therefore, the experiment was repeated with a lower amount of pyrrolidine (2 wt% and 1 wt%), with copolymers containing 10 %, 20 %, 30 %, 40 % and 50 % TLaAm (by weight) and with an increased concentration of Span 80 (10 %). None of these individual changes in experimental parameters nor combinations thereof yielded polymeric particles via a water-in-oil emulsion.

VII.7.3 Instrumentation

Liquid chromatography - mass spectrometry (LC-MS) LC-MS analyses were performed on an Agilent Technologies 1100 series LC/MSD system with a diode array detector (DAD) and a single quad MS. Analytical reversed phase HPLC-analyses were performed with a Phenomex Luna C18 (2) column (5 µm, 250 mm × 4.6 mm) and a solvent gradient (0 % to 100 % acetonitrile in H_2O in 15 min). The eluted compounds were analysed via UV detection (214 nm).

Nuclear magnetic resonance (NMR) NMR spectra were recorded on a Bruker Avance 300 (300 MHz) or a Bruker Avance 400 (400 MHz) FT-NMR spectrometer in the indicated solvent at room temperature. Chemical shifts are presented in parts per million (δ) with the residual solvent peak as an internal standard. The resonance multiplicities are described as [br. (broad)] s (singlet), d (doublet), t (triplet), q (quadruplet), quint (quintuplet), sext (sextuplet) or m (multiplet). The obtained spectra were analysed with the ACD/NMR Processor Academic Edition of ACD/Labs.

Size exclusion chromatography (SEC) SEC was performed using a Varian PL-GPC 50 Plus instrument, using a refractive index detector, equipped with two PL-gel 5 µm MIXED-D columns 40 °C. Polystyrene standards were used for calibration and THF as eluent at a flow rate of 1 mL min^{-1}. Samples were injected using a PL AS RT autosampler.

VII.8 Bibliography

1. M. T. Gokmen, F. E. Du Prez, *Prog. Polym. Sci.* **2012**, *37*, 365–405.
2. S. Billiet, K. De Bruycker, F. Driessen, H. Goossens, V. Van Speybroeck, J. M. Winne, F. E. Du Prez, *Nat. Chem.* **2014**, *6*, 815–821.
3. Q.-Y. Hu, M. Allan, R. Adamo, D. Quinn, H. Zhai, G. Wu, K. Clark, J. Zhou, S. Ortiz, B. Wang, E. Danieli, S. Crotti, M. Tontini, G. Brogioni, F. Berti, *Chem. Sci.* **2013**, *4*, 3827–3832.
4. H. Ban, M. Nagano, J. Gavrilyuk, W. Hakamata, T. Inokuma, C. F. Barbas, *Bioconjugate Chem.* **2013**, *24*, 520–532.
5. K. De Bruycker, S. Billiet, H. A. Houck, S. Chattopadhyay, J. M. Winne, F. E. Du Prez, *Chem. Rev.* **2016**, *116*, 3919–3974.
6. O. Acevedo, M. E. Squillacote, *J. Org. Chem.* **2008**, *73*, 912–922.
7. Z. Syrgiannis, F. Koutsianopoulos, K. W. Muir, Y. Elemes, *Tetrahedron Lett.* **2009**, *50*, 277–280.
8. S. Chattopadhyay, F. Du Prez, *Eur. Polym. J.* **2016**, *81*, 77–85.
9. V. R. C. Schulz, M. Marx, H. Hartmann, *Makromol. Chem.* **1961**, *44*, 281–289.
10. G. Butler, *Cyclopolymerization and Cyclocopolymerization*, Taylor and Francis, **1992**, p. 560.
11. C. E. Hoyle, T. Y. Lee, T. Roper, *J. Polym. Sci. Part A: Polym. Chem.* **2004**, *42*, 5301–5338.
12. C. E. Hoyle, A. B. Lowe, C. N. Bowman, *Chem. Soc. Rev.* **2010**, *39*, 1355–1387.
13. L.-T. T. Nguyen, M. T. Gokmen, F. E. Du Prez, *Polym. Chem.* **2013**, *4*, 5527–5536.
14. T. M. Roper, C. A. Guymon, E. S. Jönsson, C. E. Hoyle, *J. Polym. Sci. Part A: Polym. Chem.* **2004**, *42*, 6283–6298.
15. C. Hoyle, C. Bowman, *Angew. Chem. Int. Ed.* **2010**, *49*, 1540–1573.
16. P. Espeel, F. E. Du Prez, *Eur. Polym. J.* **2015**, *62*, 247–272.
17. P. Espeel, F. Goethals, F. E. Du Prez, *J. Am. Chem. Soc.* **2011**, *133*, 1678–1681.
18. Z. Paryzek, I. Skiera, *Org. Prep. Proced. Int.* **2007**, *39*, 203–296.
19. C. M. Stevens, D. S. Tarbell, *J. Org. Chem.* **1954**, *19*, 1996–2003.
20. R. Benesch, R. E. Benesch, *J. Am. Chem. Soc.* **1956**, *78*, 1597–1599.
21. A. B. Lowe, *Polym. Chem.* **2010**, *1*, 17–36.
22. D. P. Nair, M. Podgórski, S. Chatani, T. Gong, W. Xi, C. R. Fenoli, C. N. Bowman, *Chem. Mater.* **2014**, *26*, 724–744.

23. P. Espeel, F. E. Du Prez, *Macromolecules* **2015**, *48*, 2–14.

24. F. Goethals, *Ph.D. Thesis*, Ghent University, **2015**.

25. C. Resetco, *Ph.D. Thesis*, Ghent University, **2017**.

26. P. Espeel, F. Goethals, F. Driessen, L.-T. T. Nguyen, F. E. Du Prez, *Polym. Chem.* **2013**, *4*, 2449–2456.

27. N. ten Brummelhuis, C. Diehl, H. Schlaad, *Macromolecules* **2008**, *41*, 9946–9947.

28. N. B. Cramer, J. P. Scott, C. N. Bowman, *Macromolecules* **2002**, *35*, 5361–5365.

29. N. B. Cramer, S. K. Reddy, M. Cole, C. Hoyle, C. N. Bowman, *J. Polym. Sci. Part A: Polym. Chem.* **2004**, *42*, 5817–5826.

30. C. Boeckler, B. Frisch, S. Muller, F. Schuber, *Journal of Immunological Methods* **1996**, *191*, 1–10.

31. K. L. Holmes, L. M. Lantz in *Chapter 9 Protein labeling with fluorescent probes*, *Vol. 63*, Academic Press, **2001**, pp. 185–204.

32. G. Mantovani, F. Lecolley, L. Tao, D. M. Haddleton, J. Clerx, J. J. L. M. Cornelissen, K. Velonia, *J. Am. Chem. Soc.* **2005**, *127*, 2966–2973.

33. M. A. Azagarsamy, K. S. Anseth, *ACS Macro Lett.* **2013**, *2*, 5–9.

34. J. W. Chan, C. E. Hoyle, A. B. Lowe, M. Bowman, *Macromolecules* **2010**, *43*, 6381–6388.

35. B. D. Mather, K. Viswanathan, K. M. Miller, T. E. Long, *Prog. Polym. Sci.* **2006**, *31*, 487–531.

36. D. Wu, Y. Liu, C. He, T. Chung, S. Goh, *Macromolecules* **2004**, *37*, 6763–6770.

37. G.-Z. Li, R. K. Randev, A. H. Soeriyadi, G. Rees, C. Boyer, Z. Tong, T. P. Davis, C. R. Becer, D. M. Haddleton, *Polym. Chem.* **2010**, *1*, 1196–1204.

38. F. Goethals, S. Martens, P. Espeel, O. van den Berg, F. E. Du Prez, *Macromolecules* **2014**, *47*, 61–69.

39. G. B. Fields, R. L. Noble, *Int. J. Pept. Protein Res.* **1990**, *35*, 161–214.

40. P. Espeel, L. L. G. Carrette, K. Bury, S. Capenberghs, J. C. Martins, F. E. Du Prez, A. Madder, *Angew. Chem. Int. Ed.* **2013**, *52*, 13261–13264.

41. S. Martens, J. Van den Begin, A. Madder, F. E. Du Prez, P. Espeel, *J. Am. Chem. Soc.* **2016**, *138*, 14182–14185.

42. J. Garel, D. S. Tawfik, *Chem. - Eur. J.* **2006**, *12*, 4144–4152.

43. P. Espeel, F. Goethals, M. M. Stamenovic, L. Petton, F. E. Du Prez, *Polym. Chem.* **2012**, *3*, 1007–1015.

44. S. Reinicke, P. Espeel, M. M. Stamenović, F. E. Du Prez, *ACS Macro Lett.* **2013**, *2*, 539–543.

45. Y. Chen, P. Espeel, S. Reinicke, F. E. Du Prez, M. H. Stenzel, *Macromol. Rapid Commun.* **2014**, *35*, 1128–1134.

46. S. Reinicke, P. Espeel, M. M. Stamenovic, F. E. Du Prez, *Polym. Chem.* **2014**, *5*, 5461–5470.

47. S. Belbekhouche, S. Reinicke, P. Espeel, F. E. Du Prez, P. Eloy, C. Dupont-Gillain, A. M. Jonas, S. Demoustier-Champagne, K. Glinel, *ACS Appl. Mater. Interfaces* **2014**, *6*, 22457–22466.

48. W. C. Griffin, *J. Soc. Cosmet. Chem.* **1949**, *1*, 311–326.

49. L. L. Schramm, *Emulsions, Foams, and Suspensions: Fundamentals and Applications*, Wiley-VCH, **2006**.

50. J. Tan, C. Li, H. Li, H. Zhang, J. Gu, B. Zhang, H. Zhang, Q. Zhang, *Polym. Chem.* **2015**, *6*, 4366–4373.

51. J. Skey, R. K. O'Reilly, *Chem. Commun.* **2008**, 4183–4185.

52. Q. Xu, A. Crossley, J. Czernuszka, *J. Pharm. Sci.* **2009**, *98*, 2377–2389.

53. T. Ishizone, J. Tsuchiya, A. Hirao, S. Nakahama, *Macromolecules* **1992**, *25*, 4840–4847.

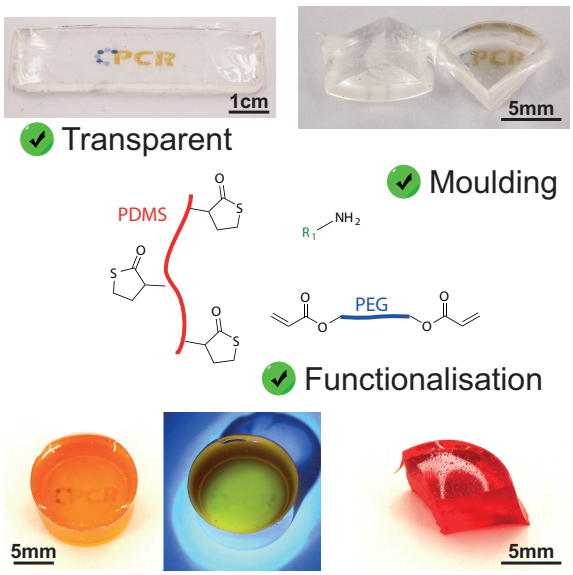

Abstract

A series of amphiphilic co-networks (ACNs) was prepared via thiolactone chemistry by cross-linking a multivalent thiolactone-functional poly(dimethylsiloxane) building block with poly(ethylene glycol) diacrylates. Formation of the networks was triggered by the addition of an amine. The nucleophilicity and steric bulk of this amine controls the curing kinetics. Furthermore, some of the cross-links can be sacrificed to introduce a fluorescent group or dye via a thia-Michael addition, without affecting the bulk mechanical properties and swelling capabilities. These ACNs exhibit a unique set of properties because of their nanophase separation, resulting in hydrophilic PEG and hydrophobic PDMS phases. Hence, swelling in both water and organic solvents was observed, of which the extent can be tuned by varying the overall PEG content.

Chapter VIII

Polydimethylsiloxane-based amphiphilic co-networks

VIII.1 Introduction

When cross-linked polymers are submerged in a good solvent, *i.e.* when there is a strong favourable thermodynamic interaction between solvent and polymer, they are known to absorb large amounts of solvents, which leads to the expansion of the network. Moreover, this swelling behaviour can be altered by incorporating two or more polymers with an affinity for different solvents into a segmented network. In this class, amphiphilic co-networks (ACNs) play an important role, since they have the contradicting ability to swell in both apolar organic solvents and water.[1]

An amphiphilic co-network consists of both a hydrophobic and a hydrophilic polymer, such as poly(dimethylsiloxane) ('silicone', PDMS) and poly(ethylene glycol) (PEG), respectively, while the macrophase separation that would usually occur is prevented by covalent bonds between these incompatible polymers. However, on a microscopic level, this is not the case. In fact, a phase-separated morphology with small hydrophobic and hydrophilic domains is formed,[2] which was studied by a wide variety of techniques such as atomic force microscopy (AFM),[2–5] X-ray photoelectron spectroscopy (XPS),[5] attenuated total reflectance infrared spectroscopy (ATR-FTIR),[5] small-angle X-ray scattering (SAXS)[2] and transmission electron microscopy (TEM).[2] In an aqueous environment, the hydrophilic domains will swell while the hydrophobic ones collapse. When the ACN is transferred

to an organic solvent, a morphology isomerisation occurs, *i.e.* the previously swollen hydrophilic domains will collapse while the hydrophobic ones expand.[1] Therefore, the term 'chameleon' networks was introduced by Kennedy *et al.* to describe their ability to change morphology according to the medium.[6] This phase-separated nanostructure of ACNs also results in the presence of two glass transition temperatures (T_gs) when they are analysed via differential scanning calorimetry (DSC)[1,5,7] or dynamic mechanical thermal analysis (DMTA),[8] originating from the constituting homopolymers.

One of the most important applications of amphiphilic co-networks is their use in extended-wear contact lenses. In this context, a good oxygen permeability is very important, which resulted in a large interest in PDMS-based materials, as this polymer is known to have a high gas permeability.[9–13] On the other hand, the hydrophilic phase enables the diffusion of water through the material and greatly improves the wearing comfort.[14] Recently, researchers also gained interest in the development of immuno-isolation membranes that are used to encapsulate living cells and shield them from the body's immune system.[15,16] Indeed, to keep the cells alive, similar properties as for contact lenses are required, *i.e.* rapid diffusion of water and metabolites should be possible.

Besides their use in contact lenses, ACNs have been explored for a wide range of other applications, such as the extraction of water from organic solvents,[17] controlled drug release,[18–21] scaffolds for tissue engineering[22–27] and matrices for phase transfer reactions.[3,28,29] Each of these applications is based on the nanophase separation between the hydrophobic and hydrophilic parts, while the latter also benefits from the large interfacial area inside the ACN. For example, Bruns *et al.* demonstrated that embedding enzymes in the hydrophilic phase allows enzymatically catalysed reactions to be performed in organic solvents.[28,29]

ACNs are frequently prepared based on the free radical polymerisation of a telechelic macromonomer, *i.e.* a polymer containing two polymerisable groups, and a co-monomer.[1,30] Although this approach was proven to be widely applicable, it also suffers from several deficiencies that limit the applications. First, an initiator is always necessary to produce the radical species for the polymerisation, which typically requires high temperatures or UV light, depending on the initiator. Moreover, yields are often sub-optimal while residual (unreacted) monomers remain present in the network, which can leach out over time and

cause an inflammatory response in bio-medical applications.[31–34] Furthermore, network defects, such as dangling chains, are common and do not contribute to the mechanical strength of the final material.[1]

Another way to obtain ACNs, while also preventing the problems listed above, is based on the application of polymeric precursors with multiple reactive groups that can be used in coupling reactions.[1,30,35–37] However, this strategy is not straightforward because traditional reactions are often inefficient and low yielding when performed on polymeric substrates, leading to a badly cured network with poor properties. Moreover, the thermodynamic incompatibility of the constituting polymers can lead to a high soluble fraction as a result of macrophase separation during the network formation, as demonstrated by Delerba *et al.*[38] Therefore, ideal reactions to prepare amphiphilic co-networks are fast, high yielding and produce no by products, *i.e.* so-called 'click reactions'.[39]

Recently, our research group established the use of thiolactones (TLas) as a very efficient and orthogonal conjugation strategy allowing a double modification of various substrates. In fact, TLas are cyclic thioesters that are prone to aminolysis and thereby release a thiol functionality, which can react in one of the many reported 'thiol-X' reactions. Since both the amine and the thiol-complementary reaction partner are incorporated into the final product, this strategy allows a double modification of the TLa-bearing substrate. Moreover, both the aminolysis and the subsequent reaction of the thiol can be performed in a one-pot fashion with the aminolysis as rate determining step. For a more detailed introduction to thiolactone chemistry, the reader is referred to the theoretical section of the previous chapter (section VII.3).

In this final experimental chapter, thiolactone-based chemistry was explored as an alternative cross-linking strategy for the generation of amphiphilic silicone-based co-networks. To this end, thiolactone-functional PDMS (PDMS-TLa) was prepared in a first step by linking a reactive thiolactone-bearing compound to a silicone backbone (section VIII.2). Commercially available PEG diacrylates of various chain lengths were selected as hydrophilic component, which are expected to quickly react with the thiols that are generated by the aminolysis of the TLa units. Next, the two components were mixed to obtain a stable yet curable mixture, to which an amine was added to initiate the network formation (section VIII.3). Based on the functionality of the PDMS-TLa, two essentially different

PDMS-PEG co-networks were synthesised, which are discussed and further characterised in their dedicated sections (sections VIII.3.1 and VIII.3.2). Finally, the applicability of this TLa-based strategy to both cross-link and functionalise the PDMS-PEG mixture was demonstrated.

VIII.2 Synthesis of thiolactone-functional PDMS

Previous reports of our research group on TLa chemistry describe the use of a thiolactone bearing an isocyanate functional group (**139**, TLa-NCO) as a versatile compound for the functionalisation of various substrates with thiolactone units.[40] Therefore, the modification of either an alcohol- or amine-functional commercial silicone with this TLa-NCO should represent a facile, one-step procedure to obtain TLa-functional PDMS (PDMS-TLa), required for the synthesis of amphiphilic co-networks. The isocyanate itself is readily obtained on a multigram scale by treating the cheap and renewable DL-homocysteine thiolactone hydrochloride (**142**) with triphosgene in the presence of a base (Scheme VIII.1). In this section, the synthesis of both bivalent and multivalent PDMS-TLa will be discussed in more detail.

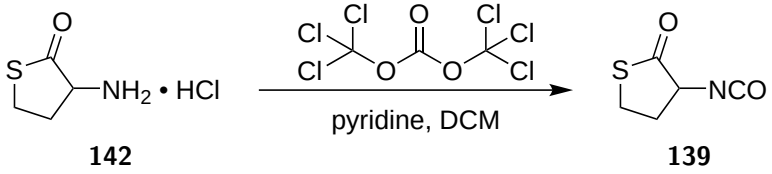

142 **139**

Scheme VIII.1: Synthesis of thiolactone-isocyanate (**139**, TLa-NCO) from DL-homocysteine thiolactone hydrochloride (**142**) by treatment with triphosgene.

VIII.2.1 TLa-terminated PDMS

As a first example of a TLa-functional silicone, hydroxypropyl terminated PDMS (**143**, M_w = 600–850 g mol^{-1}) was functionalised with TLa groups via a reaction with TLa-NCO (Figure VIII.1). Because both reaction partners are miscible and low viscous liquids, the reaction could be performed in bulk. By simply adding a few drops of dibutyltin dilaurate (DBTL), nucleophilic addition of the alcohol to the isocyanate occurs, thereby yielding a carbamate that links the TLa to the silicone backbone (**144**).

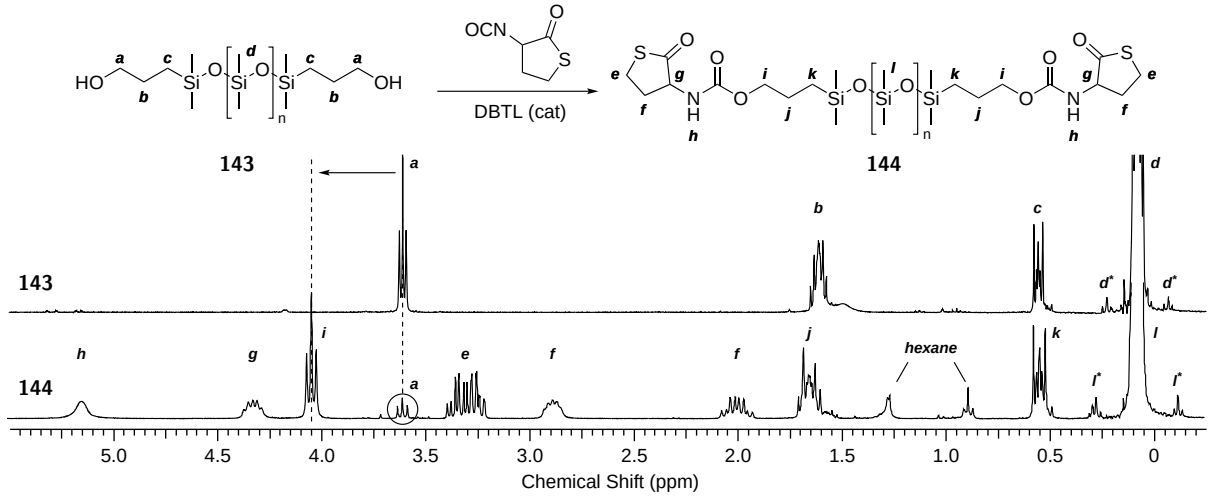

Figure VIII.1: Synthesis of TLa-functional silicone (**144**) from hydroxypropyl terminated PDMS (**143**) and their ^{1}H-NMR spectra in $CDCl_3$. The arrow indicates the downfield shift of the protons in the α-position of the hydroxyl group after reaction.

The progress of the reaction was monitored via ^{1}H-NMR spectroscopy, because the resonance corresponding to the protons in the α-position of the hydroxyl group should significantly shift downfield. However, as displayed in Figure VIII.1, we always found that ∼10 % of the alcohol groups remained unreacted based on this resonance. Initially, we assumed that full conversion was not yet obtained, but even when taking extra care in drying the PDMS, prolonging the reaction times and using an excess of thiolactone isocyanate, no improved conversion was obtained. Even after the addition of a few drops of trichloroacetyl isocyanate (TAIC) to the NMR tube, a compound that instantaneously reacts with any free hydroxyl groups at room temperature, no significant change was observed in the resulting spectrum. Therefore, despite the NMR analysis suggesting otherwise, we concluded that the reaction was finished and that all free hydroxyl groups were successfully modified with a thiolactone group.

One possible explanation for the apparent residual amount of free hydroxyl groups, is the commercial silicone that is not properly described by structural formula **143**. During the production of the hydroxypropyl terminated PDMS, especially in equilibrium ROP,[41–44] a reactive alkoxylate anion can be formed that results in chain transfer reactions, as illustrated in Scheme VIII.2. These chain transfers yield a side product (**145**) with an alkoxypropyl group in the chain that should give similar peaks in the ^{1}H-NMR spectrum compared to the hydroxypropyl termini.

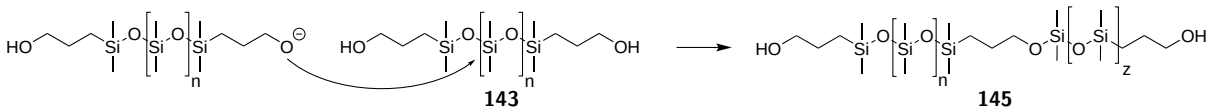

Scheme VIII.2: Suggested mechanism for the formation of side product (**145**) during the production of hydroxypropyl terminated PDMS.

The presence of these alkoxypropyl groups was confirmed by a $^{1}H,^{29}Si$ heteronuclear multiple-quantum correlation (HMQC) NMR experiment. In fact, the resulting spectrum can be interpreted as the Si counterpart of a well-known $^{1}H,^{13}C$-HMBC analysis, which correlates chemical shifts of protons with carbons separated by two or three covalent bonds. If only the expected polymer (**143**) is present in the commercial product, without any contaminants, only cross-peaks between Si and the closest protons in the α and β position should be expected (α and β in Figure VIII.2). However, a third cross-peak between a Si atom and the protons closest to the hydroxyl group is observed in the spectrum (γ in Figure VIII.2), while a difference in the chemical shift of the Si atom indicates that this third coupling originates from a differently shielded Si atom compared to the cross-peaks originating from the hydroxypropyl termini. This observation can only be explained by the presence of our proposed by-product (**145**).

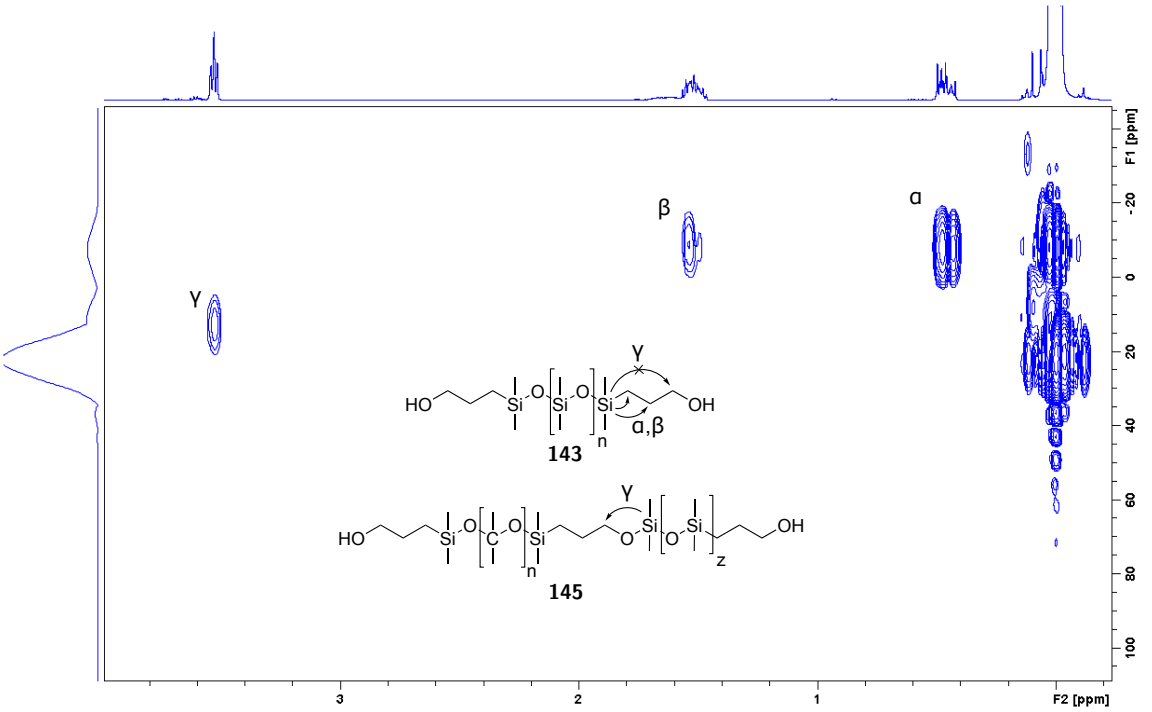

Figure VIII.2: ^{29}Si-^{1}H HMQC NMR spectrum of the commercial hydroxypropyl terminated PDMS. The third cross-peak can only be explained by the presence of side product **145**.

In conclusion, TLa-NCO was successfully used to synthesise a TLa-terminated PDMS with a carbamate linker (**144**). The presence of ∼10 % of alkoxypropyl groups in the main chain of the polymer causes no problems for the intended applications, since each chain should still contain two hydroxypropyl chain-ends that were fully transformed into a thiolactone functionality.

VIII.2.2 Multivalent TLa-functional PDMS

Besides the synthesis of a (bivalent) thiolactone-terminated PDMS, the functionalisation of a silicone with multiple thiolactone groups was targeted as well. Similarly to the synthesis described in section VIII.2.1, we searched for a silicone with hydroxyalkyl side chains in order to link the thiolactone moieties to the silicone by a carbamate group. However, the hydroxypropyl side-chains were ethoxylated in all commercial silicones, yielding PDMS grafted with short poly(ethylene glycol) (PEG) chains. Because this PEG-content was rather high, as judged by ^{1}H-NMR analysis, polymers with an overall polar structure would be obtained. Although functionalisation of these substrates should proceed without any problem, we aimed to synthesise apolar components for the production of amphiphilic networks. Therefore, the range of hydroxyalkyl-functionalised silicones were not useful in the framework of this doctoral work.

In contrast to the hydroxyalkyl-type functional silicones, which are unable to open the thiolactone ring yet quickly react with an isocyanate in the presence of a catalyst (section VIII.2.1), aminopropyl functional PDMS can in theory react with both TLa and isocyanate groups without the need for a catalyst. In this context, TLa-NCO (**139**, Scheme VIII.3)

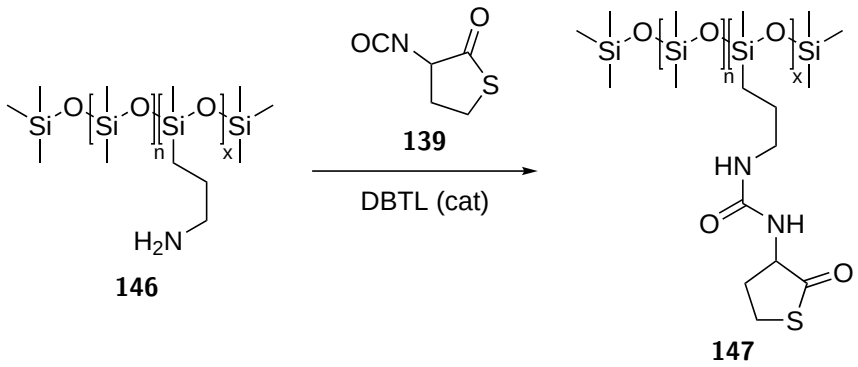

Scheme VIII.3: Synthesis of TLa-functional silicone (**147**) from aminopropylmethylsiloxane-dimethylsiloxane copolymer (**146**). Adding DBTL as a catalyst avoids the aminolysis of the thiolactone as a side reaction.

could act as a cross-linker for silicones bearing multiple amine groups. Indeed, in our initial tests to modify an aminopropylmethylsiloxane-dimethylsiloxane copolymer (**146**, M_w = 4000–5000 g mol^{-1} and 3–4 amines per chain) with TLa units, a cross-linked gel was obtained. Nevertheless, this gelation could be avoided by slowly adding the silicone to an excess of TLa-NCO with a few drops of DBTL. Because the catalyst speeds up the nucleophilic addition of the amine to the isocyanate but not the aminolysis of the TLa, no indication of this side reaction was visible in the crude NMR spectrum. Finally, the multivalent PDMS-TLa (**147**) was separated from the excess of TLa-NCO by washing the crude mixture with a water:methanol solution and evaporation of the solvent.

VIII.3 Amphiphilic PDMS-*l*-PEG co-networks via thiolactone chemistry

After the successful modification of silicones with thiolactone groups, the next phase of this work consisted of the cross-linking of these reactive polymers with a poly(ethylene glycol) (PEG) diacrylate. In this way, hydrophilic PEG and hydrophobic PDMS are combined into a single network of which the amphiphilicity is expressed in its characteristics, *i.e.* their ability to swell in both water and non-polar organic solvents.

First, the different TLa-functional silicones were mixed with a PEG diacrylate to obtain a curable mixture, after which the gelation is triggered by addition of an appropriate amine, thereby yielding a series of PDMS-*l*-PEG co-networks where '*l*' indicates that a PEG cross-linker was used. Depending on the functionality of the PDMS-TLa, different amines can be used, while the PEG content can be varied by changing the molecular weight of the cross-linker. Next, the thermal and mechanical properties of the various networks were analysed by thermogravimetric analysis (TGA), differential scanning calorimetry (DSC) and tensile testing, followed by an investigation of the amphiphilic properties by swelling them in water and hexane. Finally, it was shown that the thiolactone strategy can be used to introduce additional functionalities by incorporating a fluorescent group and a dye.

VIII.3.1 Co-networks from TLa-terminated silicone

VIII.3.1.1 Network synthesis

The first strategy for the preparation of amphiphilic PDMS-*l*-PEG co-networks used the thiolactone terminated silicone (**144**, Figure VIII.1) that was prepared in the first part of this work (section VIII.2.1). To this polymer, an equimolar amount of poly(ethylene glycol) diacrylate (**148**) was added to prepare a stable yet curable mixture. As soon as a diamine (**149**) is added, the network formation is initiated because of the aminolysis of the thiolactone rings, which initially results in a chain extension of the siloxane polymer together with the release of a free thiol (Scheme VIII.4). Subsequently, these thiols quickly react with the PEG diacrylate present in the same medium, thereby introducing cross-links and forming the final network structure.

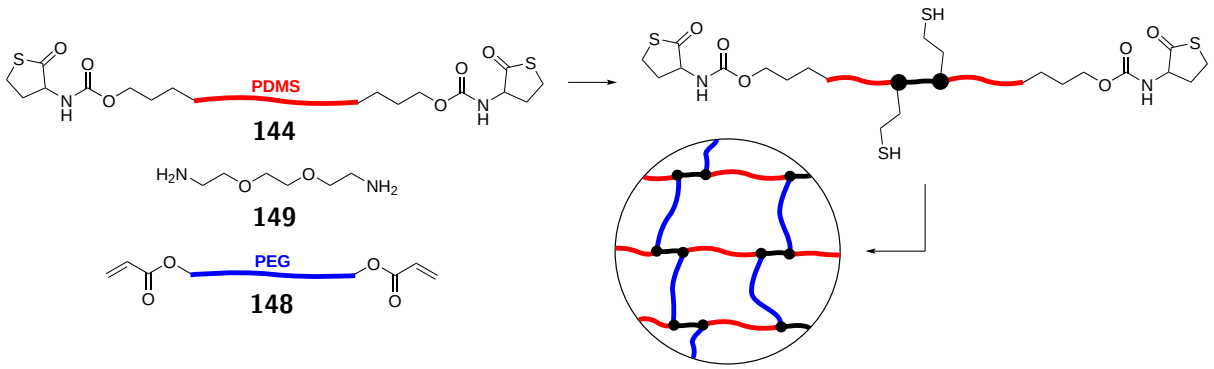

Scheme VIII.4: Synthesis of PDMS-*l*-PEG co-networks using thiolactone terminated silicones. Aminolysis of the thiolactone moiety with a diamine allows chain extension in addition to liberating the thiol. Subsequent reaction with the PEG diacrylate introduces the cross-links and thereby forms the network structure.

When the slightly viscous silicone and PEG diacrylate are mixed, an opaque blend is formed as a result of the limited miscibility of these polymers. Therefore, we expected that a macroscopic phase separation could occur during curing, leading to a badly cured or inhomogeneous network with poor mechanical properties. In order to prevent this, a common solvent such as tetrahydrofuran (THF) was added during the first cross-linking experiments until a homogeneous and transparent solution was obtained. Once the diamine was added, gelation occurred after approximately 20 minutes.

Despite the anticipated problems related to the limited miscibility of the components, the curing was tested in bulk as well. Surprisingly, only seconds after the diamine was added

to the opaque blend of PEG and PDMS, the mixture became completely transparent and a non-sticky elastomer was retrieved after 30 minutes. Consequently, the formation of covalent bonds between the immiscible polymers effectively avoids the large scale phase separation. This approach, *i.e.* without the use of a solvent, has several advantages. Most importantly, when solvent is used, the network is formed in a highly swollen state, which leads to a large shrinkage when the solvent is removed, typically accompanied by the formation of cracks and fractures. Moreover, the evaporation of solvents during curing often causes bubbles that compromise the mechanical properties of the final network.

Next, the solvent-free approach was used to prepare a series of co-networks with a varying PEG content (Table VIII.1). This variation was achieved by using PEG diacrylates with different molecular weights, *i.e.* 250, 575 and 700 g mol^{-1}, while an equal stoichiometry of the individual compounds was maintained. The samples were cured in a mould at room temperature and were left undisturbed for 24 hours to ensure a complete network formation, although a transparent, non-sticky and solid elastomer (Figure VIII.3) was already obtained in 15–30 minutes for every composition.

Table VIII.1: Synthesised PDMS-*l*-PEG co-networks based on the bivalent PDMS-TLa with a varying PEG content, together with their soluble fraction (SF).

Sample code	PEG content (wt%)	SF (%)
B-PEG$_{250}$	16.3	2.3
B-PEG$_{575}$	30.9	5.4
B-PEG$_{700}$	35.3	1.6

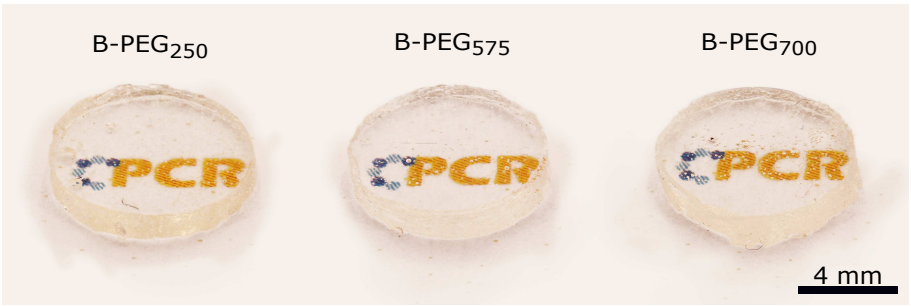

Figure VIII.3: Pictures of the PDMS-*l*-PEG co-networks (Table VIII.1).

The soluble fraction was determined for all the synthesised networks by a soxhlet extraction for 24 hours with THF, which is a common solvent for both PDMS and PEG (*vide supra*) and should thus be able to remove any polymer residue that is not incorporated in the network. Subsequently, the network was dried and weighted, after which the soluble faction

could be calculated from the mass loss during the extraction (section VIII.5.2.1). In all cases, the obtained value was very low (Table VIII.1), which indicates that the formation of the co-network is not only successful, but also very efficient. Therefore, all the following analyses were performed on untreated samples, *i.e.* without prior removal of the soluble fraction.

VIII.3.1.2 Thermal analysis and mechanical properties

After the successful synthesis of the first thiolactone-based PDMS-*l*-PEG networks, thermogravimetric analyses (TGA) and differential scanning calorimetry (DSC) measurements were performed on all materials, in order to obtain more information about their thermal stability and phase behaviour. The resulting thermograms (Figure VIII.4a) show two distinct degradation steps at 260 °C and 340 °C, respectively. Because the first mass loss is inversely proportionate to the PEG content while PDMS is known to have a high thermal stability, the initial degradation can be attributed to the thermolysis of the cross-links, *i.e.* mainly thioethers and esters, followed by a degradation of the homopolymers at higher temperatures.

As previously discussed (section VIII.1), amphiphilic co-networks are known to have a phase-separated morphology with microscopic domains of the immiscible components. Moreover, transparency of the networks suggests that the dimensions of these domains are smaller than the wavelength of visible light.[35] Indeed, DSC analysis confirmed the existence of these domains in the synthesised networks by the presence of two distinct glass transition temperatures, *i.e.* one in the usual region of PDMS (approximately −120 °C[45]) and the other corresponding to the PEG segments between −50 °C and −30 °C (Figure VIII.4b). Although the exact value of the T_g might be slightly influenced by the residual soluble fraction (Table VIII.1), this effect is expected to be very low. In principle, AFM measurements could elucidate the size of the different domains (*vide supra*, not done).

Next, the mechanical properties of the synthesised networks were investigated by tensile testing, yielding the maximum elongation, Young's modulus (E) and maximum stress as a function of the composition. All the samples are brittle materials with ruptures in the elastic region, as evidenced in the stress-strain curves (Figure VIII.5a). While the tensile

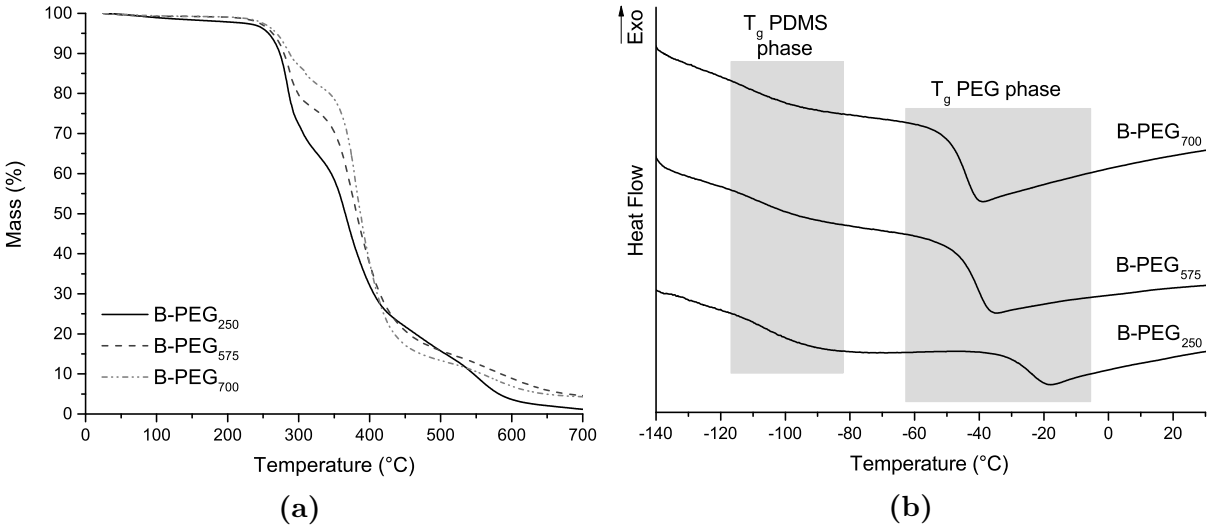

Figure VIII.4: Thermal analysis of the prepared samples based on the bivalent PDMS-TLa (Table VIII.1). **(a)** TGA and **(b)** DSC.

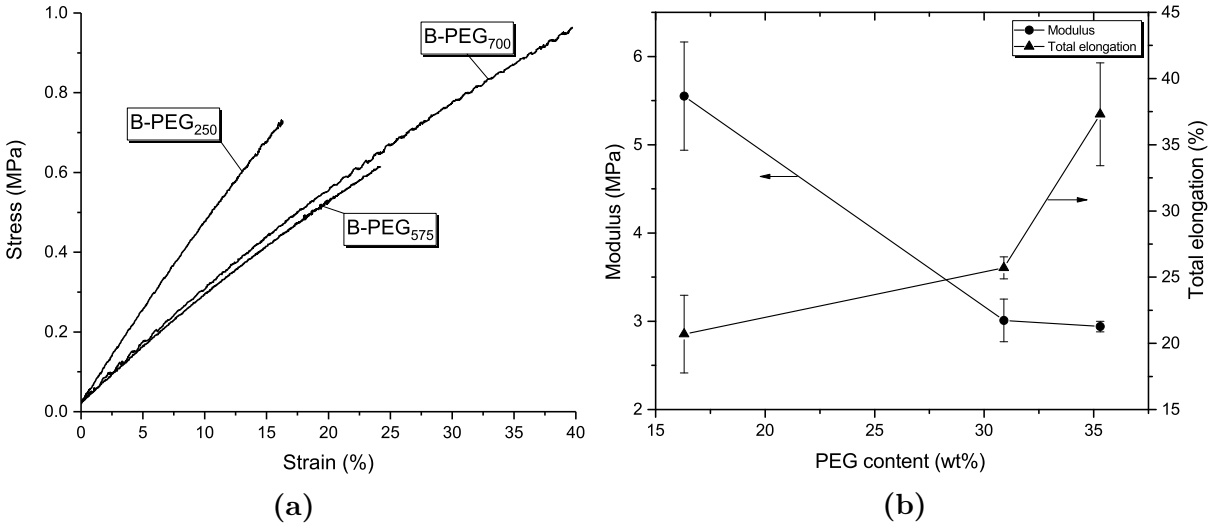

Figure VIII.5: Results of the tensile tests on the samples based on the bivalent PDMS-TLa (Table VIII.1) with **(a)** representive stress-strain curves and **(b)** the measured modulus and total elongation as a function of the sample composition. The error bars indicate the standard deviation of at least three different measurements.

strength is shown to be dependent on the exact composition of the elastomers, no apparent relation with the amount of PEG could be identified. Nevertheless, a clear relation was found between the composition and both the modulus and maximum elongation of the resulting materials (Figure VIII.5b). This trend can be explained by the lower cross-linking density when the amount of PEG is increased, which allow the segments to stretch more when stressed, resulting in a decreasing modulus and an increasing maximum elongation as a function of the PEG content.

VIII.3.1.3 Swelling behaviour

Once the DSC analysis of the synthesised PDMS-*l*-PEG co-networks indicated a phase-separated morphology with microscopic domains of the different components, in agreement with earlier reports on amphiphilic co-networks (section VIII.1), their amphiphilic character was assessed by swelling them in two immiscible solvents. Polymer networks tend to absorb solvent molecules, leading to an expanded solvated state, which is a result of the system trying to minimise its free energy. According to the swelling theory by Flory and Rehner,[46,47] the equilibrium swelling degree is a result of two counteracting forces. On the one hand, the mixing of solvent and polymer chains during swelling leads to a favourable mixing energy, while on the other hand, the extent of swelling is limited by the elastic forces of the network and thus dependent on the cross-linking density. Therefore, swelling will be most significant when submerged in a good solvent, *i.e.* solvents which have a high affinity for the polymer. Consequently, networks will typically either swell in water, *i.e.* hydrogels, or in certain organic solvents when they are made from only one type of polymer. In contrast, the networks in this study are synthesised by combining a polar and a non-polar polymer, *i.e.* so-called amphiphilic co-networks (ACNs), and should thus swell in both water and apolar organic solvents.

The swelling of the synthesised networks was tested in both water and hexane as immiscible solvents, of which the former only dissolves the PEG fragments, while the latter only dissolves the PDMS segments,[48] making it an ideal combination to test the amphiphilicity. Preweighted dry samples were placed in vials filled with water or hexane and were periodically shaken to facilitate the swelling. After 7 days, the gels were weighed again to calculate the mass swelling ratio (section VIII.5.2.2).

As depicted in Figure VIII.6, all the samples were able to swell in both water and hexane, thereby demonstrating the first successful application of thiolactone chemistry for the preparation of amphiphilic structures. In correspondence to the previously reported PDMS-*l*-PEG co-networks by Erdodi and Kennedy,[7,35] the degree of swelling in water proved to be highly dependent on the polymer composition and directly proportional to the PEG content. On the other hand, while a similar dependence yet opposite trend was expected in the case of the swelling ratio in hexane, it was found to decrease only slightly when the PEG content increases. A plausible explanation for the fairly constant

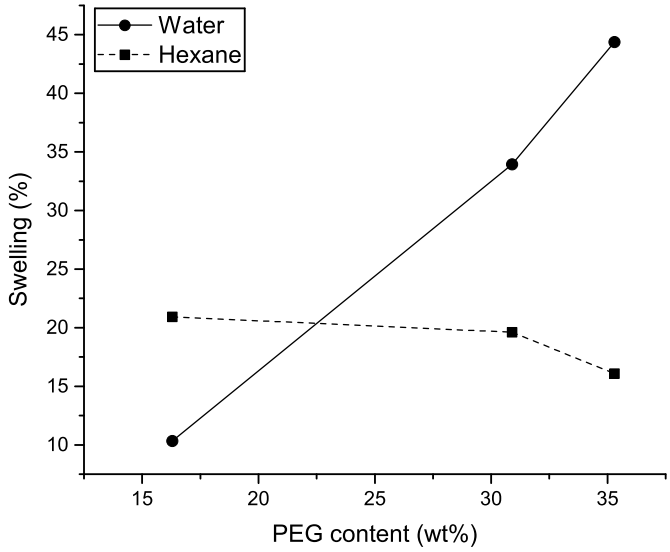

Figure VIII.6: The swelling behaviour of PDMS-*l*-PEG amphiphilic co-networks based on the bivalent PDMS-TLa in water and hexane as a function of the composition.

swelling in hexane is that an increase in PEG content is accompanied with an increase in size of the PEG segments (section VIII.3.1.1), thereby lowering the cross-linking density. This decreased cross-linking density results in a higher conformational freedom of the individual chains and a more efficient absorption of hexane molecules (*vide supra*), which compensates for the decrease in the relative amount of PDMS.

Even at a PEG content of 35 wt%, the short PDMS and PEG segments resulted in a material that is still characterised by a high cross-linking density, as evidenced by the low overall swelling ratios of 45 % and 16 % in water and hexane, respectively. Erdodi and Kennedy, for example, obtained a degree of swelling up to 75 % and 50 % in the respective solvents for a material with a similar PDMS/PEG ratio yet much lower cross-linking density.[7] Therefore, we believe that the thiolactone-based approach already shows promising results, while a further increase of both the PDMS and PEG chain-lenghts or a variation in the polarity of the applied diamine (**149**) should yield very competitive materials in the future.

In conclusion, a new thiolactone-based strategy was developed for the preparation of PDMS-*l*-PEG co-networks. In all cases, curing proceeded rapidly (<15 min) and networks with a low soluble fraction were obtained, showing the effectiveness of this chemistry in coupling the polymeric precursors into one cross-linked structure. DSC analysis revealed the presence of two distinct T_gs from the corresponding homopolymers, which indicates

the characteristic phase-separated nanostructure of amphiphilic networks. Indeed, these networks swell in both water and hexane, and despite an overall low swelling in hexane, the one in water was found to be proportional to the PEG content. Nevertheless, while we expect that the swelling behaviour can be further optimised, this system will always be limited by the requirement for both a diamine and diacrylate to obtain a network from the bivalent PDMS-TLa, which prevents a facile structural variation or introduction of functionalities in the elastomer. Therefore, we focussed on further exploring the possibilities of thiolactone chemistry by using a multivalent PDMS-TLa instead.

VIII.3.2 Co-networks from multivalent TLa-functional PDMS

In the previous section, a bivalent thiolactone-functional PDMS (PDMS-TLa) was already successfully applied to synthesise amphiphilic PDMS-*l*-PEG co-networks. However, this approach did not fully exploit the benefits offered by the thiolactone group because both a diamine and a diacrylate were required for a good network formation, thereby limiting the structural variability. Nevertheless, this limitation can be overcome by using silicones functionalised with multiple TLa moieties ($f \geq 3$) . Consequently, either the diamine or the diacrylate can be substituted by a monofunctional alternative, allowing to introduce various functionalities during the synthesis of the network. Moreover, because the aminolysis of the thiolactone unit is the rate determining step in the overall curing mechanism (section VII.3), a variation in cross-linking kinetics should be expected when different amines are used.

Here, a silicone with on average three to four thiolactone groups (**147**, Scheme VIII.5), of which the synthesis was described in section VIII.2.2, will be combined with a PEG diacrylate and a monofunctional amine. First, the influence of the exact amine on the cross-linking kinetics was investigated. When an optimal gelation time was achieved, mainly from a practical point of view, the PEG content was again varied to obtain a series of different PDMS-*l*-PEG co-networks. After assessing the thermal and mechanical properties, as well as the swelling behaviour of these new elastomers, we finally demonstrated that the thiolactone chemistry can also be used to introduce additional functionalities, such as a fluorescent dye.

VIII.3.2.1 Influence of the amine on the gelation time

Earlier research by our group already showed that the kinetics of the aminolysis are strongly influenced by the structure and electronic properties of the amine (section VII.3.1). Hence, the used amine also directly influences the curing rate and thereby the gelation time, *i.e.* the time between addition of amine and the transition from a liquid to a solid elastomer. Therefore, various amines were tested to measure the influence on the gelation time, but also to investigate their compatibility with the applied synthesis method. Knowledge of the time-frame in which gelation occurs is very important, as shaping or moulding has to occur within this processing window.

Similarly to the previous procedure (section VIII.3.1.1), a curable mixture containing the multivalent PDMS-TLa (**147**) and the PEG diacrylate (**148**, 250 g mol^{-1}) was first prepared. Then, a simple (mono)amine (**150**) of choice was added, which initiates the network formation by aminolysis of the thiolactone group, followed by the reaction of the liberated thiol with the present PEG diacrylate (Scheme VIII.5).

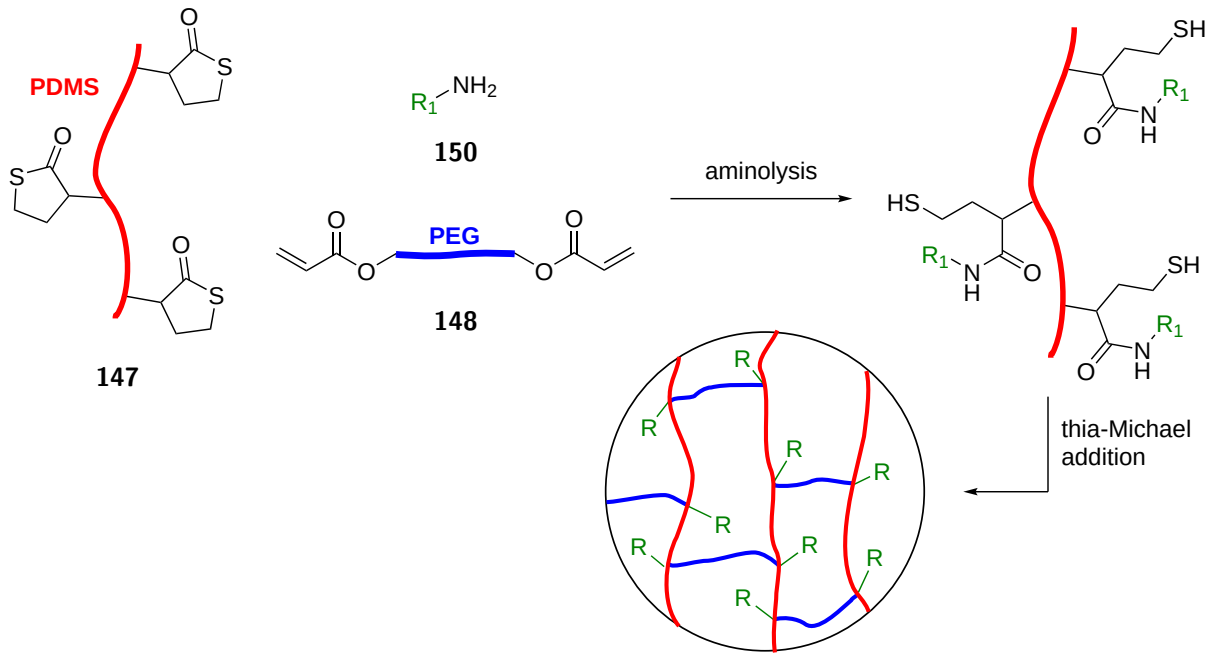

Scheme VIII.5: Synthesis of PDMS-*l*-PEG co-networks from multivalent PDMS-TLa (**147**).

The network formation can be visualised by monitoring the dynamic moduli as a function of time using a rheometer. Shortly after the addition of the amine, the sample is still liquid and its viscous behaviour dominates over its elastic one, *i.e.* $G' \ll G''$. While both moduli increase as soon as cross-links are formed, the storage modulus (G') increases more

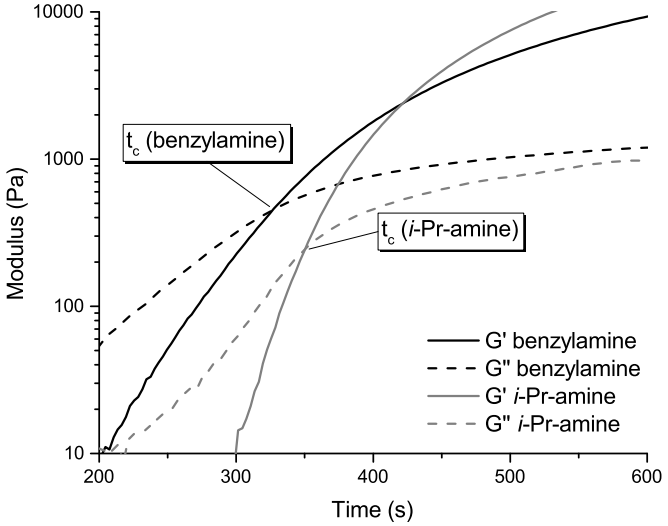

Figure VIII.7: Evolution of the dynamic moduli as a function of time. The time is corrected for the dead time between the addition of the amine and the start of the measurement and thus represents the actual reaction time.

rapidly than the loss modulus (G″), leading to a crossing of both curves at a certain time (t_c). From this point onwards, the elastic behaviour dominates, which means that t_c can be used to quantify the gelation time. The results of these rheology measurements are illustrated in Figure VIII.7, where the progress of the moduli is shown for samples cured with either benzylamine or isopropylamine. Unfortunately, the gelation time could not be quantified via this method for several other amines and could only be estimated visually, as gelation already occured before a measurement could be started. The tested amines and accompanied gelation times are summarised in Table VIII.2.

From these initial cross-linking experiments, it was clear that the choice of amine has a profound impact on the curing times. Pyrrolidine, propylamine and octylamine resulted in the shortest gelation times, in agreement with the previous reports on the kinetics of thiolactone aminolysis (section VII.3.1). In fact, when these amines were added to the reaction mixture, partial gelation occurred almost instantaneously, after which the

Table VIII.2: Effect of the amine on the gelation time of a curable mixture of multivalent PDMS-TLa and PEG diacrylate. [a]Visual observation. [b]Determined via rheology.

Amine	Time (s)
Pyrrolidine	<10[a]
Propylamine	<10[a]
Octylamine	<10[a]
Benzylamine	327[b]
Isopropylamine	349[b]

complete blend solidified. This remarkable observation can be explained by a high local concentration upon addition of the amine, leading to a fast cross-linking prior to a homogeneous mixing of all the reactants. Consequently, the reaction rate was too fast for our intended application in the case of these amines, since there was not enough time to mix and process the reactive blend prior to gelation. However, this rate can be decreased by using either benzylamine or isopropylamine, which are reported to be at least an order of magnitude slower in their reaction with thiolactones. Indeed, because of the electron-withdrawing effect of the benzyl group and the increased steric bulk in isopropylamine, a processing time of approximately 5 minutes was obtained, which is a feasible time for lab-scale mixing and moulding.

VIII.3.2.2 Network synthesis

As demonstrated in the previous section, the exact amine that is added to the reaction mixture has a large influence on the cross-linking kinetics of the polymer blend. For our intended application, a gelation time of at least 60 seconds is desired from a practical perspective, because a slower curing time allows to homogenise the reaction mixture after addition of the amine and to transfer it to a mould. Therefore, we decided to use benzylamine to prepare a series of ACNs with a varying PEG content. Although isopropylamine was found to have a similar curing time, its high volatility makes it impractical to work with.

First, a mixture was prepared of the highly viscous multivalent PDMS-TLa (**147**) and the PEG diacrylate (**148**), to which a small amount of THF (0.1 mL for 1 g PDMS) was added in order to lower the viscosity and to facilitate mixing. Variation in the PEG content was again achieved by using PEG diacrylates with different molecular weights, *i.e.* 250, 500 and 700 g mol^{-1}, while an equal stoichiometry of the individual compounds was maintained (Table VIII.3). Finally, network formation was initiated by the addition

Table VIII.3: Synthesised PDMS-*l*-PEG co-networks based on the multivalent PDMS-TLa with a varying PEG content, together with their soluble fraction (SF).

Sample code	PEG content (wt%)	SF (%)
M-PEG$_{250}$	8.9	7.2
M-PEG$_{575}$	18.3	9.0
M-PEG$_{700}$	21.4	8.7

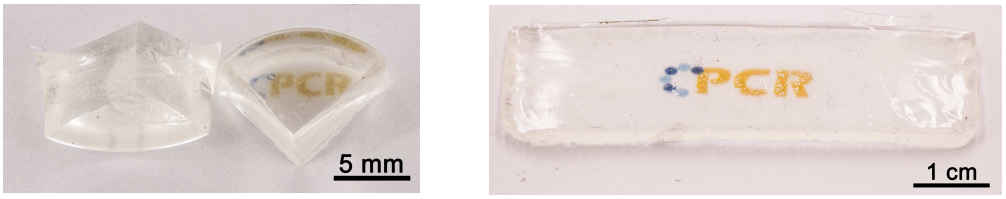

(a) **(b)**

Figure VIII.8: Pictures of **(a)** sample M-PEG$_{250}$ and **(b)** sample M-PEG$_{700}$ (Table VIII.3).

of benzylamine, after which the reaction mixture is quickly mixed and transferred to a mould. The samples were cured at room temperature and were left undisturbed for 24 hours to obtain a transparent, non-sticky, flexible elastomer (Figure VIII.8).

After the successful synthesis of the PDMS-*l*-PEG co-networks, their soluble fraction was determined by a soxhlet extraction for 24 hours with THF (section VIII.5.2.1). The current materials are generally characterised by a higher soluble fraction compared to the co-networks prepared from the TLa-terminated PDMS (Table VIII.3, *cf*. Table VIII.1). Nevertheless, the obtained values were still similar to earlier reports from comparable co-networks in literature, which indicates the efficient formation of the co-networks.[26] Again, the following analyses were performed on untreated samples, without prior removal of the soluble fraction.

VIII.3.2.3 Thermal analysis and mechanical properties

The obtained co-networks, prepared from multivalent PDMS-TLa, were analysed similarly as the previously prepared ACNs, *i.e.* by TGA, DSC and tensile testing. Degradation of the materials starts also around 250 °C regardless of the composition (Figure VIII.9a), but proceeds somewhat gradually over a broad temperature range of 450 °C rather than by two distinct steps (*cf*. Figure VIII.4a), which makes a further interpretation impossible. The DSC analysis again revealed two separate T_gs that can be attributed to the microscopic phase-seperated domains of PDMS and PEG, thereby marking the synthesised networks as structures with potential amphiphilic behaviour (Figure VIII.9b). While the exact value of the T_g might be influenced by the residual soluble fraction (Table VIII.3), this effect is expected to be rather low.

In contrast to the materials based on the bivalent PDMS-TLa (section VIII.3.1.2), tensile tests on the current networks reveal that the modulus increases while the total elongation

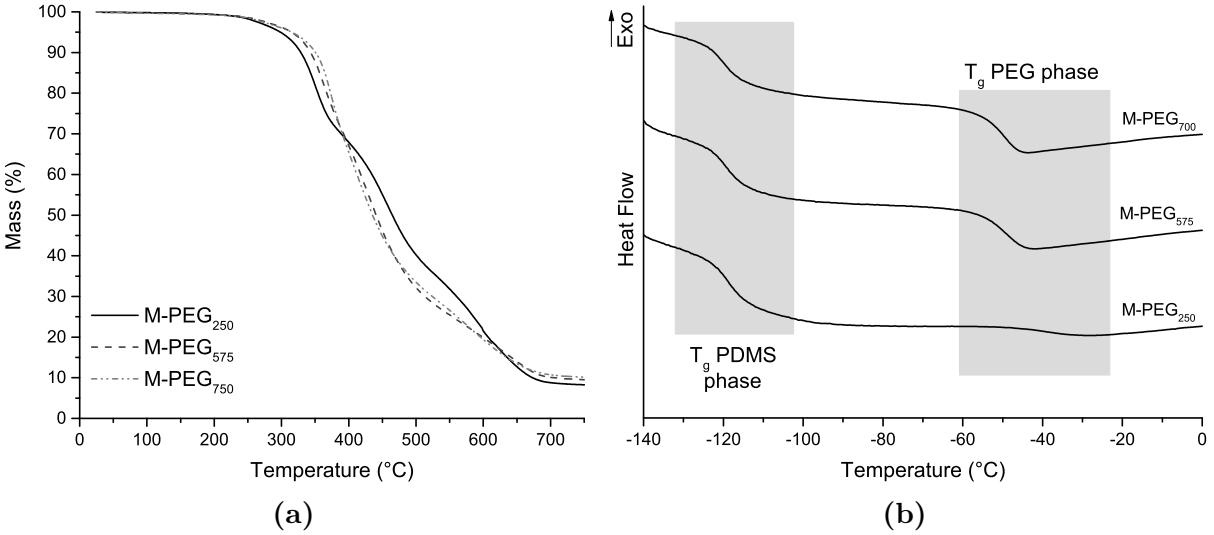

Figure VIII.9: Thermal analysis of the prepared samples based on the multivalent PDMS-TLa (Table VIII.3). **(a)** TGA and **(b)** DSC.

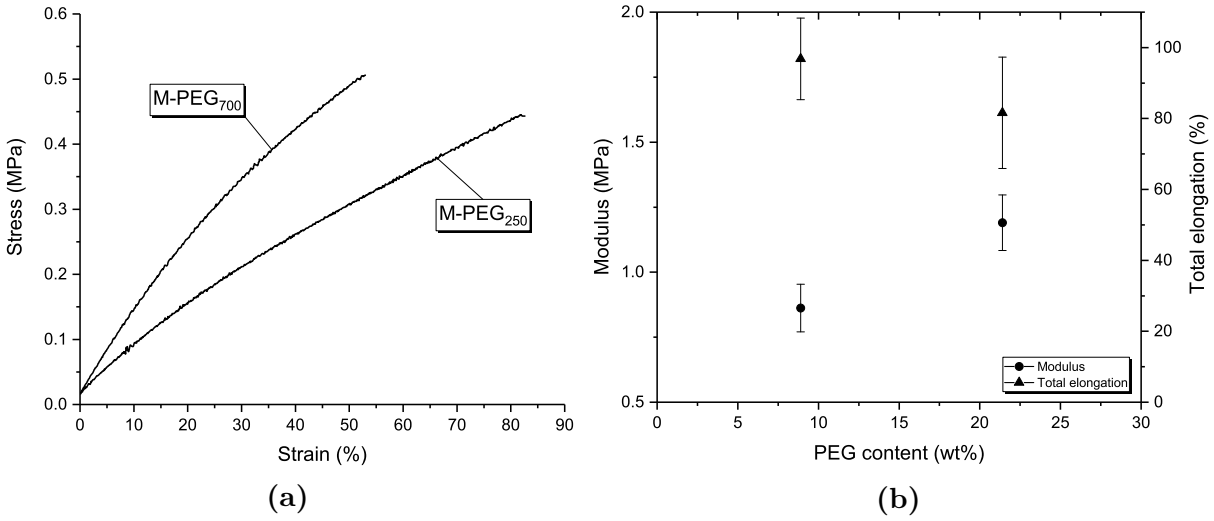

Figure VIII.10: Tensile testing results of the samples based on the multivalent PDMS-TLa (Table VIII.3) with **(a)** representive stress-strain curves and **(b)** the measured modulus and total elongation as a function of the sample composition. No void-free tensile sample could be obtained for M-PEG$_{575}$.

decreases when the molar mass of the PEG diacrylate is increased from 250 g mol^{-1} to 700 g mol^{-1} (Figure VIII.10). Nevertheless, this unexpected observation might be explained by the lower overall cross-linking density compared to the former materials, as evidenced by the lower moduli for both compositions (*cf.* Figure VIII.5b). Therefore, while a decreasing cross-linking density is expected to result in a decreasing modulus and an increasing maximum elongation as a function of the PEG content, the phase-separated PEG domains in these elastomers might act as a filler for the PDMS, thereby yielding an opposite effect as the content of this toughener increases.

VIII.3.2.4 Swelling behaviour

Once again, the swelling of the prepared PDMS-*l*-PEG co-networks was tested in both water and hexane, similarly to section VIII.3.1.3. As depicted in Figure VIII.11, this swelling study confirmed the ability of the materials to swell in both solvents. In contrast to the networks based on the bivalent PDMS-TLa, the swelling in hexane is significantly larger and shows the expected decrease as a function of the PEG content, while the swelling in water is rather low. Nevertheless, because the latter values clearly show a positive correlation with the amount of PEG, we believe that the swelling in water can be further improved by preparing networks with a higher PEG content, *i.e.* by using PEG diacrylates with higher molecular weights. However, such an in-depth optimisation of the swelling behaviour was considered out of scope of this doctoral work.

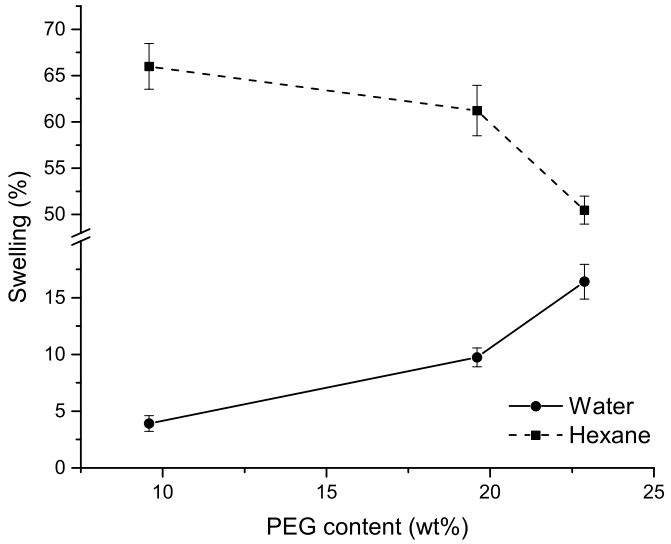

Figure VIII.11: Equilibrium swelling degree of PDMS-*l*-PEG co-networks based on the multivalent PDMS-TLa (Table VIII.3) in water and hexane as a function of the PEG content.

VIII.3.2.5 Functionalisation of ACNs via a thia-Michael addition

In the previous sections, we demonstrated that the multivalent PDMS-TLa is a suitable precursor for the effecient preparation of PDMS-*l*-PEG ACNs. Moreover, not all of the thiols that are generated via aminolysis of the thiolactone units, *i.e.* three to four per chain, are necessary to obtain a cross-linked material. Therefore, we envisioned that a small amount of these thiols can be used to introduce functionalities into the network via a 'thiol-click' reaction, without significantly altering the mechanical properties and swelling

characteristics. This section will provide a proof of concept of such a functionalisation by modifying networks with either a dye or a fluorescent group, because only a small quantity of these moieties is usually enough to cause a strong visual effect. Furthermore, the transparency of the synthesised ACNs makes them very suitable for the introduction of such features and to easily visualise a successful functionalisation.

As a first example of a covalent functionalisation, the transparent network was coloured with a red dye. To this end, the alcohol functionality of Disperse Red 1 (DR1), an azobenzene-based dye that is often used to colour textile fibres,[49] was first transformed into the corresponding acrylate (**151**, Figure VIII.12). Next, 1 mol % of the acrylates in the curable mixture of multivalent PDMS-TLa and PEG diacrylate was substituted for this DR1-acrylate, after which curing was triggered by the addition of benzylamine. The

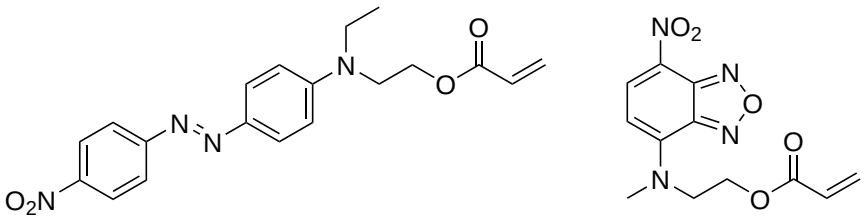

151 **152**

Figure VIII.12: The Disperse Red 1 acrylate (**151**) and the fluorescent NBD-acrylate (**152**) that were used to functionalise the PDMS-*l*-PEG ACNs.

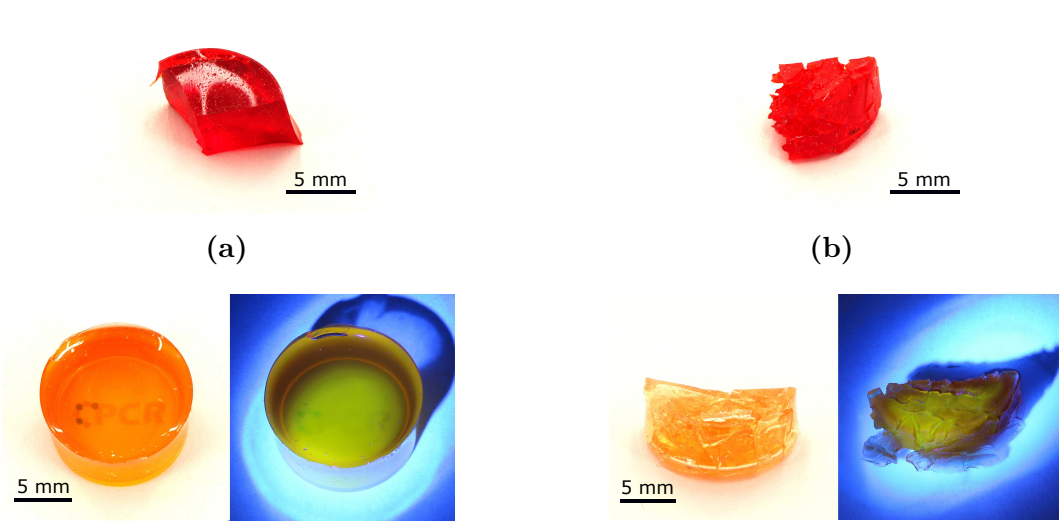

(a) **(b)**

(c) **(d)**

Figure VIII.13: PDMS-*l*-PEG co-network based on the multivalent PDMS-TLa functionalised with either **(a)** DR1-acrylate (**151**) or **(c)** NBD-acrylate (**152**, without and with UV irradiation). **(b, d)** No significant change in colour or fluorescent activity were observed after a soxhlet extraction.

obtained gel was coloured dark red (Figure VIII.13a), although only a small amount of dye was present in the material (0.27 wt%). As expected, such a small amount of additive did not significantly influence the swelling behaviour of the material.

Besides the introduction of Disperse Red, the transparent network was also coloured with the green fluorescent nitrobenzoxadiazole acrylate (NBD-acrylate, **152**, Figure VIII.12). While this acrylate was previously co-polymerised in poly(methyl acrylate) brushes (section VI.3.2.4), a small amount (0.12 wt%) was now added to the curing formulation to covalently link the fluorescent moieties in the ACN. Illumination of the transparent, yet faintly orange coloured network with UV light results in a bright green fluorescence, as shown in Figure VIII.13c. Moreover, the fluorescence was found to be especially pronounced in hydrophobic solvents while it is reported to be rather weak in water.[50,51] Hence, this opens possibilities for potential sensor applications where the fluorescent response is dependent on the polarity of the medium.

Finally, a soxhlet extraction with THF was performed on both materials to prove that the functionalities are indeed covalently linked in the network. While a small amount of unreacted acrylate was extracted for each material, which can be expected as a result of the soluble fraction of ∼7 %, no significant change in colour or fluorescent activity could be observed (Figure VIII.13b and Figure VIII.13d, respectively).

In conclusion, we demonstrated that the multivalent PDMS-TLa offers various advantages over the previously used TLa-terminated silicone (section VIII.3.1) for the production of PDMS-*l*-PEG co-networks. The exact amine that was used to initiate the network formation was found to have a large influence on the cross-linking kinetics and could be varied independently from the desired PDMS/PEG ratio. The amphiphilic structure of the networks was again confirmed by DSC analyses, while their amphiphilic behaviour was demonstrated by the ability to swell in both water and hexane. Although the swelling ratio was significantly higher in hexane than in water, the expected correlation as a function of the PEG content was found in both solvents. In a final proof of concept, the elastomers were covalently functionalised via a thia-Michael addition with dyes and fluorescent molecules.

VIII.4 Conclusions and perspectives

Thiolactone-based conjugation chemistry was investigated as a new cross-linking strategy for the preparation of PDMS-based amphiphilic co-networks. First, thiolactone units were attached to functional polysiloxanes to yield both a bivalent or a multivalent TLa-functional silicone as the hydrophobic component of the network. Commercially available PEG diacrylates of varying chain-lengths were selected as hydrophilic cross-linkers, which were added to either of the TLa-bearing polymers to obtain a stable yet curable mixture.

By addition of an amine to the polymer blends, the thiolactone generates a thiol via aminolysis, which subsequently reacts with the acrylates in the mixture. For all formulations, the cross-linking proceeded quickly and efficiently at room temperature, yielding a range of transparent elastomers with a low soluble fraction. Thermal characterisation of the PDMS-*l*-PEG co-networks revealed the presence of two distinct T_gs, indicating the characteristic phase-separated nanostructure of ACNs. Indeed, the co-networks displayed the ability to swell in both water and hexane, while their swelling ratio could be rationalised by a combination of the PEG content and the cross-linking density.

The main drawback of the TLa-terminated silicone is the requirement of a diamine to obtain a cross-linked material, which prevents a facile structural variation in the elastomer. In the case of the multivalent PDMS-TLa, on the other hand, any TLa-reactive amine can be used to generate an amphiphilic network. Moreover, because the aminolysis is the rate determining step in the overall process, the gelation kinetics could be tuned by varying the nature of the amine. Finally, we showed that a small fraction of the TLas can be used to introduce additional functionalities without significantly altering the swelling properties.

In summary, TLa chemistry was shown to be a very efficient approach to couple hydrophobic PDMS and hydrophilic PEG into an amphiphilic network. Especially the multivalent PDMS-TLa proved to be a versatile building block that allows the introduction of various functional acrylates. Future research should mainly target the optimisation of the swelling behaviour of the produced materials. For example, the produced ACNs should profit from a decrease in cross-linking density by using longer PDMS and PEG segments. Moreover, for the networks based on the multivalent PDMS-TLa, the structural freedom in the applied amine should also allow the introduction of extra functionalities into the network.

VIII.5 Experimental section

All materials, solvents and their corresponding purification are presented in appendix A.

VIII.5.1 Synthesis

The synthesis of NBD-acrylate (**152**) is described in section VI.6.1.5.

VIII.5.1.1 α-Isocyanato-γ-thiolactone (139)

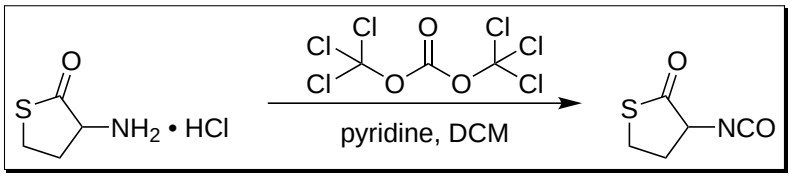

The synthesis of α-isocyanato-γ-thiolactone was based on a literature procedure.[52] Triphosgene (50.0 g, 168 mmol, 0.35 eq) was dissolved in ice-cooled dichloromethane (500 mL) in a two-neck flask and stirred for 15 minutes. Afterwards an extra dichloromethane (400 mL) was added. Subsequently, dry D,L-homocysteine thiolactone hydrochloride (74.0 g, 482 mmol, 0.35 eq) was added. Next, dry pyridine (120 mL, 1.5 mol, 3.11 eq) was added dropwise using an addition funnel. After 1 hour the ice-bath was removed and the mixture was stirred for another 5 hours. The aqueous work-up of the crude mixture was done fast to avoid degradation. The crude mixture was directly filtered into a separation funnel to remove the pyridinium hydrochloride salt and was rinsed with 300 mL cold dichloromethane. The organic phase was washed with a cold 2 M HCl solution (500 mL), brine (500 mL) and ice water (500 mL). Subsequently, the water phase was extracted with dichloromethane (200 mL) and all the organic phases were collected. Magnesium sulfate was added to remove residual water and after filtration the product was concentrated *in vacuo*. Finally, a brown residue was obtained that was further purified by distillation and the fraction between 83–95 °C (0.08 mbar) was collected.

Yield: 61.04 g colourless liquid (88.52 %).

Molecular weight: 143.16 g/mol.

^{1}H-NMR (300 MHz, $CDCl_3$): δ (ppm) = 4.23 (dd, 1 H, CO−C*H*), 3.30 (m, 2 H, S−CH_2), 2.64 (m, 1 H, S−CH_2−CH_2), 2.11 (m, 1 H, S−CH_2−CH_2).

VIII.5.1.2 Thiolactone-terminated PDMS with a carbamate linker (144)

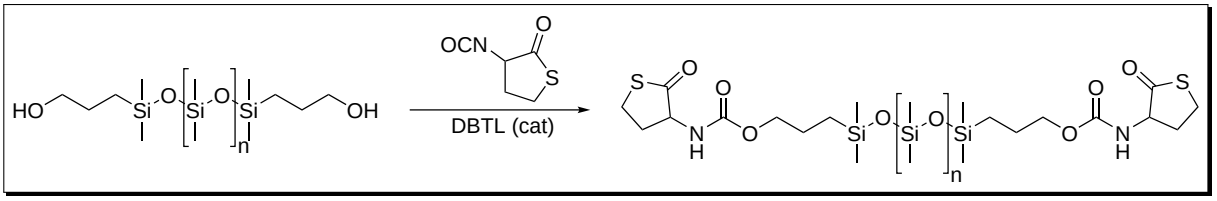

For all calculations, the molecular weight of the hydroxypropyl terminated PDMS (M_w = 600–800 g mol^{-1}) was assumed to be 600 g mol^{-1}. This compound (10 g, ∼16.67 mmol, 1 eq) was mixed in bulk with thiolactone isocyanate (5 g, 35 mmol, 2.1 eq) in a 50 mL flask. Followed by addition of a catalytic amount of dibutyltin dilaurate (2 drops). This mixture was placed under inert atmosphere and stirred at room temperature for 3.5 h, reaction progress was monitored by NMR spectroscopy. Next, the crude mixture was transferred to a separation funnel and hexane (100 mL) was added, the organic layer was washed two times with a methanol:water (10:1, 2x 200 mL) solution. The hexane phase was dried over magnesium sulfate and concentrated *in vacuo* to obtain the bivalent PDMS-TLa (**144**) with carbamate linker.

Yield: 7.78 g (∼52.7 %).

Molecular weight: 886–1086 g/mol.

^{1}H-NMR (400 MHz, $CDCl_3$): δ (ppm) = 5.15 (s, 2 H, N*H*), 4.32 (m, 2 H, NH−C*H*−CO), 4.04 (t, 4 H, CH_2−O−CO), 3.34 (m, 2 H, S−CH_2), 3.24 (m, 2 H, S−CH_2), 2.88 (m, 2 H, CH−CH_2−CH$_2$), 2.00 (m, 2 H, CH−CH_2−CH$_2$), 1.65 (m, 4 H, Si−CH$_2$−CH_2), 0.54 (m, 4 H, Si−CH_2).

^{13}C-NMR (100 MHz, $CDCl_3$): δ (ppm) = 66.96 (CH$_2$), 59.71 (CH), 31.06 (CH$_2$), 26.14 (CH$_2$), 21.86 (CH$_2$), 12.84 (CH$_2$).

VIII.5.1.3 Multivalent thiolactone-funtional PDMS with a urea linker (147)

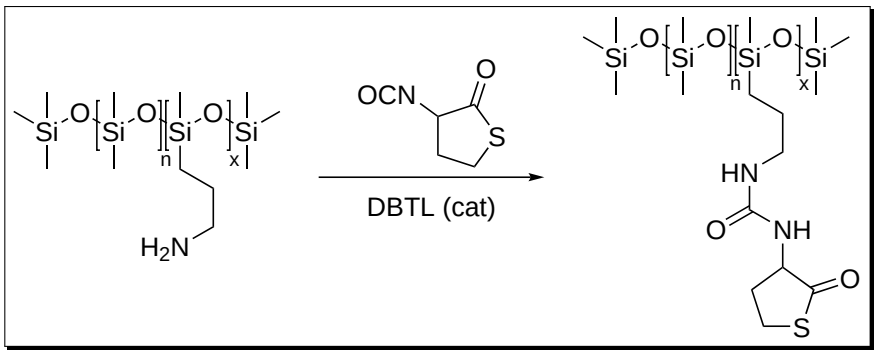

The molecular weight of the average repeat unit in the aminopropylmethylsiloxane-co-dimethylsiloxane polymer (M_w = 4000–5000 g mol^{-1}) was determined via ^{1}H–NMR spectroscopy. When the Si−CH_2 protons, originating from the aminopropyl group, are used as a reference, a total amount of 89 Si−CH_3 protons is obtained. Consequently, an equivalent weight of 1180 g mol^{-1} was calculated for this copolymer, which means that the multifunctional polymer can be treated as a (mono)amine with a molar mass of 1180 g mol^{-1} when calculating the required amounts of reactants.

A solution of thiolactone isocyanate (3.1 g, 21.7 mmol, 1.27 eq), dry tetrahydrofuran (10 mL) and a catalytic amount of dibutyltin dilaurate (4 drops) was made in a two neck flask. This mixture was put under nitrogen atmosphere and stirred at room temperature, while a solution of the aminopropylmethylsiloxane-co-dimethylsiloxane polymer (20 g, 17 mmol, 1 eq) in tetrahydrofuran (20 mL) was added dropwise. Conversion was monitored by NMR spectroscopy and after 3 h the reaction was found to be finished. The crude mixture was transferred to a separation funnel and hexane (300 mL) was added, this phase is washed three times with a methanol:water (10:1, 2x 200 mL), afterwards the hexane phase was dried over magnesium sulfate and concentrated *in vacuo* to obtain the pure compound.

Yield: 21.042 g (∼94 %).

^{1}H-NMR (300 MHz, $CDCl_3$): δ (ppm) = 4.44 (m, 1 H, NH−CH−CO), 3.35 (m, 1 H, S−CH_2), 3.22 (m, 1 H, S−CH_2), 3.15 (m, 2 H, NH−CH_2−CH_2), 2.91 (m, 1 H, CH−CH_2−CH_2), 1.94 (m, 1 H, CH−CH_2−CH_2), 1.54 (m, 2 H, Si−CH_2−CH_2), 0.51 (m, 2 H, Si−CH_2).

^{13}C-NMR (100 MHz, $CDCl_3$): δ (ppm) = 60.22 (CH), 43.06 (CH_2), 32.71 (CH_2), 27.12 (CH_2), 23.36 (CH_2), 14.22 (CH_2).

VIII.5.1.4 PDMS-*l*-PEG co-networks from thiolactone-terminated PDMS (section VIII.3.1)

Sample code	PDMS-TLa **144** (mg)	PEG (mg)	EDEA (µL)	PEG content (wt%)
B-PEG$_{250}$	1000	220	128	16.3
B-PEG$_{575}$	1000	506	128	30.9
B-PEG$_{700}$	1000	616	128	35.3

A series of co-networks were prepared with varying PEG content (see table). This variation was achieved by using PEG diacrylates with different molecular weight, *i.e.* 250, 575 and 700 g mol^{-1}, as indicated by the sample code. All these samples were prepared by the following procedure. First, the bivalent PDMS-TLa (**144**) and PEG diacrylate were weighted in the same vial. Next, this mixture was vortexed for 5 minutes at 3000 rpm in order to obtain a homogeneous (opaque) blend. Immediately afterwards, 2,2′-(ethylenedioxy)-bis-(ethylamine) (EDEA) was added with a micropipette to initiate the network formation. The curing mixture was vortexed for an additional 10 seconds and subsequently transferred to a mold (40 x 30 x 1.5 mm) with a syringe. The sample was cured at room temperature. After 1 hour the sample was removed from the mold and was left undisturbed overnight, before characterisation. In all cases, a non-sticky and transparent elastomer was obtained.

VIII.5.1.5 PDMS-*l*-PEG co-networks from multivalent thiolactone-functional PDMS (section VIII.3.2)

Sample code	PDMS-TLa **147** (mg)	PEG (mg)	Bn$-NH_2$ (µL)	PEG content (wt%)
M-PEG$_{250}$	2000	211	185	8.9
M-PEG$_{575}$	2000	487	185	18.3
M-PEG$_{700}$	2000	593	185	21.4

A series of co-networks were prepared with varying PEG content (see table). This variation was achieved by using PEG diacrylates with different molecular weight, *i.e.* 250, 575 and 700 g mol^{-1}, as indicated by the sample code. All these samples were prepared by the following procedure. First, the multivalent PDMS-TLa (**147**) and PEG diacrylate were weighted in the same vial. A small amount of tetrahydrofuran (0.2 mL) was added to lower the viscosity. Next, this mixture was vortexed for 5 minutes at 3000 rpm in order to obtain a homogeneous (opaque) blend. Immediately afterwards, benzylamine (R_1 = Bn) was added with a micropipette to initiate the network formation. The curing mixture

was vortexed for an additional 10 seconds and subsequently transferred to a mold (40 x 30 x 1.5 mm) with a syringe. The sample was cured at room temperature. After 1 hour the sample was removed from the mold and was left undisturbed overnight, before characterisation. In all cases, a non-sticky and transparent elastomer was obtained.

VIII.5.2 Methods

VIII.5.2.1 Soluble fraction

Soxhlet extractions with tetrahydrofuran were performed on a preweighed sample (m_d). After 24 hours, the sample was removed from the solvent and dried in a vacuum oven at 40 °C for 24 hours. Subsequently, the final mass was determined (m_f). The soluble fraction was then calculated using equation VIII.1.

$$SF(\%) = (m_d - m_f)/m_d * 100 \tag{VIII.1}$$

VIII.5.2.2 Swelling of amphiphilic co-networks

The equilibrium swelling characteristics of the networks were determined at room temperature. Preweighed dry samples (150–200 mg) were placed in vials filled with either water or hexane and sealed with a screw cap. Periodically the vials were shaken to facilitate the swelling. After 7 days, the gels were removed from the solvent and were quickly blotted with a paper tissue – to remove the remaining solvent on the surface – and weighed. From both masses, the (mass) swelling ratio was calculated using equation VIII.2, where m_d and m_s is the initial dry mass and the mass of swollen co-network, respectively.

$$S(\%) = \frac{m_s - m_d}{m_d} * 100 \tag{VIII.2}$$

VIII.5.3 Instrumentation

Differential scanning calorimetry (DSC) Differential scanning calorimetry (DSC) analyses were performed with a Mettler-Toledo 1/700 under nitrogen atmosphere. The samples were analysed in aluminium sample pans which contained 5–15 mg of the sample. T_gs were determined from the midpoints in the second heating using the STARe software of Mettler-Toledo. Measurements were performed in a temperature range of -150–70 °C with a rate of 10 K min^{-1}.

Fourier transform infrared spectroscopy (FT-IR) Infrared spectra were recorded with a Perkin Elmer FTIR SPECTRUM 1000 spectrometer, equipped with a PIKE Miracle attenuated total reflectance (ATR) unit. All spectra were recorded with a resolution of 4 cm^{-1} and 16 scans were made for each measurement.

Nuclear magnetic resonance (NMR) All ^{1}H and ^{13}C NMR spectra were recorded with a Bruker Avance 300 (300 MHz) or a Bruker Avance 400 (400 MHz) device. ^{29}Si-^{1}H HMQC spectrum was recorded on a Bruker Avance II 700 (700 MHz). Chemical shifts (δ) are reported in units of parts per million relative to tetramethylsilane. All ^{1}H spectra were referenced to proton signals of residual undeuterated solvents.

Tensile testing All tensile tests were performed on a Tinius-Olsen H10KT tensile tester, equipped with a 100 N load cell, using a flat dog bone type specimen with an effective gauge length of 13 mm, a width of 2 mm, and a thickness of 1 mm. The samples were cut using a RayRan dog bone cutter. The tensile tests were run at a speed of 10 mm min^{-1}.

Thermogravimetric analysis (TGA) All the TGA analyses were performed on a Mettler-Toledo TGA/SDTA 851e under N_2-atmosphere with a heating rate of 10 °C/ min from 25 °C to 800 °C. The thermograms were analysed with the STARe software from Mettler-Toledo.

Rheology Dynamic rheology measurements were performed using a parallel plate configuration (8 mm diameter) with an Anton-Paar MCR 302 rheometer. The gap distance was fixed at 1 mm and the dynamic moduli were measured over time at a constant oscillation frequency (1 Hz), strain (0.1 %) and temperature (25 °C).

VIII.6 Bibliography

1. G. Erdodi, J. P. Kennedy, *Prog. Polym. Sci.* **2006**, *31*, 1–18.
2. J. Scherble, R. Thomann, B. Iván, R. Mülhaupt, *J. Polym. Sci. Part B: Polym. Phys.* **2001**, *39*, 1429–1436.
3. N. Bruns, M. Hanko, S. Dech, R. Ladisch, J. Tobis, J. C. Tiller, *Macromol. Symp.* **2010**, *291-292*, 293–301.
4. D. Park, B. Keszler, V. Galiatsatos, J. P. Kennedy, B. D. Ratner, *Macromolecules* **1995**, *28*, 2595–2601.
5. N. Bruns, J. Scherble, L. Hartmann, R. Thomann, B. Iván, R. Mülhaupt, J. C. Tiller, *Macromolecules* **2005**, *38*, 2431–2438.
6. J. P. Kennedy, *J. Macromol. Sci. Part A: Pure Appl.Chem.* **1994**, *31*, 1771–1790.
7. G. Erdodi, J. P. Kennedy, *J. Polym. Sci. Part A: Polym. Chem.* **2005**, *43*, 4965–4971.
8. Z. Hu, L. Chen, D. E. Betts, A. Pandya, M. A. Hillmyer, J. M. DeSimone, *J. Am. Chem. Soc.* **2008**, *130*, 14244–14252.
9. G. Erdodi, J. P. Kennedy, *J. Polym. Sci. Part A: Polym. Chem.* **2005**, *43*, 3491–3501.
10. J. Kunzler, J. Salamone, *Elastomeric, expandable hydrogel compositions*, **2004**.
11. J. F. Künzler, *Trends Polym. Sci. (Cambridge U. K.)* **1996**, *2*, 52–59.
12. C. Aguado, P. C. Nicolson, L. C. Winterton, Y. Qiu, J. M. Lally, J. M. Schremmer, *Polymeric materials for making contact lenses*, **2004**.
13. T. Chirila, D. Harkin, *Biomaterials and regenerative medicine in ophthalmology*, Woodhead Publishing, **2016**.
14. P. C. Nicolson, J. Vogt, *Biomaterials* **2001**, *22*, 3273–3283.
15. J. Kang, G. Erdodi, J. P. Kennedy, H. Chou, L. Lu, S. Grundfest-Broniatowski, *Macromol. Biosci.* **2010**, *10*, 369–377.
16. G. Guzman, T. Nugay, I. Nugay, N. Nugay, J. Kennedy, M. Cakmak, *Macromolecules* **2015**, *48*, 6251–6262.
17. F. E. Du Prez, E. J. Goethals, R. Schué, H. Qariouh, F. Schué, *Polym. Int.* **1998**, *46*, 117–125.
18. B. Iván, J. P. Kennedy, P. W. Mackey in *Amphiphilic Networks*, *Vol. 469*, American Chemical Society, **1991**, book section 18, pp. 194–202.
19. J. C. Tiller, C. Sprich, L. Hartmann, *J. Controlled Release* **2005**, *103*, 355–367.
20. C. Lin, I. Gitsov, *Macromolecules* **2010**, *43*, 10017–10030.
21. J. Xu, X. Li, F. Sun, *Drug Delivery* **2011**, *18*, 150–158.

22. R. Haigh, N. Fullwood, S. Rimmer, *Biomaterials* **2002**, *23*, 3509–3516.

23. K. Tanahashi, A. G. Mikos, *J. Biomed. Mater. Res. Part A* **2003**, *67A*, 448–457.

24. J. P. Kennedy, *J. Polym. Sci. Part A: Polym. Chem.* **2005**, *43*, 2951–2963.

25. Y. Sun, J. Collett, N. J. Fullwood, S. Mac Neil, S. Rimmer, *Biomaterials* **2007**, *28*, 661–670.

26. S. K. Jewrajka, G. Erdodi, J. P. Kennedy, D. Ely, G. Dunphy, S. Boehme, F. Popescu, *J. Biomed. Mater. Res. Part A* **2008**, *87A*, 69–77.

27. Q. V. Nguyen, D. P. Huynh, J. H. Park, D. S. Lee, *Eur. Polym. J.* **2015**, *72*, 602–619.

28. N. Bruns, J. C. Tiller, *Nano Lett.* **2005**, *5*, 45–48.

29. E. M. Hensle, J. Tobis, J. C. Tiller, W. Bannwarth, *J. Fluorine Chem.* **2008**, *129*, 968–973.

30. L. Mespouille, J. L. Hedrick, P. Dubois, *Soft Matter* **2009**, *5*, 4878–4892.

31. J. Scherble, B. Iván, R. Mülhaupt, *Macromol. Chem. Phys.* **2002**, *203*, 1866–1871.

32. A. T. Metters, K. S. Anseth, C. N. Bowman, *J. Phys. Chem. B* **2001**, *105*, 8069–8076.

33. E. Fournier, C. Passirani, C. N. Montero-Menei, J. P. Benoit, *Biomaterials* **2003**, *24*, 3311–3331.

34. Y. Yuan, A.-K. Zhang, J. Ling, L.-H. Yin, Y. Chen, G.-D. Fu, *Soft Matter* **2013**, *9*, 6309–6318.

35. G. Erdodi, J. P. Kennedy, *J. Polym. Sci. Part A: Polym. Chem.* **2005**, *43*, 4953–4964.

36. G. Lin, X. Zhang, S. R. Kumar, J. E. Mark, *Silicon* **2009**, *1*, 173–181.

37. J. Cui, M. A. Lackey, G. N. Tew, A. J. Crosby, *Macromolecules* **2012**, *45*, 6104–6110.

38. M. Delerba, J. R. Ebdon, S. Rimmer, *Macromol. Rapid Commun.* **1997**, *18*, 723–728.

39. H. C. Kolb, M. G. Finn, K. B. Sharpless, *Angew. Chem. Int. Ed.* **2001**, *40*, 2004–2021.

40. D. Frank, P. Espeel, S. Claessens, E. Mes, F. E. Du Prez, *Tetrahedron* **2016**, *72*, 6616–6625.

41. W. Noll, *Chemistry and technology of silicones*, Elsevier, **1968**, p. 716.

42. T. C. Kendrick, B. M. Parbhoo, J. W. White in *25 - Polymerization of Cyclosiloxanes A2 - Allen, Geoffrey* (Ed.: J. C. Bevington), Pergamon, Amsterdam, **1989**, pp. 459–523.

43. R. G. Jones, W. Ando, J. Chojnowski, *Silicon-Containing Polymers*, Springer Netherlands, **2000**, p. 768.

44. M. A. Brook, *Silicon in organic, organometallic, and polymer chemistry*, J. Wiley, **2000**, p. 704.

45. A. C. Kuo, *Polymer Data Handbook* **1999**, 411–435.

46. P. J. Flory, J. R. Jr., *J. Chem. Phys.* **1943**, *11*, 521–526.

47. L. H. Sperling, *Introduction to physical polymer science*, John Wiley and Sons, **2005**, p. 880.

48. J. N. Lee, C. Park, G. M. Whitesides, *Anal. Chem.* **2003**, *75*, 6544–6554.

49. I. Steyaert, G. Vancoillie, R. Hoogenboom, K. De Clerck, *Polym. Chem.* **2015**, *6*, 2685–2694.

50. S. Fery-Forgues, J.-P. Fayet, A. Lopez, *J. Photochem. Photobiol. A* **1993**, *70*, 229–243.

51. S. Mukherjee, A. Chattopadhyay, A. Samanta, T. Soujanya, *J. Phys. Chem.* **1994**, *98*, 2809–2812.

52. S. Martens, J. Van den Begin, A. Madder, F. E. Du Prez, P. Espeel, *J. Am. Chem. Soc.* **2016**, *138*, 14182–14185.

Chapter IX

General conclusions and perspectives

IX.1 Conclusions

The aim of this doctoral work was the development of interfacial systems based on reactions of triazolinediones (TADs) with isolated and conjugated double bonds (Scheme IX.1). While reactions at the solid-liquid interface, *i.e.* surface modifications, can have a significant impact on the interaction of the material with its surroundings, reactions at the liquid-liquid interface were expected to yield polymeric beads and microcapsules. Although TAD compounds already found many applications in both organic chemistry and polymer science, only very few reports were available at the start of this work on the surface modification of polymers with simple, non-functional TADs.[1,2]

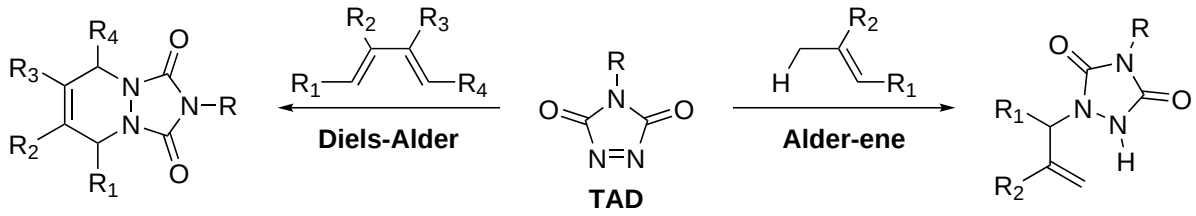

Scheme IX.1: Diels-Alder (left) and Alder-ene reaction (right) of a triazolinedione (TAD) with a diene or an isolated alkene, respectively.

Despite the positive characteristics of triazolinediones, their widespread use is still hampered because they are often considered as exotic reagents by chemists or industrial partners. Therefore, this PhD research started with an overview of the reported work on this fascinating chemistry (Chapter II).[3] The first part of this chapter focussed on the synthesis of these compounds and summarises the various synthetic routes that can yield a TAD compound. Next, the reactivity of TAD moieties is briefly discussed, with a focus on both

the desired reactions in the context of this work and the possible side-reactions that should be taken into account. Finally, an overview of the most important applications in the field of polymer science is provided, together with the most recent advances in our research group that were the foundations of this doctoral work.

Until now, the most important limiting factor for the development of TAD-based applications, is the absence of a general synthesis strategy that affords functional triazolinediones. While some functional compounds are already described in literature, Chapter III reports scalable synthesis strategies for two essentially different fluorinated triazolinediones as well as two TAD-based dyes. Once these functional TADs were obtained, a first proof of concept provided evidence of their applicability for surface modifications. On the other hand, the substrates that were necessary for this proof of concept were also synthesised via TAD chemistry. Indeed, combining an excess of a multivalent unsaturated compound with a TAD cross-linker represented an elegant strategy to produce polymeric materials with residual unsaturations. The structure of the unsaturated monomer was shown to have a significant impact on the the glass transition temperature of the final material and – most importantly – on the cross-linking kinetics.

Multiple different research projects originated from the successful syntheses and concepts presented in the aforementioned chapter (Chapter III). Firstly, the two synthesised fluorinated triazolinediones were investigated as reactive additives, *i.e.* additives that cannot leach from the material over time, to modify the wetting properties of polydienes. Both a surface modification, in which the solid material is submerged in a solution of the TAD compound, and a homogeneous treatment was performed. While all the modifications were successful, the most remarkable results were obtained when an aliphatic fluorinated triazolinedione was reacted with the polymer in solution. When this polymer was cast, the fluorinated chains were found to assemble at the surface, leading to a high apparent additive content, even at low modification degrees (Figure IX.1).[4] Moreover, the TAD-based approach resulted in fast functionalisations at room temperature, was not limited to a specific solvent and thus outperformed previously reported functionalisation strategies.

During the synthesis of TAD-based polymeric materials from trivalent unsaturated monomers (Chapter III), we found that the diene-containing compounds reacted too fast with the TAD cross-linker to obtain a homogeneous mixture prior to gelation. In

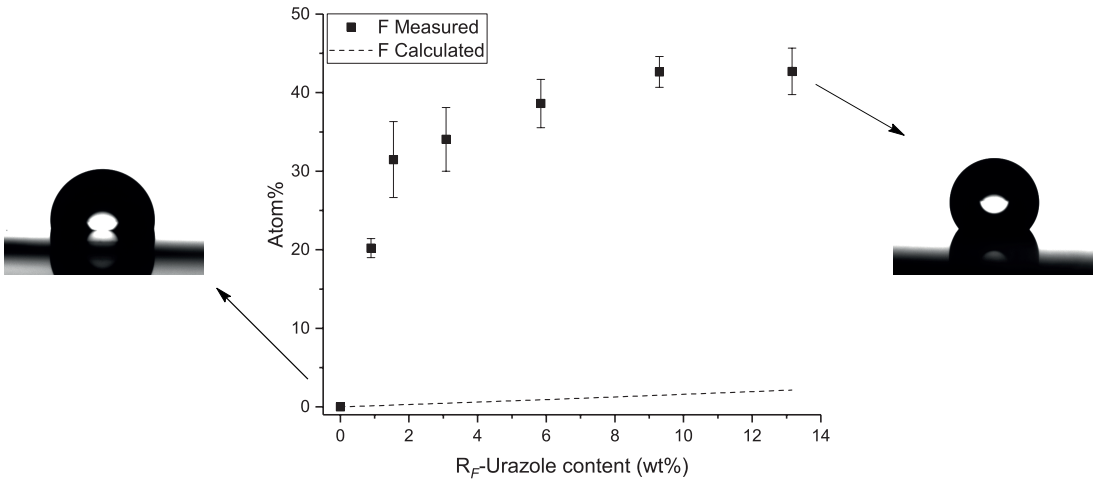

Figure IX.1: XPS analysis of R_FTAD modified SIS shows a higher fluorine content than expected for a homogeneous distribution of the additive, indicating an assembly of fluorinated chains at the surface of the material.

Chapter V, such a reactive pair was deposited on a surface in an alternating fashion to obtain a coating rather than a homogeneous material. Even in a 'simple' conventional setup, requiring only a set of beakers and a pair of tweezers, the TAD-based layer-by-layer assemblies outperformed all previously reported click chemistries in terms of speed. While a comparable system required more than 6.5 hours to obtain 20 layers,[5–7] we demonstrated the deposition of 58 layers in merely 20 minutes.[8]

While layer-by-layer assemblies result in a full surface coverage of a TAD-compatible substrate, we showed in Chapter VI that a patterned surface functionalisation could be obtained by using microcontact chemistry instead. Moreover, by grafting a reversibly reacting indole on a silicon wafer, a surface was generated on which the TAD 'ink' could be printed, removed and reprinted. As reactive ink, a TAD-bearing ATRP-initiator was applied, which could be used to graft polymer brushes from the surface after every printing step. Consequently, a truly rewritable substrate was obtained for the first time, on which micropatterned polymer nanofilms could be repeatedly grafted and degrafted (Figure IX.2).[9] To the best of our knowledge, this initial report on rewritable surfaces still represents the fastest and mildest strategy to (chemically) write and rewrite patterned polymer brushes on a substrate.

Besides the development of TAD-based reactions at the solid-liquid interface, as discussed in chapters IV–VI, we also aimed to apply this chemistry for the synthesis and functionalisation of polymeric beads and microcapsules in a liquid-liquid biphasic system. However, the

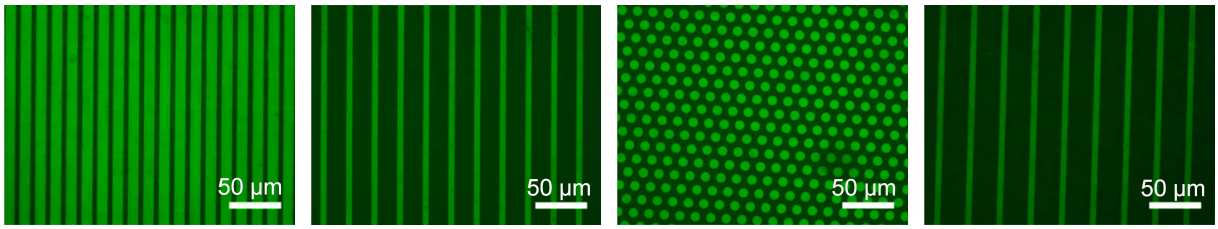

Figure IX.2: Four consecutive write and erase cycles of polymer brushes on a single substrate, visualised by fluorescence microscopy imaging.

development of such interfacial polymerisations revealed some limitations in the reactivity of TAD moieties. Therefore, Chapter VII discussed these limitations and proposed a thiolacone-based one-pot multi-component reaction as a complementary alternative to triazolinediones. This chapter also includes the development of the first interfacial polymerisations using a chloroform-soluble polystyrene containing multiple thiolactone moieties. When this polymer was mixed with a multivalent acrylate and subsequently dispersed in an aqueous solution containing an amine, aminolysis of the thiolactone units triggered the cross-linking process, which resulted in the generation of polymeric particles.

Finally, because of the possibility to covalently link both an amine and an acrylate to a single thiolactone unit in a one-pot fashion, Chapter VIII investigated this chemistry as a new cross-linking strategy for the preparation of silicone-based amphiphilic co-networks. First, thiolactone units were attached to hydrophobic yet functional polysiloxanes, which were then mixed with poly(ethylene glycol) diacrylates of various chain lengths as hydrophilic cross-linkers. Similarly to the interfacial polymerisations, addition of an amine triggered the cross-linking of the polymer blend. The networks were shown to consist of nanophase separated hydrophilic and hydrophobic domains, while the swelling ratio in both water and hexane could be rationalised by the PEG content and the cross-linking density. Furthermore, functionalisation of the amphiphilic networks was demonstrated by adding a functional acrylate to the curable polymer mixture. While the thiolactone-based chemistry already showed promising results in its new applications, as described in chapters VII and VIII, more research will be necessary to further demonstrate the added value of this strategy over the current state of the art.

IX.2 Future perspectives

Since the intermediate conclusions of each experimental chapter already provide a detailed topic-specific outlook, only the most important future perspectives will be summarised in this section. As already pointed out, the synthesis of functional triazolinediones as well as their complementary reaction partners can be considered as the key to success in this work, since multiple research projects originated from the compounds described in Chapter III. On the other hand, multiple application-driven ideas could not be successfully accomplished because of the failure to synthesise the required TAD compounds. Typically, the chemoselective modification of 4-functionalised urazoles is the crucial step in the overall synthesis as a result of the acidity and nucleophilic reactivity of the urazole moiety. Therefore, a simple, robust and cheap 'polymer-chemist-proof' protecting group strategy, to temporarily block the urazole reactivity, should greatly facilitate the development of a general synthesis strategy for functional triazolinediones. This challenge has now been taken up in an ongoing PhD research, supervised by Prof. Johan Winne.

Apart from this general suggestion to help the overall research on TAD chemistry, various topic-specific future research projects can be identified. For example, while the orange azobenzene-functional triazolinedione (Chapter III) was already applied in our group to visualise a successful transclick reaction,[10] we originally envisioned its application as a visual demonstrator for a bead-to-bead transclick system. In this system, a surface-bound or solid-supported indole (the 'sender') would be first modified with a (functional) triazolinedione, *i.e.* the 'message', whereas a solid-supported diene would act as the 'recipient'. When both these materials are then submerged in a heated solution of a second indole, the latter molecule should act as the 'messenger' that transfers the TAD compound from the solid-supported indole to the diene, without the need for a physical contact between the two materials.

For the patterning of surfaces via microcontact chemistry, multiple improvements should be possible through additional research. On the one hand, an indole could be grafted on the surface which is characterised by a lower reversibility temperature after its reaction with a triazolinedione,[10] and consequently allows for milder conditions for the rewriting procedure. On the other hand, when an indole is synthesised bearing a highly reactive trichlorosilane,

this compound could be grafted directly to a silicon substrate, without the need for the hydrothiolation step in the current system. Moreover, by synthesising a catechol-type TAD-complementary molecule, the applicability of this microcontact printing might be expanded to other substrates as well. Finally, when a suitable (di-)ene is attached to the surface in a patterned fashion, microcontact chemistry can be combined with layer-by-layer assemblies to easily obtain patterned coatings with a controllable thickness.

In the case of liquid-liquid biphasic systems, we believe that the future for triazolinediones is less bright. While additional research might eventually result in the development of a working system, we expect that only a strict set of experimental parameters will successfully yield polymeric particles, which cancels out the advantages of the TAD cross-linking. In contrast, the application of thiolactones for the production of polymeric particles proved to be much more promising. With an additional experimental effort, it should be possible to tune the particle size and to introduce extra chemical or physical functionalities, as long as they are compatible with the thiolactone strategy.

In summary, this doctoral work might have come to an end, but the work is far from over. Many challenges as well as opportunities remain for the application of both triazolinedione- and thiolactone-based chemistry at the interface, where small molecules and polymer materials meet.

IX.3 Bibliography

1. E. Cutts, G. Knight, *Surface treatment of polymers*, **1974**, US3966530.

2. G. Chen, M. Gupta, K. Chan, K. Gleason, *Macromol. Rapid Commun.* **2007**, *28*, 2205–2209.

3. K. De Bruycker, S. Billiet, H. A. Houck, S. Chattopadhyay, J. M. Winne, F. E. Du Prez, *Chem. Rev.* **2016**, *116*, 3919–3974.

4. K. De Bruycker, M. Delahaye, P. Cools, J. Winne, F. E. Du Prez, *Macromol. Rapid Commun.* **2017**, *38*, 1700122.

5. G. K. Such, J. F. Quinn, A. Quinn, E. Tjipto, F. Caruso, *J. Am. Chem. Soc.* **2006**, *128*, 9318–9319.

6. C. Schulz, S. Nowak, R. Fröhlich, B. J. Ravoo, *Small* **2012**, *8*, 569–577.

7. W. J. Yang, D. Pranantyo, K.-G. Neoh, E.-T. Kang, S. L.-M. Teo, D. Rittschof, *Biomacromolecules* **2012**, *13*, 2769–2780.

8. B. Vonhören, O. Roling, K. De Bruycker, R. Calvo, F. E. Du Prez, B. J. Ravoo, *ACS Macro Lett.* **2015**, *4*, 331–334.

9. O. Roling, K. De Bruycker, B. Vonhören, L. Stricker, M. Körsgen, H. F. Arlinghaus, B. J. Ravoo, F. E. Du Prez, *Angew. Chem. Int. Ed.* **2015**, *54*, 13126–13129.

10. H. A. Houck, K. De Bruycker, S. Billiet, B. Dhanis, H. Goossens, S. Catak, V. Van Speybroeck, J. Winne, F. Du Prez, *Chem. Sci.* **2017**, *8*, 3098–3108.

Hoofdstuk X

Nederlandstalige samenvatting

X.1 Introductie

In 2001 introduceerden Sharpless en medewerkers het 'klikchemie' concept, wat gedefinieerd werd door een lijst van criteria.[1] Deze reacties moeten onder meer robuust en snel zijn, moeten toelaten om een variëteit aan moleculen te koppelen met een hoge opbrengst en met bijproducten die eenvoudig te scheiden zijn. Los van deze definities kan het gewenste product meestal afgezonderd worden van bijproducten en reagentia door een brede waaier aan technieken in de organische synthese, terwijl dit veel lastiger is in het geval van polymeren. Bovendien worden polymeren veelal gesynthetiseerd op een grote schaal, wat de opzuivering verder bemoeilijkt. Daarom is het klik concept vooral nuttig gebleken voor polymeermodificaties, wat resulteerde in de synthese van polymeerarchitecturen die niet makkelijk te verkrijgen zijn via traditionele reacties.[2–4]

De Cu (I)-gekatalyseerde azide-alkyn cycloadditie (CuAAC) staat algemeen bekend als de eerste klikreactie,[5] waarna veel andere koppelingsstrategieën herontdekt werden als klikchemie, zoals de nucleofiele ring-opening van epoxiden of additiereacties aan onverzadigde koolstof-koolstof bindingen. Omdat echter weinig tot geen reacties voldoen aan alle originele criteria van Sharpless, werd de term 'klik' allesbehalve strikt toegepast en werd hij al snel een synoniem voor een snel en efficiënt proces. Daarom stelde Barner-Kowollik *et al.* een licht aangepaste lijst van criteria voor, die de ware klikchemie definieert in de context van polymeerchemie.[6] Zo werd bijvoorbeeld bijvoorbeeld een vereiste van equimolariteit toegevoegd voor de reagentia, die toestaat om polymeer-polymeerkoppelingen uit te voeren zonder dat het product uit een mengsel van polymeren moet afgezonderd worden.[7]

Ondanks het blijvende misbruik van de term 'klik' en het lopend onderzoek naar de perfecte klikreactie, is het concept van klikchemie reeds heel nuttig gebleken, en moet het misschien eerder aanzien worden als een manier van denken bij het ontwikkelen van een experiment in plaats van een strikte set van regels en definities. In deze context halen veel toepassingen in de materiaalkunde winst uit snelle en efficiënte klik geïnspireerde reacties. Zo worden bijvoorbeeld de meeste commerciële polymeren gemengd met additieven voordat ze hun finale vorm krijgen om de bulkeigenschappen te verbeteren, of worden ze achteraf gecoat om de interactie met de omgeving te wijzigen.[8,9] Omdat in de meeste gevallen noch de additieven, noch de coatings chemisch aan het polymeer verankerd worden, is het lekken resp. delamineren een vaak voorkomend probleem dat leidt tot een verandering in materiaaleigenschappen over de tijd.[10,11] Deze problemen kunnen aangepakt worden door specifieke groepen covalent te binden aan het polymeer, terwijl een significante stijging in verwerkingstijd uitblijft door een van de klik geïnspireerde reacties toe te passen.

Chemie op basis van triazolinedionen (TAD's) vertegenwoordigt een ander voorbeeld van een welbekende en goed onderzochte koppelingsmethode die recent opnieuw aan interesse gewonnen heeft, hoofdzakelijk omwille van het klik-karakter van de reacties met een variëteit aan onverzadigde componenten. De onderzoeksgroepen van Barbas en Madder hebben bijvoorbeeld de efficiënte bioconjugatie beschreven van TAD reagentia met tyrosine en furylalanine in peptiden en proteïnen,[12–14] terwijl onze groep de hoge reactiviteit tussen TAD's en geconjugeerde diënen of geïsoleerde alkenen heeft aangetoond door middel van de synthese van blokcopolymeren en vernette plantoliën.[15,16] Triazolinedionen worden dan ook algemeen beschouwd als de sterkste diëno- en enofielen in de organische chemie (Figuur X.1a).[17,18] TAD reacties zijn typisch afgelopen in enkele seconden tot minuten, gaan door bij kamertemperatuur zonder een katalysator, geven een hoge opbrengst, en voldoen dus aan veel criteria van een klikreactie. Wanneer bovendien TAD's reageren met een indool in plaats van een simpel alkeen, wordt reversibiliteit waargenomen in het Alder-*een* product bij verwarming (Figuur X.1b). Onze groep heeft dit dynamisch TAD-indool koppel verder onderzocht en ontwikkelde uiteindelijk het 'transklik' concept, dat een cascade van een achterwaartse en voorwaartse klikreactie beschrijft waardoor netto een TAD component overgedragen wordt van een indool naar een andere reactiepartner, gelijkaardig aan een omestering.[15] Dit concept werd vervolgens toegepast voor de synthese van reversibele blokcopolymeren en dynamisch vernette materialen.

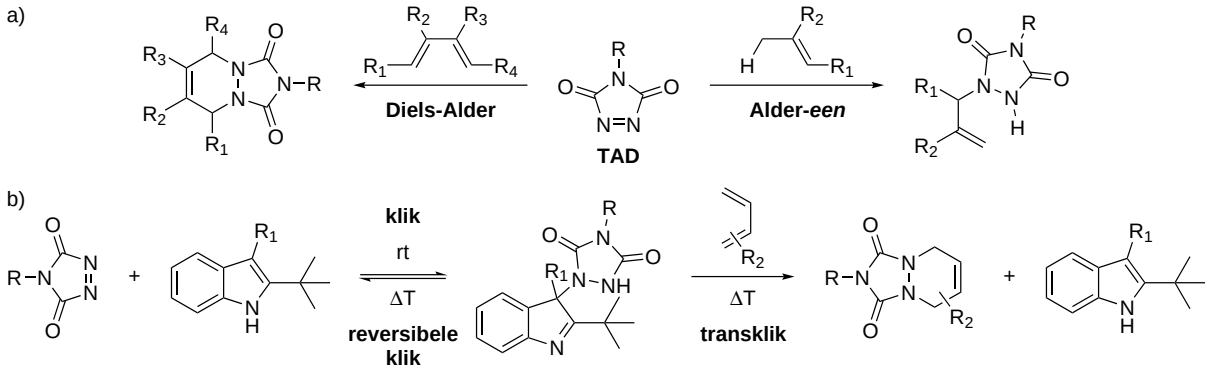

Figuur X.1: **(a)** Reactie van een triazolinedion (TAD) met een diëen (links) or een geïsoleerd alkeen (rechts) in een Diels-Alder- resp. Alder-*een*-reactie. **(b)** Een reversibele Alder-*een*-reactie tussen een TAD en een indool, gevolgd door een irreversibele Diels-Alderreactie. Deze netto overdracht van de TAD component naar van het indool naar het diëen is een voorbeeld van een transklik reactie.

Het doel van dit doctoraat is de verkenning van triazolinedion chemie als basis voor heel efficiënte reacties in het raakvlak tussen twee fasen. Deze interfaciale reacties omvatten zowel modificaties van vaste substraten met TAD componenten in oplossing, *i.e.* reacties aan de vast-vloeistof interfase, alsook de synthese en functionalisatie van polymeerpartikels of microcapsules, namelijk reacties in een vloeistof-vloeistof tweefasensysteem. In het eerstgenoemde geval wordt verwacht dat locale concentratie-effecten de reactiekinetiek significant zullen beïnvloeden, terwijl de identificatie van geschikte complementaire reactiepartners, die oplosbaar zijn in twee orthogonale vloeistoffen, de grootste uitdaging zal zijn in het laatste geval. Hoewel sommige niet-functionele triazolinedionen kunnen worden vervluchtigd onder vacuum, zullen reacties aan de gas-vloeistof of de gas-vast interfase – zoals chemische dampafzetting – niet worden onderzocht in dit werk.

X.2 Overzicht van het proefschrift

Triazolinedionen zijn – ondanks hun exotische reputatie – unieke reagentia in de organische synthese die reeds veel toepassingen gevonden hebben in verschillende onderzoeksdisciplines. Daarom zal **Hoofdstuk II** een gedetailleerd overzicht geven over de beschikbase TAD componenten, samen met de bijhorende synthesestrategieën.[19] Verder zullen de reactiviteit en de belangrijkste toepassingen op het gebied van polymeerchemie besproken worden. Het eerste deel van dit manuscript voorziet dus de theoretische achtergrond voor de chemie die zal gebruikt worden doorheen dit doctoraatsonderzoek.

Omdat geen algemene synthesestrategie voorhanden is voor de productie van functionele triazolinedionen, zal **Hoofdstuk III** de ontwikkeling van schaalbare syntheses bespreken voor dergelijke producten. Los van deze componenten, gericht op de introductie van functionaliteit in een materiaal, zullen vernette materialen gesynthetiseerd en gekarakteriseerd worden die TAD-complementaire groepen bevatten. Deze materialen zullen ten slotte gebruikt worden om de toepasselijkheid van de functionele TAD's voor oppervlakmodificaties aan te tonen.

Hoofdstuk IV onderzoekt de mogelijkheid om de bevochtigingseigenschappen van verschillende veelgebruikte bulkpolymeren te beïnvloeden met behulp van gefluoreerde triazolinedionen die gesynthetiseerd werden in het kader van Hoofdstuk III.[20] Zowel oppervlakmodificaties – waarbij een vast materiaal ondergedompeld wordt in een oplossing van de TAD component – als een homogene behandeling in oplossing zullen bestudeerd worden. De impact van de modificaties op de eigenschappen van het oppervlak worden gekwantificeerd door contacthoekmetingen, terwijl deze resultaten zullen verklaard worden door een combinatie van bulk- en oppervlakanalyses.

In tegenstelling tot de modificatie van een onverzadigd polymeer, zal **Hoofdstuk V** de mogelijkheid demonstreren tot afzetting van een TAD gebaseerde coating met een gecontroleerde dikte op een anorganisch substraat.[21] In een eerste stap zal een onverzadigd silaan verankerd worden op een silicium *wafer*, dat vervolgens afwisselend gereageerd wordt met een tweewaardige TAD-component en een driewaardig diëen. Via een dergelijke strategie kan een coating laag per laag afgezet worden.

In plaats van het volledige oppervlak van een substraat te bedekken met een TAD gebaseerde coating, beschrijft **Hoofdstuk VI** het gebruik van microcontactchemie om een functionele TAD-component aan te brengen volgens een specifiek patroon.[22] In de eerste fase zal een eenvoudig TAD-compatibel substraat gesynthetiseerd worden – dat irreversibel reageert – om het printen van een triazolinedion 'inkt' te optimaliseren. Vervolgens zal reversibiliteit geïntroduceerd worden door het verankeren van een indool op een silicium *wafer*. Op die manier kunnen TAD transklik reacties ontwikkeld worden in een interfaciaal systeem, namelijk van een indool op een vast substraat naar een competitieve reactiepartner in oplossing.

Net zoals andere 'klik' geïnspireerde reacties, is het triazolinedion platform niet perfect en onthulde het enkele van zijn nadelen in de loop van dit doctoraatsonderzoek. **Hoofdstuk VII** zal een overzicht geven van deze beperkingen in de context van vloeistof-vloeistof tweefasensystemen. Vervolgens zal thiolactonchemie geïntroduceerd worden als een complementaire strategie die gekenmerkt wordt door gelijkaardige voordelen, maar niet belemmerd wordt door de TAD-gerelateerde problemen. Ten slotte zal de toepasselijkheid van deze thiolactonchemie aangetoond worden voor de synthese van polymeerpartikels via een interfaciale polymerisatie.

Omdat thiolactonen een snelle *one-pot* dubbele modificatie toelaten, zal **Hoofdstuk VIII** deze chemie onderzoeken als alternatieve vernettingsstrategie voor de productie van amfifiele co-netwerken gebaseerd op siliconen. In plaats van een macroscopische faseschеiding zoals bij interfaciale polymerisaties, worden deze netwerken gekenmerkt door de aanwezigheid van microscopische hydrofiele en hydrofobe domeinen die ervoor zorgen dat het materiaal kan zwellen in zowel water als organische solventen. Na de synthese van meerdere thiolacton-bevattende siliconen, zullen deze hydrofobe polymeren gereageerd worden met tweewaardige acrylaten – gebaseerd op poly(ethyleen glycol) – als hydrofiele component. Verschillende netwerken zullen gesynthetiseerd en gefunctionaliseerd worden, gevolgd door een karakterisatie van hun amfifiele eigenschappen.
Hoofdstuk IX geeft een algemene conclusie van het beschreven doctoraatswerk en licht enkele toekomstplannen toe voor de TAD-chemie in tweefasensystemen.

X.3 Overzicht van de resultaten

De afwezigheid van een algemene strategie voor de synthese van functionele triazolinedionen is de belangrijkste limiterende factor voor de ontwikkeling van TAD gebaseerde toepassingen.[19] Terwijl sommige functionele componenten reeds beschreven zijn in de literatuur, beschrijft Hoofdstuk III schaalbare syntheses voor twee essentieel verschillende gefluoreerde TAD's en twee TAD kleurstoffen. Na de synthese van deze componenten, leverde een eerste *proof of concept* bewijs van hun toepasselijkheid voor oppervlakmodificaties. Anderzijds werden de substraten die nodig waren voor dit *proof of concept* ook gesynthetiseerd met behulp van TAD-chemie. Door een overmaat van een meerwaardig onverzadigde component the combineren met een TAD vernetter, werden polymeermaterialen met resterende

onverzadigdheden op een elegante manier verkregen. De structuur van de onverzadigde monomeren bleek een significante impact the hebben op de glastransitietemperatuur van het finale material en – nog belangrijker – op de kinetiek van de vernetting.

Meerdere onderzoeksprojecten ontstonden uit de succesvolle syntheses en concepten die gepresenteerd werden in het eerder vermelde hoofdstuk (Hoofdstuk III). De twee gesynthetiseerde gefluoreerde triazolinedionen werden bijvoorbeeld onderzocht als reactieve additieven, namelijk additieven die niet uit het materiaal kunnen logen, om de bevochtigingseigenschappen van polydiënen te beïnvloeden. Hoewel alle modificaties – zowel oppervlaktemodificaties als homogene behandelingen – succesvol waren, werden de meest merkwaardige resultaten bekomen wanneer een alifatisch gefluoreerd triazolinedion gereageerd werd met het polymeer in oplossing. Wanneer dit polymeer afgezet werd op een substraat bleken de gefluoreerde ketens zich te ordenen aan het oppervlak, wat resulteerde in een schijnbaar hoge additiefgehalte, zelfs bij een lage modificatiegraad (Figuur X.2).[20] Deze TAD-gebaseerde aanpak maakte een snelle functionalisatie bij kamertemperatuur mogelijk, was niet gelimiteerd tot één specifiek solvent, en overtreft bijgevolg de eerder gerapporteerde functionalisatiestrategieën.

Tijdens de synthese van TAD gebaseerde polymeermaterialen uit driewaardig onverzadigde monomeren (Hoofdstuk III), reageerden de diëen-bevattende componenten zo snel met de TAD vernetter dat het onmogelijk was om een homogeen reactiemengsel te bekomen

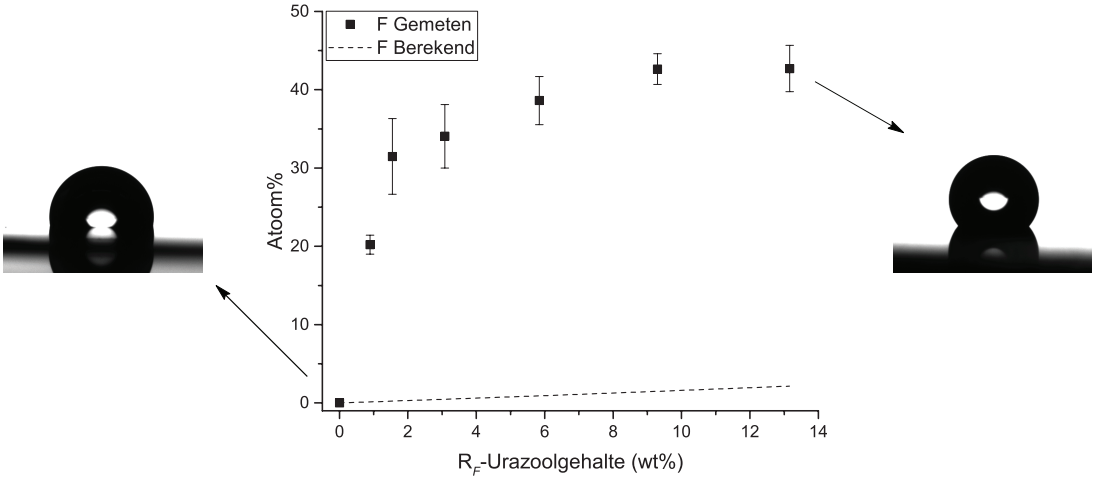

Figuur X.2: XPS analyse van een styreen-isopreen-styreen triblock copolymeer dat gemodificeerd werd met een alifatisch gefluoreerd triazolinedion. Het opgemeten fluorgehalte is significant hoger dan de waarde die verwacht wordt op basis van een homogene distributie van het additief, wat wijst op een ordening van de gefluoreerde ketens aan het oppervlak van het materiaal.

voordat gelering optrad. In Hoofdstuk V werd een dergelijk reactief paar op alternerende wijze op een substraat afgezet om een coating te verkrijgen in plaats van een homogeen materiaal. Zelfs in een 'simpele', conventionele setup – waarvoor slechts een paar bekers en een pincet nodig is – presteerde deze TAD gebaseerde laag-per-laagafzetting beter dan alle eerder gerapporteerde klik-geïnspireerde chemieën op het gebied van reactiesnelheid. Waar een vergelijkbaar systeem nog meer dan 6.5 uur vereist voor de synthese van een coating met 20 lagen,[23–25] werden in dit hoofdstuk 58 lagen afgezet in slechts 20 minuten.[21]

Waar laag-per-laagafzettingen resulteren in een volledige bedekking van het oppervlak van het TAD-compatibele substraat, demonstreerde Hoofdstuk VI dat een patroon op het oppervlak kan aangebracht worden door gebruik te maken van microcontactchemie. Bovendien kan een indool – dat op reversibele wijze reageert met TAD's – verankerd worden op een silicium *wafer* om een oppervlak te genereren waarop een TAD 'inkt' kan geprint en gewist worden. Als reactieve inkt werd een TAD component gebruikt die gelijktijdig ook een ATRP initiator is, waardoor polymeerketens konden gegroeid worden van het oppervlak na elke print. Bijgevolg werd voor het eerst een waar herschrijfbaar oppervlak verkregen, waarop polymeerfilms volgens een specifiek patroon konden gegroeid worden, om deze vervolgens meermaals te vervangen door polymeerfilms met een ander patroon (Figuur X.3).[22] Tot op heden is de TAD-indool strategie nog steeds de snelste en mildste methode om patronen van polymeerketens (chemisch) te schrijven en te herschrijven op een oppervlak.

Naast de ontwikkeling van TAD gebaseerde reacties aan de vast-vloeistof interfase, zoals beschreven in hoofdstukken IV–VI, werd ook geprobeerd om deze chemie toe te passen voor de synthese en functionalisatie van polymeerpartikels en microcapsules in een vloeistof-vloeistof tweefasensysteem. Tijdens de ontwikkeling van dergelijke interfaciale polymerisaties werden echter enkele beperkingen ontdekt in de reactiviteit van de TAD

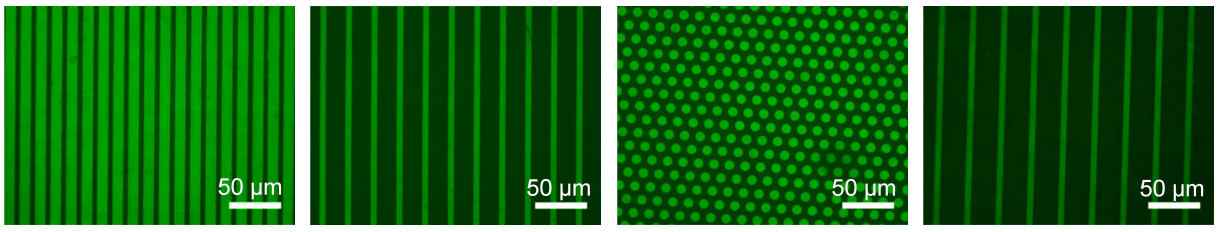

Figuur X.3: Vier opeenvolgende schrijf- en wiscycli van polymeerfilms op hetzelfde substraat, gevisualiseerd door fluorescentie microscopie.

groepen. Daarom bespreekt Hoofdstuk VII in een eerste plaats die beperkingen en stelt het een thiolacton *one-pot* multicomponentreactie voor als een complementaire strategie voor triazolinedionen. Dit hoofdstuk beschrijft eveneens de ontwikkeling van de eerste interfaciale polymerisaties met een polystyreen dat meerdere thiolactongroepen bevat. Wanneer dit polymeer met een meerwaardig acrylaat gemengd werd in chloroform en vervolgens gedispergeerd werd in een waterige oplossing van een amine, zette de aminolyse van thiolactongroepen het vernettingsproces in gang met de uiteindelijke productie van polymeerpartikels tot gevolg.

Wegens de mogelijkheid om zowel een amine en een acrylaat covalent te binden aan één thiolactongroep, werd in Hoofdstuk VIII ten slotte de mogelijkheid onderzocht om deze chemie te gebruiken als nieuwe vernettingsstrategie voor de productie van amfifiele conetwerken. Eerst werden thiolactonbevattende polysiloxanen gesynthetiseerd die vervolgens gemengd werden met poly(ethyleen glycol) diacrylaten met een variabele ketenlengte als hydrofiele vernetters. Gelijkaardig aan de interfaciale polymerisaties, werd de vernetting van het polymeermengsel gestart door toevoeging van een amine. Via DSC-analyse kon aangetoond worden dat de netwerken bestaan uit een kenmerkende fasegescheiden structuur van microscopische hydrofiele en hydrofobe domeinen, terwijl de zwellingsgraad in water en hexaan kon verklaard worden door het gehalte aan PEG en de vernettingsdichtheid. Ten slotte werd de mogelijkheid tot functionalisatie van deze netwerken aangetoond door het toevoegen van een functioneel acrylaat aan het polymeermengsel. Terwijl reeds veelbelovende resultaten behaald werden in de nieuwe toepassingen van de thiolactongebaseerde strategie, zoals beschreven in hoofdstukken VII en VIII, zal meer onderzoek nodig zijn om de toegevoegde waarde van deze chemie ten opzichte van de huidige *state-of-the-art* aan te tonen.

X.4 Vooruitblik

Zoals eerder beschreven kan de synthese van functionele triazolinedionen en de bijhorende reactiepartners aanzien worden als de sleutel tot succes in dit doctoraatswerk, aangezien meerdere onderzoeksprojecten ontstonden uit de componenten die beschreven werden in Hoofdstuk III. Langs de andere kant konden meerdere toepassingsgedreven ideeën niet tot een goed einde worden gebracht omdat de vereiste TAD-verbindingen niet konden worden

gesynthetiseerd. De cruciale stap in the algemene synthese is typisch de chemoselectieve modificatie van 4-gefunctionaliseerde urazolen, als gevolg van de aciditeit en nucleofiele reactiviteit van de urazoolgroep. Daarom wordt verwacht dat een goedkope en *dummy-proof* beschermgroep voor urazolen de ontwikkeling van een algemene synthesestrategie voor functionele triazolinedionen moet mogelijk maken. De zoektocht naar een dergelijke beschermgroep is momenteel onderdeel van een lopend doctoraatsonderzoek.

Los van deze algemene suggestie om het onderzoek naar toepassingen van TAD-chemie te vereenvoudigen, kunnen meerdere onderwerp-specifieke onderzoeksprojecten gedefinieerd worden. Zo werd bijvoorbeeld de oranje azobenzeen-gefunctionaliseerde TAD component (Hoofdstuk III) reeds toegepast in onze onderzoeksgroep om een succesvolle transklik reactie aan te tonen,[26] hoewel deze origineel werd gesynthetiseerd als een visuele hulp voor een partikel-naar-partikel transklik systeem. In dit vooropgestelde systeem kan een indool dat gebonden is aan een vaste fase – gelijkaardig aan vastefasesynthese voor peptiden of DNA – optreden als afzender wanneer het gemodificeerd wordt met een (functioneel) triazolinedion, de boodschap. Een diëen op een vaste fase is in dat geval de ontvanger. Wanneer beide materialen vervolgend ondergedompeld worden in een warme oplossing van een tweede indool, zou deze laatste molecule moeten optreden als boodschapper en de TAD-component over brengen van de ene vaste fase naar de andere, zonder de nood aan fysiek contact tussen zender en ontvanger.

Extra onderzoek moet meerdere verbeteringen mogelijk maken voor de productie van patronen op oppervlakken via microcontact chemie. In de eerste plaats moet het mogelijk zijn om een indool aan het oppervlak te verankeren die gekenmerkt wordt door een lagere reversibiliteitstemperatuur wanneer hij reageert met een TAD,[26] wat het herschrijven mogelijk moet maken onder mildere condities. Wanneer daarnaast een indool gesynthetiseerd wordt dat een reactief trichlorosilaan bevat, kan deze component direct verankerd worden aan een silicium substraat, zonder de bijkomende hydrothiolering in het huidige systeem. Bovendien kan een TAD-complementaire molecule mogelijk aan andere (metallische) oppervlakken verankerd worden door het incorporeren van een catechol-type groep, wat de mogelijkheden van dit systeem nog verder uitbreidt. Ten slotte kan de mictocontact chemie gecombineerd worden met de laag-per-laagafzettingen door een geschikt (di-)*een* volgens een patroon op het oppervlak aan te brengen om op een eenvoudige wijze polymeercoatings

met een controleerbare dikte en patroon te verkrijgen.

Voor toepassingen in vloeistof-vloeistof tweefasensystemen is er wellicht geen toekomst voor triazolinedionen weggelegd. Terwijl extra onderzoek uiteindelijk zou kunnen resulteren in de ontwikkeling van een werkend systeem, wordt verwacht dat deze systemen slechts heel beperkt zullen toepasbaar zijn, wat de voordelen van de TAD-chemie teniet doet. De toepassing van thiolactonen voor de productie van polymeerpartikels lijkt langs de andere kant wel veelbelovend. Met een bijkomende experimentele inspanning moet het mogelijk zijn om de partikelgrootte te variëren en om extra chemische of fysische functionaliteiten te introduceren, zolang deze maar compatibel zijn met de thiolactonchemie.

Samengevat is dit doctoraatswerk wel tot een einde gekomen, maar is er nog steeds ruimte voor verbetering. Voor de toepassingen van zowel TAD- als thiolactonchemie aan de interfase zijn er nog veel uitdagingen en mogelijkheiden die moeten onderzocht worden.

X.5 Bibliografie

1. H. C. Kolb, M. G. Finn, K. B. Sharpless, *Angew. Chem. Int. Ed.* **2001**, *40*, 2004–2021.
2. C. J. Hawker, V. V. Fokin, M. G. Finn, K. B. Sharpless, *Aust. J. Chem.* **2007**, *60*, 381–383.
3. A. Inglis, S. Sinnwell, M. Stenzel, C. Barner-Kowollik, *Angew. Chem. Int. Ed.* **2009**, *48*, 2411–2414.
4. P. L. Golas, K. Matyjaszewski, *Chem. Soc. Rev.* **2010**, *39*, 1338–1354.
5. M. Meldal, C. W. Tornøe, *Chem. Rev.* **2008**, *108*, 2952–3015.
6. C. Barner-Kowollik, F. E. Du Prez, P. Espeel, C. J. Hawker, T. Junkers, H. Schlaad, W. Van Camp, *Angew. Chem. Int. Ed.* **2011**, *50*, 60–62.
7. W. Xi, T. F. Scott, C. J. Kloxin, C. N. Bowman, *Adv. Funct. Mater.* **2014**, *24*, 2572–2590.
8. G. Pritchard, *Plastics Additives: A Rapra Market Report*, iSmithers Rapra Publishing, United Kingdom, **2005**, p. 208.
9. I. Holme, *Surf. Coat. Int. Part B* **2006**, *89*, 343–363.
10. D. Price, K. Pyrah, T. R. Hull, G. J. Milnes, J. R. Ebdon, B. J. Hunt, P. Joseph, C. S. Konkel, *Polym. Degrad. Stab.* **2001**, *74*, 441–447.
11. D. J. Kind, T. R. Hull, *Polym. Degrad. Stab.* **2012**, *97*, 201–213.
12. H. Ban, J. Gavrilyuk, C. F. Barbas, *J. Am. Chem. Soc.* **2010**, *132*, 1523–1525.
13. H. Ban, M. Nagano, J. Gavrilyuk, W. Hakamata, T. Inokuma, C. F. Barbas, *Bioconjugate Chem.* **2013**, *24*, 520–532.
14. K. Hoogewijs, D. Buyst, J. M. Winne, J. C. Martins, A. Madder, *Chem. Commun.* **2013**, *49*, 2927–2929.
15. S. Billiet, K. De Bruycker, F. Driessen, H. Goossens, V. Van Speybroeck, J. M. Winne, F. E. Du Prez, *Nat. Chem.* **2014**, *6*, 815–821.
16. O. Türünç, S. Billiet, K. De Bruycker, S. Ouardad, J. Winne, F. E. Du Prez, *Eur. Polym. J.* **2015**, *65*, 286–297.
17. W. H. Pirkle, J. C. Stickler, *Chem. Commun. (London)* **1967**, *1967*, 760–761.
18. G. B. Butler, *Polym. Sci. U.S.S.R.* **1981**, *23*, 2587–2622.
19. K. De Bruycker, S. Billiet, H. A. Houck, S. Chattopadhyay, J. M. Winne, F. E. Du Prez, *Chem. Rev.* **2016**, *116*, 3919–3974.
20. K. De Bruycker, M. Delahaye, P. Cools, J. Winne, F. E. Du Prez, *Macromol. Rapid Commun.* **2017**, *38*, 1700122.

21. B. Vonhören, O. Roling, K. De Bruycker, R. Calvo, F. E. Du Prez, B. J. Ravoo, *ACS Macro Lett.* **2015**, *4*, 331–334.

22. O. Roling, K. De Bruycker, B. Vonhören, L. Stricker, M. Körsgen, H. F. Arlinghaus, B. J. Ravoo, F. E. Du Prez, *Angew. Chem. Int. Ed.* **2015**, *54*, 13126–13129.

23. G. K. Such, J. F. Quinn, A. Quinn, E. Tjipto, F. Caruso, *J. Am. Chem. Soc.* **2006**, *128*, 9318–9319.

24. C. Schulz, S. Nowak, R. Fröhlich, B. J. Ravoo, *Small* **2012**, *8*, 569–577.

25. W. J. Yang, D. Pranantyo, K.-G. Neoh, E.-T. Kang, S. L.-M. Teo, D. Rittschof, *Biomacromolecules* **2012**, *13*, 2769–2780.

26. H. A. Houck, K. De Bruycker, S. Billiet, B. Dhanis, H. Goossens, S. Catak, V. Van Speybroeck, J. Winne, F. Du Prez, *Chem. Sci.* **2017**, *8*, 3098–3108.

Appendix A

Materials

The isocyanurate-based trimers of hexamethylene diisocyanate (HDI_3, Desmodur N 3600, neat), toluene diisocyanate (TDI_3, Desmodur IL EA, 51 % in ethyl acetate) and isophorone diisocyanate ($IPDI_3$, Desmodur Z 4470 BA, 70 % in butyl acetate) were kindly provided by Bayer MaterialScience (now Covestro) and – when applicable – concentrated *in vacuo* prior to use.

Acrylonitrile butadiene styrene terpolymer (ABS, Terluran GP-35) and styrene-butadiene copolymer (SBC, Styrolux 693D) were kindly provided by Styrolution as spherical pellets.

Poly(styrene-block-isoprene-block-styrene) (SIS, Kraton D1161 K) with a polystyrene content of 15 % was kindly provided by Kraton Polymers LLC as undusted porous pellet. The molecular weight ($M_\mathrm{n} = 200 \times 10^3\,\mathrm{g\,mol^{-1}}$) and dispersity ($Đ = 1.1$) were determined via SEC analysis (section IV.6.3).

Silicon wafers were supplied by Siltronic AG (Germany) and Sylgard 184 was provided by Dow Corning.

When indicated, tetrahydrofuran was dried over sodium and pyridine was dried over calcium hydride.

All other products and solvents (Table A.1) were used as received without further purification.

Table A.1: Used products and solvents.

Name	**CAS**	**Supplier**	**Purity (%)**
Acetic acid	64-19-7	Fiers	99.8
Acetone	67-64-1	Sigma-Aldrich	99.8
Acetone-d_6	666-52-4	Euriso-Top	99.8
Acetonitrile	75-05-8	Fisher Chemical	99.99
Acryloyl chloride	814-68-6	ABCR	96
Aliquat 336	63393-96-4	Sigma-Aldrich	-
Allyl vinyl ether	3917-15-5	Alfa Aesar	95
Aluminiumoxide (activated, basic, Brockmann I)	1344-28-1	Sigma-Aldrich	-
4-Aminoazobenzene	60-09-3	TCI	98
6-Aminocaproic acid	60-32-2	Acros Organics	99
Aminopropyl terminated PDMS (M_w = 900–1000, 3000, 5000)	106214-84-0	Gelest	-
Aminopropylmethylsiloxane-dimethylsiloxane copolymer (M_w = 4000–5000)	99363-37-8	Gelest	-
α,α′-Azoisobutyronitrile	78-67-1	Sigma-Aldrich	98
Benzylamine	100-46-9	Sigma-Aldrich	99.5
Bromine	7726-95-6	Sigma-Aldrich	99
α-Bromoisobutyryl bromide	20769-85-1	Sigma-Aldrich	98
Celite	91053-39-3	Sigma-Aldrich	-
Chloroform	67-66-3	Sigma-Aldrich	99.8
Chloroform-d	865-49-6	Euriso-Top	99.8
4-Chloro-7-nitrobenzofurazan	10199-89-0	Sigma-Aldrich	98
Citronellol	106-22-9	Sigma-Aldrich	95
2-(1-Cyclohexenyl)ethylamine	3399-73-3	Alfa Aesar	98
1,4-Diazabicyclo[2.2.2]octane	280-57-9	TCI	98
Dibutyltin dilaurate	77-58-7	TCI	95
Dichloromethane	75-09-2	Sigma-Aldrich	99.8
Diethyl ether	60-29-7	VWR Chemicals	99.5
3,4-Dihydro-2*H*-pyran	110-87-2	Sigma-Aldrich	97
Diisopropyl ether	108-20-3	Sigma-Aldrich	99
N,*N*-Dimethylacrylamide	2680-03-7	Sigma-Aldrich	99
N,*N*-dimethylformamide	68-12-2	Acros Organics	99.8
Dimethylsulfoxide	67-68-5	Acros Organics	99.7
Dimethylsulfoxide-d_6	2206-27-1	Euriso-Top	99.8
Dioxane	123-91-1	Sigma-Aldrich	99.5

Table A.1: Used products and solvents (continued).

Name	CAS	Supplier	Purity (%)
Dioxane (dry)	123-91-1	Acros Organics	99.8
Diphenylphosphoryl azide	26386-88-9	TCI	97
Ethanol	64-17-5	Sigma-Aldrich	99.8
Ethyl 4-bromobutyrate	2969-81-5	TCI	97
Ethyl acetate	141-78-6	Sigma-Aldrich	99.7
Ethyl carbazate	4114-31-2	Acros Organics	97
2,2′-(Ethylenedioxy)bis-(ethylamine)	929-59-9	Sigma-Aldrich	98
trans,*trans*-2,4-hexadien-1-ol	17102-64-6	Alfa Aesar	98
n-hexane	110-54-3	VWR Chemicals	98
D,L-Homocysteine thiolactone hydrochloride	6038-19-3	Haihang Industry	99
Hydrochloric acid	7647-01-0	Chem-Lab	36
Hydrochloric acid in dioxane	7647-01-0	Sigma-Aldrich	4 M
Hydroxypropyl terminated PDMS (M_w = 600–800)	104780-66-7	Gelest	-
Hypermer™ B246	-	Croda	-
Isopropylamine	75-31-0	Sigma-Aldrich	99.5
Magnesium sulfate	7487-88-9	Carl Roth	99
Methanesulfonyl chloride	124-63-0	Acros Organics	99.5
Methanol	67-56-1	Sigma-Aldrich	99.9
Methanol-d_4	811-98-3	Euriso-Top	99.8
2-(Methylamino)ethanol	109-83-1	Sigma-Aldrich	98
4,4′-methylene diphenyl diisocyanate	101-68-8	Sigma-Aldrich	98
Natrium chloride	7647-14-5	Carl Roth	99
4-Nitrophenyl chloroformate	7693-46-1	TCI	98
4-Nitrophenyl isocyanate	100-28-7	TCI	98
Octylamine	111-86-4	Sigma-Aldrich	99
Oleyl alcohol	143-28-2	Sigma-Aldrich	85
Palladium on carbon	7440-05-3	Sigma-Aldrich	5
2,3,4,5,6-Pentafluoroaniline	771-60-8	Fluorochem	99
1*H*,1*H*,2*H*,2*H*-Perfluorodecyl iodide	2043-53-0	Fluorochem	97
Petroleum ether (40–60 °C)	64742-49-0	Acros Organics	-
Phenyl chloroformate	1885-14-9	TCI	98
Phenyl isocyanate	103-71-9	Sigma-Aldrich	98
2-Phenylindole	948-65-2	Alfa Aesar	95

Table A.1: Used products and solvents (continued).

Name	**CAS**	**Supplier**	**Purity (%)**
Poly(ethylene glycol) diacrylate ($M_n = 250$)	26570-48-9	Sigma-Aldrich	92
Poly(ethylene glycol) diacrylate ($M_n = 575$)	26570-48-9	Sigma-Aldrich	-
Poly(ethylene glycol) diacrylate ($M_n = 700$)	26570-48-9	Sigma-Aldrich	-
Potassium carbonate	584-08-7	Carl Roth	99
Potassium hydroxide	1310-58-3	Sigma-Aldrich	90
Prenol	556-82-1	Sigma-Aldrich	99
Propylamine	107-10-8	Sigma-Aldrich	99
Pyridine	110-86-1	Acros Organics	99.5
Pyrrolidine	123-75-1	Sigma-Aldrich	99
Silica gel 60 Å	7631-86-9	Rocc	99.5
Sodium azide	26628-22-8	Acros Organics	99
Sodium bicarbonate	144-55-8	Carl Roth	99.5
Sodium carbonate	497-19-8	Carl Roth	99.5
Sodium chloride	7647-14-5	Carl Roth	99
Sodium ethoxide	141-52-6	Acros Organics	96
Sodium hydroxide	1310-73-2	Acros Organics	97
Sodium sulfate	7757-82-6	Carl Roth	99
Span® 80	1338-43-8	Sigma-Aldrich	-
Sudan II	3118-97-6	Sigma-Aldrich	90
Sulfuric acid	7664-93-9	Sigma-Aldrich	95
Tetrahydrofuran	109-99-9	Sigma-Aldrich	99.9
Tetrahydrofuran (dry)	109-99-9	Acros Organics	99.85
Thioacetic acid	507-09-5	Sigma-Aldrich	96
Toluene	108-88-3	Sigma-Aldrich	99.9
3-(Triethoxysilyl)propyl isocyanate	24801-88-5	Sigma-Aldrich	95
Triethylamine	121-44-8	Acros Organics	99
Triethylsilane	617-86-7	Sigma-Aldrich	97
Trifluoroacetic acid	76-05-1	Sigma-Aldrich	99
Triphosgene	32315-10-9	TCI	98

Appendix B

List of publications

Peer-reviewed articles

Ultrafast Layer-by-Layer Assembly of Thin Organic Films Based on Triazolinedione Click Chemistry.
B. Vonhören, O. Roling, K. De Bruycker, R. Calvo, F. E. Du Prez, B. J. Ravoo, *ACS Macro Letters* **2015**, *4*, 331–334.

Rewritable Polymer Brush Micropatterns Grafted by Triazolinedione Click Chemistry.
O. Roling, K. De Bruycker, B. Vonhören, L. Stricker, M. Körsgen, H. F. Arlinghaus, B. J. Ravoo, F. E. Du Prez, *Angewandte Chemie International Edition* **2015**, *54*, 13126–13129.

Triazolinediones as Highly Enabling Synthetic Tools.
K. De Bruycker, S. Billiet, H. A. Houck, S. Chattopadhyay, J. M. Winne, F. E. Du Prez, *Chemical Reviews* **2016**, *116*, 3919–3974.

Covalent Fluorination Strategies for the Surface Modification of Polydienes.
K. De Bruycker, M. Delahaye, P. Cools, J. Winne, F. E. Du Prez, *Macromolecular Rapid Communications* **2017**, *38*, 1700122.

Peer-reviewed articles outside this doctoral work

Triazolinediones Enable Ultrafast and Reversible Click Chemistry for the Design of Dynamic Polymer Systems.
S. Billiet, K. De Bruycker, F. Driessen, H. Goossens, V. Van Speybroeck, J. M. Winne, F. E. Du Prez, *Nature Chemistry* **2014**, *6*, 815–821.

Straightforward Functionalization and Crosslinking of Natural Plant Oils with Triazolinediones.
O. Türünç, S. Billiet, K. De Bruycker, S. Ouardad, J. Winne, F. E. Du Prez, *European Polymer Journal* **2015**, *65*, 286–297.

Use of Triazolinedione Click Chemistry for Tuning the Mechanical Properties of Electrospun SBS-Fibers.
S. van der Heijden, K. De Bruycker, R. Simal, F. Du Prez, K. De Clerck, *Macromolecules* **2015**, *48*, 6474–6481.

ADMET and TAD Chemistry: A Sustainable Alliance.
L. Vlaminck, K. De Bruycker, O. Türünç, F. E. Du Prez, *Polymer Chemistry* **2016**, *7*, 5655–5663.

Novel Composite Materials with Tunable Delamination Resistance Using Functionalizable Electrospun SBS Fibers.
S. van der Heijden, L. Daelemans, K. De Bruycker, R. Simal, I. De Baere, W. Van Paepegem, H. Rahier, K. De Clerck, *Composite Structures* **2017**, *159*, 12–20.

Design of a Thermally Controlled Sequence of Triazolinedione-Based Click and Transclick Reactions.
H. A. Houck, K. De Bruycker, S. Billiet, B. Dhanis, H. Goossens, S. Catak, V. Van Speybroeck, J. Winne, F. Du Prez, *Chemical Science* **2017**, *8*, 3098–3108.

Recyclable Cross-Linked Hydroxythioether Particles with Tunable Structures Via Robust and Efficient Thiol-Epoxy Dispersion Polymerizations.
J. Tan, C. Li, K. De Bruycker, G. Zhang, J. Gu, Q. Zhang, *RSC Advances* **2017**, *7*, 51763–51772.

Ultrafast Tailoring of Carbon Surfaces via Electrochemically Attached Triazolinediones.
W. Laure, K. De Bruycker, P. Espeel, D. Fournier, P. Woisel, F. E. Du Prez, J. Lyskawa, *submitted.*

Patent application

Urazole compounds
Billiet S., De Bruycker K., Winne J.M., Du Prez F.E., **WO 2015/018928 A1**

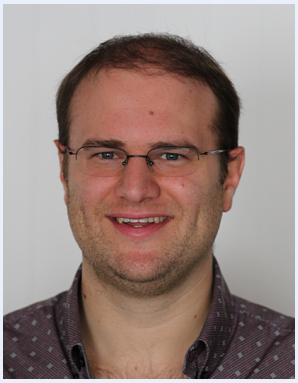

Triazolinediones (TADs) are very reactive compounds with a long-standing history in various research fields. The very first TAD has been described already in the late 19th century, followed by the first practical applications in organic synthesis and polymer chemistry in the 1970s. Recently, the launch of the concept of 'click chemistry' has renewed the scientific interest in these unique reagents, which has resulted in new applications, such as the bioconjugation to synthetic or natural peptides or proteins and the ultrafast production of various polymeric materials.

The main focus of this research is the application of triazolinedione chemistry in interfacial systems. Both reactions at the solid-liquid interface and in liquid-liquid biphasic systems are investigated. However, in each case, tailored TAD compounds and complementary reaction partners are necessary, of which the synthesis represents the first part of this work. Subsequent parts describe various TAD-based surface modifications. Firstly, fluorinated compounds are applied as reactive additives for polydienes and are shown to greatly influence the surface properties. Secondly, an inorganic yet TAD-reactive substrate is alternatingly submerged in solutions of mutually reactive monomers to afford a coating in a layer-by-layer approach. Finally, similar substrates are used to print a triazolinedione 'ink' via microcontact chemistry, which allows to write, erase and rewrite patterns when reversibility is introduced in the system.

Triazolinedione chemistry proves to be less suitable for reactions in liquid-liquid interfacial systems. Therefore, the next part discusses the limitations of the TAD strategy and introduces the thiolactone-based multicomponent reaction as a complementary alternative for the production of polymeric beads. Finally, the latter ligation is demonstrated to be a promising cross-linking method for the synthesis of amphiphilic networks.

www.CMaC.UGent.be

www.PCR.UGent.be

Ghent University
Department of Organic and Macromolecular Chemistry
Centre of Macromolecular Chemistry (CMaC)
Polymer Chemistry Research Group (PCR)
Krijgslaan 281, S4-bis
9000 Ghent, Belgium